ALMA MATER STUDIORUM
UNIVERSITÀ DI BOLOGNA

in cotutela con **Universitat Autònoma de Barcelona (UAB)**

DOTTORATO DI RICERCA IN

IL FUTURO DELLA TERRA, CAMBIAMENTI CLIMATICI E SFIDE SOCIALI

Ciclo XXXVI

Settore Concorsuale: 07/B1 AGRONOMIA E SISTEMI COLTURALI ERBACEI ED ORTOFLORICOLI

Settore Scientifico Disciplinare: AGR/04 ORTICOLTURA E FLORICOLTURA

TITOLO TESI

Emission Factors from Urban Food Systems in a Circular City

Presentata da: Gaia Stringari

Coordinatore Dottorato

Prof. ssa Silvana Di Sabatino

Supervisori

Prof. Francesco Orsini

Prof. Xavier Gabarrell Durany

Esame finale anno 2024

Emission Factors from Urban Food Systems in a Circular City

Gaia Stringari Astori

Doctoral thesis

Supervisors: Dr. Xavier Gabarrell Durany (UAB)
Dr. Francesco Orsini (UNIBO)

Academic tutor: Dr. Xavier Gabarrell Durany (UAB)

A thesis submitted in fulfillment of the requirements for the Doctoral degree in Environmental Sciences and Technology

Sostenipra research group
Institut de Ciència i Tecnologia Ambientals (ICTA–UAB)
Universitat Autònoma de Barcelona (UAB)
Maria de Maeztu program for Units of Excellence in R&D (CEX2019-0940-M)

UAB Universitat Autònoma de Barcelona

ALMA MATER STUDIORUM UNIVERSITÀ DI BOLOGNA
DIPARTIMENTO DI SCIENZE E TECNOLOGIE AGRO-ALIMENTARI

sostenipra

ICTA-UAB

EXCELENCIA MARÍA DE MAEZTU

Emission Factors from Urban Food Systems in a Circular City

By

Gaia Stringari

A thesis submitted in fulfilment of the requirements for the PhD degree in Environmental Science and Technology

May 2024

The present doctoral thesis was developed thanks to the financing of the FI 2020 and Joan Oró FI 2023 predoctoral scholarships awarded to Gaia Stringari (FI_B 01004 2020 and FI-4 00145 2023) from the Catalan Agència de Gestió d'Ajuts Universitaris i de Recerca (AGAUR).

“Αρχή δε αυτών δεν υπάρχει, αφού τα άτομα και το κενό είναι αιώνια.”

Ἐπίκουρος

(Επιστολή προς Ηρόδοτο)

[“*Non esiste alcun principio di ciò, poiché gli atomi e il vuoto sono eterni*.”

Epicuro
(Lettera a Erodoto)

“No hay principio de esto, ya que los átomos y el vacío son eternos.”

Epicuro
(Carta a Erodoto)]

The present thesis entitled Emission Factors from Urban Food Systems in a Circular City by Gaia Stringari, has been realized at the Institute of Environmental Science and Technology (ICTA) at the Universitat Autònoma de Barcelona (UAB).

Gaia Stringari

Under the supervision of Dr. Xavier Gabarrell from the ICTA and the Department of Chemical, Biological and Environmental Engineering at the UAB, and Francesco Orsini from the Department of Agricultural and Food Sciences (DISTAL) of the University of Bologna (UNIBO, Italy).

Bellaterra (Cerdanyola del Vallès), May 2024

Xavier Gabarrell Francesco Orsini

Table of Contents

Abbreviations & Acronyms

Anasorb CSC – coconut-shell activated charcoal
AGAUR – Catalan Agència de Gestió d'Ajuts Universitaris i de Recerca
BV – Breakthrough Volume
BVOC – Biogenic Volatile Organic Compound
CC – Calibration Curve
C=C – Carbo-Carbon bond
CCITUB – Centres Científics i Tecnològics of the Universitat de Barcelona
CEA – Controlled-Environment Agriculture
COVID-19 – CoronaVirus Desease of 2019
DAS – Day After Sowing
DAT – Day After Transplanting
DCM – Dichloromethane
DE – Desorption Efficiency
DISTAL – Department of Agricultural and Food Sciences
DNA – Deoxyribonucleic acid
DOI –Direct Object Identifier
EC – Electrical Conductivity
ECA – European Collaborative Action
ECHA – European Chemicals Agency
EF – Emission Factor
EFSA – European Food Safety Authority
EI – Emission Index
EO – Essential Oil
EPA – Environmental Protection Agency
ER – Emission Rate
EU – European Union
FID – Flame Ionization Detector
FoodE – Food Systems in European Cities, EU project
GC – Gas Chromatography
GC-MS – Gas Chromatograph coupled to Mass Spectrometer
GC-FID – Gas Chromatograph coupled to Flame Ionization Detector
GHG – Greenhouse Gas
G_s – Stomatal conductance
HDDs – Heating Degree Days
HSE – Health and Safety Executive
HT – Homoterpene
HVAC – Heating, Ventilation and Air Conditioning
IAQ – Indoor Air Quality
IARC – International Agency for Research on Cancer
ICS – Ion Chromatography System
ICTA – Institut de Ciència i Tecnologia Ambientals
INSHT – Spanish National Institute of Safety and Health at Work
IPC – Institut Paleontológic de Catalunya

IPCC – Intergovernmental Panel on Climate Change
iRTG – integrated Rooftop Greenhouse
IS – Internal Standard
ISO – International Organization for Standardization
ISQ – Ion Single Quadrupole
LAI – Leaf Area Index
LAU – Laboratory of Urban Agriculture in ICTA
LE – Liquid Extracted
LED – Light Emitting Diode
LC – Liquid Chromatography
LCI – Lower Concentration of Interest
LDPE – Low-Density Polyethylene
LOD – Lowest Limit of Detection
LOQ – Lowest Limit of Quantitation
LOX – Lipoxygenase
LED – Light Emitting Diode
m/z – mass-to-charge ratio
MDHS – Methods for the Determination of Hazardous Substances
MT – Monoterpene
NIOSH – National Institute for Occupational Safety and Health
NIST – National Institute of Standards and Technologies
NO_x – Nitrogen oxides
NTP – Notas Técnicas de Prevención
OMT – Oxygenated monoterpene
PAR – Photosynthetic Available Radiation
PCA – Principal Component Analyses
PH – Phenylpropanoid
PMs – Particulate Matters
Pn – Net Photosynthesis
PPFD – Photosynthetic Photon Flux Density
Ppb – Parts per billion
Ppm – parts per million
PTR-MS – Proton transfer Mass Spectrometer
REACH – Registration, Evaluation, Authorisation and Restriction of Chemicals
RB – Red Blue ratio
RB_1 – Red Blue ratio equal to 1
RB_3 – Red Blue ratio equal to 3
RO_2 – Organic peroxy radicals
RT – Retention Time
RSD – Relative Standard Deviation
SEM – Standard Error of the Mean
SIM – Selected ion Monitoring
S/N or SNR – signal-to-noise ratio
SO_x – Sulphur oxides
SOAs – Suspended Organic Aerosols

Sostenipra – Sustainability and Environmental Prevention research group
SPME – Solid Phase Microextraction
SSV – Safe Sample Volume
ST – Sesquiterpene
STRATEX – Strategies to determine and control the contributions of indoor air pollution to total inhalation exposure
TA – Tenax
TD – Thermally Desorbed
TIC – Total Ion Chromatogram
TMTT – (3E,7E)-4,8,12-Trimethyltrideca-1,3,7,11-tetraene
VF – Vertical Farm
VOC – Volatile Organic Compound
UA – Urban Agriculture
UAB – Universitat Autònoma de Barcelona
UNIBO – University of Bologna
UV – Ultraviolet
WHO – World Health Organization

List of Figures, Tables, and Equations

List of Figures

list of tables

List of Equations

Research Funding

The work presented was supported by the following Institutions:

- The co-funded European Interreg NWE Programme for the financial support to G. Stringari under the Greenhouses to Reduce CO2 on Roofs (Groof) project.
- The Catalan Agència de Gestió d'Ajuts Universitaris i de Recerca (AGAUR) for the grants awarded to G. Stringari no 2020 FI_B 01004 and no 2023 FI-4 00145.
- The Catalan Agència de Gestió d'Ajuts Universitaris i de Recerca (AGAUR) for the grants awarded to Sostenipra no 2021SGR00734, no AGAU 2020 PANDE 00021, and no 2023CLIMA0041 (WEF4Build).
- The European Research Council under the European Horizon2020 research and innovation program for the grant agreement No 862663 (FoodE).
- The Spanish Ministry of Economy, Industry and Competitiveness for the grants awarded under the MOVE4EDU (MCIN/AEI/10.13039/501100011033/FEDER) no PID2021-126845OB-C21 and the BINAFET (MCIN/AEI/10.13039/501100011033/) no TED2021-130047B-C21.
- The “María de Maeztu” program for Units of Excellence and R&D (MDM-2015-0552 and CEX2019-0940-M).
- The European Union for the grant awarded under the NextGenerationEU/PRTR.

Acknowledgements

¡Por fin llegó ese día!

Me gustaría agradecer en primer lugar a mis supervisores Xavier y Francesco por haber hecho posible la realización de estos 4 cuatros años de investigación.

A Joan Villanueva por la paciencia y toda la ayuda con el trabajo del lab y a Nuria y Pau por el soporte técnico. A Gara por prestarme sus equipos siempre (me has salvado muchos ensayos!) y a Carme también. A Josep Antoni por la inspiración (aun me acuerdo nuestra charla!) y a Joan Rieradevall por su motivación y por el tema de investigación :)

Al despacho #321 por las risas cotidianas y el marujeo y por dejarme siempre algún detalle encima de mi mesa… a Vero por su apoyo femenino en el medio de tantos…y esfuerzo por aprender italiano, a Ramiro por las aventuras en el iRTG, las cámaras construidas, las ideas empresariales (sí, ya tú sabes que piensa mi madre) y por acogerme en su casa el día siguiente de conocerme, a Guido por las apuestas Norte vs Sur –ya sabes quién gana –, a Jonatan por llevarnos al equilibrio, y a Felipe por todo su inmenso soporte personal y científico (bendita estadística!), sin ti estaría perdida!

También a todas las personas del grupo Sostenipra actuales y anteriores. A los que estuvieron desde mi TFM (¡cuantos años llevo aquí!) pero que ya no están: Ana Maria, Ana Nadal, Mireia, Martí, Perla, Alexandra, Joan y Susana T. (fashioners inspiradores), Maria Raja, os echo de menos! ♡

Al equipo Surana (por las jaranas): Mateo, Pietro, Juan David, Anna, Miquel, Sara, Gemma, Susana, Berta, Albert, Borja… sois muchos y siempre hay más.

A l@s precarious predocs del ICTA, a l@s que ya no están y a l@s que siguen aquí, falta poco! Y a la gente de administración (la burocracia no es lo mío). También a los seguratas, siempre me tenéis cariño aunque me salte las normas…!

Al equipo de Bologna por acogerme en el grupo en tan poco tiempo juntos: Laura, Vito, Ila, Andrea, Ale, Matteo, Michele, Giuseppina y sobretodo a Elisa por haber compartido conmigo las aventuras con los tomates (mannaggia).

Quiero agradecer a tod@s l@s de la mítica casa Montflorit (sí, el reino), a todos los que me han aguantado y a los que me siguen aguantando por mis manías de orden y limpieza (no os preocupéis, aún no tengo planes de irme!), a Javi por haberme salvado en aquel día (quizás no estaría aquí ahora), a la primera (Naza, Anna, Marc, Marina), segunda, tercera,

cuarta,..generación de compañer@s y de gatunos. A Juli por quererme y comprenderme siempre, te quiero *zi* ♡. A Aurora por *le minghiate* (¡vuelve!) y a Stefanone por las fuertes emociones (espero te hayas recuperado 100%).

Quiero darle un agradecimiento especial a Luca por todo el apoyo personal, emotivo y laboral (la química!!!) a lo largo de estos años, sin ti creo que no hubiera llegado al final, te debo un montón :')

Finalmente, a mi familia, mi mamá, mi hermano y mi padre (y a las gatas, Recel y Lola siempre en mi corazón) y familiares y a mis amig@s de Italia/España por haber estado presentes, aunque lejos en todo ese tiempo, os quiero.

Y a tod@s l@s que no haya citado (perdón perdón perdón), por haber estado en estos años compartiendo aventuras conmigo!!!

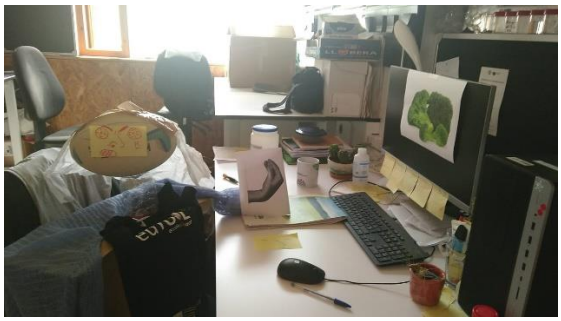

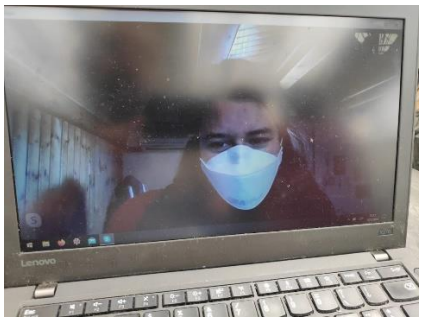

Vuestra Gaia (*Gallina*)

Summary

Recognized for its potential to foster resilient and sustainable cities, Urban Agriculture (UA) seeks to ensure reliable and attainable food supply while generating various benefits across environmental, economic, and societal domains. Various applications of UA exist, including indoor, outdoor, and mixed typologies, with installations ranging from traditional ground-level setups to integrated rooftop greenhouses (iRTGs) and vertical farms (VFs). These installations are considered as part of the green strategies aimed at improving air quality, reducing carbon emissions, creating job opportunities, and promoting technological advancements in production systems. Despite the multiple benefits reported, their implementation faces challenges, particularly concerning human health and environmental safety. Issues such as air quality, contamination, and regulatory frameworks often hinder UA initiatives, necessitating the involvement of local authorities and the development of appropriate policies and regulations. Concerning air quality, the accumulation of indoor pollution is a topic frequently debated due to the acknowledged health risks associated. Among indoor pollutants, Volatile Organic Compounds (VOCs) generally rank at the top of official lists due to their multiple sources and sustained emission. Beside anthropogenic causes, also living organisms emit VOCs, better knowns as biogenic ones (BVOCs). Plants are known to be high emitters of BVOCs, whose tropospheric reactivity can greatly affect the air quality of different environments. However, the influence of external factors often produces fluctuations in plant emissions, making it difficult to accurately predict the true impact of BVOCs. With the expansion of indoor UA installations, the overall emissions of BVOCs in urban areas are expected to rise. Despite limited research on this topic to date, existing studies have highlighted both positive and negative effects of BVOC emissions. Therefore, it is essential to monitor BVOC emissions to better understand their implications for air quality and human health, particularly in the context of UA systems. This action was endeavoured by multiple assessments conducted specifically in an iRTG and in an indoor VF, involving widely cultivated plant species, such as, green bean, tomato, and basil. The present dissertation aims to define the safety of the investigated systems based on the measured BVOC emissions, by addressing the following questions:

Q.1 What are actual BVOC emission levels in the considered UA environments and which volatile compounds accumulate more?

Q.2 Are the measured BVOC emission levels within the safety range fixed by official frameworks and/or most updated databanks?

Q.3 Which are the factors implicated in final BVOC emissions in the considered UA environments?

Q.4 Based on the overall investigation, do UA environments bring about unsafe conditions to human health? And if so, how could the BVOCs accumulation be contained and/or prevented?

The development of this research followed a methodological approach consisting of 5 main parts, the sampling setup, field emissions collection, post sampling setup, data analysis, and validation of the results. These steps involved the utilization of specific tools and protocols, such as chambers for the BVOCs collection, as well as chemical reagents and analytical instruments for the qualitative and quantitative determination of the BVOCs. Additionally, official table lists and factsheets were used as reference limit guidelines.

The results obtained from the research can be wrapped up in the following 4 sections.

Qualitative and quantitative BVOC emission trends within UA systems

The research investigated the environmental levels and BVOC emission profiles of different crops grown under protected cultivation systems in UA. On average, BVOC levels were within parts per billion (ppb) across both UA environments, with peak levels typically observed during the initial growth phase before gradually declining throughout the plant cycle. However, exceptions to this trend were primarily attributed to specific environmental conditions. In the iRTG, similar emission trends were observed for beans and tomato plants, with monoterpenes dominating early in the cycle, followed by lipoxygenase derivatives and oxygenated monoterpenes. Sesquiterpenes and phenylpropanoids were less common or barely detected. In the indoor VF, emission patterns varied depending on the light treatment applied to the plants. Under blue light spectra, high emissions of various BVOCs were observed early in cultivation, while under red light, higher emissions were detected later in the cultivation period, although for fewer volatiles. Overall, oxygenated monoterpenes were the most abundant, followed by lipoxygenase derivatives, sesquiterpenes, monoterpenes, and phenylpropanoids. Interestingly, for the same cultivated species (basil), emission trends differed between the iRTG and VF environments.

Compliance with safety risk-levels of BVOC emissions produced by UA

The safety determination in each UA environment was based on the BVOC concentrations measured. Their levels were usually compared against official indoor limits established by the European Collaborative Action (ECA), designated as the Lower Concentrations of Interest (LCIs) or when missing against detailed factsheets compiled for the individual compound by the European Chemicals Agency (ECHA). To date, only a few LCIs have been provided for BVOCs.

Therefore, multiple BVOCs were compared to the same LCI based on their volatile structure (class). None of the BVOCs were found to exceed the established thresholds. Average emission measured were considerably lower than reference LCIs, often by at least one order of magnitude. However, scattered bursts were identified during individual samplings, such as the case of aldehyde emissions detected in both building-integrated and indoor spaces, evaluated against the LCI of 2-hexenal (7 µg m^{-3}). These emissions were deemed not relevant for health concerns due to their limited occurrence and duration along the cultivation cycle. Further emission bursts were observed for volatiles β-caryophyllene, trans-β-farnesene, and 1.8-cineole, in the indoor VF. According to specific factsheets, adverse health effects related to the measured concentrations were considered unlikely. Overall, it was suggested that mild sensitization (e.g., localized irritation) could occur due to exceptionally high emissions in both investigated environments, varying based on individual sensitivity. This assumption was further supported by a comparative assessment conducted at the end of the research, which revealed much higher emission exposure in common indoor environments unrelated to plants compared to UA spaces.

BVOC emissions sensitivity to external factors excited by the background and the sampling approach

The research findings highlighted the multifaceted impact of various factors on BVOC emissions in UA conducted in building-integrated and indoor environments. The static enclosure maintained during sampling revealed that environmental parameters such as temperature and relative humidity significantly reduce plant emissions. Additionally, the variation in CO_2 concentration, particularly its decrease, interfered with normal emission activity, although its full implication at normal (iRTG) and higher (VF) concentrations was not entirely clear. Lighting settings, especially in the VF, were found to play a crucial role in influencing plant emission responses. Furthermore, in the iRTG, radiation was considered to have a negligible impact on BVOC emissions due to strong screening by the surrounding façade. Conversely, artificial lighting in the VF was believed to modulate the emission blend and quantity, but this hypothesis was not confirmed due to low correlations between emissions and different light spectra. The morphological development of plants was identified as another factor affecting BVOC emissions in both UA environments. Qualitative and quantitative variations in emissions were observed across different stages of plant growth. However, due to the lack of significant morphological differences between stages and further evaluative elements, the exact impact of plant development on emissions could not be conclusively determined. Overall, the research pointed out the complex interplay of environmental factors and plant biology on the total BVOCs emission in the frame of UA.

Multi-application of volatile sampling techniques for BVOC emission study

For the collection and analysis of plant emissions, multiple techniques were carried out, following revised literature and established protocols. Initially, in a preliminary study, open (without chamber), semi-open (open chamber), and closed (closed chamber) sampling approaches were tested, combining both active and passive collection for short or long collection terms. Based on the results obtained, the main assessments were conducted using active sampling in a static enclosure tailored to the size of the plant species under investigation. The efficiency of this method was evaluated based on the reliability of the emissions measured, determined by the precision and accuracy of the analytical results, which were consistently validated throughout the assessment process. Additionally, the entire methodology was evaluated against an alternative approach using a different sorbent material (Tenax instead of activated carbon) and analytical technique (thermal instead of liquid extraction). Consistent findings between the two approaches not only corroborated the research outcomes obtained with the main methodology but also highlighted relevant technical advances for the implementation of BVOC sampling.

Future explorations

Firstly, in relation to Controlled-Environment Agriculture (CEA), the investigation of further plant species and/or variety under standard and specific cultivation regimes, including alternative fertilizers recovered from the urban environment, could integrate the knowledge acquired from this study on qualitative and quantitative BVOCs emission. This also comprises the application of further combinations of light, CO_2, temperature, and relative humidity. Secondly, in terms of sampling methodology, the exploration of alternative sorbent materials, like Carbopack and Solid Phase Microextraction (SPME), was recommended to enhance the efficiency and the feasibility of sampling and analysis processes. These technical improvements could broaden the scope of BVOC investigation to encompass various indoor environments beyond UA, thus contributing to a deeper understanding of air quality assessment. Furthermore, exploring BVOCs-ozone derivatives from the tropospheric activity could improve the understanding of the environmental dynamics of BVOCs in relation to air quality. Lastly, shifting the perspective of the study on the positive effects associated to BVOCs, such as their bio-stimulant activity and their potential relaxant effects, on both plant system and human well-being, could hold significant promise for agronomic development and the expansion of building-integrated and indoor UA in the city.

Resumen

Reconocida por su potencial para fomentar ciudades resilientes y sostenibles, la Agricultura Urbana (AU) busca garantizar un suministro de alimentos seguro y alcanzable al mismo tiempo que genere diversos beneficios en los ámbitos ambiental, económico y social. Existen varias aplicaciones de AU, incluidas tipologías interiores, exteriores y mixtas, con instalaciones que van desde configuraciones tradicionales a nivel del suelo hasta invernaderos integrados en azoteas (iRTG) y granjas verticales (VF). Estas instalaciones se consideran parte de las estrategias verdes encaminadas a mejorar la calidad del aire, reducir las emisiones de carbono, crear oportunidades de empleo y promover avances tecnológicos en los sistemas de producción. A pesar de los múltiples beneficios reportados, su implementación enfrenta desafíos, particularmente con respecto a la salud y la seguridad ambiental. Cuestiones como la calidad del aire, la contaminación y los marcos regulatorios a menudo obstaculizan las iniciativas de AU, lo que requiere la participación de autoridades locales y el desarrollo de políticas y regulaciones apropiadas. En cuanto a la calidad del aire, la acumulación de contaminación interior es un tema de debate frecuente debido a los riesgos reconocidos y asociados para la salud. Entre los contaminantes de interior, los compuestos orgánicos volátiles (COV) suelen encabezar las listas oficiales debido a sus múltiples fuentes y a su emisión sostenida. Además de las causas antropogénicas, también los organismos vivos emiten COV, más conocidos como biogénicos (COVB). Se conoce que las plantas son grandes emisoras de COVB, cuya reactividad troposférica puede afectar en gran medida a la calidad del aire de distintos entornos. Sin embargo, la influencia de factores externos suele provocar fluctuaciones en las emisiones de las plantas, lo que dificulta la predicción exacta del verdadero impacto de los COVB. Con la expansión de las instalaciones de AU de interior, se espera que aumenten las emisiones globales de COVB en las zonas urbanas. A pesar de la limitada investigación sobre este tema hasta la fecha, los estudios existentes han evidenciado los efectos tanto positivos como negativos de las emisiones de COVB. Por lo tanto, es esencial monitorizar estas emisiones para comprender mejor sus implicaciones en la calidad del aire y la salud humana, especialmente en el contexto de los sistemas de AU. Esta acción se ha llevado a cabo mediante múltiples evaluaciones realizadas específicamente en un sistema integrado a un edificio, iRTG, y de interior, VF, con especies vegetales ampliamente cultivadas, como la judía verde, el tomate y la albahaca. La presente tesis pretende definir la seguridad de los sistemas investigados basándose en las emisiones de COVB medidas, abordando las siguientes cuestiones:

P.1 ¿Cuáles son los niveles reales de emisión de COVBs en los entornos de AU considerados y qué compuestos volátiles se acumulan más?

P.2 ¿Los niveles de emisiones de COVBs medidos están dentro del rango de seguridad fijado por los marcos oficiales y/o las bases de datos más actualizados?

P.3 ¿Cuáles son los factores implicados en las emisiones finales de COVBs en los entornos de AU considerados?

P.4 Según la investigación general, ¿los entornos de AU generan condiciones inseguras para la salud humana? Y en caso afirmativo, ¿cómo se podría contener y/o prevenir la acumulación de COVBs?

El desarrollo de esta investigación siguió un enfoque metodológico que consta de 5 secciones principales, la configuración del muestreo, la recolección de emisiones en campo, la configuración posterior al muestreo, el análisis de datos y la validación de los resultados. Estos pasos implicaron la utilización de herramientas y protocolos específicos, como cámaras para la recolección de COVBs, así como reactivos químicos e instrumentos analíticos para la determinación cualitativa y cuantitativa de los COVBs. Además, se utilizaron listas de tablas oficiales y hojas informativas como pautas de límites de referencia.

Los resultados obtenidos de la investigación se pueden resumir en los siguientes 4 apartados.

Tendencias cualitativas y cuantitativas de emisiones de COVB dentro de sistemas de AU

La investigación estudió los niveles ambientales y los perfiles de emisión de COVB de diferentes plantas crecidas en sistemas de cultivo protegidos en AU. En promedio, los niveles de COVBs se situaron dentro del rango de partes por billón (ppb) en ambos entornos considerados, con niveles máximos observados típicamente durante la fase de crecimiento inicial y disminuyendo gradualmente a lo largo del ciclo de cultivo. Sin embargo, las excepciones a esta tendencia se atribuyeron principalmente a condiciones ambientales específicas. En un iRTG, se observaron tendencias de emisiones similares para las plantas de judías y tomates, en las cuales los monoterpenos prevalieron al principio del ciclo, seguidos por los derivados de la lipoxigenasa y los monoterpenos oxigenados. Los sesquiterpenos y los fenilpropanoides fueron menos comunes o apenas se detectaron. En un VF de interior, los patrones de emisión variaron dependiendo del tratamiento lumínico aplicado a las plantas. Bajo los espectros de luz azul, se observaron altas emisiones de varios COVBs al principio del cultivo, mientras que bajo luz roja, las emisiones más altas se detectaron más tarde, aunque menos variadas. En general, los monoterpenos oxigenados fueron los más abundantes, seguidos por los derivados de la

lipoxigenasa, los sesquiterpenos, los monoterpenos y los fenilpropanoides. Curiosamente, para la misma especie cultivada (albahaca), las tendencias de emisión difirieron entre los entornos iRTG y VF.

Cumplimiento de los niveles de riesgo de seguridad de las emisiones de COVB producidas por la AU

La determinación de seguridad en cada ambiente de AU se basó en las concentraciones de COVBs medidas. Sus niveles generalmente se compararon con los límites oficiales en interior establecidos por la Acción Colaborativa Europea (ECA), designados como Concentraciones de Interés Inferiores (LCI) o, en su defecto, con fichas técnicas especificas del compuesto considerado redactadas por la Agencia Europea de Sustancias Químicas (ECHA). Hasta la fecha, sólo se han proporcionado unas pocas LCIs para los COVBs. Por lo tanto, se compararon varios COVBs con el mismo LCI en función de su clase volátil. Ninguno de los COVBs superó los umbrales establecidos. Las emisiones medias medidas fueron considerablemente inferiores a las de los LCI de referencia, a menudo en al menos un orden de magnitud. Sin embargo, se identificaron picos aislados a lo largo del muestreo, como el caso de las emisiones de aldehídos detectadas tanto en espacios integrados y de interior, evaluadas frente al LCI del 2-hexenal (7 μg m^{-3}). Estas emisiones no se consideraron relevantes para la salud debido a su escasa presencia y duración a lo largo del ciclo de cultivo. Se observaron otros picos de emisión de los volátiles β-cariofileno, trans-β-farneseno y 1,8-cineol en la VF. Según las relativas fichas técnicas, se consideraron improbables los efectos adversos para la salud en relación con las concentraciones medidas. En términos generales, en ambos entornos, se determinó más probable la ocurrencia de una sensibilización leve-moderada (ej., irritación localizada) en respuesta a los niveles excepcionalmente elevados, según la sensibilidad individual. Esta hipótesis se vio respaldada por una evaluación comparativa realizada al final de la investigación, que reveló una exposición a las emisiones evidentemente mayor en los ambientes interiores comunes no relacionados con las plantas en comparación con los espacios de AU.

Sensibilidad de las emisiones de COVB a factores externos asociados al medio ambiente y al método de muestreo

Los hallazgos de la investigación resaltaron el impacto multifacético de varios factores sobre las emisiones de COVB en entornos integrados o de interior de AU. El cierre estático mantenido durante la toma de muestras demostró que parámetros ambientales como la temperatura y la humedad relativa pueden reducir significativamente las emisiones de las plantas. Además, variaciones en la concentración de CO_2, particularmente su reducción, se vieron interferir con la normal actividad de emisión, aunque su implicación en concentraciones normales (iRTG) y

superiores (VF) no fue aclarada. Se encontró que los ajustes de iluminación, especialmente en la VF, desempeñan un papel crucial a la hora de influir en las respuestas volátil de las plantas. Además, en el iRTG, se atribuyó un impacto irrelevante a la radiación debido a la fuerte filtración ejercida por la fachada circundante. Por el contrario, se planteó la hipótesis de que la iluminación artificial en el VF influyera en la composición y la concentración de las emisiones, aunque esa suposición no fue corroborada debido a las escasas correlaciones observadas entre las emisiones y los distintos espectros de luz aplicados. El desarrollo morfológico de las plantas fue identificado como siguiente factor influyente en las emisiones de COVB en ambos entornos investigados. Se observaron variaciones cualitativas y cuantitativas en diferentes etapas del crecimiento de las plantas. Sin embargo, debido a la falta de diferencias morfológicas significativas entre las etapas y de otros elementos de evaluación, no se pudo determinar de manera concluyente el impacto exacto de este factor en las emisiones de COVB. En general, la investigación señaló la compleja interacción de los factores ambientales y de la biología vegetal en las emisiones totales medidas en el marco de la AU.

Aplicación múltiple de técnicas de muestreo de volátiles para el estudio de las emisiones de COVB

Para la recolección y el análisis de las emisiones de las plantas se llevaron a cabo múltiples técnicas, siguiendo la literatura de referencia y los protocolos establecidos. Inicialmente, en un estudio preliminar, se probaron enfoques de muestreo abierto (sin cámara), semiabierto (cámara abierta) y cerrado (cámara cerrada), combinando recolección activa y pasiva para tiempos de muestreo cortos o largos. A partir de los resultados obtenidos, las medidas principales se realizaron mediante muestreo activo en una cámara estática adaptada al tamaño de la especie vegetal investigada. La eficiencia de este método se evaluó en función de la fiabilidad de las emisiones medidas, determinada por la precisión y exactitud de los resultados analíticos, los cuales fueron validados consistentemente durante todo el proceso de toma de muestra. Además, toda la metodología se evaluó frente a un método alternativo utilizando un material absorbente (Tenax en lugar de carbón activado) y una técnica analítica (extracción térmica en lugar de líquida) diferentes. Los resultados coherentes entre los dos enfoques no sólo corroboraron los resultados de la investigación obtenidos con la metodología principal, sino que también pusieron de relieve los avances técnicos pertinentes para la aplicación del muestreo de COVB.

Exploraciones futuras

En primer lugar, en relación con la Agricultura en Ambiente Controlado (ACE), la investigación de otras especies y/o variedades de plantas bajo regímenes de cultivo estándar y específicos,

incluidos fertilizantes alternativos recuperados del ambiente urbano, podría integrar el conocimiento adquirido en este estudio sobre aspectos cualitativos y cuantitativos de las emisiones de COVBs. Esto también incluye la aplicación de otras combinaciones de luz, CO_2, temperatura y humedad relativa. En segundo lugar, en términos de metodología de muestreo, se recomendó la exploración de materiales absorbentes alternativos, como Carbopack y la microextracción en fase sólida (SPME), para mejorar la eficiencia y la viabilidad de los procesos de muestreo y análisis. Estas mejoras técnicas podrían ampliar el alcance de la investigación de COVB para abarcar varios entornos interiores más allá de la UA, contribuyendo así a una comprensión más profunda de la evaluación de la calidad del aire. Además, la exploración de los derivados de la actividad troposférica entre COVBs-ozono podría mejorar la comprensión de la dinámica ambiental de los COVBs en relación con la calidad del aire. Por último, cambiar la perspectiva del estudio sobre los efectos positivos asociados a los COVB, como su actividad bioestimulante y sus potenciales efectos relajantes, tanto en el sistema vegetal como en el bienestar humano, podría ser muy prometedor para el desarrollo agronómico y la expansión de la AU integrada en edificios y de interior en la ciudad.

Resum

Reconeguda pel seu potencial per fomentar ciutats resilients i sostenibles, l'Agricultura Urbana (AU) cerca garantir un subministrament d'aliments segur i assolible alhora que generi diversos beneficis en els àmbits ambiental, econòmic i social. Hi ha diverses aplicacions d'AU, incloses tipologies interiors, exteriors i mixtes, amb instal·lacions que van des de configuracions tradicionals a nivell del terra fins a hivernacles integrats en terrats (iRTG) i granges verticals (VF). Aquestes instal·lacions es consideren part de les estratègies verdes encaminades a millorar la qualitat de l'aire, reduir les emissions de carboni, crear oportunitats d'ocupació i promoure avenços tecnològics als sistemes de producció. Tot i els múltiples beneficis reportats, la seva implementació enfronta desafiaments, particularment pel que fa a la salut i la seguretat ambiental. Qüestions com la qualitat de l'aire, la contaminació i els marcs reguladors sovint obstaculitzen les iniciatives d'AU, fet que requereix la participació d'autoritats locals i el desenvolupament de polítiques i regulacions apropiades. Pel que fa a la qualitat de l'aire, l'acumulació de contaminació interior és un tema de debat freqüent pels riscos reconeguts i associats per a la salut. Entre els contaminants d'interior, els compostos orgànics volàtils (COV) solen encapçalar les llistes oficials a causa de les múltiples fonts i l'emissió sostinguda. A més de les causes antropogèniques, també els organismes vius emeten COV, més coneguts com a biogènics (COVB). Es coneix que les plantes són grans emissores de COVB, la reactivitat troposfèrica del qual pot afectar en gran mesura la qualitat de l'aire de diferents entorns. Tot i això, la influència de factors externs sol provocar fluctuacions en les emissions de les plantes, la qual cosa dificulta la predicció exacta del veritable impacte dels COVB. Amb l'expansió de les instal·lacions d'AU d'interior, s'espera que augmentin les emissions globals de COVB a les zones urbanes. Tot i la limitada investigació sobre aquest tema fins ara, els estudis existents han evidenciat els efectes tant positius com negatius de les emissions de COVB. Per tant, és essencial monitoritzar aquestes emissions per comprendre millor les implicacions en la qualitat de l'aire i la salut humana, especialment en el context dels sistemes d'AU. Aquesta acció s'ha dut a terme mitjançant múltiples avaluacions realitzades específicament en un sistema integrat a un edifici, iRTG, i d'interior, VF, amb espècies vegetals àmpliament cultivades, com la mongeta tendra, el tomàquet i l'alfàbrega. Aquesta tesi pretén definir la seguretat dels sistemes investigats basant-se en les emissions de COVB mesures, abordant les qüestions següents:

P.1 Quins són els nivells reals d'emissió de COVB als entorns d'AU considerats i quins compostos volàtils s'acumulen més?

P.2 Els nivells d'emissions de COVB mesurats estan dins del rang de seguretat fixat pels marcs oficials i/o les bases de dades més actualitzades?

P.3 Quins són els factors implicats en les emissions finals de COVB als entorns d'AU considerats?

P.4 Segons la investigació general, els entorns d'AU generen condicions insegures per a la salut humana? I en cas afirmatiu, com es podria contenir i/o prevenir l'acumulació de COVB?

El desenvolupament d'aquesta investigació va seguir un enfocament metodològic que consta de 5 seccions principals, la configuració del mostreig, la recol·lecció d'emissions a camp, la configuració posterior al mostreig, l'anàlisi de dades i la validació dels resultats. Aquests passos van implicar la utilització d'eines i protocols específics, com ara càmeres per a la recol·lecció de COVBs, així com reactius químics i instruments analítics per a la determinació qualitativa i quantitativa dels COVBs. A més, es van utilitzar llistes de taules oficials i fulls informatius com a pautes de límits de referència.

Els resultats obtinguts de la investigació es poden resumir en els 4 apartats següents.

Tendències qualitatives i quantitatives d'emissions de COVB dins de sistemes d'AU

La investigació va estudiar els nivells ambientals i els perfils d'emissió de COVB de diferents plantes crescudes en sistemes de cultiu protegits a l'AU. De mitjana, els nivells de COVBs es van situar dins del rang de parts per bilió (ppb) en tots dos entorns considerats, amb nivells màxims observats típicament durant la fase de creixement inicial i disminuint gradualment al llarg del cicle de cultiu. Tot i això, les excepcions a aquesta tendència es van atribuir principalment a condicions ambientals específiques. En un iRTG, es van observar tendències d'emissions similars per a les plantes de mongetes i tomàquets, en què els monoterpens van prevaldre al principi del cicle, seguits pels derivats de la lipoxigenasa i els monoterpens oxigenats. Els sesquiterpens i els fenilpropanoides van ser menys comuns o amb prou feines es van detectar. En un VF d'interior, els patrons d'emissió van variar segons el tractament lumínic aplicat a les plantes. Sota els espectres de llum blava, es van observar altes emissions de diversos COVBs al principi del cultiu, mentre que sota llum vermella, les emissions més altes es van detectar més tard, encara que menys variades. En general, els monoterpens oxigenats van ser els més abundants, seguits pels derivats de la lipoxigenasa, els sesquiterpens, els monoterpens i els fenilpropanoides. Curiosament, per a la mateixa espècie cultivada (alfàbrega), les tendències d'emissió van diferir entre els entorns iRTG i VF.

Compliment dels nivells de risc de seguretat de les emissions de COVB produïdes per l'AU

La determinació de seguretat a cada ambient d'AU es va basar en les concentracions de COVB mesurades. Els seus nivells generalment es van comparar amb els límits oficials en interior establerts per l'Acció Col·laborativa Europea (ECA), designats com a Concentracions d'Interès Inferiors (LCI) o, si no, amb fitxes tècniques específiques del compost considerat redactades per l'Agència Europea de Substàncies Químiques (FET). Fins ara, només s'han proporcionat unes quantes LCI per als COVB. Per tant, es van comparar diversos COVBs amb el mateix LCI en funció de la classe volàtil. Cap dels COVBs va superar els llindars establerts. Les emissions mitjanes mesurades van ser considerablement inferiors a les dels LCI de referència, sovint en almenys un ordre de magnitud. Tot i això, es van identificar pics aïllats al llarg del mostreig, com el cas de les emissions d'aldehids detectades tant en espais integrats i d'interior, avaluades davant del LCI del 2-hexenal (7 μg m-3). Aquestes emissions no es van considerar rellevants per a la salut degut a la seva escassa presència i durada al llarg del cicle de cultiu. Es van observar altres pics d'emissió dels volàtils β-cariofilè, trans-β-farnesè i 1,8-cineol a la VF. Segons les relatives fitxes tècniques, es van considerar improbables els efectes adversos per a la salut en relació amb les concentracions mesurades. En termes generals, en tots dos entorns, es va determinar més probable l'ocurrència d'una sensibilització lleu-moderada (ex., irritació localitzada) en resposta als nivells excepcionalment elevats, segons la sensibilitat individual. Aquesta hipòtesi es va veure recolzada per una avaluació comparativa realitzada al final de la investigació, que va revelar una exposició a les emissions evidentment més gran en els ambients interiors comuns no relacionats amb les plantes en comparació dels espais d'AU.3. Sensibilitat de les emissions de COVB a factors externs associats al medi ambient i al mètode de mostreig.

Sensibilitat de les emissions de COVB a factors externs associats al medi ambient i al mètode de mostreig

Les troballes de la investigació van ressaltar l'impacte multifacètic de diversos factors sobre les emissions de COVB en entorns integrats o d'interior d'AU. El tancament estàtic mantingut durant la presa de mostres va demostrar que paràmetres ambientals com ara la temperatura i la humitat relativa poden reduir significativament les emissions de les plantes. A més, variacions en la concentració de CO2, particularment la reducció, es van veure interferir amb la normal activitat d'emissió, encara que la seva implicació en concentracions normals (iRTG) i superiors (VF) no va ser aclarida. Es va trobar que els ajustaments d'il·luminació, especialment a la VF, tenen un paper crucial a l'hora d'influir en les respostes volàtil de les plantes. A més, a l'iRTG, es va atribuir un impacte irrellevant a la radiació a causa de la forta filtració exercida per la façana circumdant. Per contra, es va plantejar la hipòtesi que la il·luminació artificial al VF influís en la composició i la concentració de les emissions, encara que aquesta suposició no va ser corroborada a causa de

les escasses correlacions observades entre les emissions i els diferents espectres de llum aplicats. El desenvolupament morfològic de les plantes va ser identificat com a següent factor influent en les emissions de COVB en ambdós entorns investigats. Es van observar variacions qualitatives i quantitatives en diferents etapes del creixement de les plantes. Tot i això, a causa de la manca de diferències morfològiques significatives entre les etapes i d'altres elements d'avaluació, no es va poder determinar de manera concloent l'impacte exacte d'aquest factor a les emissions de COVB. En general, la investigació va assenyalar la complexa interacció dels factors ambientals i de la biologia vegetal a les emissions totals mesurades en el marc de l'AU.

Aplicació múltiple de tècniques de mostreig de volàtils per a l'estudi de les emissions de COVB

Per a la recol·lecció i anàlisi de les emissions de les plantes es van dur a terme múltiples tècniques, seguint la literatura de referència i els protocols establerts. Inicialment, en un estudi preliminar, es van provar enfocaments de mostreig obert (sense càmera), semiobert (càmera oberta) i tancat (càmera tancada), combinant recol·lecció activa i passiva per a temps de mostreig curts o llargs. A partir dels resultats obtinguts, les mesures principals es van fer mitjançant mostreig actiu en una cambra estàtica adaptada a la mida de l'espècie vegetal investigada. L'eficiència d'aquest mètode es va avaluar en funció de la fiabilitat de les emissions mesurades, determinada per la precisió i l'exactitud dels resultats analítics, els quals van ser validats consistentment durant tot el procés de presa de mostra. A més, tota la metodologia es va avaluar davant d'un mètode alternatiu utilitzant un material absorbent (Tenax en lloc de carbó activat) i una tècnica analítica (extracció tèrmica en lloc de líquida) diferents. Els resultats coherents entre els dos enfocaments no només van corroborar els resultats de la investigació obtinguts amb la metodologia principal, sinó que també van posar en relleu els avenços tècnics pertinents per a l'aplicació del mostreig de COVB.

Exploracions futures

En primer lloc, en relació amb l'Agricultura en Ambient Controlat (ACE), la investigació d'altres espècies i/o varietats de plantes sota règims de cultiu estàndard i específics, inclosos els fertilitzants alternatius recuperats de l'ambient urbà, podria integrar el coneixement adquirit en aquest estudi sobre aspectes qualitatius i quantitatius de les emissions de COVBs. Això també inclou l'aplicació daltres combinacions de llum, CO_2, temperatura i humitat relativa. En segon lloc, en termes de metodologia de mostreig, es va recomanar l'exploració de materials absorbents alternatius, com ara Carbopack i la microextracció en fase sòlida (SPME), per millorar l'eficiència i la viabilitat dels processos de mostreig i anàlisi. Aquestes millores tècniques podrien ampliar l'abast de la investigació de COVB per abastar diversos entorns interiors més enllà de la UA i contribuir així a una comprensió més profunda de l'avaluació de la qualitat de l'aire. A més,

l'exploració dels derivats de l'activitat troposfèrica entre COVB-ozó podria millorar la comprensió de la dinàmica ambiental dels COVB en relació amb la qualitat de l'aire. Finalment, canviar la perspectiva de l'estudi sobre els efectes positius associats als COVB, com la seva activitat bioestimulant i els seus potencials efectes relaxants, tant al sistema vegetal com al benestar humà, podria ser molt prometedor per al desenvolupament agronòmic i l'expansió de l'AU integrada a edificis i d'interior a la ciutat.

Preface

The dissertation offers a glimpse into the dissemination of the research through scientific publications and oral presentations at relevant congresses. It is followed by a description of the activities undertaken during the PhD program to advance the professional career, which includes cotutelle assignments, collaboration on projects, participation in training courses, and a research stay:

Research dissemination

Professional career development

The research content has been structured into five parts including the Annexes.

The first part includes a comprehensive introduction about the research subject followed by the postulated questions and objectives, and a detailed chapter dedicated to the materials and methods used for the development of the research.

PART I: Introduction, research hypothesis, questions, and objectives, materials & methods

- Chapter 1: Introduction
- Chapter 2: Research hypothesis, questions, and objectives
- Chapter 3: Materials & Methods

The second part gathered four chapters reporting the experimental assessments on BVOC emissions that were conducted in the two case studies considered, representing the building-integrated and the indoor setting of UA. Respectively, chapters 4, 5, and 6 report the assessments carried out in an iRTG (=building-integrated), whereas chapter 7 describes an assessment performed in an independent VF (=indoor). Each chapter follows the format of a scientific publication, structured into introduction, materials and methods, results, discussion, and conclusion sections. Chapters 4, 5, and 6 have been published in open access in relevant impact journals. Each chapter presents independent experiments with specific objectives and methodologies aligned with the general ones described in Part I.

PART II: BVOCs Field measurement

- Chapter 4: Potential volatile organic compounds emission in indoor urban farming: a case study
- Chapter 5: Assessment of greenhouse emissions of the green bean through the static enclosure technique

- Chapter 6: Measuring BVOC emissions released by tomato plants grown in a soilless integrated rooftop greenhouse
- Chapter 7: Biogenic volatile organic compounds emitted by basil grown in a vertical farm under two different red:blue LED ratios

The third part comprises a single chapter divided into two interconnected sections. The first section validates the results obtained from the field collections described in part two by comparing them with qualitative and quantitative outcomes derived from an alternative methodology using different sorbent tools and analytical techniques. In the second section, a comparative multi-site assessment presents preliminary findings on BVOCs exposure between common indoor spaces and UA environments.

PART III: Evaluation of field collection results and further relevant insights

- Chapter 8: Research methodology assessment and additional relevant BVOC emission findings

In the fourth part, the research outputs are discussed in accordance with the preconditions outlined in chapter 2. This is followed by the conclusions drawn from the study and proposals for further investigations. Altogether:

PART IV: Discussion of the research outcomes, general conclusions, further investigation

- Chapter 9: Discussion of the research outcomes
- Chapter 10: General conclusions
- Chapter 11: Further investigation

The last section (part V) comprises three annex sections. Annex I provide detailed information regarding the methodological approach of the research, encompassing the sampling and post sampling procedures. Annex II wrapped up main BVOC emission results in addition to those reported in the individual assessment. Finally, Annex III contains supporting information for the understanding of all chapters reported in part two.

PART V: Annexes

- Annex I: Elements of the experimental methodology for practical BVOC emissions measurement and analysis
- Annex II: Summary of complete BVOC emissions and Emission Factors
- Annex III: Supplementary Information

Research dissemination

Collaboration as co-author in the scientific publications included in the PhD thesis

* Potential volatile organic compounds emission in indoor urban farming: a case study. **Gaia Stringari**, Nuria Moraleda-Cibrián, Antoni Rosell, Joan Rieradevall, Francesco Orsini, Xavier Gabarrell; (2022) ISHS Acta Horticulturae, 1356. DOI: 10.17660/ActaHortic.2022.1356.17.
* Assessment of greenhouse emissions of the green bean through the static enclosure technique. **Gaia Stringari**, Joan Villanueva, Antoni Rosell-Melé, Nuria Moraleda-Cibrián, Francesco Orsini, Gara Villalba, Xavier Gabarrell; (2023) Science of the Total Environment, 874. DOI: 10.1016/j.scitotenv.2023.162319.
* Measuring BVOC emissions released by tomato plants grown in a soilless integrated rooftop greenhouse. **Gaia Stringari**, Joan Villanueva, Elisa Appolloni, Francesco Orsini, Gara Villalba, Xavier Gabarrell Durany; (2023) Heliyon (CellPress), 10. DOI: 10.1016/j.heliyon.2023.e23854.

Collaboration as co-author in other scientific publications during the PhD thesis

* Extended use and optimization of struvite in hydroponic cultivation systems. Verónica Arcas-Pilz, Felipe Parada, Martí Rufí-Salis, **Gaia Stringari**, Ramiro González, Gara Villalba, Xavier Gabarrell; (2022) Resources, Conservation and Recycling, 179. DOI: 10.1016/j.resconrec.2021.106130.
* Supplemental LED Lighting Improves Fruit Growth and Yield of Tomato Grown under the Sub-Optimal Lighting Condition of a Building Integrated Rooftop Greenhouse (i-RTG). Elisa Appolloni, Ivan Paucek, Giuseppina Pennisi, **Gaia Stringari**, Xavier Gabarrell, Francesco Orsini, Giorgio Gianquinto; (2022) Horticulturae, 771. DOI:10.3390/horticulturae8090771.
* Preliminary results on N_2O emission factor calculation in hydroponic struvite fertilization of lettuce production. Veronica Arcas-Pilz, **Gaia Stringari**, Ramiro González, Gara Villalba, Xavier Gabarrell; (2022) ISHS Acta Horticulturae, 1356. DOI: 10.17660/ActaHortic.2022.1356.36.

Attendance at Conferences, Congresses, and Symposia

* **XI Scandinavian Plant Physiology Society (SPPS) PhD Student conference organized by the Turku University, from the 2nd to the 4th of September 2020.**

Oral presentation: Potential volatile organic compounds emission in indoor urban farming: impact assessment in building integrated-Rooftop Greenhouses (i-RTG). Stringari G., Rosell-Melé A., Rieradevall-Pons J., Orsini F., Gabarrell X.

* **I ICTA-UAB Winter Symposium conference from the 15th to the 16th of December 2020.**

Oral presentation: Emission Factors from Urban Food Systems in a Circular City. Stringari G., Gabarrell X., Orsini F.

* **XV Congreso Nacional del Medio Ambiente (CONAMA) organized by the CONAMA Fundation, from the 31st of May to the 3rd of June 2021.**

Poster: FoodE Food Systems in European Cities. **Stringari G.**, Tonini P., Orsini F., Odina Muñoz P., Atero Gonzalez R.

* **XXXI International Horticultural Congress (IHC) from the 14th the 20th of August 2022.**

Oral presentation: Potential volatile organic compounds emission in indoor urban farming: a case study. **Stringari G.**, Moraleda-Cibrián N., Rosell-Melé A., Rieradevall-Pons J., Orsini F., Gabarrell X.

* **XV Mediterranean Congress of Chemical Engineering (MeCCE) from 30th of May to 1st of June 2023.**

Oral presentation: Timeline of the development of a reproducible and easy methodology for volatile emissions assessment in the framework of urban agriculture. **Stringari G.**, Villanueva J., Orsini F., Villalba G., Gabarrell X.

* **III ICTA-UAB Winter Symposium conference 14th of December 2023.**

Oral presentation: Reconsidering the Impact of Plant Emissions on Indoor Air Quality: Did We Underestimate the Surrounding Environment? **Stringari G.**, Gabarrell X., Orsini F.

* **3rd International Workshop on Vertical Farming from the 16th to the 19th of January 2024.**

Poster presentation: Measuring indoor emissions in vertical farm under different LED lighting. **Stringari G.**, Villanueva J., Carotti L., Zauli I., D'Aprile A., Pistillo A., Pennisi G., Orsini G., Gabarrell X.

Professional career development

Cotutelle

This doctoral thesis has been led under the international joint supervision of the Universitat Autònoma de Barcelona (UAB) within the Environmental Sciences and Technology PhD program and the Alma Mater Research Institute on Global Challenges and Climate Change - Alma Climate (University of Bologna) within the 36th cycle of the PhD program Future Earth, Climate Change and Societal Challenges (Frontiers).

Collaboration in projects

- (2020-2024) **FoodE** (EU Horizon2020) funded by the European Research Council [862663]. The main scope of the project is the involvement of European Union local initiatives in the design, implementation, and monitoring of environmentally, economically, and socially sustainable City/Region Food Systems, promoting job creation, local economy, and communities in complying with Sustainable Development Goals, identifying, and strengthening the relations between the different actors of the food chain.
- (2021-2022) **Pandemies** funded by Generalitat de Catalunya AGAUR 2020PANDE00021. This project aims at making the cities resilient, sustainable, and healthier in the framework of the COVID-19 pandemia and future ones, by supporting local indoor agriculture, recycling activities such as domestic and community composting in buildings and schools, and waste reduction through the analysis of the emissions produced and of the environmental impact along different levels of the municipality.
- (2022-2025) **MOVE4EDU** (MCIN/AEI/10.13039/501100011033/FEDER) funded by the Spanish Ministry of Economy, Industry and Competitiveness [PID2021-126845OB-C21]. The aim of the project is to develop and implement a natural modular ventilation solution that is adaptable, ensures indoor air quality, increases building sustainability, and introduces circular economy principles in the operation of buildings.
- (2022-2024) **BINAFET** (MCIN/AEI/10.13039/501100011033/) funded by the Spanish Ministry of Economy, Industry and Competitiveness [TED2021-130047B-C21]. The aim of the project is to advance in the design of a strategy for the integration of resource flows (CO_2, energy, and nutrient exchanges) between buildings and urban agriculture to demonstrate the viability and scalability of new smart solutions for building-integrated agriculture.

Internship supervision & coordination

- Merce Marinello Rosell (2020-2021) – professional training Institut 'La Romanica' (440 hours)
- Marta Gonzalez Sedano (2021) – professional training Institut 'La Romanica' (440 hours)
- Ismael Jurado Medina (2021-2022) – professional training (Dual) 'Institut Terrassa - INS'
- Paula Meseguer Prat (2021) – professional training bachelor of Biosciences UAB (280 hours)
- Miquel Vallejo (2021-2022) – professional training 'Institut Terrassa - INS' (416 hours)
- Joan Vázquez Dueñas (2022-2023) – professional training 'Institut Terrassa - INS' (416 hours)
- Izan Córcoles Rodriguez (2023) – professional training 'Institut Terrassa - INS' (416 hours)
- Jan de Rueda Sánchez (2022-2023) – professional training 'Institut Terrassa - INS' (416 hours)

Courses and Certifications

- Online course on chemical risk prevention in laboratories, Egarsat (03/2020)
- Online course on digital skills, module 3-4-6 (word, access and excel) and use of data display screens, UAB Escola de Doctorat (03/2020)
- Basic level for Phytosanitary product handling and application, ESCOLA AGRÀRIA DE MAS BOVÉ (05/2020)
- Basic course on life cycle assessment digital edition, Rete LCA Italiana (09/2020)
- First (Theme A, B and C) and second (specialized Theme C) term courses of cotutelle PhD Frontiers (36 cycle) (Theme A, B and C), UNIBO (11/2020-02/2021)
- Online course on Thesis Writing in English (Science), UAB Escola de Doctorat (11/2020)
- FoodE Winter school, UNIBO (02/2021)
- Basic course of statistic on design and data analysis with R studio, ICTA-UAB (03/2021)
- Online course on HPC and Big Data, CINECA (04/2021)
- Online course on how to write a scientific paper, VPH Institute (06/2021)
- Certificacio tutoria d'empresa en la formació professional dual (08/2022)

Research Stay

3 months (June-September 2022) of research stay at the DISTAL-UNIBO for the realization of the experimental work in the *AlmaVFarm* under the supervision of Francesco Orsini.

PART I

Introduction

Research hypothesis, questions, and objectives

Materials & Methods

Chapter 1

Introduction

Chapter 1: Introduction

1.1 Urban Agriculture meaning in the current century

The way cities are growing and affecting the environment, along with the increasing problems of climate change and health issues for people worldwide, highlighted the importance of timely actions (IPCC, 2022). In the last years Urban Agriculture (UA) has been recommended to seek more resilient and sustainable cities to face current issues (Langemeyer et al., 2021; Rao et al., 2022). UA concurrently engages the environmental, economic, and societal sectors to attain a reliable and fresh food supply, thereby generating benefits within each of these domains (Puppim de Oliveira et al., 2022; Rao et al., 2022). For instance, by simply regreening urban environments, air quality (Ysebaert et al., 2021; Saeed Meo and Karim, 2022) and buildings environmental performance (Li et al., 2022; Oquendo-Di Cosola et al., 2022) can improve significantly. By supporting local food ventures, carbon emissions associated with land exploitation and long-distance transportation can be reduced (LLorach Massana, 2017; Saeed Meo and Karim, 2022). Moreover, UA promotes the creation of new markets, job opportunities and entrepreneurs (Cirone et al., 2023; Wiśniewska-Paluszak et al., 2023), and supports the technological development related to the production systems (Q. Yang et al., 2023). For instance, the implementation of techniques like hydroponics and aquaponics for urban farming allows a much more efficient use of space and resources (Rufí-Salís et al., 2020; Engler and Krarti, 2021) enabling year-round and safe production (Magwaza et al., 2020; Gumisiriza et al., 2022). In this context, the role of citizens is a key factor for the expansion of UA, promoting both adults and young generations awareness about food systems, agriculture, and the environment (Colston et al., 2015; Kutralam-Muniasamy et al., 2023; Simon, 2023). This also has an impact on health and dietary concerns, as UA helps people access nutritious, freshly grown fruits, vegetables, and herbs, leading to improved overall well-being (Pradhan et al., 2023). However, the implementation of UA is often hindered by multiple factors (Orsini et al., 2020), especially when topics concerning human health and environmental safety are involved (Domingo and Nadal, 2009; Buscaroli et al., 2021). This normally implies the intervention of local authorities requiring addressed policies and regulations (Fox-Kämper et al., 2023).

1.1.1 Applications of Urban Agriculture

UA can be applied in the city under different typologies, indoor, outdoor, and mixed ones, on traditional ground level or lifted, as for rooftops and terraces, on soil or soilless conditions (Appolloni et al., 2021; HUI et al., 2022; Toboso-Chavero et al., 2023). Systems integrated to the buildings became fashionable as they optimize space utilization in densely populated areas and

may adapt to the complexity of the urban centers (D'Ostuni et al., 2022). These comprise simple but also structured installations open-air and semi-closed or closed, Controlled-Environment Agriculture (CEA), based on the greenhouse technology, including respectively integrated Rooftop Greenhouses (iRTGs) (Sanyé-Mengual et al., 2018) and Vertical Farms (VFs) (Benke and Tomkins, 2017). Both can be integrated into different kinds of urban buildings and operated autonomously, although an iRTG and the hosting edifice are generally bound under a symbiotic relationship (Muñoz-Liesa et al., 2020). With respect to the last one, the iRTG of the Institut de Ciència i Tecnologia Ambientals of the Universitat Autònoma de Barcelona (ICTA-UAB) represents an excellent example for the Mediterranean area (Sanyé-Mengual et al., 2014; Pons et al., 2015; Montero et al., 2017; Sanjuan-Delmás et al., 2018). The architectural design of the building, indeed, ensures a sustainable and efficient utilization of available resources such as water, sunlight, and natural ventilation (Rufí-Salís et al., 2020; Parada et al., 2021), establishing a natural heating, ventilation, and air conditioning (HVAC) system throughout the different floors (Zambrano et al., 2021; Muñoz-Liesa et al., 2022).

Instead, vertical farming not only improves space and energy efficiency (Kobayashi et al., 2022; Martin et al., 2022), but also constitutes an innovative market sector for the indoor cultivation (Gumisiriza et al., 2022; Shao et al., 2022). Plants are grown under controlled conditions (Benke & Tomkins, 2017b; Naranjani et al., 2022), regardless of external factors, and using automated systems (Delorme and Santini, 2022; Popkova, 2022), ensuring continuous production and high yields, with automated management. More specifically, climatic (temperature, humidity, CO_2, and ventilation), feeding (fertigation) and light (artificial lightning) parameters can be set according to the requirements of the crop and adjusted over the cycle (Wada et al., 2019; Weidner et al., 2021; Wang and Iddio, 2022). Additionally, the introduction of Light-Emitting Diode (LED) technology allows for both a more efficient use of the energy (F. Orsini et al., 2020; Wong et al., 2020a; Avgoustaki and Xydis, 2021), and to specifically affect certain quality traits and secondary metabolites, relevant for the nutritional profile of the production (Nicole et al., 2019; Hammock et al., 2021; Veremeichik et al., 2023). An exemplary Vertical Farm (VF) is the Italian AlmaVFarm of the Department of Agricultural and Food Sciences (DISTAL) of the University of Bologna (UNIBO), a closed system organized in stacked shelves dedicated to the soilless cultivation (hydro and aeroponics) under artificial lightning (LED), and optimal conditions (Carotti et al., 2023). Here, the cultivation of short cycle crops, such as, lettuce, basil, and microgreens, is studied and the best light settings are identified (Pennisi et al., 2020; Pistillo et al., 2022; Zauli et al., 2022).

1.2 Accumulation of indoor pollutants in the urban settings

The proper arrangement of interior spaces within urban buildings is essential for creating secure environments. From this perspective, the design of HVAC systems is becoming important also to improve building's sustainability and efficiency (Syed and Hachem, 2019; Mehdizadeh Khorrami et al., 2023). Similarly, the implementation of these solutions to building's integrated greenhouses can significantly increase their environmental performance and the indoor quality (Muñoz-Liesa et al., 2022). In addition to thermal considerations, indoor environmental quality also relies on air conditions. In enclosed spaces, frequent high contamination levels have direct health consequences, which is why they are regarded as a primary concern (Prabhakaran et al., 2022). Among most common pollutants are reported airborne ones, like the Volatile Organic Compounds (VOCs), PMs, N_2O, and combustion derivatives, such as CO, CO_2, NO_x, and SO_x, (IARC, 2016) deriving from the outdoor but also from indoor materials (Baek et al., 1997; ECA, 1997a; Xu et al., 2016). Even relatively sustainable materials, like wood, can represent a source of indoor pollution, substantially VOCs (Y. Yang et al., 2023). All these have been also reported in indoor farming systems, from traditional greenhouses (EFSA, 2014) to modern iRTGs (Tong et al., 2016) and occasionally VFs (Shao et al., 2021a). In common greenhouse as well as in an iRTG, biological and dust contaminants have been documented, in the specific, fungal spores and bacteria (Madsen et al., 2013; Ercilla-Montserrat et al., 2017), and toxic particles derived from chemicals application (Wang et al., 2009; Caballero-Casero and Rubio, 2022). In addition, the same plants cultivated indoor have been noticed to affect air quality due to the irregular emission of Biogenic VOCs (BVOCs) (Burge et al., 1982; Yang et al., 2009a; Tiwari et al., 2019).

1.3 BVOCs: definitions, sources, and ecosystem interactions

BVOCs, much like general VOCs, are characterized as low-weight organic molecules with high vapor pressure. They are categorized as semi-volatile, volatile, or very volatile, depending on the boiling point of the respective molecules (ECA, 1997b). Their primary sources are the living organisms, basically plants, animals, and human beings, though vegetation represents the main producer and emitter into the environment (Seco et al., 2007; Mohd Hanif et al., 2021; Duan et al., 2023), releasing almost the totality of global VOCs annually (Fisch, 2004; Guenther et al., 2006; Duhl et al., 2008). In terms of the chemical structure BVOCs comprise a wide range of classes, having different or common biosynthetic pathways and activity on the ecological system (Herrmann, 2010; Dudareva et al., 2013; Picazo-Aragonés et al., 2020). At biological level, they constituted the plant-to-plant and plant-to-animal intercommunication, for the purpose of pest-defense, growth regulation and reproduction (Catola et al., 2018; Bouwmeester et al., 2019). At environmental level, especially isoprene-based ones, they essentially contribute to the

composition and the dynamic of the atmospheric chemistry at different scale levels, depending on the size of the emitting source (Herrmann, 2010; Cai et al., 2021; Mohd Hanif et al., 2021). BVOCs release is regulated not only by the internal plant metabolism but also by a bunch of external factors of variable nature, either biotic and abiotic ones, that affect significantly the final qualitative and quantitative emission response (Loreto et al., 2006; Loreto and Schnitzler, 2010; Niinemets et al., 2013; Chen et al., 2020)

1.3.1 Environmental implications of BVOCs

BVOCs study is originally associated with open field monitoring of the isoprene fluxes released by the vegetation continuously (Holzke et al., 2006; Sharkey and Monson, 2014; Seco et al., 2015; Malik et al., 2018), because of the relevant impact on the atmosphere (Karl et al., 2008; Laothawornkitkul et al., 2009; Calfapietra et al., 2013b; Hantson et al., 2017). Indeed, BVOCs instability at tropospheric level is documented (IPCC, 2022), and it is responsible of the formation of several radical species, namely, OH^-, NO_x, and RO_2, and secondary organic particles aerosols (SOAs). These in turn undergo cascade reactions increasing, the radicals, the population of greenhouse gases, such as, O_3, N_2O, CO_2, and CH_4, the SOAs, that of PMs that besides intrinsic detrimental effect on the health also perform a screening activity against the sunlight (Kulmala et al., 2013; Mahilang et al., 2021; Dodman et al., 2022). Most of these oxidative reactions occur right after BVOCs release because of atmospheric O_2, though others require certain conditions, as for the case of ozone and hydroxyl, carried on by temperature and UV radiation. BVOCs oxidation may occur even at nighttime leading to the formation of nitrogen oxide radicals (NO_3). The simultaneous occurrence of these reactions over the long-term impacts not only air quality but also various Earth systems due to the rise in global temperatures, thereby exacerbating climate change (Peñuelas and Staudt, 2010; Glotfelty et al., 2016; Nowak, 2019). Locally, they favor the accumulation of airborne pollutants, as observed in the urban area (Niinemets and Peñuelas, 2008; Churkina et al., 2017; Zhang et al., 2020; Coggon et al., 2021), especially inside the buildings (Tiwari et al., 2019; Prabhakaran et al., 2022), affecting the quality and the safety of indoor environments.

1.3.2 BVOC emissions management in indoor environments within the framework of human health

The regulation of indoor emissions on a global and European level is overseen by the United States Environmental Protection Agency (EPA), the collaborative efforts of the World Health Organization (WHO) and the International Agency for Research on Cancer (IARC), as well as the European Collaborative Action (ECA). These institutions periodically contribute with updated reports and publications, offering vital information and guidelines concerning various aspects

related to human health. As regards VOCs, there is a widespread consensus on their greatest indoor exposure due to people spending most of their lives inside buildings (residences, workplaces, and recreational spaces), coupled with their rapid accumulation. A significant portion of these compounds originates from outdoor sources, emitted by industrial activities, fossil fuel consumption, and transportation, with estimated emissions ranging from 27 to 34 Tg y^{-1} (IARC, 2016).Among these compounds, which are harmful to human health as they contribute to the formation of oxidant species with carcinogenic properties (e.g., DNA methylation and strand breaks), are aldehydes (e.g., formaldehyde), ketones, aromatics (e.g., benzene), and alkanes. Moreover, their photooxidative reactions with other anthropogenic pollutants like NO_x and SO_x, as well as with tropospheric ozone and organic particulate matter, enhance their reactivity and total residence time, exerting significant consequences on urban air quality.

Regarding the European environment, ECA drafted several reports for the management of indoor VOCs, from their definition and sources (Report no. 19, 1997b), their effects on human health (Report no. 10, 1991), until targeting strategies (*STRATEX*) to monitor and reduce their amount (Report no. 25 and 30, 2006, 2020), as well as detail guidelines for the assessment of the associated risk (Report no.22, 2000) and the determination of corresponding levels (Report no. 29, 2013). A comprehensive compilation documenting measured indoor levels was compiled by the EPA in the 90s (EPA, 1988). However, the limited accuracy of the measurements raises doubts about their reliability. Similarly, in Europe, the ECA conducted a comprehensive review of all available studies on indoor pollution, encompassing both its causes and effects. The findings were summarized in a comprehensive project inventory (Report no. 9, 1991a).

Considering BVOC emissions, none of the publications in force put much concern on the potential harm to human health. Only in ECA Report no. 26 (2007) they were treated separately, focusing on terpene compounds, as the most abundant in the total amount of indoor VOCs. However, only products based on concentrated BVOC mixtures, such as detergents, varnishes, and paints, were listed among main sources being widespread in these environments. Biological sources such as plants and humans were not considered in the Regulation. Among biogenic emitters, were mentioned the wooden materials, such as wooden floors and furniture. Following the Report highlights, main issues would be related to the terpene's reactivity, due to multiple double C=C bonds in the molecule, with indoor ozone leading to an increment of the air pollutants, namely radicals, such as OH^-, OH_2, and RO_2. This process is strongly affected by the amount of both these volatiles (sources), the air exchange rates, the environmental conditions (e.g., UV light penetration, humidity levels, etc.), and the physical state of the volatiles, which affects the chemical reaction pathway and therefore the total produced radicals. Considering

epidemiological studies conducted, insufficient data were referred for human exposure, since health effects were mainly measured in animal assays (mouse) and/or under short terms, and unrealistic exposure levels which would make difficult the risk assessment associated to both BVOCs and their mixture with ozone. Still, assumed referencing values are those provided by Report no. 29 (ECA, 2013), calculated on the concept of the Lower Concentration of Interest (LCI) that is the concentration at which an adverse effect on health is measured. However, only for few terpenes (α- and β-pinene, 3-carene, limonene and general hydrocarbons) these were determined. This open gap provided space for the active contribution of the scientific panel to update LCI tables. As stated in the Reports, official Regulations about the Registration, Evaluation, Authorisation and Restriction of Chemicals (REACH) should be followed in assessing the risk and the levels, providing detailed information about the exposure scenarios, the emission sources, and the performing conditions.

1.3.3 Official Methods for BVOCs assessment

The determination of BVOC emissions follows the procedures established for the assessment of indoor VOCs. This traditionally consisted in the collection of the volatiles through elective methods, namely, active, and passive sampling, followed by analytical screening carried out with chromatographic techniques. Sampling and post sampling methods have been comprehensively revised by the EPA under the Compendium Method TO-17 (1999), the Health and Safety Executive (HSE) and the WHO Methods (no 72, 1993 and no 96, 2002; 2020), and the ECA Reports, in the specific, no. 6, 14 and 19 (1989, 1994, 1997b). European guidelines, additionally, lean on dedicated ISO (International Organization Standards), 16017-1 (2000) and 16017-2 (2003) that are periodically revised, referring each to the active and the passive sampling including post sampling analysis. In both the cases sampling is the result of volatiles accumulation onto an adsorbent surface (=sorbent) contained in a stainless steel, glass or fused silica lined stainless steel tube. In the first, this is achieved by actively pumping air on the sorbent, whereas in the second air freely diffuses onto it. Indoor VOCs assessment can be carried out either directly within the environment or within a chosen volume, preferably with active pumping. This approach allows for improved control over sampling conditions and parameters. Further post sampling step includes destructive and non-destructive techniques, depending on the sorbent type, for the extraction and the preparation of the trapped material prior to its qualitative and quantitative analysis.

1.3.3.1 Active and passive sampling methods

Technical information related to these methods has been retrieved from ECA Reports no. 14, 16, and 18 (1994, 1995, 1997), WHO Publication (2020), EPA Compendium Method TO-17 (1999), and the Spanish National Institute of Safety and Health at Work (INSHT) NTP (Notas Técnicas de Prevención) no 151 (1983).

Active sampling, also referred to dynamic, consists in the use of a pumping system that pulls a volume of air through a sorbent tube. Sampling flow and duration are set depending on the properties of the sorbent material (density and size) and of the compounds to be trapped, as well as on the environmental concentration of these last. Usually short-term and low flow rate are recommended to increase sampling performance and avoid sample loss. Active sampling of BVOCs has been frequently implemented using a headspace system for qualitative and quantitative reason (Ortega and Helmig, 2008; Ortega et al., 2008; Soria et al., 2015; Tholl et al., 2021). This method follows the traditional one used for the assessment of VOC emissions from indoor materials and products (ECA, 1995) and its extended version (ECA, 1997) by means of small chambers where internal conditions can be easily controlled and properly corrected to minimize background noise and artifacts production in the total sampled volume. Sampling in the headspace may be carried out in static condition or under a continuous flow crossing in and out the system. In both cases volatiles concentration in the sampled air (*C*, µg m^{-3}) is expressed through a corresponding Emission Factor (*EF*, µg h^{-1} m^{-2}) that can be calculated with the simplified equations (1.1) and (1.2) determined by Li et al. (2019) for practical BVOCs assessment.

$$EF = \frac{C\ x\ (V + V_0) - C_0\ x\ V_0}{\Delta t\ x\ A} \quad (1.1)$$

$$EF = \frac{F\ x\ (C_{emission} - C_{blank})}{A} \quad (1.2)$$

In the case of (1), *EF* is the volatile amount (µg) in the sampled air by the time of sampling or enclosure time (Δt, h) and the emitting surface (*A*, m^2); the volatile amount is given by its concentration, *C*, that should be corrected on a background samples (C_0, µg m^{-3}), taken usually from the empty headspace, related each to the corresponding volume where sample is taken. Having the headspace, a fixed volume, both volume of scrubbed air purged into the headspace (*V*, m^3) and of the residual air in the headspace before air purging (V_0, m^3) are considered in the calculation. In the case of (2), *EF* is the volatile amount (µg) in the outlet air sampled by the

emitting surface *A*. Volatile amount is calculated from the relation (multiplication) between the volatile concentration of the emitting surface enclosed ($C_{emission}$, µg m^{-3}) corrected on that measured without the emitting surface (C_{blank}, µg m^{-3}) and the rate flow of scrubbed air purged crossing in and out the headspace (*F*, L h^{-1}).

Overall, the performance of this method may be time-consuming and complex with regards to the conservation of the sampling conditions during its realization, especially in a static headspace. The control of key parameters, such as, the humidity levels, the sampling length and flow rate, and the steady state concentration provides reliability and accuracy to the collected samples.

Passive sampling, also referred to diffusive, instead, does not require any power system since volatiles are collected by the time of the exposure to the air in the sorbent tube. Besides volatiles features, the total trapped amount rather depends on the surrounding ventilation, the sorbent position, the tube's section (diameter) and length, and the adsorbent surface. Altogether these factors affect the duration of the sampling that is usually longer (hours to weeks) with respect to the active method, increasing the sensitivity towards the volatiles present in the environment. In addition, the performance of this method entails less expertise and management, although the contemplation of the elements mentioned above is crucial.

This method allows the calculation of volatiles concentration (*C*, µg m^{-3}) in the indoor environment, as shown in the equation (1.3), that is the amount of the volatile (*m*, µg) accumulated in the sorbent along the exposure time (Δt, h) related to the volatile diffusive uptake rate (*Q*, ml h^{-1}). The determination of *Q* is based on the diffusion coefficient of the compound itself (m^2 h^{-1}) and on section area (m^2), and the longitudinal length (m) of the sorbent tube, to which the diffusion coefficient is respectively directly and inversely correlated.

$$C = \frac{m}{Q \; x \; \Delta t}$$

(1. 3)

In contrast to the active, the determination of an EF is less precise and accurate, due to the diffusive nature of the sampling method. In addition, factors such as ambient air temperature, wind speed, and other environmental conditions can influence the volatile uptake in the adsorbent surface. Thus, additional corrections or assumptions are generally required.

In the research field of BVOCs most frequently used sorbent materials are Tenax®, Carbotrap/pack™ and Anasorb®. Each consists of a variable percentage of a porous polymer, preconditioned, and adjusted to the polarity of the volatiles, the sampling, and the post-sampling conditions. An important parameter contemplated while performing both active and

passive sampling is the breakthrough volume (BV). The breakthrough occurs when the adsorbent bed is unable to retain the volatiles contained in the volume of air passing through the sorbent leading to loss and thus underestimation. The BV is determined in the back-up of the sorbent tube when more than 5% (or higher percentage) of the total amount of a compound detected in the front part is individuated. BV is affected by multiple factors, among which the environmental conditions and the volatile chemical affinity for the sorbent. However, it is more common during active sampling, associated with high pumping rates or saturation of the sorbent bed.

1.3.3.2 Post sampling: sample handling and analytical techniques for qualitative and quantitative determination

Technical information related to these methods has been retrieved from ECA Reports no. 14, 16, and (1994, 1995), WHO Publication (2020), EPA Compendium Method TO-17 (1999), HSE Methods for the Determination of Hazardous Substances (MDHS) no72 and 96 (1993, 2002), and the National Institute for Occupational Safety and Health (NIOSH) protocol no. 2549 (1995).

Depending on the sorbent type and the analytical technique, post sampling procedure consists in the extraction of the trapped compounds prior to the analysis. This can be achieved through destructive and non-destructive techniques, basically, liquid (solvent) extraction and thermal desorption. The choice of extraction is usually provided by the sorbent tube's manufacturer, following the reported features.

Destructive extraction involves the usage of target solvents where volatile analytes can elute. During this step the adsorbent material gets in direct contact with the solvent and therefore cannot be restored. On the contrary, non-destructive extraction implies the use of thermal energy, namely, temperature, to release retained volatiles from the sorbent while preserving the integrity and activity of the adsorbent material, which can be reconditioned and reused.

Liquid extraction is recommended for sorbents that are especially susceptible to elevated temperatures, such as activated charcoal that constitutes the Anasorb® tubes. This method provides a viable alternative to expensive desorbing machines or in incompatibility situations with available analysers. This procedure has been reported thoroughly by NIOSH in the protocols no. 2549 (1995) and no. 1552 (1996), addressing respectively VOCs and terpenes (BVOCs).

On the other hand, the thermal desorption technique is widely implemented, having on the destructive one multiple advantages. Among these, rapidity and automation, since right after desorption volatiles are transferred into the analyzer, reducing sample loss and artifacts occurrence connected to intermediate steps and solvent contact. In addition, sensitivity and

sample recovery can be increased adjusting the desorbing temperature, usually in the range of 200-350 °C, to the different boiling points of target volatiles.

Elective post sampling analytical technique is the Gas Chromatography (GC), although Liquid Chromatography (LC) is also utilized. In the GC the total extracted sample or a part of it is injected (in its liquid or gas form) and carried along a capillary column with specific polarity, thickness, length, and stationary phase, characteristics that altogether determines the separation of the different volatiles present in the mixture. Finally, a Mass Spectrometer (MS) or a Flame Ionization Detector (FID) coupled to the GC machine allows their identification and quantitation. In the case of an MS volatiles assessment is performed on specific m/z (mass-to-charge ratio) response of the constituting ions, while in the FID this is done on the electric response of the carbon ions derived from the molecule's combustion. In both cases, this response is returned as a signal expressed as abundance (number of ions) and voltage, in the MS and FID respectively, and represented as peaks with determined area, weight, and width, and a specific retention time (RT) in the Total Ion Chromatogram (TIC) separating the different compounds. In the MS peaks identification can be realized on their mass spectra with supporting datasets, like the National Institute of Standards and Technology (NIST) mass spectral library, or through external analytes (standards); in the FID peaks identity is achieved exclusively through external standards. Moreover, in the MS qualitative and quantitative assessment on the acquired TIC can be performed under full scan mode or targeting individual m/z under the Selected Ion Mode (SIM). For both, quantitation is achieved by interpolation with calibration curves built on standards injected at known amounts in the instrument. The two fundamental parameters for a reliable and reproducible analytical method are, respectively, accuracy and precision. Depending on the analytical technique, their evaluation follows fixed procedures and given limits. In general, accuracy is calculated on the recovery or extraction efficiency of the blanks (=no sample). Precision is calculated on the variation of repetitive injections of blanks (usually 5) under the working conditions. Following, Lowest Limit of Detection (LOD) and Lowest Limit of Quantitation (LOQ) should be determined. These represent the smallest measure (signal-to-noise ratio) that can be detected, for the first, and that can be quantified, for the second, among a calculated confidence level which can be determined with related equations, as the general (1.4):

$$LOD\ or\ LOQ = \frac{k\ x\ \sigma}{b}$$

(1. 4)

In the formula both parameters are reported as concentrations, where *k* is a factor of 3 and 10 times the instrument's noise level, for LOD and LOQ respectively, σ is the standard deviation of

multiple measures of the lowest concentration detected, and *b* the slope of the calibration curve. When building a calibration curve, the linear response of the machine should be assessed using multiple increasing concentrations (minimum 5) according to the expected concentrations in the samples. Further additional steps suggested for the validation of both the sampling and the analytical method involve the collection and analysis of replicate samples and (field and laboratory) blanks at the set conditions. Commonly acceptable error between replicate samples is $\leq$ 30%.

1.3.4 BVOCs assessments in micro-scale indoor environments

Currently, the study on BVOCs' impact on human health at micro-scale environments (room level) is limited to few conducted assessments. Literature is divided between the positive and negative effects attributed to plants or their derivative products indoors. Positive effects are supported by evidence related to human physiology and mood (Maffei et al., 2011; Song et al., 2016), as well as improvements in the air quality (Kim et al., 2011; Zorić et al., 2019). On the other hand, negative effects were initially hypothesized (Yang et al., 2009a), subsequently quantitatively assessed (Yamada et al., 2015; Wang et al., 2020), and more recent studies have even challenged previously claimed benefits (Cummings and Waring, 2020). Numerous traditional assessments were carried out using the headspace system, a recommended method that has been extensively documented (Tholl et al., 2006; Ortega and Helmig, 2008; Li et al., 2019) and consolidated in comprehensive reviews (Soria et al., 2015; Tholl et al., 2021). However, employing this method can potentially result in sampling errors and failures, which need to be thoroughly anticipated to prevent inaccurate estimations that could undermine overall reliability (Ortega and Helmig, 2008; Niinemets et al., 2011; Pérez-Priego et al., 2015). Using headspace coupled with dynamic sampling technique has also been commonly employed to evaluate plant emissions (Komenda et al., 2001; Ortega et al., 2008; Jansen et al., 2011; Takayama et al., 2012; Wang et al., 2019). Another noteworthy aspect emphasized by various studies is the influence of external elicitors that can significantly affect final emission sampled as compared to normal plant conditions. Indeed, BVOCs release can be particularly enhanced by increasing temperature (Owen et al., 2002; Pazouki et al., 2016; Chen et al., 2020) and light intensity (Velikova et al., 2009), drought (Copolovici et al., 2014; Tiiva et al., 2017; Fabbri et al., 2020), wounding associated to a mechanical injury (Copolovici et al., 2014; Cozzolino et al., 2016) or infectious disease (Quintana-Rodriguez et al., 2015; Kasal-Slavik et al., 2017; Catola et al., 2018), ozone (Llusi et al., 2002; Souza et al., 2013; Li et al., 2017) and CO_2 (Vuorinen et al., 2004; Daussy and Staudt, 2020; Copolovici et al., 2021) exposure, different light spectra (Pennisi et al., 2019; Lauria et al., 2023) and growth stage (Holzke et al., 2006; Fischer et al., 2011; Chen et al., 2020).

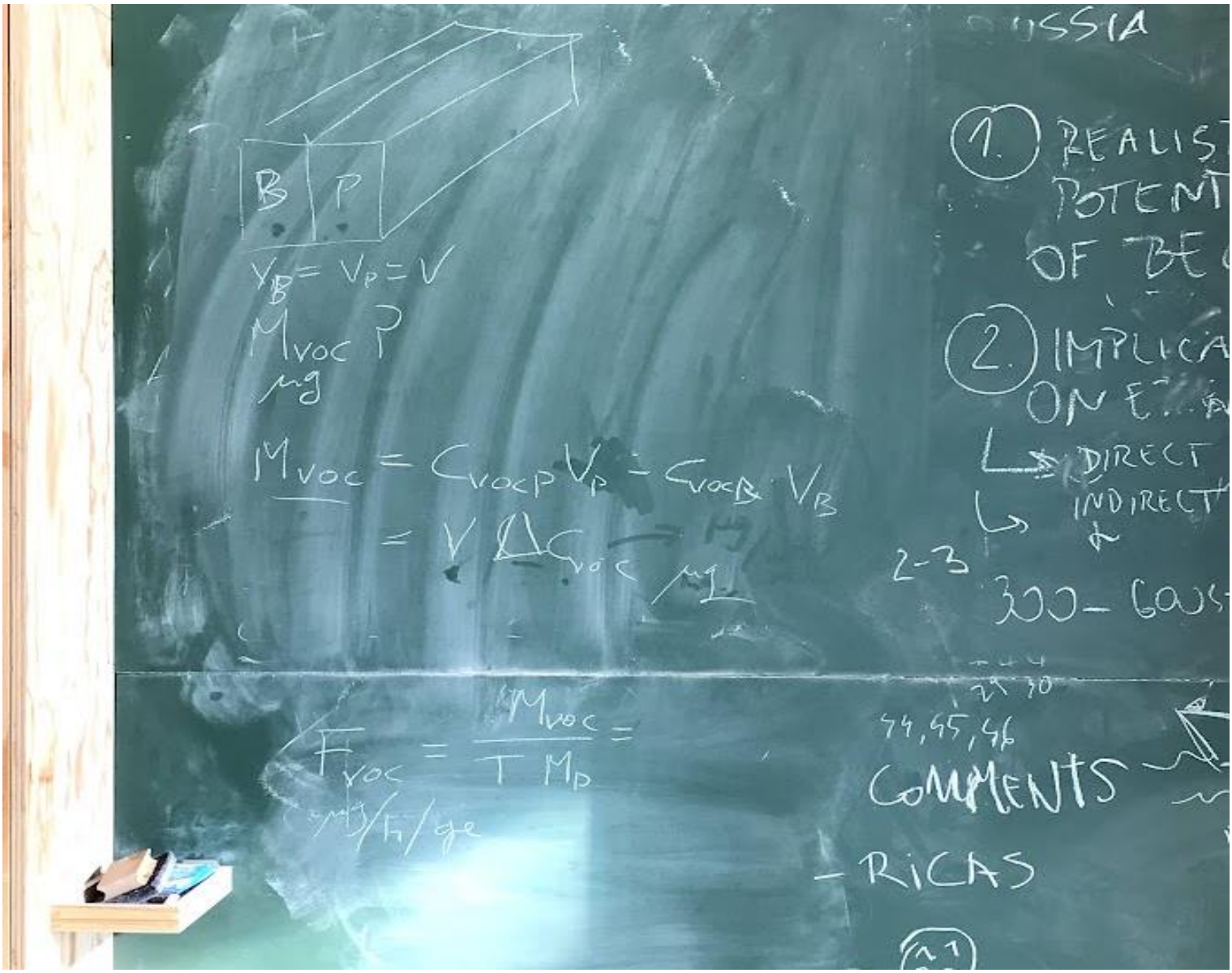

Chapter 2

Research hypothesis, questions, and objectives

Chapter 2: Research hypothesis, questions, and objectives

2.1 Justification for the research

The primary motivation behind this doctoral research derived from the scarcity of comprehensive data concerning BVOC emissions in indoor environments, given their potential to accumulate and exacerbate air quality issues. The reason for addressing this knowledge gap lies in the safeguard of people's health in the framework of UA, of private households particularly and of professionals (e.g., technicians, researchers, etc.) involved in this sector. As previously remarked, the health implications associated with BVOCs strongly depend on factors, such as the space configuration, the emission source, and the exposure time, other than their intrinsic activity. The multiple combinations of all these variables play a pivotal role in determining the ultimate impact of BVOC emissions on both individuals and the environment. On the other hand, supporting the integration of UA, especially within existing buildings, represents one of the key strategies to promote alternative solutions to food accessibility and sustainable food production.

2.2 Research questions and objectives

The principal scope of this dissertation is:

- The determination of the safety of UA environments, focusing on building-integrated and indoor ones, from the perspective of the BVOC emissions released by traditionally cultivated horticultural species that in this study were green bean, tomato, and basil plant.

To achieve the scope the research went through the following questions (**Q.**):

Q.1 What are actual BVOC emission levels in the considered UA environments and which volatile compounds accumulate more?

Q.2 Are the measured BVOC emission levels within the safety range fixed by official frameworks and/or most updated databanks?

Q.3 Which are the factors implicated in final BVOC emissions in the considered UA environments?

Q.4 Based on the overall investigation, do UA environments bring about unsafe conditions to human health? And if so, how could the BVOCs accumulation be contained and/or prevented?

Each of these questions were related to a determined objective (**Obj.**) defined below:

Due to a lack of focused studies (Q.0) → **Obj.0** The set-up a reproducible and easy-to-implement sampling and post sampling protocol to measure BVOC emissions in different UA environments.

Q.1 → **Obj.1** The qualitative and quantitative determination of the BVOC emissions of the plant species cultivated in building-integrated and indoor UA environments and of a BVOC EFs for the most relevant detected.

Q.2 → **Obj.2** The characterization of the safety or unsafety intervals where detected BVOC emissions fall in with respect to official thresholds measured by the Institutions.

Q.3 → **Obj.3** Understanding the influence of different UA settings on the total BVOC emissions.

Q.4 → **Obj.4** The principal scope of the dissertation above stated.

Objectives were addressed in the research by field experiments and analytical tests, which proceeding results and discussions were reported in 11 chapters (part II, III, and IV) and 3 annexes (part V) of the presented dissertation.

Obj.0 was first approached in **chapter 4** describing a preliminary screening conducted in advance of the PhD (master thesis) and in the supporting information of **Annex I** detailed in section **A1.1** and **A1.2**, and finally in **chapter 8**:

Ch.4 *Potential volatile organic compounds emission in indoor urban farming: a case study.*

A1.1 *Testing the sampling system;* **A1.2** *Sampling length.*

Ch.8 *Research methodology assessment and additional relevant BVOC emission findings.*

In Ch.4, having as investigated building-integrated UA environment the iRTG, two sampling methods (active and passive) were performed and the system for the collection of the emissions was tested (open chamber) along with the analytical technique (GC-MS). According to these outcomes, elected method (active) and system (static headspace) were then applied in the assessments presented in the further chapters.

In Ch.8 BVOCs measuring protocol adopted over the whole PhD was compared with a side sampling method (active-TA tube) and post sampling technique (thermal desorption) in the same iRTG to corroborate the results obtained from the different field collections. Additionally, further relevant highlights related to BVOC sampling and indoor levels were reported.

Obj.1, **2**, and **3** were addressed by each of the following investigations reported in **chapter 5**, **6**, **7** and partially **8**:

Ch.5 *Assessment of greenhouse emissions of the green bean through the static enclosure technique.*

Ch.6 *Measuring BVOC emissions released by tomato plants grown in a soilless integrated rooftop greenhouse.*

Ch.7 *Biogenic volatile organic compounds emitted by basil grown in a vertical farm under two different red:blue LED ratios.*

Ch.8 *Research methodology assessment and additional relevant BVOC emission findings.*

Along the individual investigations, a set of environmental variables (temperature, relative humidity, radiation, and CO_2 concentration) was monitored, including occasional monitoring of plant physiological status (net photosynthesis and stomatal conductance) and their contribution on the measured emissions were evaluated. In chapters 5, 6, and 8 assessments were conducted in the iRTG on short- and long-cycle crops. Similarly, in Ch.7 assessment was carried out in an independent UA environment, an indoor VF, on short-cycle crop.

Obj.4 was therefore comprehensively approached in final chapters 9 and 10, targeting Q.4 based on the overall outcomes provided, both chapters, and addressing it with a series of recommendations, chapter 10 mainly:

Ch.9 *Discussion of the research outcomes.*

Ch.10 *General conclusions.*

Finally, future investigations including suggestions on the methodological approach and research targets related with the topic of this dissertation were introduced in last chapter 11:

Ch.11 *Further investigation.*

Chapter 3

Materials & Methods

Chapter 3: Materials & Methods

3.1 Methods

The methodology of this doctoral thesis can be divided into five principal sections (Table. 3.1): sampling setup, field emissions collection, post sampling setup, data analysis, and validation of the results.

The first (sampling setup) and the third (post sampling setup) sections are closely related because they describe the development of the method for the BVOC emissions collection in the field experiments and their qualitative and quantitative analysis, respectively. Both these sections are treated in **chapters 4** and **5**. The second (field emissions collection) and the fourth (data analysis) sections interest all **chapters from 4 to 8** that altogether report multiple BVOC investigations conducted in two UA environments (case studies), the statistical analyses performed on the collected data, and the comparison of BVOC levels with the official limits. The fifth section (validation of the results) is addressed in dedicated **Ch. 8**. Because here a comparative analysis of the outcomes proceeding from an alternative sampling and post sampling method is carried out, the first and the third section are once again debated. Additional methodological information related to the first, the third and the fifth section is detailed in Annex I.

Table 3. 1 Methodological framework used in the research.

Sections of the Methodology

Thesis part	Chapter	UA case study*	1st sampling setup	2nd field emissions collection	3rd post sampling setup	4th data analysis	5th validation of the results
II	Ch. 4	○	X	X	X	X	
	Ch. 5	○	X	X	X	X	
	Ch. 6	○		X		X	
	Ch. 7	●		X		X	
III	Ch. 8	○ □	X	X	X	X	X
V	Annex I	○ ●	X		X		X

*○: iRTG (ICTA-UAB); □: office (ICTA-UAB); ●: VF (*AlmaVFarm*-UNIBO).

3.1.1 UA case studies

Field emissions collection was principally carried out in two UA systems reflecting building-integrated and indoor environmental setting, respectively, an iRTG (**Chapters 4**, **5**, **6**, and **8**) and an indoor VF (**Ch. 7**). Emissions collection was secondary performed in a further indoor space represented by a working office (**Ch. 8**).

3.1.1.1 The iRTG and the office

This environment comprises two iRTGs of the ICTA-UAB, respectively, the Urban Agriculture Laboratory 1 (LAU1) and 2 (LAU2). (Figure 3.1). These spaces are located on the top floor of the building (142 m above sea level) immediately below the roof, each measuring 122.8 m^2. Each greenhouse is equipped with an elevated hydroponic system delivering a mineral solution via drip irrigation into perlite substrate bags. The system makes use of the rainwater stocked below the building and allows leachates collection and recirculation throughout. The main differences between the iRTGs are constituted by the geographical orientation and cultivation management. SE-oriented LAU1 usually hosts one or two cultivation rounds along the year addressed to long-cycle crops distributed on 84.3 m^2, whereas the SW-oriented LAU2 provides multiple cultivations per year being dedicated to short-cycle crops, which are organized in 70 m^2. The internal climatic conditions are regulated through the automatic opening/closing of the surrounding façade according to the conditions desired. The iRTG environment is essentially exposed to the building, with only superficial separation provided by a lateral reflecting curtain. Plant emissions were investigated during the mild term of the year (March/July) in LAU2 mainly (**chapters 4, 5,** and **8**) and once in LAU1 (**Ch. 6**) that was also involved in the last part of the research (**Ch. 8**).

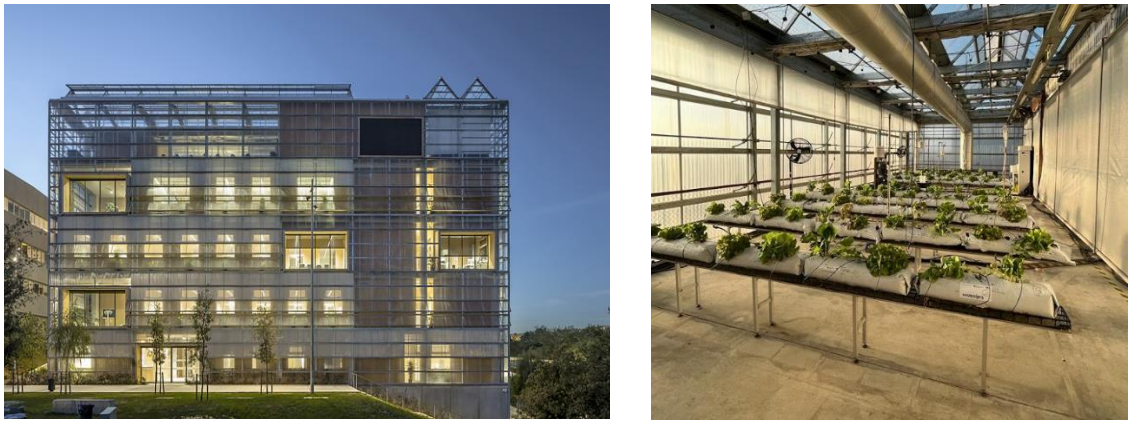

Figure 3. 1 The ICTA-UAB building (left) and an overview of the SE-oriented iRTG-LAU1 and the reflecting curtain on the right side separating it from the atrium (right).

The lower floors of the ICTA building host several indoor working spaces, mainly laboratories and offices of similar dimensions, situated in its perimeter all around the main open atrium. The walls

and both the ceiling and the floor of these spaces are constituted of recycled materials, respectively wood plywood, and concrete. In **Ch. 8** emissions were collected inside a randomly chosen office of 52.5 m^3 (Figure 3.2), representative of the building's environments separated from the cultivated area (iRTG), for the level's comparison purpose.

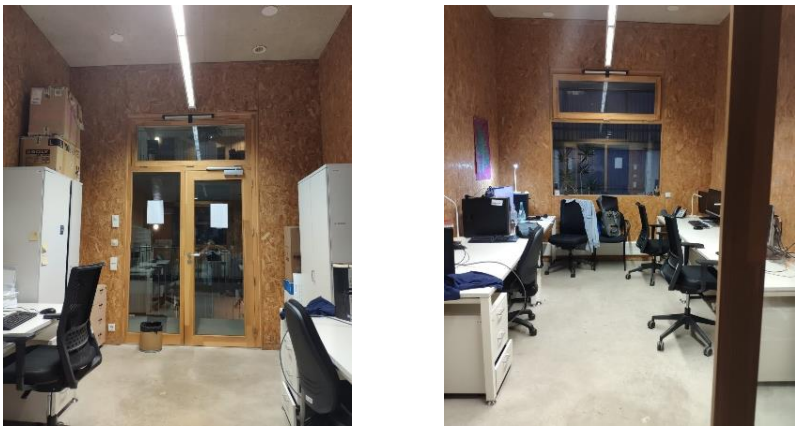

Figure 3. 2 Internal view of the office located on the 1st floor of ICTA-UAB where air samples were taken.

3.1.1.2 The VF

This indoor VF (*AlmaVFarm*) is located at the Department of Agricultural and Food Sciences (DISTAL) of the University of Bologna (Viale G. Fanin 40, Italy). The inner space is designed as an isothermal growth chamber of 45 m^2 composed of 22 cultivation lines, where plants are illuminated by LED fixtures and grown in two soilless systems, hydroponics (10 lines) and aeroponics (12 lines) (Figure 3.3). The cultivation lines are vertically arranged in 3 separate levels, where cultivation trays (each 0.53 m^2 of productive surface) are hosted. Additionally, 3 germination lines arranged in 5 vertical levels are also present within the VF chamber. Fertigation systems feature closed loop (with full water recirculation). Differently from the hydroponics' drip irrigation, water in aeroponics is pressurized at 70 bar and sprayed by nozzles (orifice = 0.2 mm) into the roots directly. Internal conditions can be controlled and maintained constant throughout the growing cycle independently of the external by means of a central HVAC and CO_2 cylinder-pump systems set on desired parameters that simultaneously recirculates the air and recovers the water transpired by the plants. In **Ch. 7** the emission response of plants grown in aeroponic conditions under two different LED light spectra were investigated.

Figure 3. 3 Overview of the indoor space of the AlmaVFarm (left) and the aeroponic LED cultivation (right).

3.1.2 BVOC emissions sampling setup

This part involved a comprehensive bibliographic review on BVOC sampling reported by both official guidelines and experimental works mentioned in the introductive paragraph 1.3.3.1. As described in this paragraph both active and passive methods were implemented for the first time in **Ch. 4**, testing the sampling performance in terms of their feasibility, reproducibility, and reliability. These features comprised the use of affordable and easy-to-handle materials under a working setup providing analogous results along repetitive measurements and comparable outcomes among different experiments. Throughout this process, different sampling intervals and locations were tested and are reported in Annex I (A1.2). Based on this preliminary trial, dynamic (active) sampling in static enclosure was established as the elective method, refined in **Ch. 5**, applied in all principal field experiments (**chapters 6** and **7**), then corroborated in **Ch. 8**.

3.1.3 Post sampling

Depending on the sampling method and the materials used, all samples collected were properly handled prior to their analysis. Dynamic sampling performed with consumable sorbents in **chapters 4, 5, 6,** and **7** followed the solvent extraction according with the NIOSH protocol no. 1552 (1996), while that performed with reusable ones in **Ch. 8** followed the thermal desorption according with the indications given by manufacturer. Both these techniques were realized in **Ch. 8**. Qualitative and quantitative analysis was then carried out with the GC-MS in all the chapters, and in addition with the GC-FID, in **Ch. 8**. All the analyses were performed with the laboratory facilities of ICTA-UAB, except for the samples collected passively (**Ch. 4**) analysed externally by the Centres Científics i Tecnològics of the Universitat de Barcelona (CCITUB). Volatiles identification was achieved through the NIST library provided by the working software only, in **Ch. 4**, and also on purchased standards in **chapters 5, 6, 7,** and **8**. Their quantitation was carried out on the peaks relative abundance with respect to an internal standard (IS) (**Ch.4**), or on the calibration curves (CC) built with multiple standard dilutions(**chapters 5, 6, 7,** and **8**).

3.1.4 Evaluation of the emission levels and related emission factors

BVOC levels (µg m^{-3}) found were compared with the most updated LCIs listed by ECA (EU-LCIs) of corresponding volatiles, among which, terpenes (no 3-1, 3-2, 3-3, 3-4, and 3-5), aliphatic alcohols (no 4-5), and aldehydes (no 7-6). When reference LCIs were not provided levels were compared with those reported in the European Chemicals Agency (ECHA) databank, retrieved from empirical trials. Moreover, BVOC levels were used for the derivation of corresponding EFs (ng or µg h^{-1} m^{-2} and ng or µg h^{-1} g^{-1}) of the source plant, based on the equation reported in paragraph 1.3.3.1. Emission levels and factors of all the BVOCs detected in the different field collections can be found in Annex II.

3.2 Materials

3.2.1 Investigated plants

Different plant species traditionally grown in UA were object of this study to derive the emission profile of both short- and long-cycle crops. Overall, BVOCs sampling was conducted on fully developed plants, except in one case (**Ch. 7**) in which young and mature stage emissions were compared. Due to the relatively short cultivation cycle (about 30 days) and easier maintenance, leafy vegetables and herbs were more frequently used than long-cycle sprawling bushes, which instead required approximately 180 days (6 months) and higher labour. Among the first ones, green bean (*Phaseolus vulgaris* L. var. Pongo) and sweet basil (*Ocimum basilicum* L. var. Genovese) interested **chapters 4** and **5**, and **chapters 7** and **8**, respectively; among the second ones, tomato plant (*Solanum lycopersicum* L. cv. Arawak and cv. Siranzo) was investigated in **Ch. 6** and partially in **Ch. 8**.

3.2.2 Cultivation management

3.2.2.1 Fertigation and nutrient status monitoring

In the iRTG, nutrient solution was divided in two separated tanks to avoid mineral precipitations or incomplete dissolution. It usually comprised the elements reported in Table X.9 of Annex I (A2.1) under different concentrations depending on the crop type. Water solution was dripped multiple times per day and adjusted on plant requirements along the cycle. Only in the case of basil plant (**Ch. 8**) the irrigation was constituted by the water leached from the cultivation of a tomato crop in the neighbour greenhouse (LAU1). Nutrient balance was checked by measuring the pH (G-PHT1, XS instruments) and the Electric Conductivity (EC) (G-CONDT5, XS instruments) every day and by analysing different water samples collected (irrigated, leached, and rainwater)

under their anions and cations content via Liquid Chromatography (ICS-1000 and AS-DV, both Dionex) once per week.

In the VF, nutrient solution was nebulized every 15 min for 60 s and its pH and CE frequently monitored (96 times per day) and corrected automatically by a fertigator (NidoPro®, LogicSun, Cattolica, RN, Italy).

3.2.2.3 Pest management

Due to the exposure to the surrounding environment, iRTG was more vulnerable to pests than the VF, usually aphid, white fly, and spider mite. Therefore, treatments were applied preventively and only when strongly necessary on iRTG crops except for the aromatic species (basil). Applications were performed far from the volatile sampling with chemicals based on organic products, respectively, sulphur at 0.6% (Heliosufre S®) and potassium soap at 2 or 4%.

3.2.2.4 Plants management

In addition to daily and weekly checks of the fertigating conditions, along plant cultivation leaves shaving and fruits harvesting were periodically carried out. Both these tasks and the second one only was performed on tomato and green bean plants respectively. No management was necessary in the case of basil plant.

3.2.3 Environmental monitoring

Each building-integrated and indoor UA space was equipped with multiple sensors monitoring temperature (T, °C), relative humidity (RH, %), solar radiation (W m^{-2}) or Photosynthetic Photon Flux Density (PPFD, µmol m^{-2} s^{-1}), wind speed (m s^{-1}), and occasionally the concentration of CO_2 (ppm). In the iRTG sensors (Siemens and Campbell Scientific) were located inside and outside it and connected with an automated station (Siemens Building Technologies Ltd) controlling the opening of the building's façade based to the set climatic parameters. These were frequently adjusted to keep standard growing conditions along the cycle. Data was recorded every minute and related 10 min averages were stored by dataloggers (CR1000 and 3000, Campbell Scientific). Likewise, in the VF the settled HVAC system (Monti&C srl, Borgo a Buggiano, PT, Italy) allowed the maintenance of the internal conditions that were instead fixed, respectively, 0.03 m^3 h^{-1} of air turnover, 24/21 ± 1°C of day/night T, 70/75 ±10% of RH, and 850 ppm of CO_2 concentration. Table 3.2 reports a comprehensive list of the sensors and their location.

Table 3. 2 Fixed and portable sensors placed in the iRTGs, in the VF, and in the static enclosure.

Climatic variable	**Sensor details**	**Location**	**UA space**
T (°C)	Thermistor T107 (Campbell)	LAU1 and LAU2: multiple points (1 and 1.70 m above ground), rooftop (outside): one point	iRTG
		Static enclosure of LAU1 and LAU2: 2 points	
RH (%) & Air T (°C)	Thermistor CS215 (Campbell)	LAU1: 3 points (1.70 m above ground), LAU2: 2 points (1.50 m above ground), rooftop (outside): one point	
		Static enclosure of LAU1 and LAU2: 1 point	
Solar radiation (W m^{-2})	Pyranometer LP02 (Hukseflux)	LAU1: 3 points (2 at 1.70 m and 1 at 2m above ground), LAU2: 2 points (1.50 m above ground), rooftop (outside): one point	
		Static enclosure of LAU1 and LAU2: 1 point	
CO_2 (ppm)	U-CO2-915, GLA132 Series (LGR)	LAU1 and LAU2: 1 point (1.50 m above ground)	
		Static enclosure of LAU1 and LAU2: 1 point	
wind speed (m s^{-1})	Anemometer 03002-5 (Campbell)	LAU1: 2 points (2 m above ground), rooftop (outside): one point	
		Static enclosure of LAU1: 3 points (before sampling)	
T (°C) & RH (%)	EWHS 2840-3040-3140 (Eliwell)	Walls: 3 points distributed along the chamber	VF
	BL30 Trotec (GmbH)	Static enclosure: 1 point	
PPFD (µmol m^{-2} s^{-1})	MQ-610 PAR meter (Apogee Instruments)	Cultivation lines and static enclosure: 3 points (before sampling)	
W (J s^{-1})	Fluke 189 multimeter (Fluke Corporation)	Cultivation lines and static enclosure: 3 points (before sampling)	
CO_2 (ppm)	CO2E (POLA)	Walls: 3 points distributed along the chamber	
	CARBOCAP® GMP343 probe (Vaisala)	Static enclosure: 1 point	
Gs (mmol m^{-2} s^{-1})	AP4 (Delta-T Devices)	Static enclosure: 1 point	

3.2.4 Light setting

Artificial illumination in the VF was provided by LED lamps (Flytech s.r.l., Belluno, Italy) on each level of the cultivation lines, featuring red (peak at 669 nm) and blue (peak at 465 nm) wavelengths (OSRAM Hyper Red and Blue, OSLON® Square GH) at 200 µmol m^{-2} s^{-1} PPFD under a light/dark photoperiod of 16/8 h d^{-1}. Indoor cultivation and plant emission collection was carried out under two red:blue (RB) light ratios, determined on the areas retrieved from the spectral intervals of red (600–700 nm) and blue (400–500 nm). According to the calculated ratios these were assigned as RB_1 and RB_3. Their performance was checked periodically measuring the electricity absorbance (W = J s^{-1}) and the PPFD.

3.2.5 Dynamic sampling

3.2.5.1 Static enclosure

Many chambers were designed along the experimental research to fit with the different dimensions of the investigated plants and environments (Table 3.3). Enclosures were commonly made of low emitting materials, namely, Low-Density Polyethylene (LDPE) for the cloth and steel for the frame, to minimize the background emission level on the total BVOCs sample. Apart from the first, all enclosures were designed to be entirely closed to facilitate BVOCs gathering through the dynamic sampling. Plants were carefully enclosed along with the growing system (substrate and fertigation) to maintain their physiological conditions under the respective cultivation environment. In **Ch. 4**, an open chamber was preliminary tested and compared with a smaller and closed one (A1.1), as well as in **Ch. 6** chamber's inertia was measured (A1.2). In these tests short and long sampling intervals were included. Based on the proceeded outcomes all experiments performed with the same sampling method (**chapters 5, 6, and 7**) were carried out in static conditions (=closed chamber) along small closing intervals.

Table 3. 3 Chambers specifications.

Enclosure type	Dimensions (m) W x L x H D x H *	Vol. (m^3)	Picture or planimetry	Place	Nº plants	Plant species	Ch.
Open	2 x 4.5 x 1.95	9		LAU2 (iRTG)	32	bean	**4**
Closed	0.5 × 1 × 0.6	0.33		LAU2 (iRTG)	4	bean	**4**

Closed	0.35 x 0.85 x 3.5	1		LAU2 (iRTG)	12, 8	bean, basil	**5, 8**
Closed	1.16 x 2.23 *	2.36		LAU1 (iRTG)	1	tomato	**6**
Closed	0.6 x 1.25 x 0.23	0.17		VF	55	basil	**7**

3.2.5.2 Sorbent material and pumping system

BVOCs were collected using consumable and reusable (conditionable) sorbents. Along active sampling they were trapped in coconut-shell charcoal Anasorb® tubes (Anasorb CSC) of 6 × 70 mm packed with 100/50 mg of sorbent material (SKC) in **chapters 4, 5, 6, 7,** and **8**. Whereas steel tubes packed with 150 mg of Tenax (TA) of 35/60 mesh (GL Sciences) were used for the samplings conducted in **Ch. 8**. In each case, drying tubes (6 ×70 mm) packed with 250 mg of glass wool of 10/60 mesh (SKC) were mounted upstream to reduce sample loss due to the high humidity levels of the environment. Active flow was generated by a controlled pumping system (Electro A.D. pump and flow meter E-7000 Series, Bronkhorst®) set at 0.25 L min^{-1} and carried out for generally short intervals during plant enclosing. (Figure 3.4). Indeed, sampling times were established according to the evolution of the climatic conditions inside the chamber to contain as much as possible their impact on the normal plant emission activity. Most of the time internal conditions were preserved among 5–15 minutes of sampling, although even longer intervals (30 and 45 minutes) were tested. In **Ch. 8** sampling was conducted with and without enclosure allowing testing of longer intervals, between 10 and 120 minutes, that overall showed best chromatographic resolution at sampling $\leq$ 30 minutes (see A3.2.2). Conversely, passive (diffusive) sampling described in **Ch. 4** was carried out with stainless-steel tubes packed with Carbograph 1TD and Carbosieve SIII both of 60/80 mesh (CAMSCO).

Figure 3. 4 Consumable Anasorb CSC (a) and drying (b) tubes and reusable stainless- steel TA tube (c) (left) and the pumping system (right).

3.2.5.3 Static conditions control

During the sampling the internal conditions of the chamber were tracked continuously (every minute) by the sensors indicated in Table 3.3. This information was also used throughout the static enclosure design (dimensions) and the determination of sampling lengths to contain the impacts related with the enclosing condition on plant's constitutive (normal) emission. T and RH were always monitored as being tightly correlated with BVOCs release (Niinemets et al., 2004; Pérez-Priego et al., 2015). Radiation was also measured but its contribution was disregarded due to the low sunlight transmissivity through the polycarbonate windows and the LDPE cloth (<50% of the total external radiation). In addition, CO_2 monitoring and supply via pure gas cylinders (**chapters 6, 7** and **8**) was also conducted as relevant indicator of plant physiological performance. Among the parameters related, main considered ones were the net photosynthesis (Pn, µmol m^{-2} s^{-1}) and stomatal conductance (g_s, mmol m^{-2} s^{-1}). Depending on instrument availability these were measured directly, as for the g_s (**Ch. 7**), or retrieved by theorical formulas (**Ch. 6**), both g_s (Ball et al., 1987; Miner et al., 2017) and Pn (Yin et al., 2019), based on further data recorded.

3.2.6 Plant material processing

During the experiments crop morphological features were periodically measured along the cycle to monitor plants development and adjust the cultivation regime on their requirements. This consisted in non-destructive measurements of the leaves area and/or the Leaf Area Index (LAI) obtained with a free mobile application (Easy Leaf Area, University of California) in one case and dividing the average leaf area by the plant spacing in the other, and of the stem height. In the case of tomato plants, the sum of the Heat Degree Days (HDDs) accumulated by the crop along the whole season were also calculated according to the reference formula of Aguilar-Rodríguez et al. (2020). Destructive measurements were carried out nearby the volatile sampling and at the end of the crop cycle on a minimum of 4 harvested plant samples. These included biomass weighting (entire and separated organs) and leaves and fruits counting. Fresh biomass was then dry at 60 or 70 °C in static oven for repeated cycles until weight variation was <5%. Finally, data

related with fresh and/or dry biomass (g) and leaves area (m^2) or LAI were used as meaningful inputs in the calculation of the EFs of the detected BVOCs.

3.2.7 Sorbent handling

Depending on the sorbents type this procedure was carried out using the techniques described in the introductive paragraph 1.3.3.2.

3.2.7.1 Liquid extraction

Following NIOSH method no. 1552 (1996) consumable Anasorb CSC tubes were broken in a half to recover the adsorbent material in a vial and eluted with 1 mL of CS_2 solvent (≥99.9%, ACROS ORGANIC). (Figure 3.5). In each sample a small aliquot of 1-bromodecane (98% purity, Sygma-Aldrich) as IS was added directly or eluted in dichloromethane (≤100% purity, Supelco) or CS_2 according to Ballhorn et al. (2008). To favour the extraction, vial was occasionally agitated during 30 minutes in advance to the analysis. Prior to real field collection, BV was determined on test samples, analysing separately the front and the back segment of the sorbent bed (A3.1.1). Because of low BV individuated for the representative volatile (<5%), segments were therein extracted together. In addition, Desorption Efficiency (DE) of the sorbent material was tested by adding different (known) amounts of analytes mixture to blanks (=virgin tubes) subjected to the extractive procedure described and then analysed (A3.1.2). Both BV and DE tests were carried out following dedicated sorbent's protocol (HSE, 2002; NIOSH, 1996). Related results are reported in A3.1.

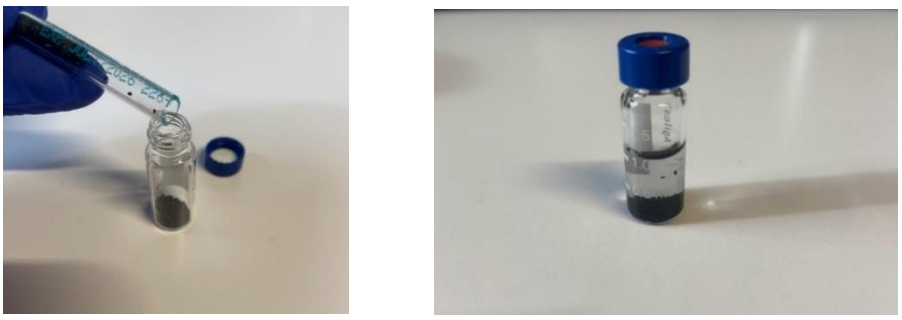

Figure 3. 5 Collection of the adsorbent material in a vial and solvent liquid extraction.

3.2.7.2 Thermal desorption and sorbent conditioning

Steel TA tubes were subjected to thermal desorption in the Handy machine (TD 265, GL Sciences) before their analysis (Figure 3.6). The whole method (pre- and desorption) was defined according to reference examples reported in the instrument manual and after repetitive tests on side collected samples (A3.2). In the specific, pre-desorption was led at 40°C under constant 5 mL min^{-1} of helium flow followed by pressurization at 96.5 kPa (14 psi). At the end of the chromatographic analysis sorbents were re-conditioned for 50 minutes at 300 °C under 5 mL

min^{-1} of N_2 flow. As for Anasorb CSC tubes, the BV (**Ch. 8.1**) was determined for TA tubes as well, following both EPA (1999) and HSE (1993) Methods. Due to the poor sampling performance given with most of the targeted volatiles (BV> 5%), beside few exceptions, BVOCs quantitation was untrustworthy (see Table 8.1). However, sorbents provided reproducible qualitative information.

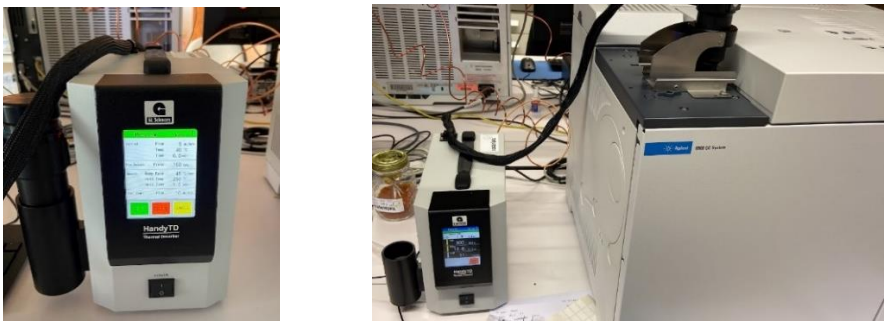

Figure 3. 6 TD probe Handy 265 and the thermal desorption throughout sample injection.

3.2.8 Chromatographic analysis

The analysis of both Liquid Extracted (LE) and Thermally Desorbed (TD) samples was carried out using different GC instruments, depending on laboratory availability, coupled to either the MS or the FID (Figure 3.7; Table 3.4). When consecutive analysis was not possible, LE samples were stored in cold conditions (at 4°C) for a maximum of 4 months, achieved if sample recovery was ≥50% (A3.1.3). Instead, TD samples were always analysed right after the field collection. In **Ch. 8** LE samples underwent also thermal desorption (LE-TD) prior to their analysis in the GC-FID and in the GC-MS.

Figure 3. 7 RACE 1300/1310 GC and ISQ7000 MS (top-left), 7890A GC and 5975C MS (top-right), 8860 GC and FID (bottom).

Table 3. 4 Instruments specifications and methods according to the prepared samples.

Ch.	Sample	Instrument	Analytical Conditions	Detection Conditions	Software
4	**LE**	7890A GC coupled to 7975C MS (Agilent)	Injection: splitless, 1 µL at 240 °C (1 min) GC: Ultra Inert DB-5 MS capillary column (25 m × 0.25 mm × 0.25 µm, Agilent); 1 mL min^{-1} He flow; T: initial 40°C (2 min), gradient 6°C min^{-1} (20 min), final 280°C (4 min)	Transfer line T: 250°C Ion source T: 150°C Ionization: 70 eV Acquisition: scan mode, 35-400 amu at 0.2 scan s^{-1} Detection: mass spectra comparison in the NIST08 library	MassHunter Workstation 10.1 (Agilent GC-MS data)
4	**TD**	Unity Series 2-Ultra Series 2 TD probe (Markes International) Thermo Focus DSQII GC coupled to MS (ThermoFisher Scientific)	1st TD: 300°C (for 10 min) under 55 mL min^{-1} He flow; Injection: double split or splitless, at -27°C Cold trap: U-T15ATA-2S (TO-15/TO-17 Air Toxics trap, Markes International), 11 mL min^{-1} 2nd TD: 300°C (for 10 min) 55 under mL min^{-1} GC: ZB-624 capillary column (Zebron™, 60 m × 0.32 mm × 1.8 µm, Phenomenex); 1.8 mL min^{-1} He flow; T: initial 40°C (1 min), gradient 6 °C min^{-1} (min), final 230 °C (5 min)	Transfer line T: 250°C Ion source T: 200°C Ionization: 70 eV Acquisition: scan mode, 30-300 amu at 0.2 scan s^{-1} Detection: mass spectra comparison in the NIST08 library	Analyses led by the CCITUB
5	**LE**	RACE 1300/1310 GC coupled to ISQ7000 MS (Thermo Scientific)	Injection: splitless, 2 µL at 240 °C (1 min) GC: TG-WAXMS capillary column (TraceGOLD™, 30 m × 0.32 mm × 1 µm, Thermo Scientific); 2.7 mL min^{-1} He flow; T: initial 35 °C (1 min), gradient 10 °C min^{-1} (10 min), final 215 °C (1 min)	Transfer line T: 240 °C Ion source T: 200 °C Ionization: 70 eV Acquisition: scan mode, 50–600 amu at 0.2 scan s^{-1} Detection: SIM mode (55–178 m/z)	Chromeleon Studio 7.2 software (Thermo Scientific)
6 and 7	**LE**	7890A GC coupled to a 5975C MS (Agilent)	Injection: splitless, 2 µL at 240 °C (1 min) GC: TG-WAXMS capillary column (see Ch. 5); 3 mL min^{-1} He flow;	Transfer line T: 250°C Ion source T: 150°C Ionization: 70 eV Acquisition: scan mode, 50–600 amu at 0.2 scan s^{-1}	MassHunter Workstation 10.1 (Agilent GC-MS data)

			T: initial 35 °C (2 min), gradient 10 °C min^{-1} (10 min), final 215 °C (4 min)	Detection: SIM mode (55–178 m/z)	
8	**TD** & **LE** + **TD**	*Handy 265 (GL Sciences) TD probe 8860 GC coupled to a FID (Agilent) *7890A GC coupled to a 5975C MS (Agilent)**	TD: gradient T 45 °C s^{-1} up to 250°C (for 1.5 min) under 10 mL min^{-1} He flow Injection: 1.5 split ratio at 250 °C GC: TG-WAXMS capillary column (see Ch. 5); 1.5 mL min^{-1} He flow; T: initial 50 °C (1 min), gradient 20 °C min^{-1} (10 min), final 240 °C (4.5 min)	Transfer line T: 250°C H_2 flow: 35 mL min^{-1} Air flow: 380 mL min^{-1} Makeup flow: (N_2): 25 mL min^{-1}	OpenLab CDS ChemStation Edition C.01.10 (Agilent)

*At same working conditions reported above for chapters 6 and 7 but injecting 7 µL of LE sample.

3.2.8.1 Qualitative and quantitative characterization

BVOCs determination for most of the collected samples was carried out on external standards (Figure 3.8), except for the preliminary assessment described in **Ch. 4** where identification and quantitation on scan acquired TICs were led respectively on the comparison of mass spectra in the NIST library, the first, and on the peaks area ratio between target analytes and the IS, the second. Identification and quantitation of samples analysed in the GC-MS were led in SIM targeting specific m/z ions for the assessment presented in **chapters 5**, **6**, and **7**, and in SIM and scan mode for those reported in **Ch. 8**. Instead, BVOC determination in samples analysed in the GC-FID (**Ch. 8**) was entirely based on the RT of chromatographic peaks. A total of 33 analytes were purchased (purity 80-99%, TCI America and Sigma-Aldrich) according to the volatile profile of the investigated species. RT and m/z ions of the analytes were retrieved from the NIST Standard Reference Database Number 69 and confirmed by chromatograms obtained by single injections of each of them. Quantitation was performed on CCs (Figure 3.8) built with known concentrations of analytes eluted in CS_2. Curves fitting (proportionality between instrument response and the concentration) was achieved with 5-6 standard solutions of increasing amount and applying the best calibration algorithm provided by the software. In addition, the precision of the quantitative method was determined on the analytes' LOQ. This parameter was retrieved on the relative standard deviation (RSD) ≤25% between the peaks area of a minimum of 5 standard solutions of the lowest CC's level (0.001 ng μL^{-1} in the GC-MS; 1.5 ng μL^{-1} in the GC-FID), in **chapters 5**, **6**, **7**, and in **Ch. 8.3** and **8.2** with regards to, respectively, TA samples analysed in

the GC-FID and LE samples analysed in the GC-MS. Conversely, in **Ch. 8.2** LOQ of TA and LE-TD samples analysed in the GC-FID was retrieved from the general formula detailed in paragraph 1.3.3.2 using CC and blank (pure CS_2) data in the calculation, LOQ of LE-TD samples analysed in the GC-MS was attributed to the blank noise (pure CS_2) in absence of CC data. In all cases the final sample concentration was divided by the total volume of air sampled through the sorbent. Usually, this was corrected on blanks collected from pure air cylinders (**chapters 5**, **6**, and **7**) and on solutions containing only the eluent (**Ch. 8**). Additional information about the overall LOD-LOQ and CC calculated can be found in the Tables reported in section A3 of Annex I.

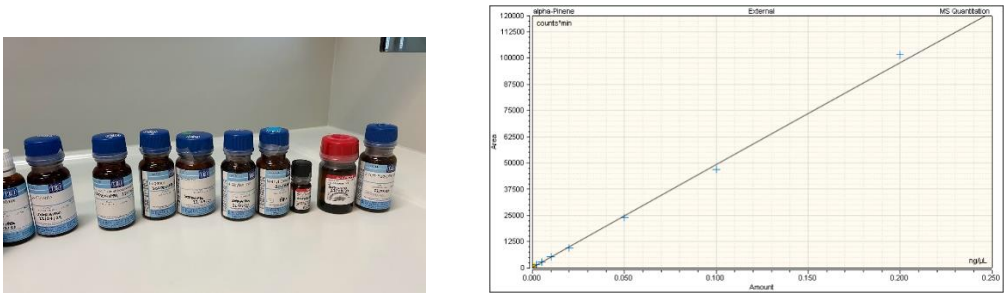

Figure 3. 8 Part of the standards used (left) and an example of a CC for α-pinene obtained injecting 7 dilutions in the RACE 1300/1310 GC coupled to the ISQ7000 MS (right).

3.2.9 Statistical analysis

Statistical tests were performed to evaluate the reliability of the results obtained and their reproducibility according to the sampling method used. In general, emission levels and monitored or predicted variables (environmental and physiological ones) were compared between the sampling intervals and between the treatments applied. Depending on the data distribution, evaluated a priori, statistical analysis was carried out with parametric (one-way Anova, Linear Regression Analysis, LSD test, and Pearson correlation) and non-parametric (two-way Anova, Wilcox signed-rank, Kruskal-Wallis, Dunn test, and Spearman correlation). Significant differences between ($p \leq 0.05$) samples were measured on the variance through one-way Anova with parametric data and on assigned ranks through paired/unpaired Wilcox signed-rank or Kruskal-Wallis test with non-parametric data. When significant differences were found further post-hoc tests, LSD, and Dunn test respectively, were used to highlight them between each sample of a batch. Dependencies between the samples, usually between the emissions and the variables, were analysed through LRA or two-way Anova. Positive and negative correlations (R= ±0.5 or ±0.8) between them were also assessed in plot matrices measuring the correlation coefficient under Pearson (r) and Spearman (r_s) method according to the data distribution. In addition, Principal Component Analyses (PCA) were run to preliminary test the relationships between all the considered data (emissions, environmental and physiological conditions). All statistical tests were performed in R Studio (v. 3.6.3 and 4.2.2).

PART II

BVOCs Field measurement

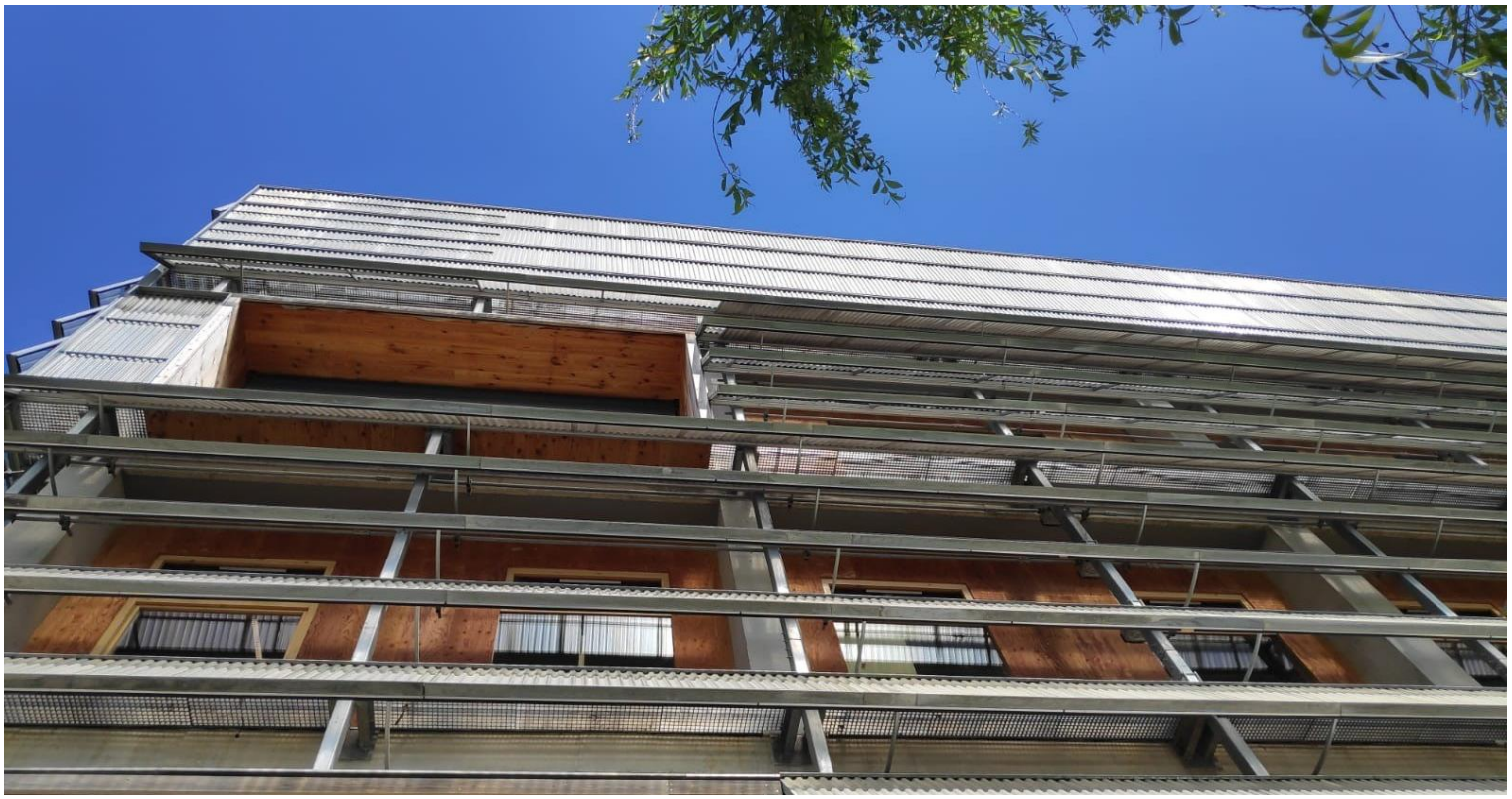

Chapter 4

Potential volatile organic compounds emission in indoor urban farming: a case study

Gaia Stringari[1], Nuria Moraleda-Cibrián [1], A. Rosell-Melé[1,2†], Joan Rieradevall-Pons[4,1], Francesco Orsini[3], Xavier Gabarrell[1,4]

[1]Institut de Ciència i Tecnologia Ambientals ICTA-UAB MdM Unit (CEX2019-0940-M), Universitat Autònoma de Barcelona (UAB), Bellaterra, Spain
[2]Institució Catalana de Recerca i Estudis Avançats (ICREA), Barcelona, Spain
[3]Department of Agricultural and Food Sciences, University of Bologna Alma Mater Studiorum, Bologna, Italy
[4]Department of Chemical, Biological and Environmental Engineering, Universitat Autònoma de Barcelona (UAB), Bellaterra, Spain
† Deceased on December 2021

Journal: ISHS Acta Horticulturae
DOI: 10.17660/ActaHortic.2022.1356.17
DDD: https://ddd.uab.cat/record/273257?ln=en

Chapter 4: Potential volatile organic compounds emission in indoor urban farming: a case study

Abstract

A possible solution to cope with climate change and food insecurity is city greening, through extensive adoption of green infrastructures and urban agriculture. Little consideration is given to potential impacts that could be derived from elevate BVOCs released by plants. BVOCs can account for up to 90% of global VOC emissions. In indoor spaces, their levels are still unknown, although they may raise as much concern as for GHGs. The study presents the monitoring BVOCs emitted by a mature crop of green beans (*Phaseolus vulgaris* L. 'Pongo') cultivated inside an iRTG in the Mediterranean area. Long-term air measurements were taken by passively sampling the atmosphere inside the iRTG and in an inner open chamber hosting plants to monitor physiological emissions, as well as from the external outdoor environment, as control. An additional short measurement was taken on four plants in static-head space conditions to check detected BVOCs. Among a wide range of different volatiles terpenes, methanol and acetic acid were always found (including in the control), suggesting that their origin should not be associated with iRTG plants. However, the detected signals were below the analytical procedure's LOQ. In the static-head space sample, most GC-MS signals could be identified as terpenoid compounds based on their mass spectra and by comparison of their chromatographic retention times with standards; though signals were faint, estimated values were below ppb. Accordingly, the results suggested passive sampling as a practical and easy-to-implement method to produce preliminary tracking of BVOC emissions. However, active sampling may improve the quantitative assessment of their levels inside the iRTG.

4.1 Introduction

Implementing urban green spaces represents one of the strategies embraced by the European programme Horizon 2020 to contain climate change impacts and improve citizens' life quality (European Commission, 2019). In this framework, urban agriculture supports city resilience and liveability (Armanda et al., 2019) and simultaneously tackles issues related to food security and sustainable food production (Opitz et al., 2016; Langemeyer et al., 2021). Due to the limited land available for farming, innovative configurations for urban agriculture that make smart use of existing buildings and available resources have emerged in the last years (Orsini et al., 2014). Nowadays, multiple urban farming systems are available, including indoor, open-air or mixed systems, eventually combined with the urban built environment as for the cases of iRTGs (Iaquinta and Drescher, 2015; Sabeh, 2020). One direct benefit of city greening relates to plants'

sequestration of tropospheric CO_2 (Jamloki et al., 2021; Saeed Meo and Karim, 2022). Currently, global CO_2 levels have increased and showed a rising future tendency (IPCC, 2021). Including urban farming can therefore improve the environmental performance of the city. However, plants are also big emitters of BVOCs, especially terpenes (isoprenoids) that are regularly released into the environment physiologically and under external elicitation (Niinemets et al., 2004; Calfapietra et al., 2013a). Some studies forecasted annual levels of BVOCs up to ten times higher than VOCs emitted by anthropogenic activity (Geron et al., 1995; Guenther et al., 2006). Moreover, it was highlighted a disbalancing effect towards the atmosphere (Laothawornkitkul et al., 2009; Peñuelas and Staudt, 2010) connected to BVOCs, e.g., increased residence time of air pollutants (NO_x, O_3 and CH_4) (Karl et al., 2008; Peñuelas and Staudt, 2010). Indoors, only abiogenic VOCs were extensively argued by the European Regulation (European Parliament, 2021) and supported by comprehensive guidelines (ECA, 2013; World Health Organization, 2021). Regarding biogenic ones (BVOCS), few studies have been reported on plants' emissions at the urban level (Niinemets and Peñuelas, 2008; Yang et al., 2009a) and still no dedicated directions about their management have been provided. Hence, to better assess plant BVOCs levels inside innovative urban farming systems we performed a study on the measurement of crop emissions inside an iRTG of the European Mediterranean area (Pons et al., 2015). Since multiple techniques are suggested (Heiden et al., 2003b; ECA, 1994) and given the exposed conditions of iRTG, we selected the passive sampling for the collection of dynamic flows of cultivated plants (Bartual et al., 1986). Finally, obtained results were compared with those provided by a proofing measurement conducted once in static headspace (Ortega and Helmig, 2008).

4.2 Materials and Methods

4.2.1 Experimental setting and investigated plants

The experiment was performed from September 13 to October 30, 2018. Crop cultivation was carried out in the South-West oriented iRTG of ICTA-UAB institute, a building situated on the campus of the UAB (41°29'51.6"N 2°06'31.2"E). Unlike conventional greenhouses, iRTG shares the environmental flows of the building in which it integrates and communicates with the surrounding outdoor through semi-moving façades (Sanyé-Mengual et al., 2014).

4.2.2 Plant material

Common green bean was selected for the study, a vegetable quite spread in traditional horticulture and broadly consumed by the population of the Mediterranean area. The emission profile of this plant was retrieved from collected literature (Ballhorn et al., 2008; Quintana-

Rodriguez et al., 2015; Martins et al., 2019). About 256 seedlings of *Phaseolus vulgaris* L. 'Pongo' of ±10 cm height was equally distributed on lifted perlite bags inside the cultivable area (40 m^2) of the 122.8 m^2 iRTG. Plants fertigation with standard nutrient solution for leafy crops dissolved in rainwater was administered via a drip system, several times during the day. Plant feeding was checked daily measuring EC and pH of the rainy, delivered, and leached water. Climatic conditions inside the iRTG were tracked by temperature ('T') and relative humidity ('RH') sensors (CS215, Campbell Scientific) and pyranometers (L202, Hukseflux) for the radiation, distributed at different points of the greenhouse; averages of 10 minutes data were collected by data-loggers (model CR3000 and CR1000X, Campbell Scientific Inc., USA) and used by the automated system (Siemens Building Technologies Ltd) on facades opening to modulate iRTG's environmental conditions. Routine greenhouse and crop management, including old leaves shaving, fruit harvesting, and organic chemicals treatment, were carried out for the whole duration of plants cultivation.

4.2.3 Chambers' design

An open chamber for BVOCs measurements was built aside in the iRTG (Figure 4.1), assembling a steel frame (2 m width x 4.50 m length x 1.70 height x 1.95 m roof height) wrapped by LDPE cloth divided into two halves of 9 m^3 on the long side and left open on the short one. Inside a half, two lines of 32 seedlings on perlite bags (=iRTG crop arrangement) were placed and grown under the same regime. Air was sustained by an extractor fan (170 m^3 h^{-1} airflow) positioned on the backside to improve plant to grant climatic conditions comparable to the iRTG. Environmental parameters were recorded by sensors arranged in the chamber, two for T, displaced at the entrance and the end of the section, one for RH, and solar radiation.

A small chamber entirely closed (0.5 m width x 1 m length x 0.6 m height) of 0.33 m^3 was constructed to sample volatile emissions in static headspace conditions on a module of four plants (=one perlite bag).

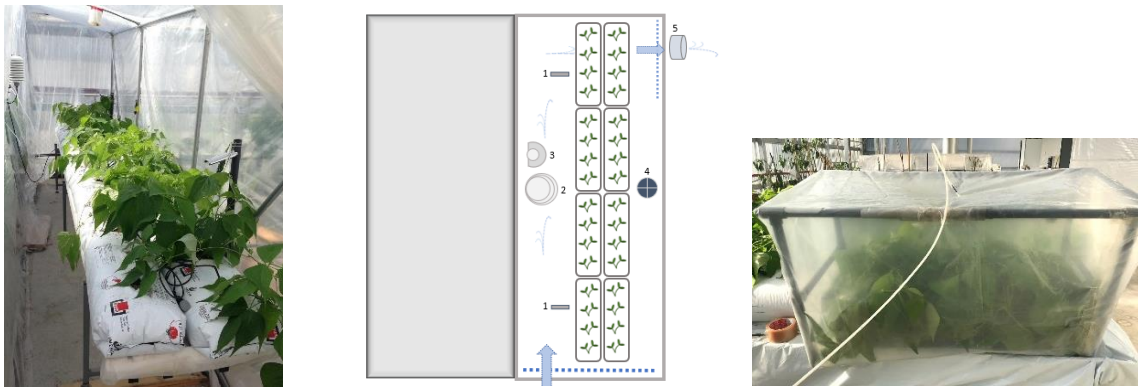

Figure 4. 1 Arrangement of green beans cultivation inside the open chamber and a schematic representation (left) showing sensors for T (1) and RH (2), pyranometer for radiation (3), extractor fan (5) and the diffusive canister for BVOCs collection (4); static headspace sampling in the close chamber (right).

4.2.4 BVOCs sampling

The sampling period began in the 3rd week of transplanting, at the stems' average height of 30–35 cm, when plants were fully developed (Ballhorn et al., 2008; Li et al., 2017). The collection of BVOCs was performed with passive sampling carried out twice along the season, either for one week (between Sept 26 and Oct 2), or for two weeks in a row (from Oct 2 to 22), for comparative volatiles accumulation in response to the time of exposure (Bartual et al., 1986). Sampling was performed with diffusive canisters, containing preconditioned stainless-steel tubes (Carbograph 1TD 60/80, Carbosieve SIII 60/80, CAMSCO), positioned in three distinctive spots: one in the midpoint of the open chamber, one in the centre of the iRTG and one outside, on the building's rooftop, representing the *control* sample of indoor emissions (Figure 4.2). At the end of the experiment, one measurement of 5 hours (10 am to 3 pm) was taken in the small chamber with active sampling to check BVOCs emitted by enclosed plants. It was performed using a coconut-shell charcoal sorbent (Anasorb® CSC, 6 x 70 mm – 100/50 mg, SKC) mounted with a drying tube (6 x 70 mm, 250 mg, 10/60 mesh, SKC) – to prevent waterlogging in the sorbent– at a suction flow between 330-450 ml min^{-1}, generated and controlled with a pump (M&C) and a mass flow meter (E-7000 Series, Bronkhorst®) system. At the end of sampling, diffusive tubes were capped and stocked at 4°C before analysis that was led by an external laboratory (Centres Científics I Tecnològics, Universitat de Barcelona). Similarly, active sorbent briefly flushed with Nitrogen to prevent BVOCs oxidation was stored under the same condition; its analysis was carried out in situ.

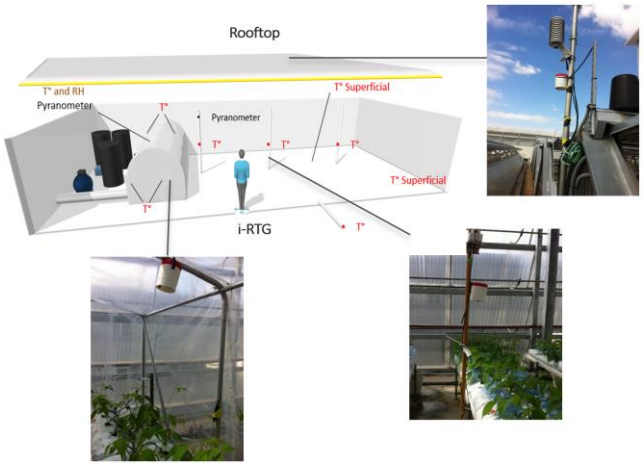

Figure 4. 2 Allocation of diffusive canisters (sampling points) for the collection of the volatiles throughout the experiment.

4.2.5 Diffusive canisters desorption and analysis

Stainless-steel tubes were analysed by the CCITUB using thermal desorption (Unity Series 2-Ultra Series 2, Markes International) coupled to GC-MS system (TD/GC-MS Thermo Focus DSQII GC-MS, ThermoFisher Scientific). To point out eventual differences in instrument response, the first batch (Sep 26) was injected in (double) split mode, while the second one (Oct 2) in splitless. Oven conditions: 300 °C (maintained for 10 min) long primary desorption transported by He gas at 55 ml min^{-1}; split injection at 11 ml min^{-1} with initial temperature -27 °C in the cold trap (U-T15ATA-2S: TO-15/TO-17 Air Toxics trap, Markes International); 300 °C (maintained for 10 min) for secondary desorption transported by He at 1.8 ml min^{-1} into ZB-624 capillary column (Zebron™, 60 m x 0.32 mm x 1.8 µm, Phenomenex). GC temperature program: initial temperature 40 °C (for 1 min), followed by a 6 °C min^{-1} temperature ramp to a final temperature of 230 °C (maintained for 5 min). MS transfer line was set at 250 °C and ion source at 200 °C achieving sample signal under mass scan mode at 30-300 amu. By screening selected ranges of m/z fragments, individuated peaks were then identified by mass spectra with the given NIST library.

4.2.6 Active sorbent extraction and analysis

Analysis of the active sorbent was performed in the ICTA laboratories following a procedure adapted from Ballhorn *et al.* (2008). The adsorbent material of the sorbent was transferred to a 4.5 mL glass vial. In the vial 50 µL of a stock solution of 25 ng $µL^{-1}$ of 1-bromodecane (1-Bromodecane 98% purity Sygma-Aldrich) IS and dichloromethane (DCM, ≤ 100 % purity, Supelco) was added and bring to volume with DCM. The resulting solution was analysed using GC-MS system (7890A-7975C GC-MS, Agilent). An aliquot (1µL) was splitless injected in the GC capillary column Ultra Inert DB-5 MS (25m x 0.25 mm x 0.25µm, Agilent) carried by He at 1 mL min^{-1} constant flow. BVOCs were eluted using the following GC temperature program: an initial

temperature of 40 °C (for 2 min) followed by a 6 °C min^{-1} temperature ramp to a final temperature of 280 °C (maintained for 4 min). MS transfer line and ion source were set at 250 °C and 150 °C, respectively achieving sample signal under mass scan mode at 35-400 amu. Identification of the chromatographic peaks was performed by comparison of the mass spectra with the NIST08 database using the MassHunter software (Agilent). Concentration estimates were obtained using peak area ratios between the target compound and the IS, and assuming the same response factor for both compounds.

4.3 Results and Discussion

4.3.1 Environmental conditions

Throughout the crop cycle, in the iRTG average T and RH were 22.5 °C and 65.1 %, though peaks below and above average T and RH were registered (12.2– 39.5 °C; 18.5–94.1 %) due to seasonal climatic variations. Between the first and the second term of sampling, average T and RH progressed inversely (-3°C; +3%), according to fall progression. In the open chamber, T was equally distributed, and levels were equivalent to iRTG's ones, except for RH, usually higher (+6%). Average radiation registered in the iRTG was barely 22% of the total outdoor radiation and even lower inside the chamber.

4.3.2 Passive sampling results

Tentatively identification of volatiles in the two sample batches is reported in Table 4.1. Due to the huge number of trapped compounds and the high variability of related peak areas in the TIC (Figure 4.3), BVOCs researched focussed on those reviewed by literature.

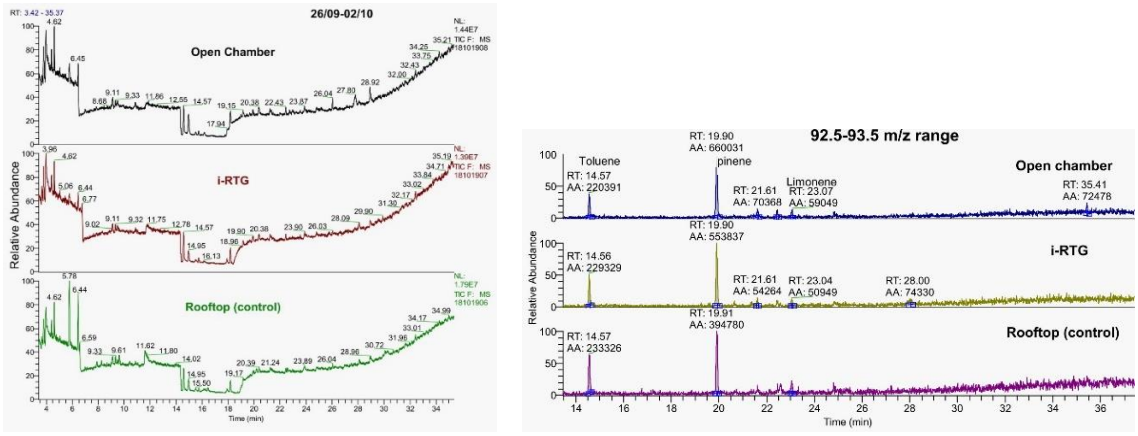

Figure 4. 3 TICs of the open chamber, iRTG and rooftop-control sample, obtained after one week (left) and example of extracted mass channel (right) for MTs (92.50-93.50 m/z).

Quantitation of identified compounds was not possible due to signals below the quantitation limit set by the instrument method. Only preliminary information was given by the peaks' area (Table 4.1). Overall, no appreciable differences were detected among the batches nor between

the sampling points (open chamber, iRTG and rooftop). In the *control* sample, a progressive increase in peaks RTs was usually observed and was attributed to tube breakthrough by particles other than VOCs (e.g., water droplets). Several peaks were identified with VOCs commonly present in the air (omitted in the summary table). Certain BVOCs were identified with MTs, found in all samples with a variation of less than 40% and with α-pinene as the most abundant. Methanol and acetic acid were also ubiquitous and from 15 to 172-folds higher than terpenes but considering multiple sources emitting, their biogenicity was unconfident. Air pollutant, toluene, was present in all the collected emissions, with variable abundance, higher than most terpenes. The remaining peaks were not identified due to the faint S/N ratio.

Table 4. 1 Identified compounds in the diffusive canisters after one week and two weeks of exposure.

Compound type	Compound name	RT (min)	Target ion range (m/z)	relative abundance range (area counts)	Sampling spot[a]
Monoterpenes	α-pinene	19.90	92.50-93.50	390000 – 660000	A, B, C
	β-pinene[b]	21.61	92.50-93.50	56600 – 75800	A, B
	cumene	22.46	92.50-93.50	54000 – 71600	A
	limonene	23.07	92.50-93.50	54700 – 63900	A, C, B
Benzenes	toluene	14.57	92.50-93.50	220000 – 233000	C, B, A
Aldehydes	acetic acid	11.70	59.50-60.50	5700000 – 11000000	C, B, A
Alcohols	methanol	4.62	30.50-31.50	8800000 – 10970000	A, C, B

[a]In order of abundance, the samples obtained from A=open chamber, B=iRTG and C=rooftop after one week of exposure.

[b]Low matching percentage with the NIST library

4.3.3 Active sampling results

Relevant detected and identified compounds are resumed in Table 4.2. Among co-eluted signals, in the first 15 minutes of the chromatographic run, separated peaks were attributed to α-pinene, 3-carene, and limonene MTs with a good matching (72-83%) with the NIST08 library. IS (1-bromodecane) was identified (>96% score) confirming the reproducibility of the analytical method performed. Detected peaks of representative mass-to-charge 100 and 173 m/z were not identified due to poor matching. (Figure 4.4).

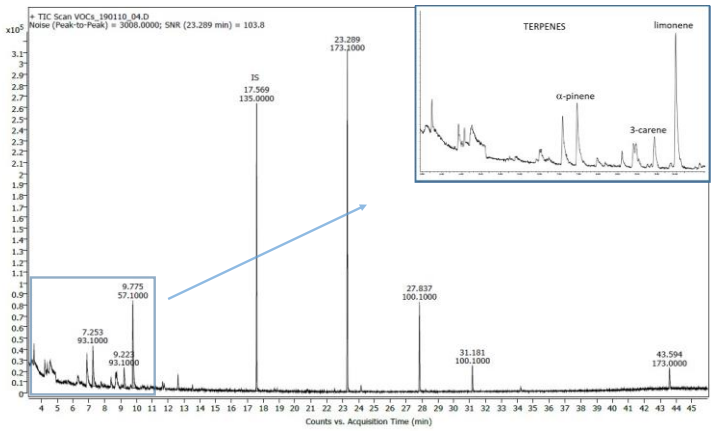

Figure 4. 4 TIC of the close chamber sample. In the magnification terpenes region and identified compounds are highlighted; in the chromatogram, relevant peaks comprise unknown compounds and the IS, with target m/z ion and RT on top.

By comparison of detected peaks' area, terpenes abundance was between 4 and 53% of the IS. From the known concentration of the IS, terpenes amount was estimated to be 0.4 – 4.9 ppb (0.1 – 1.6 µg) in the chamber. On the contrary, levels of unidentified compounds were found to be 1.0 – 11.8 ppbv (0.3 – 3.8 µg).

Table 4. 2 Detected and identified compounds in the close chamber with active sampling.

Compound type	Compound name	RT[a] (min)	Target ion (m/z)	Relative abundance (SNR)[b]
Monoterpenes	α-pinene	7.25	93.1	12.2
	3-carene	9.22	93.1	6.1
	limonene	9.78	57.1	26.5
Internal standard	1-bromodecane	17.57	135.1	87.2
Unknown	unknown 1	23.29	173	103.8
	unknown 2	27.84	100	27.2
	unknown 3	31.18	100	7.8
	unknown 4	43.59	173	6.2

[a]Retention Time.

[b]Signal-to-Noise-Ratio.

4.4 Conclusions

From the study performed the highlights derived were, for the passive sampling:

- Detected BVOCs could not be attributed with certainty to the iRTG crop, since they were found also outdoors and were not quantifiable through the method used.
- Despite occasional peaks of T and RH inside the open chamber and in the iRTG, which excite as elicitors on volatiles release (Niinemets et al., 2004), and cumulative collection, there was no significant difference between indoor and outdoor total emissions. Especially in the iRTG, the role of solar radiation on plant emissions is unclear or at least its impact is not demonstrated.
- The similarity found between indoor and outdoor volatile emissions suggested frequent air turnover in the iRTG, decreasing the concentration of indoor volatiles.
- Resemblance encountered within the open chamber and the iRTG confirmed the reproducibility of the passive sampling method for this context, though resemblance may be also due to a lack of the technical performance of the devices (e.g., water in the tubes).
- Despite the low sensitivity, passive sampling is easy-to-perform and provides a snapshot of the volatiles population of multiple environments.

And for the static headspace sampling:

- VOCs found from this sample confirmed green bean as an emitting species.
- The preliminary quantitative information suggested plant emissions did not exceed the ppb in the iRTG and BVOCs were lower than other volatiles.
- Since found BVOCs levels were much lower than those (≥ppm) provided by the European Report (No 29, 2013) for indoor environments, they were not believed to convey a relevant impact on human health.
- Active sampling on a static headspace system improved both qualitative and quantitative performance of BVOCs analysis but further improvements in its application could define more accurate the chemical profile of current BVOCs and their levels inside the iRTG.

Chapter 5

Assessment of greenhouse emissions of the green bean through the static enclosure technique

Gaia Stringari[1], Joan Villanueva[1], Antoni Rosell-Melé[1,2†], Nuria Moraleda-Cibrián[1], Francesco Orsini[3], Gara Villalba[1,4], Xavier Gabarrell[1,4]

[1]Institut de Ciència i Tecnologia Ambientals ICTA-UAB MdM Unit (CEX2019-0940-M), Universitat Autònoma de Barcelona (UAB), Bellaterra, Spain
[2]Institució Catalana de Recerca i Estudis Avançats (ICREA), Barcelona, Spain
[3]Department of Agricultural and Food Sciences, University of Bologna Alma Mater Studiorum, Bologna, Italy
[4]Department of Chemical, Biological and Environmental Engineering, Universitat Autònoma de Barcelona (UAB), Bellaterra, Spain
† Deceased on December 2021

Journal: Science of the Total Environment
DOI: 10.1016/j.scitotenv.2023.162319
DDD: https://ddd.uab.cat/record/273153?ln=en

Chapter 5: Assessment of greenhouse emissions of the green bean through the static enclosure technique

Abstract

Urban green installations are extensively promoted to increase sustainable and accessible food production and simultaneously improve the environmental performance and liveability of city buildings. In addition to the multiple benefits of plant retrofitting, these installations may lead to a consistent increase in BVOCs in the urban environment, especially indoors. Accordingly, health concerns could limit the implementation of building-integrated agriculture. In a building's iRTG, throughout the whole hydroponic cycle, green bean emissions were dynamically collected in a static enclosure. Four representative BVOCs, α-pinene (MT), β-caryophyllene (ST), linalool (OMT) and cis-3-hexenol (LOX derivative), were investigated in the samples collected from two equivalent sections of a static enclosure, one empty and one occupied by the iRTG plants, to estimate the volatile EF. Throughout the season, extremely variable BVOC levels between 0.04 and 5.36 ppb were found with occasional but not significant ($P > 0.05$) variations between the two sections. The highest emission rates were observed during plant vegetative development, with EFs equivalent to 78.97, 75.85 and 51.34 ng g^{-1} h^{-1} for cis-3-hexenol, α-pinene, and linalool, respectively; at plant maturity, all volatiles were either close to the LOQ or not detected. Consistent with previous studies significant relationships ($r \geq 0.92$; $P < 0.05$) were individuated within volatiles and temperature and relative humidity of the sections. However, correlations were all negative and were mainly attributed to the relevant effect of the enclosure on the final sampling conditions. Overall, levels found were at least 15 folds lower than the given Risk and LCI values of the EU-LCI protocol for indoor environments, suggesting low BVOC exposure in the iRTG. Statistical outcomes demonstrated the applicability of the static enclosure technique for fast BVOC emissions survey inside green retrofitted spaces. However, providing high sampling performance over entire BVOCs collection is recommended to reduce sampling error and incorrect estimation of the emissions.

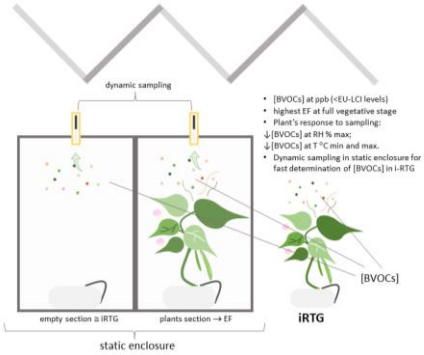

Figure 5. 1 Graphical Abstract

5.1 Introduction

Despite the current climatic emergency and COVID-19 pandemic, the global population increase is expected to reach 8 billion by the end of 2022 and approximately 9.7 billion in the next thirty years (United Nations DESA, 2022). The consequent broadening of urbanized areas in response to an increasing number of inhabitants is driving the agricultural sector toward innovative and sustainable techniques for food production that prioritizes proximity to the city (Maye, 2019; Buscaroli et al., 2021; Rao et al., 2022). Urban planning has also moved in the direction of a more sustainable design by integrating vegetation into buildings (Appolloni et al., 2021; Puppim de Oliveira et al., 2022), both for cultivation and ornamental purposes, such as indoor farming (Sabeh, 2020; Avgoustaki and Xydis, 2021; Banerjee et al., 2022) and vertical gardening (Francesco Orsini et al., 2020b; HUI et al., 2022).

Green installations have been reviewed for their positive effects on building performance in terms of temperature and noise mitigation (Li et al., 2022; Oquendo-Di Cosola et al., 2022) and energy inputs (Muñoz-Liesa et al., 2021; Zambrano et al., 2021) and considered for their capability to remove harmful VOCs from indoor spaces (Ysebaert et al., 2021) and decrease environmental carbon emissions (Lampinen et al., 2022; Saeed Meo and Karim, 2022). However, many studies on air assessment in the open field have reported the release of high BVOCs from plants (Laothawornkitkul et al., 2009; Calfapietra et al., 2013b), mainly isoprene-based compounds, and their chemical interaction with the tropospheric layer. Multiple chain reactions occurring between BVOCs and air molecules may result in significant increases in atmospheric GHGs (CO_2, N_2O, Nox, O_3, CH_4) and SOAs (Cai et al., 2021; Mahilang et al., 2021; Dodman et al., 2022), reflecting air quality and climatic condition variations (Fu et al., 2010; Peñuelas and Staudt, 2010; Glotfelty et al., 2016).

Individuating large-scale effects dependent on plant emissions is demanding, although it could be estimated via extended monitoring and real-time sampling of the urban and wild environment (for instance PTR-MS), or via prediction models (Guenther et al., 2006), which could show particular trend distributions of biogenic fluxes (Chuang et al., 2011; Seco et al., 2015; Drewer et al., 2018; Coggon et al., 2021). In the city area the impact of BVOC emissions regarding green-integrated infrastructures was already theorized (Niinemets and Peñuelas, 2008; Tiwari et al., 2019; Persiani, 2021), but currently research targeting the assessment of BVOC levels in urban environments is limited (Yang et al., 2009b; Zhang et al., 2020).

Indoors, safety levels and ventilation guidelines for anthropogenic and biogenic VOCs have been comprehensively wrapped up in harmonization frameworks of the ECA-IAQ (ECA, 2020;

European Union, 2022). Based on recognized health procedures and according to collected monographs, report nº29 provides the LCI for a VOC that does not reproduce an adverse effect on human health after long-term exposure in an indoor environment. With respect to BVOCs, LCIs are fixed between 1400-5000 µg m^{-3} but individual levels were determined only for few MTs (α-pinene, β-pinene, 3-carene and limonene) despite broad range of volatiles emitted by plants. With respect to the assessment strategies, different sampling techniques and important elements to consider have been discussed (ECA, 1994), supporting user's choice of the most adequate sampling procedure. Since indoor BVOCs can accumulate, levels may exceed safety risk values and result in serious health issues related to breathing and hypersensitivity (Müller et al., 2002; Yang et al., 2009; Maffei et al., 2011; ECA, 2013). Generating data about their potential environmental fluxes can therefore be of great interest.

In view of prospecting scenarios and current research gaps, we carried out a quali-quantitative assessment of the BVOC emissions generated by crop cultivation in iRTG that was placed in the ICTA-UAB building (Sanjuan-Delmás et al., 2018). Following proposed strategies and previous works (ECA, 1994; Soria et al., 2015; Li et al., 2019; Tholl et al., 2021) BVOCs were collected in a static enclosure with dynamic sampling technique and recovered with solvent extraction, identified, and quantified by GC-MS. Detected levels were compared with available LCIs as main referencing values for indoor emissions and additionally BVOCs EF related to the different phenological stage was calculated throughout plants development. Finally, the performance and the reproducibility of the overall sampling methodology performed was evaluated.

5.2 Materials and methods

5.2.1 IRTG arrangement and plant cultivation

Green bean *Phaseolous vulgaris* L. 'Pongo' was cultivated in the southwest-facing greenhouse located inside the iRTG of the ICTA-UAB research institute (41°29'51.6" N 2°06'31.2" E, Figure 5.2 A). Both iRTG and building specific configuration allow a constant exchange of environmental flows among the spaces and, alternately, with outdoor flows according to the programming of the façade system (Muñoz-Liesa et al., 2021). (Figure 5.2 B). Crop cultivation was carried out in spring 2020 (February 12 to May 15).

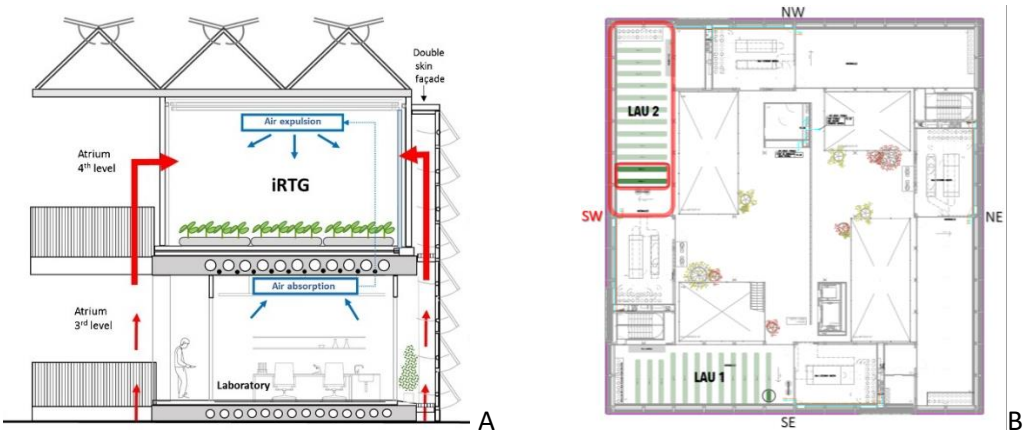

Figure 5. 2 Schematic reproduction of the environmental flow direction along the ICTA building, adapted from (Nadal et al., 2017). (A) and a planimetry of the 4th floor dedicated to urban agriculture, where current/the considered iRTG is highlighted (B).

The cultivation system was run hydroponically under drip fertigation and organized into 8 trailed lines of flanked perlite bags. A total of 256 seedlings of 10-15 cm height were transplanted with a plant spacing of 0.20 m x 0.40 m, resulting in a density of 15 plants per m^2. The cultivated area was approximately 40 m^2 (Figure 5.3). Plants were grown with a nutrient solution for leafy crops dissolved in rainwater. Water management was controlled by a programmed irrigation system that was periodically adjusted for the plants' daily requirements. Daily water pH and EC were measured in the delivered and leached solutions and in the collected rainwater to maintain an adequate nutritional supply. Ambient temperature ('T'), relative humidity ('RH'), and radiation were constantly monitored (systems CS215, Campbell Scientific and L202, Hukseflux) by averaging 10-minute time periods using dataloggers (models CR3000 and CR1000X, Campbell Scientific Inc., USA). Indoor cultivar requirements were fulfilled via the movement of the façade, handled by an automated station (Siemens Building Technologies Ltd).

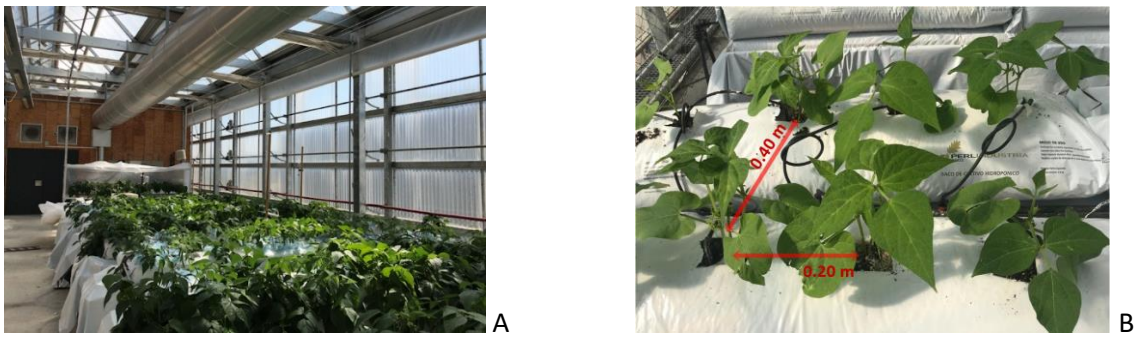

Figure 5. 3 Lateral view of the arrangement of the iRTG cultivation (A) and a picture of the plant spacing along the substrate bags (B).

5.2.2 Static enclosure design and setup

Plant emissions were collected in a chamber, which was a static enclosure (Tholl et al., 2006) built alongside the crop inside the iRTG (Figure 5.4). Chamber dimensions were established

following those of a previous test designed for preliminary emissions assessment (Stringari et al., 2022). The chamber consisted of a rectangular steel frame assembled and delimited with LDPE cloth. The chamber was divided into two equal sections of 1000 L (0.35 m width x 0.85 m height x 3.50 m length). The chamber remained open to the iRTG ambient and was isolated during the BVOC sampling process. In the right section, 12 seedlings were transplanted into perlite bags distributed inside the section and grown under the same environmental conditions as the iRTG crop. The volume occupied by the single plant (0.0867 m^3) was further applied in the calculation of the EF of the detected volatiles. The left section remained empty to provide a representative sample of iRTG ambient. T, RH, and radiation inside the chamber were continuously recorded to obtain supporting information regarding plant physiological status before and during the BVOC sampling process. In the empty section, only T was monitored.

5.2.3 BVOC dynamic sampling

Air BVOCs were extracted into charcoal cartridges (Anasorb® CSC, 6 x 70 mm – 100/50 mg, SKC) using a controlled air stream (Electro A.D. pump and flow meter E-7000 Series, Bronkhorst®). Drying tubes (6 x 70 mm, 250 mg, 10/60 mesh, SKC) were placed upstream of the cartridges to ensure adequate BVOC extraction. Air was collected from the centre of the chamber to represent its atmospheric composition. Since our purpose was the collection of the current environmental air stream in the iRTG, no air purging was performed inside the enclosure prior to sampling. For each sampling process, a total volume of 3.75 L of air was extracted during a 15 min time period (airflow 0.25 L min^{-1}). This term was decided after observing the environmental performance several times in the plant section, considering the well-known influence of abiotic stress on the plant emission response (Ortega and Helmig, 2008), and focusing mainly on RH, which usually showed the highest variation under extended closure. The sampling period started 5 weeks after transplanting, ensuring that the average stem size was above 30 cm (March 26 until May 8). Air samples were taken multiple times during individual phenological stages of the crop cycle (vegetative-reproductive-productive-senescent), individuated by periodical stem sizing, blossom counting and biomass (fallen leaves and harvested fruits) weighing. Consecutive measurements were considered repetitions of a determined stage. Samples were obtained at or near the 12 AM time point, coinciding with the maximum plant activity (Loreto et al., 2006; Ortega et al., 2008). Additional air samples were obtained before the start of the experiment to control BVOCs in the iRTG ambient environment. Procedural blank samples were also analysed to identify possible contamination during the analytical process.

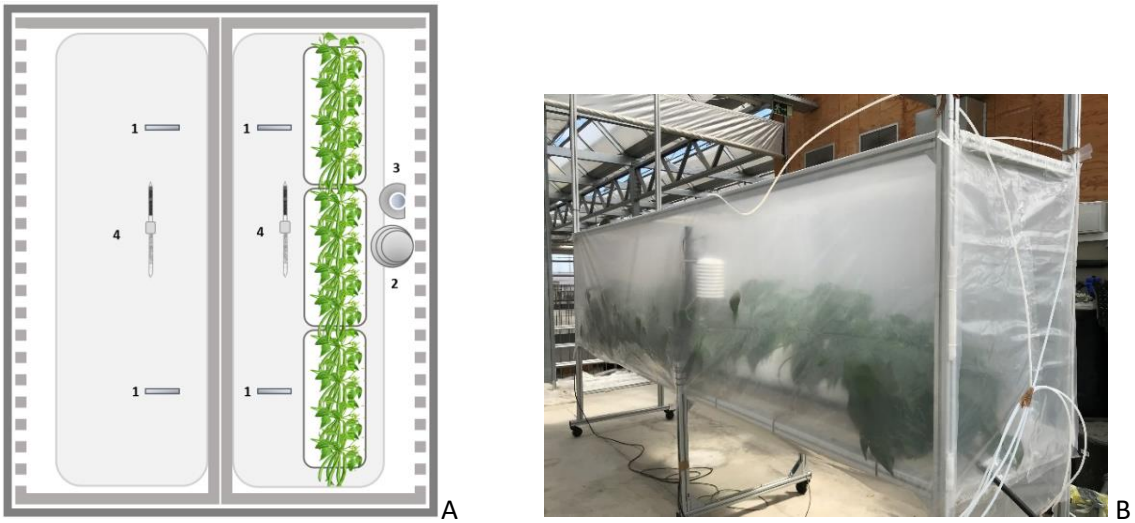

Figure 5. 4 (A) Graphical setup of the chamber for volatile collection in the empty (iRTG) and filled (12 plants) sections (sensors 1, 2 and 3 for T, RH, and radiation; 4 is the BVOC sorbent + dryer tube); (B) Picture showing the air sampling.

5.2.4 BVOC determination

The collected sorbents were flushed with nitrogen to prevent BVOC oxidation and then capped and stored at 4 °C before analysis.

BVOC characterization focused on four of the compounds usually emitted by green beans (Table 5.1) and leafy plants (Holzke et al., 2006; Fu et al., 2010; Maffei, 2010; Malik et al., 2018) and representative of their chemical class. Qualitative and quantitative analysis was performed on MT-α-pinene and OMT-linalool, on ST-β-caryophyllene and on LOX derivative-cis-3-hexenol following the NIOSH Method n. 1552 (NIOSH, 1996). Then, BVOCs were desorbed with 1 mL of CS_2 (purity ≥99.9%, ACROS ORGANIC) and transferred to 1.5 mL vials.

Sample extracts and standard solutions were analysed using a GC-MS (TRACE 1300/1310 GC coupled to an ISQ7000 MS, Thermo Scientific, USA). Extracts (2 µL) were injected in split-less mode (1 min, 240 °C), and BVOCs were separated using a TG-WAXMS capillary column (TraceGOLD^{TM}, 30 m x 0.32 mm x 1 µm, Thermo Scientific, USA) with a constant flow of 2.7 mL min^{-1} of He as carrier gas. Compounds were eluted using the following temperature gradient: initial temperature of 35 °C (for 1 min), followed by 10 °C min^{-1} temperature ramp to a final temperature of 215 °C (held for 1 min). MS transfer line and ion source temperatures were set at 240 °C and 200 °C, respectively. Compounds were ionized at 70 eV and the resulting ions were detected in scan mode at 50-600 amu (0.2 scan s^{-1}) for identification purposes. Compounds were identified by comparing their mass spectra with the NIST library (NIST 17 Mass Spectral Library Software) using Chromeleon Studio 7.2 software (Thermo Scientific). Quantitation was led in SIM to improve instrument sensitivity and specificity. Compounds were identified by comparing the

retention time with solutions containing commercially available standard compounds. The LOQ of target BVOCs was assessed by injecting six replicates of the smallest standard solution (0.001 ng μL^{-1}) detected (LOD), with RSD≤ 21%. (Table A5.1). BVOCs concentration (ng μL^{-1}) in the samples was calculated using the standards calibration curve (0.001–0.1 ng μL^{-1}).

Table 5. 1 List of typical (bold text) and induced (*) BVOCs emitted by Phaseolus vulgaris L. retrieved from the literature (Croft et al., 1993; Ballhorn et al., 2008; Souza et al., 2013; Quintana-Rodriguez et al., 2015).

Class	Terpenoids	LOX derivatives	Shikimic acid derivatives	Photosynthesis derivatives (Glucose)
MT	**α-pinene**	**cis-3-hexenol***	**methyl**	**methanol***
	β-pinene*	**cis-3-hexenal***	**salicylate***	
	cis-β-ocimene*	**trans-2-hexenal***	**indole**	
	limonene*	**trans-2-hexenol***		
	1,8-cineole*	trans-3-hexenal*		
	camphene	trans-3-hexenol*		
	linalool*	(1-hexanol)*		
ST		**acetate** (acetic acid)*		
	β-caryophyllene	cis-3-hexenyl acetate*		
	L-carveol*	1-octen-3-ol*		
	cis-α-bergamotene*	2-ethylhexan-1-ol*		
	α-terpineol*	butyrate*		
HT	farnesene*	cis-3-hexenyl isovalerate*		
Others	trans-4,8-dimethyl-1,3,7-nonatriene*	cis-jasmone*		
		methyl jasmonate		
	2-butanone*			
	nonanal*			
	decanal*			

5.2.3 BVOC emission factor calculation

Quantitative data obtained for the detected BVOCs were then applied to the calculation of an EF, following (Li et al., 2019) equation (5.1) for a static enclosure system: the EF (ng g^{-1} h^{-1}) of a BVOC species (EF_{BVOC}) is given by the difference between the total BVOC concentration (C, ng L^{-1}) emitted by the plant and its concentration in the background air sample (C_0) collected in the static enclosure (V and V_0, L) for the total time of enclosure (Δt), related either to the plant (P) leaf area (m^2), LAI, or fresh/dry biomass (g). In our experiment, no background air sample was provided prior to sampling (no air purging) inside the enclosure. Therefore, the total BVOC concentration was correct on the blank samples collected. The derived equation was then simplified (5.2), giving the EF_{BVOC} for the green bean plant.

$$EF_{BVOC} = \frac{C \times V - C_0 \times V_0}{\Delta t \times P} \quad (5.1)$$

$$EF_{BVOC} = \frac{C \times V}{\Delta t \times P}$$

(5. 2)

The leaf area and biomass of the plants were measured periodically along progressive growth stages. Specifically, four randomly chosen plants were cut at the stem base; the whole plant, stem, and leaves were weighed to provide the average weight of fresh biomass. The 25% of harvested leaves was gently spread onto a scan surface, and the acquired image was processed using an encoding Python 3.8 script (Spyder 4.1.5; Figure A5.2) that calculated the area of the leaves; the 100% area was derived by relating the area to the corresponding biomass weight. The dry weight was also provided by drying the fresh biomass in a static oven (60-70 °C). The LAI calculation was derived by the ratio between the average leaf area calculated and the plant spacing in the iRTG (0.20 m x 0.40 m).

5.2.4 Statistical analyses and environmental correlation

The reproducibility of the carried-out sampling technique was examined using statistical analyses to ensure the reliability of the results. Between the two sections of the static enclosure, BVOC emissions were compared with paired tests (Wilcoxon signed-rank test). Similarly, environmental conditions – T and RH – monitored during the closure time were compared with one-way test (ANOVA). In addition, the effect of the static enclosure was investigated by looking at significant Pearson correlations façade between environmental variables (radiation, T, and RH) and individual BVOCs. Data processing was realized in R Studio (version 3.6.3).

5.3 Results

5.3.1 Environmental performance inside the iRTG during plant cultivation

Far from the sampling, the mean T registered over the crop cycle in the iRTG and in the empty section of the static enclosure was equivalent (18 °C and 19.5 °C, respectively) and slightly higher in the plant section (20 °C); this was also found between the mean RH in the iRTG (56%) and in the plant section (54%). The mean radiation measured at the crop level in the iRTG and in the chamber was also similar (51.83 W m^{-2} and 47.90 W $m^{-2,}$ respectively). During air measurements, chamber T was higher in the plant section and on average 2.5 °C higher than in iRTG; in contrast, RH in the iRTG was still higher than levels recorded in the plant section (+16%), although these levels as well as for T ones were found to increase exponentially along the time of enclosure (Figure 5.5) with peaks close to the saturation point.

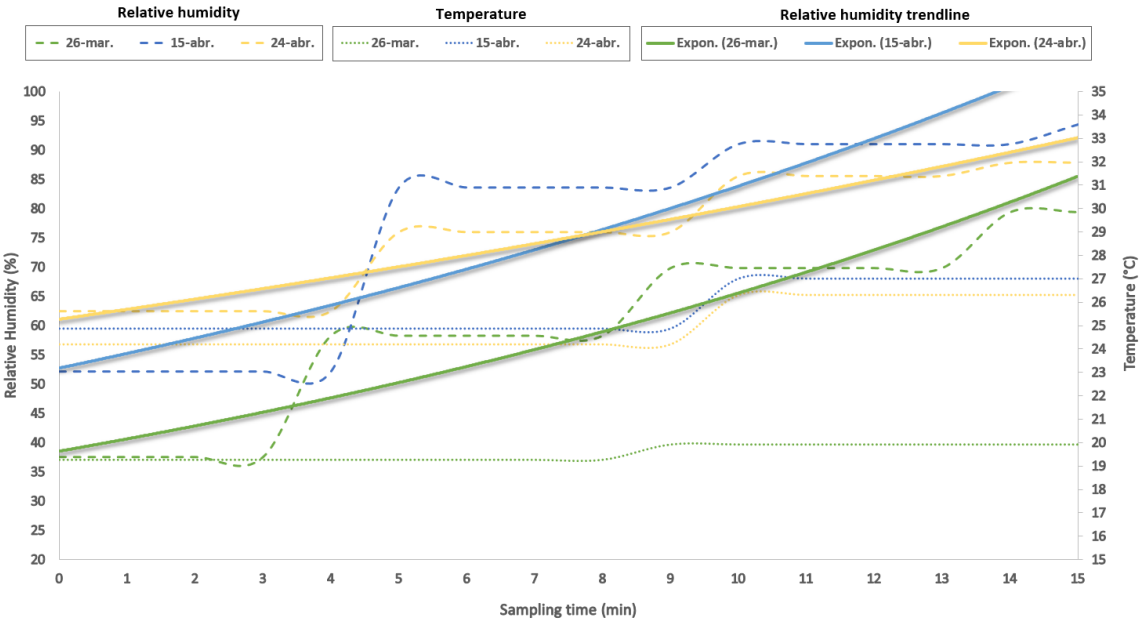

Figure 5. 5 Three representative records of Tand RH measured in the plant section during air sampling; exponential trendlines of RH are highlighted.

5.3.2 Crop emission levels in the iRTG

Throughout the cultivation cycle, the chemical profile of the collected emissions was extremely variable, ranging between 0.35 µg m^{-3} and 29.87 µg m^{-3} (0.04-5.36 ppb) or not detected (below the LOQ). The highest concentration of each detected BVOC was compared with the respective EU-LCI value (Table 5.2), which was defined only for α-pinene but not for the rest of the compounds. Therefore, these levels were compared to the given values of the corresponding terpene class, except for the missing values for cis-3-hexenol. All the investigated compounds were below the most updated EU-LCI values. The collected emissions throughout the season are shown in Figure 5.6. Considering BVOC abundance, MT-α-pinene was the most abundant (1.33-29.87 µg m^{-3}), followed by LOX derivative-cis-3-hexenol (2.13-20.64 µg m^{-3}), OMT-linalool (0.40-16.69 µg m^{-3}) and ST-β-caryophyllene (0.35-0.61 µg m^{-3}). Considering the BVOC distribution, cis-3-hexenol and linalool were typically detected throughout the season and in both sections of the chamber; in contrast, α-pinene and β-caryophyllene were occasionally detected and more often in the empty section. Emissions differences between the two sections were highlighted by subtracting the BVOC amount of the empty section from the section enclosing the plants (Figure 5.7). Although remarkable negative and positive emission variations were observed for all the detected compounds, statistical analysis did not show a significant difference between the collected emissions (lowest *P* value > 0.36). Likewise, the environmental factors measured during collections were generally similar except for RH, whose maximum and minimum values registered in the two sections were significantly different ($P < 0.001$ and $P < 0.01$, respectively).

The interpretation of such variations is addressed by the environmental load analysis in the following section (Results 5.3.3).

Table 5. 2 Compiled EU-LCI values, highest concentrations collected in the static enclosure over the crop cycle, and the instrument LOQ.

		µg m^{-3}	
BVOC	EU-LCI value	Detected level	LOQ
α-pinene	2500	29.87	0.489
linalool	1400*	16.69	0.391
β-caryophyllene	1400*	0.61	0.320
cis-*3-hexenol*	-	20.64	0.449

* This group includes all MTs, STs and their oxygen-containing derivatives

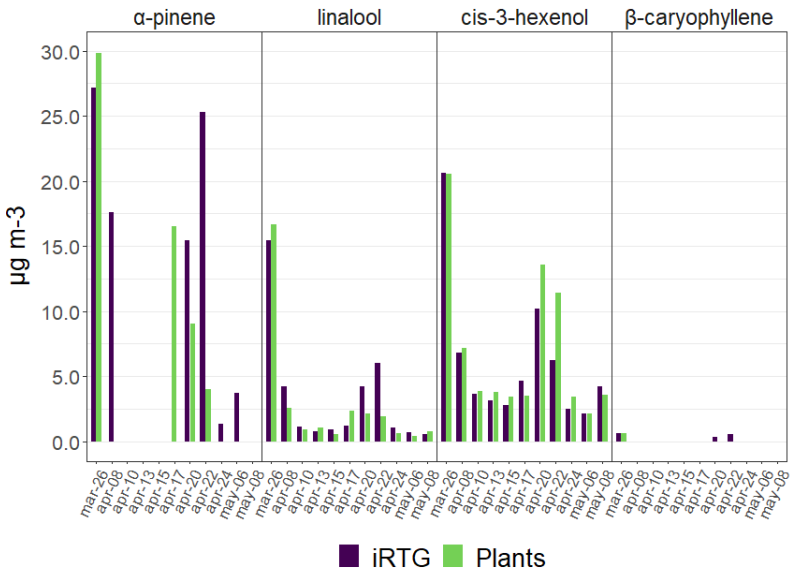

Figure 5. 6 Total BVOC emissions (µg m^{-3}) collected in the empty and plant sections of the chamber throughout the cultivation of the green beans in the iRTG.

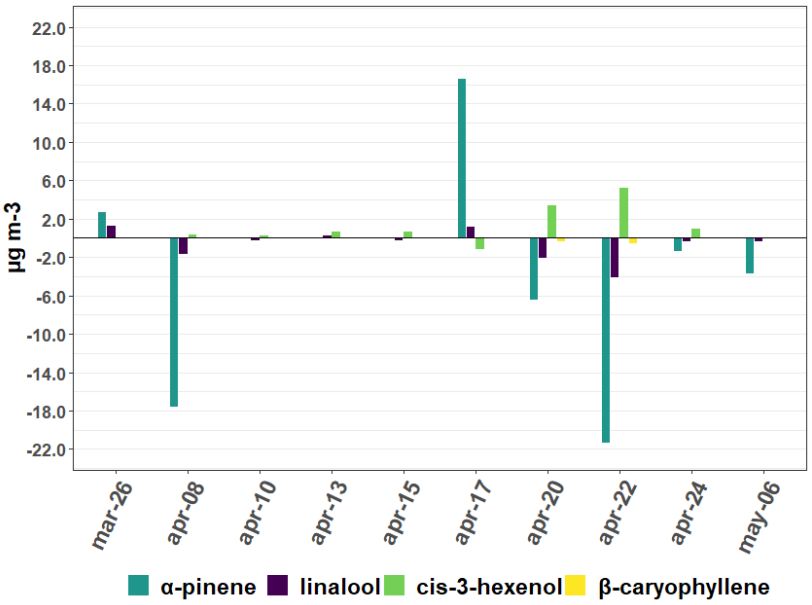

Figure 5. 7 BVOC emissions (µg m^{-3}) variation after subtraction of the total emissions collected in the empty section from those collected in the plant section.

5.3.3 Environmental load analysis of BVOC emissions

By computing individual BVOC emissions with the mean, minimum and maximum rates of the variables recorded (T, RH, and radiation) in compiled matrices, significant correlations were detected (Figure 5.8). In both the empty and the plant sections, analogous negative correlations were found between LOX derivative cis-3-hexenol and T variation ($P < 0.05$); for this volatile, the same correlation was observed with maximum RH rates, although only in the plant section, as well as OMT and ST, linalool and β-caryophyllene ($P < 0.01$). In contrast, no correlations were found for the MT α-pinene. No relevant relation was underlined with radiation. As a result of the computational matrix, a strong positive correlation among all the volatiles ($P < 0.001$) was also highlighted in both sections. Among the variables, significant negative correlations ($P < 0.01$) between RH maxima and the different patterns of T were individuated but only in the plant section.

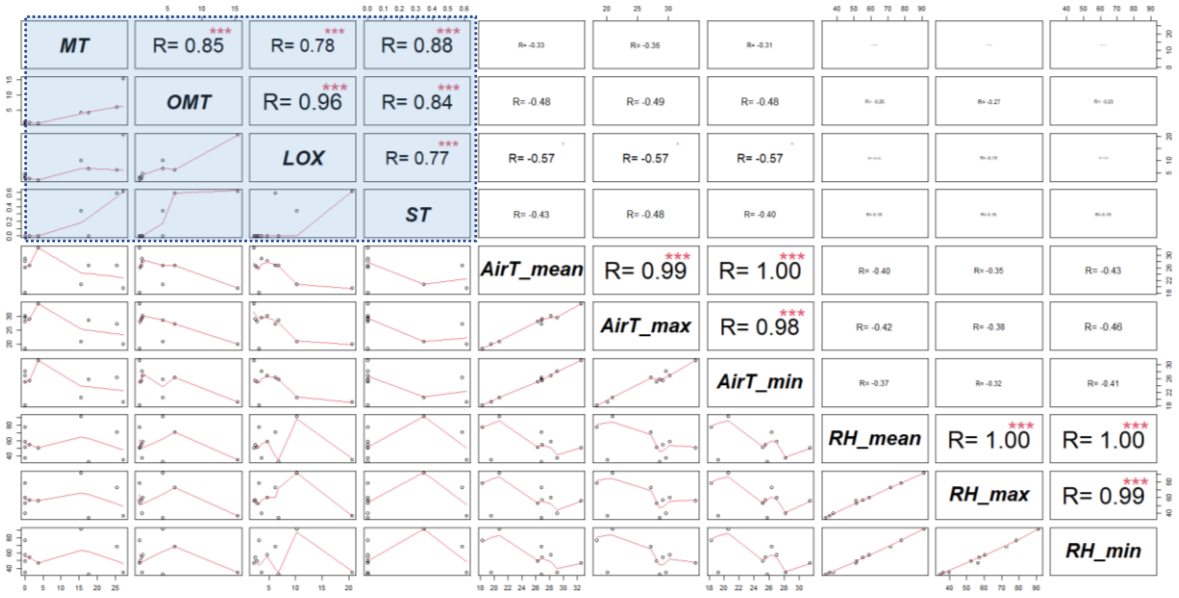

A

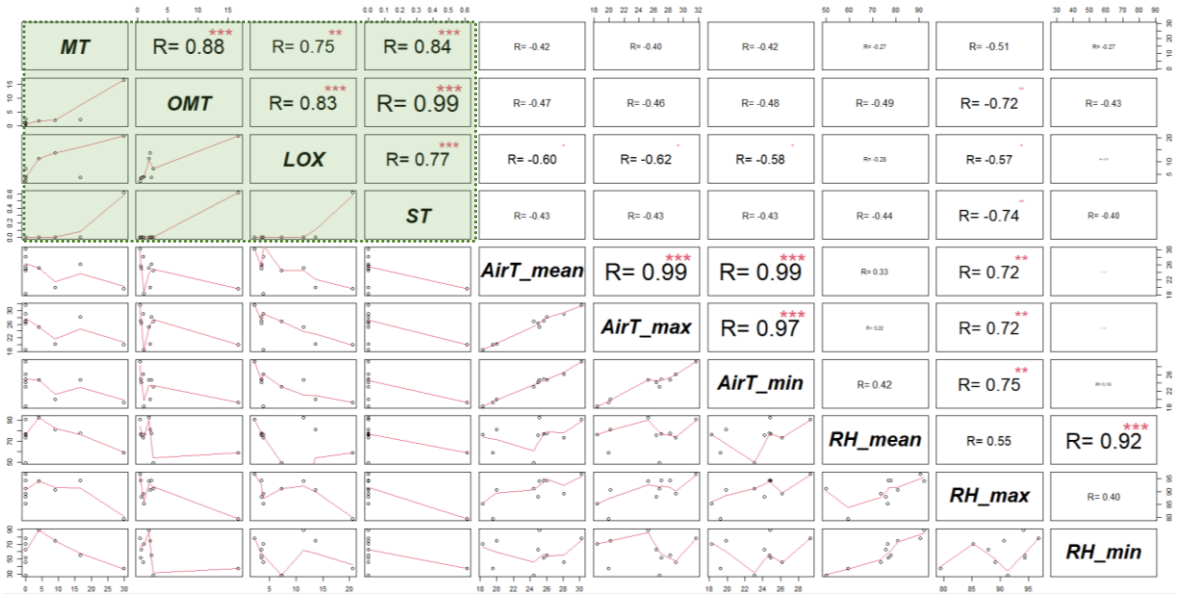

B

*Figure 5. 8 Positive and negative Pearson's r correlations between environmental variables (mean, maximum and minimum RH , and air T: RH_mean, RH_max, RH_min, AirT_mean, AirT_max, AirT_min) and individual BVOC classes (MT, OMT OMT, LOX derivative and ST) detected in the chamber during air sampling in the empty (A) and plant (B) sections; significant correlations P < 0.001, P <0.01 and P < 0.05 are indicated by the symbols '***', '**' and '*'. Correlations with radiation data are omitted here since they are not significant in any of the cases.*

5.3.4 Emission factor of detected BVOCs throughout the crop cycle in the iRTG

From the emissions collected in the plant section, the respective BVOC EFs were determined and related to the corresponding crop growing stage according to phenological measurements (Table 5.3, Table A5.3.1 and A5.3.2). General tendencies were marked, although exceptional levels were also observed. Emission bursts were associated with vegetative development completion,

decreasing progressively during blossoming and fruit production until senescence, which was characterized by the lowest EFs registered.

Table 5. 3 Emission factors (average of nearby air measurements) of the reviewed BVOCs over the crop cycle in the iRTG, and the environmental factors, mean, maximum and minimum T (a, b, c) and RH (A, B, C) most significantly correlated with them.

	BVOC EF ($ng\ g^{-1}\ h^{-1}$)			
Plant phenological stage	**α-Pinene**	**Linalool** [b, A]	**cis-3-hexenol** [a, b, c, A]	**β-caryophyllene** [b, A]
Full vegetative	75.852	51.335	78.967	1.558
Reproductive	17.715	4.257	11.286	0.000
Productive	14.294	5.067	20.683	0.000
Senescent	0.000	2.040	11.082	0.000

5.4 Discussion

Throughout the cultivation cycle, all the green bean BVOCs selected were detected. In general, levels described by measured concentrations were found to be variable. Because the building façade's screening mechanism altered the iRTG radiation, the ozone impact on the total BVOCs collected was neglected. Concentrations of all investigated volatiles were much below ascribable EU-LCI values. Additionally, taking as a reference the highest BVOC detected (29.87 µg m^{-3} or 0.0054 ppm), α-pinene, its concentration was approximatively 15 folds lower than the Risk Value (450 µg m^{-3} or 0.0803 ppm) calculated from long exposure studies (from 6 h to 5 days). Indeed, even when researchers were in the iRTG for long periods of time (e.g., during harvesting or greenhouse maintenance), their exposure to emissions was mitigated by frequent ventilation via automated windows and the edifice structure itself, which can contribute to a fast emissions decrease. Nevertheless, the main phenological EFs derived underlined high emissions at vegetative development and variable or low emissions over the progression of plant growth (Table 5.3). Individual BVOC chemistry and environmental relationships, as well as plant activity, should thus be revised. For MTs (α-pinene) and STs (β-caryophyllene), release (Loreto et al., 2006) is typically driven by Tand characterized by high reactive bursts (Guenther et al., 2006; Materić et al., 2015), although release is much slower for STs (Duhl et al., 2008), which may lead to underestimations during sampling. Emission of OMTs (linalool) and LOX derivatives (cis-3-

hexenol) is also generally inductive, regulated by both biotic and abiotic factors (Niinemets et al., 2013; Jamloki et al., 2021), but rather stable and more persistent in the atmosphere than hydrocarbon terpenes. In the literature, MTs have been reported along the vegetative stage (Holzke et al., 2006) to progressively decrease at plant maturity (Mozaffar et al., 2018), while OMT and LOX compounds have been documented over the entire productive phase (Manco et al., 2021), which is consistent with the emission rates measured. Frequent variations were tentatively explained by the environmental load analysis in the two sections (Results 5.3.3). Considering plant section, general increase of T and RH during the sampling could be reasonably associated to plants physiological response (transpiration) to the enclosing (A. C. Heiden et al., 2003; Pérez-Priego et al., 2015; Soria et al., 2015) and were significantly related with detected emissions. However, negative correlations found between many of the volatiles and RH, and in one case (cis-3-hexenol) with T are in contrast with past findings and may be questionable. A possible explanation may be found in scrutinized analysis of the molecular pattern of VOCs in conditions of high humidity levels (Zhou et al., 2017). Though the combination of increased Tand RH may improve emission amount in the environment the different interaction between individual BVOC and water molecules may also reduce substantially the total concentration of the volatiles (Kari et al., 2018).BVOC fluctuations observed between consecutive samplings could then be attributed to resulted environmental fluxes in the chamber misleading correct estimation of BVOC levels in the iRTG. Unfortunately, assumptions verification required additional analysis and eventually the monitoring of physiological parameters (e.g., CO_2 rates, stomatal conductance, etc.) that in our experiment were not conducted. Nevertheless, the reproducibility of the sampling method was assessed. Validation was performed on the blank samples in which no BVOC was detected (levels below the LOQ) and on the statistical tests on the collected emissions and the environmental records between the two sections of the static enclosure, where indeed no significant differences were highlighted in either case.

5.5 Conclusions

According to our findings, expected BVOC emissions released by a leafy crop in an iRTG can be rationally contained considering low levels found in a small fraction (1 m^3) of it, and more dispersed in relation to traditional indoor systems due to recurrent turnovers of the air enclosed. Regarding the choice of the proper sampling strategy, we suggested dynamic sampling in static enclosure because of an easy-to-implement method for preliminary screening of BVOC emissions, which can provide the indicative levels of BVOC fluxes along a short cultivation cycle (4 months). The occurrence of artifacts during the measurement leading to wrong estimation of current BVOC levels is still higher compared to most recent sampling technologies. Bias may be

reduced improving the performance of the sampling set-up where the conservation of the environmental conditions is pivotal. This could be achieved for instance by monitoring specific physiological predictors of plant response and adjusting the length of the measurement. We compared levels found with official indoor EU-LCIs values as based on rigorous protocols of exposure degree to a specific volatile. Even at the conditions of the highest emission rates for all detected BVOCs levels were much smaller than given LCIs. However, even in most updated tables (2022) detailed LCIs of BVOCs are limited to one class of compounds, basically MTs, and direct comparison of levels related to other speciates (LOX derivates and STs) is not possible. Since plants can emit simultaneously a variety of different volatile speciates having each a defined interaction with the environment their potential risks associated to the human health require attention. Their future evaluation may upgrade current knowledge and support the update of reference limits.

Chapter 6

Measuring BVOC emissions released by tomato plants grown in a soilless integrated rooftop greenhouse

Gaia Stringari[1], Joan Villanueva[1], Elisa Appolloni[2], Francesco Orsini[2], Gara Villalba[1,3], Xavier Gabarrell[1,3]

[1]Institut de Ciència i Tecnologia Ambientals ICTA-UAB MdM Unit (CEX2019-0940-M), Universitat Autònoma de Barcelona (UAB), Bellaterra, Spain
[2]Department of Agricultural and Food Sciences, University of Bologna Alma Mater Studiorum, Bologna, Italy
[3]Department of Chemical, Biological and Environmental Engineering, Universitat Autònoma de Barcelona (UAB), Bellaterra, Spain

Journal: Heliyon (CellPress)
DOI: 10.1016/j.heliyon.2023.e23854
DDD: https://ddd.uab.cat/record/287132

Chapter 6: Measuring BVOC emissions released by tomato plants grown in a soilless integrated rooftop greenhouse

Abstract

Urban design is currently promoting the inclusion of plants in buildings. However, plants emit BVOCs, which alone or in combination with other airborne molecules such as CO_2, may result in a general increase in tropospheric pollution. Many studies have documented the effects of biotic and abiotic factors on plant BVOC responses, but few have assessed the contribution of typical CO_2 levels found in indoor work and meeting spaces. To answer this question, we monitored CO_2 and constitutive (MT-limonene) and induced (LOX-cis-3-hexenal) BVOC emissions of a fully developed tomato crop grown hydroponically inside an iRTG in a Mediterranean climate. Two distinctive CO_2 assays were performed at the level of the iRTG by supplying or not CO_2. The impact of CO_2 on plant physiological emittance was then assessed, and the resulting BVOC rates were compared with reference to EU-LCI values. MT-limonene was ubiquitous among the assays and the most abundant, while LOX-cis-3-hexenal was detected only under controlled CO_2 management. The highest levels detected were below the indicated LCIs and were approximately one order of magnitude lower than the corresponding LCI for MT-limonene (50.88 *vs.* 5000 µg m^{-3}) and eightfold (6.63 µg m^{-3}) higher than the constitutive emission level for LOX-cis-3-hexenal. Over extended sampling (10 minutes) findings revealed a general emission decrease and significantly different CO_2 concentration between the assays. Despite similar decreasing rates of predicted net photosynthesis and stomatal conductance their correlation with decreasing CO_2 under uncontrolled condition indirectly suggested a negative CO_2 impact on plant emission activity. Conversely, increasing CO_2 under the controlled assay showed a positive correlation with induced emissions but not with constitutive ones. Because of significantly higher levels of relative humidity registered under uncontrolled conditions, this factor was considered to affect more than CO_2 the emission response and even its collection. This hypothesis was supported by literature findings and attributed to a common issue related with the sampling in static enclosure. Hence, we suggested careful monitoring of the sampling conditions or further improvements to avoid bias and underestimation of actual emissions. Based on the main outcomes, we observed no evidence of a hazardous effect of registered CO_2 rates on the BVOC emissions of tomato plant. Furthermore, because of the low BVOC levels measured in the iRTG, we assumed as safe the recirculation of this air along building's indoor environments.

6.1 Introduction

Worldwide climate emergencies and intense gentrification are forcing the scientific community and citizens to enact timely actions for the containment of forecasted environmental and socioeconomical contingencies (IPCC, 2023). Among the effective strategies recommended, the systematic expansion of green infrastructures in urban centres has been encouraged, particularly by European councils and local neighbourhoods (European Commission, 2019; HUI et al., 2022), to solve issues related to food accessibility and social exclusion (Gould and Caplow, 2012; Yudelson, 2012; Buehler and Junge, 2016) as well as to tropospheric contamination (Torpy and Zavattaro, 2018; Ramasubramanian et al., 2019; Shao et al., 2021b). The environmental performance of existing buildings can be improved by integrating plants inside and outside of them (Pons et al., 2015), not necessarily by means of high-cost technologies. Innovative systems, such as iRTGs (Nadal et al., 2017; Milford et al., 2019; Muñoz-Liesa et al., 2021), have demonstrated the multiple benefits provided in terms of energy use efficiency (Muñoz-Liesa et al., 2021), carbon emissions reduction (Lampinen et al., 2022), and energy and food production (Francesco Orsini et al., 2020b; Zambrano et al., 2021).

The benefits associated with plant removal capacity of air contaminants have been widely reviewed in the green retrofitting literature (Torpy and Zavattaro, 2018; Gunawardena and Steemers, 2019; Tomson et al., 2021; Ysebaert et al., 2021; Sharma et al., 2022). However, this capacity seemed to be overestimated with respect to the measured removal efficiency (Kim et al., 2011; Zorić et al., 2019; Cummings and Waring, 2020) due to species-specific plant mechanisms and to the same environment considerably affecting plant response in terms of indoor and outdoor air recovery (Brilli et al., 2018; Cummings and Waring, 2020; Tomson et al., 2021). In the wild, plants can release (Loreto et al., 2006; Arena et al., 2016) tons of BVOCs annually into the atmosphere during photosynthetic activity (Laothawornkitkul et al., 2009; Drewer et al., 2018; Lun et al., 2020), which have also been detected in urban areas (Churkina et al., 2017; Zhang et al., 2020) and domestic spaces (Yang et al., 2009a; Tiwary et al., 2013; Zorić et al., 2019). The ultimate impact of BVOCs on indoor air quality is still uncertain (Yang et al., 2009a; Tiwari et al., 2019; Tomson et al., 2021), although because of the high concentration and chemical reactivity, potential harm to human health has been warned (European Union, 2008; Maffei et al., 2011; Song et al., 2016). For some BVOCs, concern levels were assessed and included along with those of other volatiles in the EU-LCI tables for indoor spaces (ECA, 2013; European Union, 2022). Depending on indoor conditions, the composition and amount of BVOC emissions change and can increase considerably, as observed under elevated ozone (European Union, 2008; Li et al., 2017) and temperature (Loreto et al., 2006; Zhou et al., 2017) levels.

Emission blend mutations have been referred to as a substantial adaptation of plants to the presented environment (Niinemets et al., 2004; Calfapietra et al., 2013b) and were demonstrated to follow typical patterns. Without stimuli, either biotic or abiotic, plants emit constitutive BVOCs, mainly mono- and sesquiterpenes, regulated by the temperature–light gradient (Juuti et al., 1990; Kim et al., 2005; Loreto et al., 2006). Under nonphysiological conditions, commonly during a stress event (e.g., drought and insect plague), plants emit predominantly volatile derivates of the lipoxygenase pathway (Loreto et al., 2006; Loreto and Schnitzler, 2010).

Among the stress factors affecting BVOC emissions, the implication of CO_2 has also been studied (Wilkinson et al., 2009; Calfapietra et al., 2013a) given the higher levels recorded currently than in the past 30 years and those foreseen (Parmesan et al., 2022). Although there is still uncertainty about the effect of CO_2 at both ambient and elevated concentrations, a trend toward reduced plant response under elevated CO_2 has been documented (Kulmala et al., 2013; Copolovici et al., 2021; Jamloki et al., 2021), although it is connected to the length of exposure. More specifically, this has mainly been detected at short-term exposure. Longer term exposure was believed to result in plant adaptation with almost no consequences on total emission release (Calfapietra et al., 2013a; Staudt et al., 2017). Additionally, combining high CO_2 with increasing temperature and other common stresses, such as drought, was shown in the short term to have a contrasting effect to the inhibiting effect of CO_2, favouring plant emission activity (Räisänen et al., 2008; Velikova et al., 2009; Tiiva et al., 2017). In a recent study (Daussy and Staudt, 2020), different CO_2 regimes were applied for a short time, individually or in combination with defined temperature rates, to the leafy species *Artemisia annua* L. The results demonstrated that a decreasing effect on total emissions was significant only when the plant was exposed to both elevated CO_2 (800 ppm) and temperature (>30 °C); this also confirmed the predominant effect of temperature on the induction of plant emissions. However, high variability and different outcomes were also noted depending on different factors, for instance, the sampling condition (field or laboratory study), the plant status and the species (Hantson et al., 2017; Copolovici et al., 2021).

Among indoor crops, tomato (*Solanum lycopersicum* L.) is one of the top crops because of its remarkable nutritional and commercial aspects (Cruz et al., 2022; Peña et al., 2022; Richardson and Arlotta, 2022). Regarding the volatile profile, tomato plants have been investigated under conventional and stressed conditions to determine BVOC variations between constitutive and induced emissions (Jansen et al., 2011; Copolovici et al., 2012). Among the wide range of BVOC classes, terpene components are usually detected in physiological emission blends (Schilmiller et al., 2009; Falara et al., 2011). Monoterpene and sesquiterpene release via plant

photosynthesis was reported under a positive temperature gradient sustained over time (Falara et al., 2011; Takayama et al., 2012). Despite the ubiquity of terpene (Pazouki et al., 2016), induced emissions from tomato may change substantially according to elicitation and intensity subordination (Jansen et al., 2011). Lipoxygenase derivates were the volatiles most documented under extreme temperature rates (Copolovici et al., 2012), ozone fumigation (Peñuelas et al., 1999), insect wounding (Farag and Paré, 2002), and combined biotic and abiotic stresses (Degenhardt et al., 2010; Catola et al., 2018). To the best of our knowledge, potential variations in tomato emissions associated with different CO_2 levels have not been reported, since related measurements were conducted at ambient CO_2 levels only.

Compared to most horticultural species, tomato plants account for a considerable emitting surface, and therefore, BVOC amounts eventually reach levels of attention over prolonged exposure (European Collaborative Action (ECA), 2020). Few studies have been conducted on the assessment of tomato emissions into the environment (Jansen et al., 2009, 2010; Takayama et al., 2012; Fabbri et al., 2020). Among these, their association with CO_2 was briefly mentioned (Takayama et al., 2012). Additionally, in an iRTG on the ICTA building on the UAB campus, the emissions from a leafy plant (*Phaseolus vulgaris* L.) were previously investigated through a static chamber under ambient conditions by checking temperature, light, and relative humidity parameters (with the exception of CO_2), and emission rates below the advised EU-LCI (Stringari et al., 2023) were found. Emissions from larger plants (e.g., tomato), which in southeast-oriented iRTGs (Parada et al., 2021) are cultivated annually, have not yet been studied. Compared to a controlled greenhouse (Jansen et al., 2009, 2010; Takayama et al., 2012; Catola et al., 2018) and although frequently adjusted to crop requirements, climatic conditions in iRTGs are much more variable due to the top location, which enhances exchanges with the surroundings. Additionally, according to the building's recirculation system, air coming from the greenhouse floor could be efficiently exploited to warm up the lower space, increasing the living quality of indoor environments, such as offices (Muñoz-Liesa et al., 2021). Therefore, in this study, in addition to measuring tomato plant emissions, the contribution of CO_2 was also analysed. This was performed under two sampling conditions in a static chamber, one at the CO_2 concentration generated by the enclosure and one at a controlled concentration maintained at the ambient (iRTG) levels. The research questions investigated were as follows:

- Are the BVOC emissions of tomato plants grown under iRTG conditions below the reference EU-LCI values to be safely recirculated to indoor spaces?
- Does CO_2 control significantly affect constitutive BVOC emissions during sampling?
- If so, do emissions increase or decrease under uncontrolled CO_2?

6.2 Materials and Methods

6.2.1 Experimental conditions

The study was conducted in two consecutive warm seasons (spring-summer), with one experiment conducted in 2021 and the following in 2022. Plant cultivation and experimental setup were carried out hydroponically in the abovementioned iRTG. In both campaigns, *Solanum lycopersicum* cv. Arawak was grown in the greenhouse and intercropped with another cultivar, cv. Siranzo in 2021 and Rosa de Cadiz in 2022. Cultivars Siranzo and Arawak were chosen for the volatile profile investigation in 2021 and 2022, respectively. Despite slight morphological differences, the emission blend composition of the plants was assumed to be similar and consistent with previous studies (Table A6.1). In both cases, the hydroponic system consisted of 12 parallel rows of perlite substrate bags (40 L) where plants were distributed equally along the row (0.30 m) and between the rows (0.80 m) (Figure 6.1), providing a density of 3 plants per m^2 and a total cultivated area equal to 41.8 m^2 in 2021 and 27.8 m^2 in 2022. In the two years, the crop cycle in the iRTG had an equivalent duration of approximately 5 months (135 days). The duration of the cycle was defined as days after transplanting (DAT), which occurred in mid-March, and it finished at the end of July.


A


B

Figure 6. 1 Crop distribution in the iRTG in the early growing stage (A) and a panoramic view from the building's atrium of mature tomato plants in the iRTG (B). Both pictures were taken in the 2021 season.

Cultivation parameters were checked continuously and adjusted when necessary to maintain adequate and stable growing conditions over the season. This included daily measurements of the pH and EC of water tanks, dripped solution and leachates, as well as of environmental temperature, relative humidity, and radiation (CS215 system, Campbell Scientific and L202, Hukseflux). Ambient CO_2 was periodically measured in the greenhouse space with a portable gas analyser (U-CO_2-915, GLA132 Series, LGR) to provide updated ambient levels. The internal conditions of the iRTG were managed by a remote station (Siemens Building Technologies Ltd)

that regulated the opening of the surrounding façade to dissipate the passive heat collected from the building.

Plant development was monitored weekly based on morphological traits by measuring stem height and leaf area, counting the blossoms, and weighing the biomass collected from the pruning and harvested fruits. Additionally, over the whole cultivation cycle of each season, the HDDs inside the iRTG were calculated by applying Formula (6.1) of Aguilar-Rodríguez et al. (2020). The single HDD was derived from the average of the maximum and the minimum temperature (T_{max}, T_{min}) and the lowest temperature at which tomato can thrive (T_{base}), which was fixed at 10 °C. This value provided the minimum temperature required for the plant's metabolic activity. This information was then used as a direct and indirect measurement of plant growth in the iRTG to determine crop resemblance and diversity among the two cultivation seasons.

$$HDD = \frac{(T_{max} + T_{min})}{2} - T_{base} \quad (6.1)$$

6.2.2 Volatile monitoring and CO_2 management

BVOC investigation was conducted on mature plants at first fruit ripening (82 DAT) over the whole productive stage. Emissions were concentrated in a static enclosure and trapped dynamically onto Anasorb tubes (CSC, 6 x 70 mm – 100/50 mg, SKC) at 250 mL min^{-1} constant flow using the sampling settings reported in a previous study for the determination of green bean emissions (Stringari et al., 2023). The aerial part of one tomato plant was gently enclosed in a suspended LDPE cylindrical chamber (1.16 x m diameter x 2.23 m height) to avoid mechanical injury and minimize the load of the plastic wall around the plant (Figure 6.2). In our study, we investigated the emission response to CO_2 variation because of the static enclosure. First, the inertia of the static enclosure was determined by measuring solar radiation, temperature ('T'), relative humidity ('RH'), and CO_2 fluctuation in the empty chamber over different time intervals (5 to 60 minutes). Then, the variation in CO_2 before and during plant enclosure was recorded every minute with the portable gas analyser. After 5 minutes of closure, a progressive drop in CO_2 relative to the starting concentration was observed. Therefore, short consecutive samplings of 5 (1.25 L) and 10 (2.50 L) minutes were carried out to contain alterations in constitutive plant emissions under uncontrolled CO_2 (=unadministered CO_2). Feedback on plant physiological performance was derived from 1-minute records of radiation, T, RH, and CO_2. In addition, plant photosynthetic rate ('Pn') and stomatal conductance ('g_s') were estimated based on the empirical formulas of Yin et al. (2019) and Ball et al. (1987), respectively, in absence of measuring tools.

Missing input data for the calculation of g_s were retrieved from comprehensive literature (Miner et al., 2017) based on C3 plants. The results obtained in 2021 were compared with an equivalent trial performed the following season (2022). Air samples were instead collected at CO_2 levels equivalent to the ambient, achieved by controlled CO_2 purge (≥99% purity) into the chamber throughout the length of sampling (=administered CO_2). Sampling was usually carried out between 10:00 a.m. and 1:00 p.m. (CET) because most of the greenhouse tasks were performed in the morning, and this time was thus considered the longest period of exposure to plant emissions. Throughout the season, volatile collection was repeated to provide replicates for the statistical analysis. Blank samples from a pure air cylinder were generated as benchmarks for all samples collected.

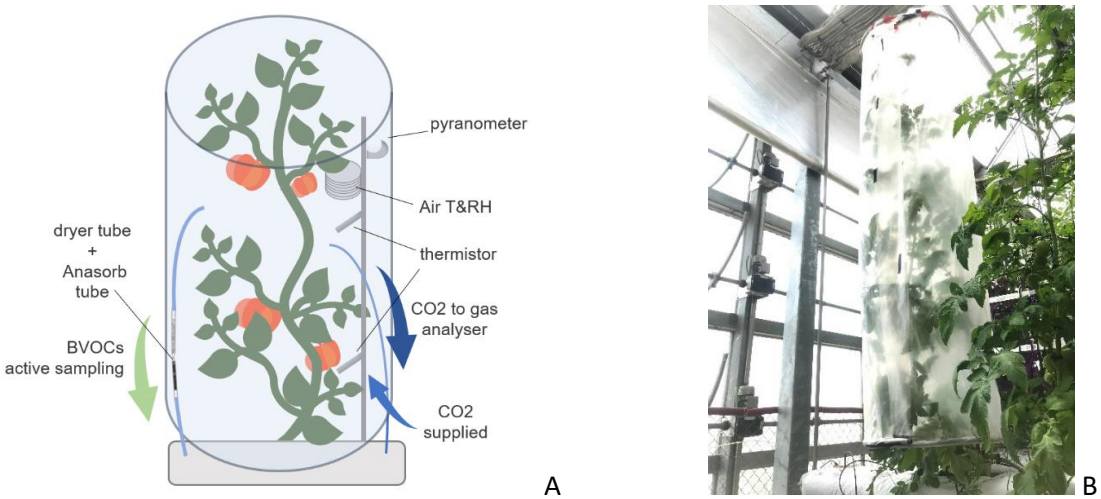

Figure 6. 2 Simplified representation of the dynamic (active) emission sampling with static enclosure, with or without CO_2 supply (A). Picture taken during the setup of the sampling chamber on a tomato plant (B).

6.2.3 Determination of selected BVOCs in the sampled emissions

Only two elective volatiles were analysed in the total emissions sampled that represented specific BVOC classes of constitutive and induced tomato plant emissions (Table A6.1): limonene for the MTs and cis-3-hexenal for the LOX derivatives.

Quantitation of BVOCs was performed following the NIOSH protocol (NIOSH, 1995) BVOCs trapped in Anasorb CSC tubes were extracted with 1 mL of liquid CS_2 (purity≥99.9%, Thermo Scientific) collected in 1.5-mL vials. Samples from 2021 were analysed using a Thermo GC-MS system (GC: TRACE 1300/1310, MS: ISQ7000, Thermo Scientific, USA) using the working conditions described elsewhere (Stringari et al., 2023). Samples obtained in 2022 were analysed using an Agilent GC-MS system (Agilent 7890A GC coupled to a 5975C MS). Calibration with external standard solutions ensured data comparability between both instruments. The instrumental conditions were maintained constant among instruments. Extract volumes of 2 µL

were injected in splitless mode (1 min, 240 °C), and BVOCs were separated using a TG-WAXMS capillary column (TraceGOLD™, 30 m x 0.32 mm x 1 µm, Thermo Scientific, USA) with a constant helium flow (3 mL min^{-1}). The GC oven programming consisted of an initial temperature step at 35 °C (held for 2 min), followed by a 10 °C min^{-1} gradient up to 215 °C (maintained for 4 min). The MS transfer line temperature was set at 250 °C, and the ion source was heated at 150 °C with 70 eV as the ionization potential. Data acquisition was performed in SIM mode to optimize instrumental sensitivity and reproducibility. Data processing and BVOC quantitation were performed with either MassHunter Workstation 10.1 (Agilent GC-MS data) or Chromeleon Software (Thermo GC-MS data). Compound identification and quantitation were performed by comparison of peak RTs and peak areas with external standard solutions as described elsewhere (Stringari et al., 2023).

In this study, the instrumental LOQ corresponds to the concentration value that can be quantified with a RSD≤ 21% upon consecutive analysis (Table A6.2). The instrumental dynamic range was typically between 10–100 ng mL^{-1}.

The calculation of the BVOC emission rate (ER_{BVOC}) was based on the canonical Equation (6.2) for the determination of the emission rate of a volatile. This is the difference between the products of the volatile emitted by the plant ($BVOC_p$, µg m^{-3}) in the sampled volume (V_c, m^3) and its amount found in a blank sample (either in the empty chamber or in scrubbed air, $BVOC_c$) divided by the product between the sampling time (h, hr) and either the fresh weight (gfw, g) of the leaves or of the total biomass (stem + leaves + fruits) enclosed, or the projected leaf area (m^2). In the results section, this is referred to as the weight of fresh leaves.

$$ER_{BVOC} = \frac{(BVOC_p \times V_c) - (BVOC_c \times V_c)}{gfw \times h} \quad (6.2)$$

6.2.4 Statistical analysis and variable impact calculation

Individual BVOC emissions were compared between the sampling intervals (5 and 10 minutes) within the same CO_2 conditions (administered or unadministered) and between the CO_2 conditions within the sampling intervals using the Wilcox test (paired or unpaired). Dependencies and independencies between the variation rates of monitored and predicted variables (radiation, T, RH, and CO_2 concentration) were also compared using linear regression models and ANOVA tests (type II). The relationships between the sampled BVOC emissions at the 5- and 10-minute intervals of each CO_2 assay and the considered variables were preliminarily assessed through principal component analysis (PCA). Finally, the variation rates of both

emissions and variables were log-transformed before their computation in paired plot matrices for the determination of the correlation coefficient (r_s). Differences were assigned as significant at a probability value $p \leq 0.05$, and correlations were considered meaningful at a r_s coefficient comprised between ±0.50 and ±1 and significant at a probability value $p \leq 0.05$. All tests were performed with R software (version 4.2.2). r_s

6.3 Results

6.3.1 Crop heat accumulation and growth during the two cultivation seasons

The sum of the HDDs calculated from the DAT in the iRTG until the last sampling day for each of the two experimental seasons (Figure A6.3) was significantly higher (p= 0.001) in 2021 (3039.82) than in 2022 (2323.41). In detail, comparing the maximum and minimum T rates of the two periods, there was a significant difference (p= 0.001) between the T_{max} average of 2022 (37.12°C) and 2021 (32.81°C). In fact, BVOC collection in 2022 covered approximately one week less than in 2021, and it was concluded 21 days before the last day of sampling in 2021. Considering plant morphological development over the growing cycles (Table A6.4), the mean total fresh biomass (stem + leaves + fruits) measured in 2021 was significantly higher (4.23 kg, p= 0.007) than that measured in 2022 (3.08 kg). However, comparing individual organ weights, the overall difference was provided only by the mean weight of fruits (p= 0.002), rather than that of leaves or stem.

6.3.2 BVOC emission rates and amounts in the iRTG with respect to indoor LCI values

Average emission rates (ERs) for the two volatiles at both the 5- and 10-minute sampling intervals under the two different CO_2 assays are reported in Figure 6.3 and summarized in Table A6.5.1 and A6.5.2.

During the two experimental seasons, MT-limonene was usually detected under both the administered and unadministered CO_2 assays, while LOX-cis-3-hexenal was detected only under administered CO_2. The emissions of both volatiles were higher in the first 5 minutes than in the following 10. Between short and long sampling intervals there was no significant difference in the levels of limonene (p> 0.1) in either of the two CO_2 assays, whereas a significant difference was observed in those of cis-3-hexenal (p= 0.002). Overall, Limonene emissions were substantially higher but not significantly different under the administered assay. Moreover, under the same condition, MT emissions were on average the most abundant in both the 5- and 10-minute samples, accounting for 65.2% and 72.8%, respectively, compared to LOX emissions, which accounted for 34.8% and 27.2%, respectively. Likewise, the average minimum and maximum percentages collected during 5 and 10 minutes were 44.4–78.9% and 50–87.2% for

limonene and 21–55.6% and 12.8–50% for cis-3-hexenal, respectively. Considering the calculated ERs (Table A6.5.1 and A6.5.2), for the constitutive MT, the highest amount was reported under unadministered CO_2 (1752.19 ng g^{-1} h^{-1}), while for the induced LOX, it was reported under the administered assay (181.8 ng g^{-1} h^{-1}).

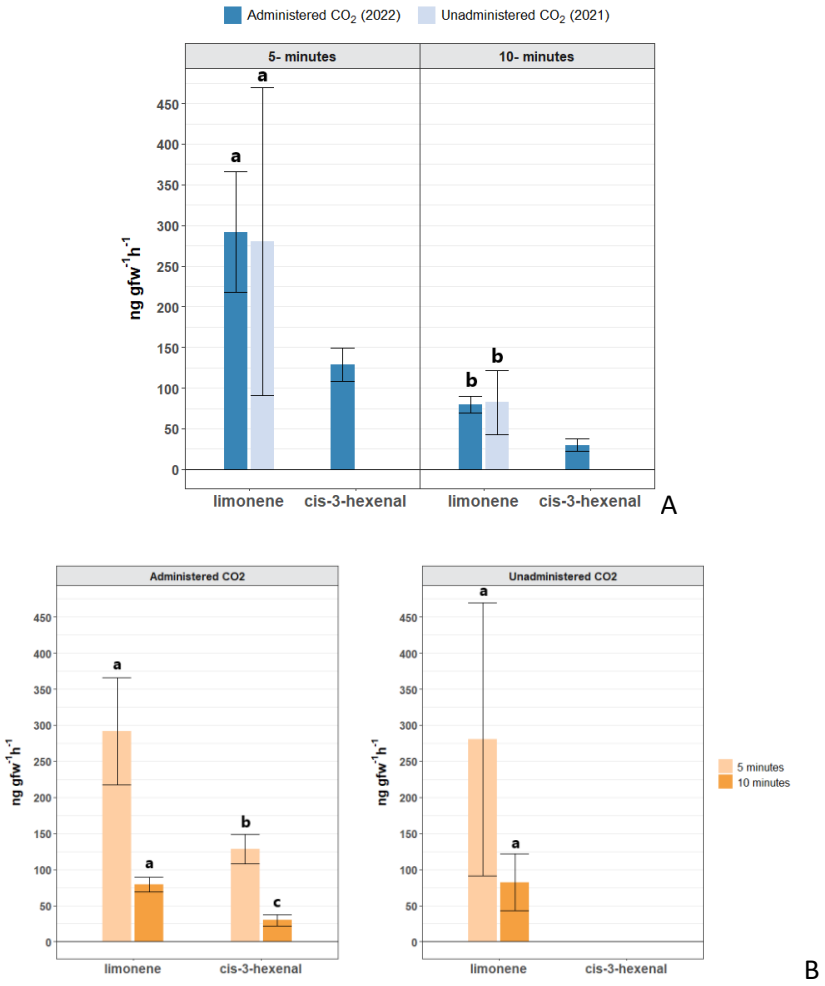

Figure 6. 3 Average ± SEM (n=9, 2021; n=5, 2022) ERs of the MT (limonene) and LOX derivative (cis-3-hexenal) detected in the static enclosure containing one mature plant at 5- and 10-minute sampling intervals under different CO_2 assays. Different lowercase letters indicate significantly different emissions ($p \leq 0.05$); average ERs of the single volatile are compared between the CO_2 assays within the same sampling interval (A) or between the sampling intervals within the same CO_2 assay (B).

6.3.3 Enclosure performance prior to emission sampling

The tested inertia of the empty chamber provided no significant variation in the measured radiation, T, RH, and CO_2 concentration during the whole enclosure time (up to 60 minutes). Radiation inside and outside the chamber did not vary significantly. Over the whole cycle, radiation recorded at the crop level (Table A6.6) was approximately 29% (2021) and 48% (2022) of the total radiation measured 2 m above the canopy, which was far below the standard illumination supplied in other greenhouses (Jansen et al., 2010; Kasal-Slavik et al., 2017; Daussy and Staudt, 2020). However, according to previous assessments performed on this iRTG

(Montero et al., 2017), such rates were still consistent with those found in common greenhouses and would ensure plant photosynthetic activity. Therefore, the effect of radiation on CO_2 assimilation was not contemplated henceforth.

6.3.4 Comparison of environmental and physiological trends across different CO_2 assays

Across the CO_2 assays, between 5- and 10-minute sampling intervals no significant differences ($p > 0.1$) were highlighted in the mean values (Table A6.6 and A6.7) of both the monitored and predicted variables. However, between the assays significantly higher levels of RH and g_s under the unadministered condition were observed at both 5- (+16%, $p = 0.04$) and 10- (+18%, $p = 0.02$) minutes sampling for RH, at 10 minutes only (+124 mmol m^{-2} s^{-1}, $p = 0.02$) for g_s. Figure 6.4 reports variables performance in relation to the CO_2 tendency during the enclosing time. According to the mean values registered, with respect to the iRTG concentration by the end of the first and the second sampling term CO_2 decreased up to 14 and 30 ppm under the unadministered condition and increased up to 8 and 11 ppm under the administered one. However, according to the variation rates, a general CO_2 drop was always observed within the first 5 minutes of enclosure across both the assays. Although the decrease was higher under unadministered (-57.01 ppm) than under unadministered (-17.60 ppm) CO_2 it was not statistically significant ($p = 0.24$). However, on the overall 10 minutes CO_2 decrease under the first condition (-69.04 ppm) was then significantly higher ($p=0.042$) than under the second one (-11.22 ppm) where partial recovery of CO_2 (+6.38 ppm) occurred. Considering T and RH, throughout the sampling a progressive increase was registered under both CO_2 assays, with overall higher RH increase (±18%) than T one (±1.50 °C). Despite slightly higher rates observed under the unadministered (0.40-0.80 °C; 9.70–11.57%) than under the administered condition (0.23–0.41 °C; 2.15-3.64%) no significant differences ($p > 0.05$) wefaçadee individuated. Consistent with CO_2 trend, also predicted Pn and g_s were found to decrease along the sampling. Within the individual assay substantial Pn and g_s decrease was higher under administered CO_2 (-21.53–22.91 µmol CO_2 m^{-2} s^{-1} and -413–442.72 mmol m^{-2} s^{-1}) rather than the unadministered condition (-6.40–10.38 µmol CO_2 m^{-2} s^{-1} and -64.39–161.41 mmol m^{-2} s^{-1}). However, their variation rates of between the assays were not significantly different.

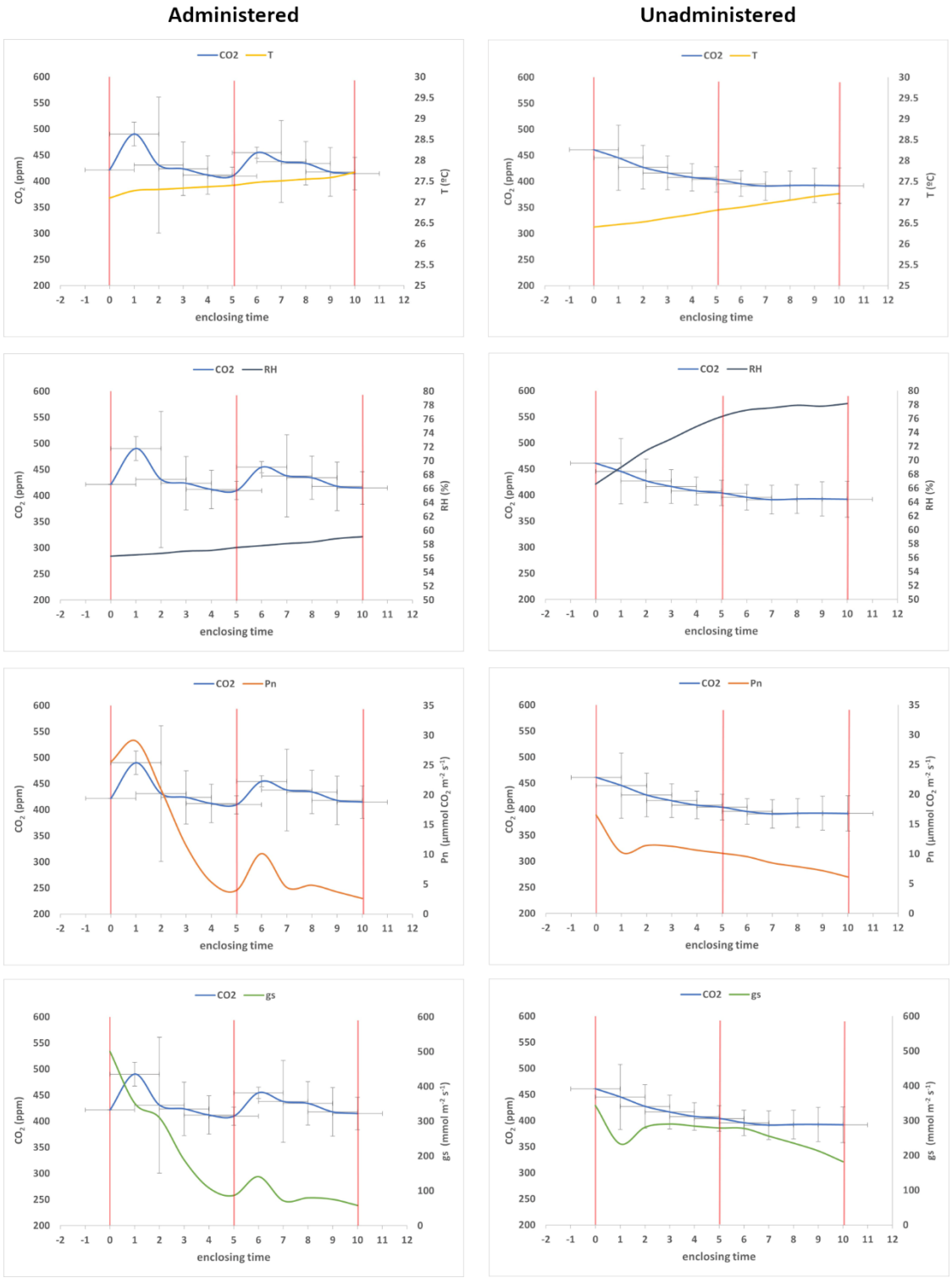

Figure 6. 4 Mean ± SD of CO_2 levels interpolated with the environmental (T and RH) and physiological (Pn and g_s) variables monitored and predicted under administered (left) and unadministered (right) CO_2 condition along plant enclosure sampling. Red bars delimit the principal sampling intervals considered (5- and 10- minutes).

6.3.4 Implication of the CO_2 assay on plant emissions and the enclosing conditions

Exploratory principal component analysis (PCA) scores and data distribution (Figure A6.8 and Table A6.9) revealed that emissions collected under administered CO_2 were primarily related to

environmental factors, especially those sampled within the 5-minute interval and mostly for the LOX volatile. T and CO_2 emerged as the main relevant variables, while Pn, g_s, and RH in this order showed less influence. Conversely, the data suggested little to no relationship between environmental and physiological factors and MT emissions.

Correlations between the five variables monitored and predicted are shown in Figure A6.10 of Annex III. Between constitutive and induced emissions there were no relationships ($r_s \leq 0.40$) under any of the CO_2 assays. Between the emissions and the five variables, there were correlations only under administered CO_2. There were negative correlations between MT emission and increasing T ($r_s = -0.60$) and RH ($r_s = -0.50$), respectively in the first and in the second sampling interval. There was a positive correlation between LOX emission and decreasing CO_2 ($r_s = 0.60$) in the second interval only. Among the variables several correlations were additionally individuated (Figure A6.10). Within the 5 and the total 10 minutes of sampling T and RH were significantly positively correlated (r_s=0.67 and 0.73, $p \leq 0.01$) and mutually explained their increasing rate ($p = 0.03$ and $p = 0.01$) under unadministered CO_2, whereas this was not found under the administered condition. The variation of CO_2 appeared to be uncorrelated with T and RH in any of the two cases. However, significant positive correlations with CO_2 were found under unadministered CO_2 for the whole enclosure time with Pn (r_s=0.78 and 0.73, $p \leq 0.01$) and g_s (r_s=0.58 and 0.68, $p \leq 0.05$ and 0.01). Decreasing CO_2 levels also explained significantly ($p \leq 0.01$ and 0.05) and partially significantly ($p \leq 0.03$ and $p = 0.07$) both Pn and g_s variations, respectively. These correlations were however not highlighted under administered CO_2, where instead both Pn and gs were correlated with T in the first sampling term and with RH in both the terms. The relationship was negative (r_s=-0.70) with the first but positive (r_s=0.5 and 0.90, $p \leq 0.01$) with the second. In contrast to CO_2 in the unadministered assay, in this case none of the variables explained ($p \geq 0.05$) the variation rates of the physiological variables.

6.4 Discussion

6.4.1 Effects of CO_2 conditions on plant emissions during the two sampling intervals

The aim of this study was to assess tomato plant emissions in an iRTG and compare them to existing LCI values and levels found in previous assessments to evaluate the potential harm to human health in the iRTG and in the offices where this air could be recirculated. Short sampling intervals of 5 and 10 minutes were used to investigate the impact of CO_2, comparing two sampling conditions: controlled (=administered) and uncontrolled (=unadministered) environmental CO_2 levels. The study also measured HDDs as a function of plant development during each separate season, which significantly differed only in terms of average T_{max} that was

higher during the experiment performed with the administration of CO_2. However, the weight of traditional emitting biomass (leaves and stem), excepting the fruits, remained similar throughout the cycles. These preliminary outcomes suggested that investigated crops were rather similar, therefore emission variations were researched in the corresponding sampling conditions.

Similar MT-limonene emissions were found across the different CO_2 assays. However, administration of CO_2 affected the detection of LOX-cis-3-hexenal volatiles, with significant differences observed between the two intervals. Overall, average emissions were higher in 5-minute samples and under administered CO_2. The most abundant and ubiquitous volatile was MT-limonene. Nevertheless, the highest emission recorded in the iRTG (50.88 µg m^{-3}) over the 2021 season was approximately one order of magnitude lower than the corresponding EU-LCI (5000 µg m^{-3}). Likewise, the highest LOX emission was at least eightfold lower (6.63 µg m^{-3}) than that of the MT. Comparing these levels with resembling studies on tomato emission assessment in greenhouse environments (Jansen et al., 2009; Takayama et al., 2012), there were some consistencies. In our iRTG limonene and cis-3-hexenal levels were comprised between 0.01–9.13 and 0.27–1.65 ppb, respectively, which fell within the intervals found by Jansen et al. (2009) under normal or stressed conditions (0.035–40.4 ppb for MTs and 0–20 ppb for LOX volatiles). Under similar experimental conditions (open bottom chamber and similar inner CO_2 trends), Takayama et al. (2012) retrieved for terpenes and LOX derivatives emission indices (EIs) at steady and stressed condition. Higher EI (> 3) was reported for terpenes than for LOX compounds in the first condition, then much lower EI (< 2) for the first ones was measured than the second ones (EI> 6) during the stress occurrence. In contrast to these results equivalent limonene and cis-3-hexenal EIs measured under our CO_2 assays were substantially similar (< 3).

Typically, emissions of MTs are observed to increase in response to a quasilinear T gradient (Niinemets and Reichstein, 2003; Loreto and Schnitzler, 2010) within a tolerant range for the plants before experiencing structural damages which may affect the normal emission activity. However, studies have reported emission disruptions due to occasional or prolonged T increases (Dani et al., 2014).

With respect to CO_2, the relatively few studies conducted on the emission responses at determined CO_2 concentrations provided conflicting or not fully consistent results (Calfapietra et al., 2013a). Physiological MT emission is generally slowed by increasing CO_2, as terpene production implies the activation of the same enzymatic system involved in the transportation of O_2 during photosynthesis (Peñuelas and Llusià, 1997; Niinemets et al., 2004, 2013; Loreto and Schnitzler, 2010; Dani et al., 2014). However, it was generally observed that supplying CO_2 up to

normal ambient concentrations (~400 ppm) did not have a relevant impact on MTs and overall emission feedback unless T rose without exceeding damage thresholds (over 35 °C and up to 47 °C) (Räisänen et al., 2008; Velikova et al., 2009; Tiiva et al., 2017; Daussy and Staudt, 2020). In contrast, applying high CO_2 concentrations (> 800 ppm) at high T would decrease overall emissions (Räisänen et al., 2008; Dani et al., 2014; Daussy and Staudt, 2020).

In our case, under administered CO_2 flush within the first 5 minutes, the relationship between the positive T gradient and limonene emissions was found to be unexpectedly negative, and no relationship at all was found with increasing RH or with (decreasing) CO_2 levels. Conversely, despite CO_2 decrease, ERs were still slightly higher within 5 minutes than after CO_2 stabilization achieved after until the end of sampling. In this second interval, MT were instead negatively correlated with the increasing RH rather than with T and still uncorrelated with CO_2. Under unadministered CO_2, no relationship was found with the constitutive emissions, but negative correlation between T and RH was maintained throughout the sampling, as well as the positive correlation between overall decreasing CO_2, Pn and g_s. Based on these outcomes, it could be rationally assumed that T and RH had a relevant implication on the MT emission response when no administration is applied. The increase of RH has been traditionally associated with a common issue individuated during volatile sampling in static enclosures. As reported by experimental tests (Niinemets et al., 2011; Pérez-Priego et al., 2015; Li et al., 2019), within a relatively short timeframe (3 minutes), despite preconditioning and thorough sampling, RH levels can increase quickly due to instant plant transpiration substantially affecting both the plant's regular emittance and the goodness of the emission sampled [89–91]. This condition would be confirmed in our study by the tight correlations found between physiological Pn and g_s and the CO_2 variation that even explained the two variables. On the other hand, under the administered condition the highest T and RH registered (T_{max}= 32 °C, RH_{max} 60%) were much below extreme levels reported, plus no correlation was found between CO_2 rates and the physiological response (Pn and g_s decrease). This suggested that supplying CO_2 up to fixed environmental levels perhaps mitigates the quenching action of RH on plant emission release and sampling bias. However, beyond 5 minutes, sampling constitutive emissions can be tricky making the sample less reliable due to the loss of stable conditions inside the static enclosure.

LOX emissions have been extensively investigated in field studies, and they have been found to be rapidly released following an abiotic or biotic stress event, usually associated with mechanical injury of the cellular structure. Instead, MT emissions are mostly subordinated to T under a characteristic slow and extended release (Herrmann, 2010; Maffei, 2010; Calfapietra et al., 2013b; Niinemets et al., 2013; Copolovici et al., 2014; Mozaffar et al., 2018). Currently, the

relationship between LOX emissions and the variation of CO_2 is unclear, mainly due to the few investigations on this topic. So far, there was no evidence of a correlation between high CO_2 levels (720 µmol mol^{-1}) and these volatiles in comparison with environmental CO_2 concentration. Furthermore, even the combination of a mechanical stressor (insect chewing) with each of these two conditions (high and ambient CO_2 levels), missed this correlation. (Vuorinen et al., 2004; Herrmann, 2010). It was also unclear the positive feedback of combined increasing T (below stress thresholds) and ambient CO_2 levels, though hypothesis was scarcely supported due to the lower correlation between LOX volatiles and T compared to the MTs (Maffei, 2010; Pazouki et al., 2016). There were exceptions, such as in the case of tomato, where Copolovici et al. (2012) found direct correlation with the increase of LOX emission and T under normal CO_2 concentration starting from chilling and heating degrees (-7 °C and 49 °C) because of a breakage in the cell membrane. However, further field studies (Degenhardt et al., 2010; Pazouki et al., 2016) found out that stress-induced LOX emissions were quite common and independent of T increases.

In the case study, under administered CO_2, the significantly higher rates of LOX emissions collected in the short sampling interval were strongly correlated with the initial CO_2 drop and still correlated when restoration of pre-sampling levels was achieved (10 minutes). Conversely, it should be noted that without CO_2 supply, emissions were not detected. It is important to consider that the occurrence or absence of LOX compounds is likely due to a stress event, which may include a combination of environmental factors such as T, RH, and CO_2 concentration. In the case of tomato plants, the connection between these volatiles and the type of elicitor (Farag and Paré, 2002; Degenhardt et al., 2010; Pazouki et al., 2016; Kasal-Slavik et al., 2017) and the role of the LOX kinetic response in the expression and the total amount of volatile released has been demonstrated (A C Heiden et al., 2003). Therefore, based on the reviewed literature, the inverse correlation between progressive CO_2 decrease plus significantly higher RH rates and LOX emissions could be hypothesized even if it was not determined. Conversely, MTs were generally found to be the most abundant and far ubiquitous under multiple stress conditions (Jansen et al., 2009; Falara et al., 2011; Pazouki et al., 2016; Kasal-Slavik et al., 2017). According to these findings and given the much higher gradient of RH (up to 71.9% at min 5 and up to 79.4% at min 10) under uncontrolled rather than controlled CO_2 assays, RH could again be considered the determining factor in the fulfilment of LOX-cis-3-hexenal collection. Eventually, RH may also be determined as the driving factor in the modulation of the stress response in plants.

6.5 Conclusions

In this study, it was observed that BVOC emissions generally decreased over extended sampling under both unadministered and administered CO_2. Similar variations of Pn and g_s observed

between the two assays suggested a similar physiological performance under the different CO_2 conditions. However, in the unadministered assay the progressive decrease of CO_2 appeared to be tightly connected with the decrease of both the physiological variables. Even if no relationships were found between constitutive nor induced BVOCs and the variation of these variables (Pn, g_s, and CO_2) lower emissions collected under this condition suggested, indirectly, the impact of low CO_2 concentration on overall plant emission activity. On the other hand, in the administered assay positive correlations individuated among increasing CO_2 and LOX emissions also suggested the implication of this variable on the release of induced emissions. Conversely, the absence of correlations with MTs made difficult to assess the actual impact of CO_2 on constitutive emissions.

Furthermore, it has been observed a significant implication of the increase of RHon both MT and LOX emissions under unadministered condition that was likely to be connected to the sampling set up, as demonstrated in the literature. Instead, this effect was not fully individuated under administered condition where indeed lower RH levels were observed and that were positively correlated with plant physiological response.

It could be reasonably assumed but not confirmed, then, that under administered condition CO_2 supply partially contributed on plant BVOCs emission, whereas under unadministered condition its contribution remained unclear and was rather prevailed by RH factor. To fill this gap, altogether proper adjustments of the sampling setting and accurate monitoring of all the variables involved may improve the performance of static sampling and reduce technical issues responsible of errors and incorrect BVOCs estimation.

Overall, monoterpene and lipoxygenase derivatives emissions released by tomato plants in an iRTG at environmental conditions (T, RH, radiation, and CO_2) are expected to be safe over longer periods of exposure. However, it should be noted that further research would be needed to confirm measured BVOC levels since for many of them referencing EU-LCI values are currently still missing (e.g., LOX derivatives). In addition, based on the configuration of the building, designed air recirculation in the closed spaces of the lower floors for energy and quality purposes is likely to be implemented in the future without bringing about dangerous conditions for human health.

Chapter 7

Biogenic volatile organic compounds emitted by basil grown in a vertical farm under two different red:blue LED ratios

Based on a scientific investigation conducted[1]

[1] Co-authors participating in the experiment and the analyses reported in this chapter: Gaia Stringari, Joan Villanueva, Laura Carotti, Ilaria Zauli, Andrea D'Aprile, Alessandro Pistillo, Giuseppina Pennisi, Francesco Orsini, Xavier Gabarrell

Chapter 7: Biogenic volatile organic compounds emitted by basil grown in a vertical farm under two different red:blue LED ratios

Abstract

Vertical Farms are becoming cutting-edge solutions for local food production, where integrated LED lighting has potential to improve both yield and quality of the cultivated crop, as in the case of basil plant. Indoor, the concentration of plant's BVOCs can easily increase, affecting the air quality. In this study we investigated the effect of two red and blue light ratio, namely, RB_1 and RB_3, on the BVOC emissions of basil grown in an indoor VF, comparing levels found with the LCIs given in the European Regulation. Emissions were collected in the young and mature plant stage at static conditions along consecutive intervals of 5-, 10- and 15-minutes, monitoring physiological and environmental parameters throughout. Selected compounds of the class of MT, OMT, ST, PH, and LOX derivative were investigated in the collected blend. BVOC emissions were generally higher under RB_1 light in the young stage and under RB_3 at plant maturity. However, while higher LOX derivatives emissions were observed in young RB_1 plants, mature plants exposed to RB_3 presented increased MT-cymene and OMT-1.8-cineole emissions. Overall, during the sampling under both light treatments and plant stages increasing temperature and relative humidity were found to negatively affect BVOC emissions and associated stomatal conductance. In fact, emissions were usually higher in the first interval and decreased over time. In contrast, the relationship with the slight variations of CO_2 observed remained unclear. Despite similar trends measured under the different light treatment, stomatal conductance was usually higher under RB_3 along with higher BVOC emissions, suggesting red light predominancy on the volatile response. On average BVOC emissions remained much below reference LCIs (10 $\mu g\ m^{-3}$). Individual LOX emissions were found to exceed the given threshold under RB_1 light only and once. Bursts of STs and OMT were occasionally collected, mostly in the mature stage, but were not sufficient to define the emissions pattern. Therefore, considering low levels found and related exposure effects we believed as worst-case scenario a sensitization to the highest emissions released, suggesting overall safe in terms of air quality the cultivation of basil in indoor VF.

7.1 Introduction

The implementation of innovative cultivation systems based on the soilless techniques (Barrett et al., 2016; Saha et al., 2016; Banerjee et al., 2022) improved the performance of agriculture and its integration in the urban environment, especially indoor (D'Ostuni et al., 2022). Among these, indoor VFs promoted the incorporation of latest technologies (Delorme and Santini, 2022;

Popkova, 2022; Q. Yang et al., 2023) bringing several benefits to traditional food production. Most of them are connected with resource's optimization provided for instance by the HVAC systems and the water (Kozai and Niu, 2016; F. Orsini et al., 2020; Engler and Krarti, 2021; Naranjani et al., 2022), recirculation that will improve energy saving and cultivation yield, reducing related costs and environmental impacts (Shao et al., 2021a; Martin et al., 2022; Tablada and Kosorić, 2022). Furthermore, VFs are often associated with improved local food production and accessibility (Pinstrup-Andersen, 2018; Shao et al., 2022). However, start-up and maintenance costs (Gumisiriza et al., 2022; Shao et al., 2022) often make challenging their implementation, which careful evaluations, such as the choice of best crops and optimal growing conditions (Wada et al., 2019; Kobayashi et al., 2022; Wang and Iddio, 2022), can dampen. Indoor vertical farming allows, indeed, a better management of the environmental parameters (e.g., temperature, humidity, and light) over the whole cultivation period (Weidner et al., 2021; Wang and Iddio, 2022). To date, VF is mostly applied to leafy plants and microgreens (Nicole et al., 2019; Wong et al., 2020b), owed to their short cycle and small size.

The cultivation of basil plant (*Ocimum basilicum* L.) in indoor VFs has recently become a fashion, thanks to its elevate value in the food market and reduced growing requirements (Bušić et al., 2014; Bajomo et al., 2022; Srbinovska et al., 2023). Basil's Essential Oil (EO) is rich in a wide range of distinctive BVOCs (Calfapietra et al., 2013b) traditionally associated with medicine and cuisine (Pandey et al., 2016; Bajomo et al., 2022; Tangpao et al., 2022). Leaf maturity (Fischer et al., 2011) and plant developmental stage (Chutimanukul et al., 2022) are strongly connected with EO composition and amount. Progressive light intensities stimulate the production of characteristic terpenes (Chang et al., 2008; Dou et al., 2018; Walters et al., 2021), although specific wavelengths can sensibly affect not only the EO contained in the leaves but also the release of BVOCs into the environment (Carvalho et al., 2016; Matysiak and Kowalski, 2019; Pennisi et al., 2019; Lauria et al., 2023).

Due to the low air turnover of indoor VFs (Yuan et al., 2019; Prabhakaran et al., 2022) BVOC levels may eventually exacerbate (Niinemets and Peñuelas, 2008; Yang et al., 2009a; Wang et al., 2014). In the open environment total released isoprene can reach up to 750 Tg $year^{-1}$ (Guenther et al., 2006; Duhl et al., 2008) and constitute most of the VOC emissions globally (Fisch, 2004; Drewer et al., 2018). Beside the positive effects on the plant ecosystem (Bouwmeester et al., 2019), BVOCs also contribute to increase the concentration of atmospheric pollutants, namely, NO_x, N_2O and OH^- (Peñuelas and Staudt, 2010; Kulmala et al., 2013; Duan et al., 2023), affecting air quality. For many species like basil their release is regulated by the stomata, where volatiles are accumulated and stocked in liquid form. Stomata opening is driven by the light (Owen et al.,

2002; Loreto et al., 2006), and on the water and CO_2 fluxes (Niinemets and Reichstein, 2003). However, emission also intrinsically depends on the nature and on the Henry's law constant of the volatile itself, as well as on the leaf anatomy, and on the in/out pressure excited on the stomata controlling the volatilization of BVOCs (Harley, 2013).

Despite described effects of LED technology on the metabolic patterns of basil plant, about the emission release some studies (Carvalho et al., 2016; Jensen et al., 2018; Pennisi et al., 2019) provided results not fully consistent with the literature on stomatal activity, leaving uncertainties behind the true mechanism modulating its response. In addition, most of the volatile assessments conducted on basil plant were carried out in the post-harvest, whether on intact leaves in small chambers (Carvalho et al., 2016; Trettel et al., 2017; Hammock et al., 2021; Lauria et al., 2023) or on smashed tissue properly extracted (Klimánková et al., 2008; Fischer et al., 2011; Jensen et al., 2018; Pennisi et al., 2019; Walters et al., 2021; Chutimanukul et al., 2022), so that actual emissions released into the surrounding environment could be significantly different. Furthermore, little is known about the environmental levels, as most of the measurements did not contemplate the emissions impact on the air quality where the cultivation of basil was carried out.

Given the relevance of LED light in the control of the qualitative traits of basil, its simplicity and cost-effectiveness, the systems adopting this technology are expected to increase fast in the next years (Benkeand Tomkins, 2017; Graamans et al., 2018; Wang and Iddio, 2022). For this reason, monitoring indoor emissions becomes important to ensure the compliance of such spaces with actual Regulations (ECA, 2020; European Parliament, 2021). From these perspectives, we carried out a real-time assessment of the BVOC emissions of basil plant cultivated in an indoor VF located in the peri-urban area of Bologna (Italy) (Carotti et al., 2023). Plant emissions were collected under two elective LED treatments in the spectral region of red and blue over the entire plant cycle. Our objectives were the elucidation of red and blue light effects on the emission response of this plant species, and the quantification of the detected BVOCs in relation to the LCIs determined by the ECA (Report no.29; 2013) and further levels reported in open databanks and updated by the ECHA (2023).

7.2 Materials and methods

7.2.1 The vertical farm system and the plant material

The experiment was performed in the *AlmaVFarm*, an experimental VF located in the Department of Agricultural and Food Sciences (DISTAL) of Bologna University (Italy) (Carotti et al., 2023). The space consisted in a controlled growth room (45 m^2) arranged in 22 cultivation

sectors, of which 12 equipped with a high pressure aeroponics (Frm srl, Rovereto, TN, Italy), distributed among 3 individual levels providing each a cultivation surface of 0.53 m^2. On the top of each level LED lamps (Flytech s.r.l., Belluno, Italy) featuring red (peak at 669 nm, OSRAM Hyper Red) and blue (peak at 465 nm, OSRAM Blue) wavelengths (OSRAM, 2017a, 2017b) were set with a PPFD of 200 µmol m^{-2} s^{-1} and a common light/dark photoperiod of 16/8 h d^{-1}. Lamps performance was assessed on the electricity absorbance (W = J s^{-1}) measured with a multimeter (Fluke 189, Fluke Corporation, Everett, WA, United States) and the PPFD with an Extended PAR meter (model MQ-610, Apogee Instruments, Logan, UT, United States). LED treatments were characterized by two RB ratios, 1 and 3 referred as RB_1 and RB_3, respectively. Ratio between red and blue portions was calculated by defining the relative areas of the spectrum within the red (600–700 nm) and the blue (400–500 nm) regions (Singh et al., 2015). In total, two cultivation sectors were used for the experiment, each consisting of 3 cultivation layers. Aeroponic fertigation consisted in a closed-loop pumping system, pressurized at 70 bar, and nebulized to the roots for 60 seconds every 15 minutes by nozzles (orifice = 0.2 mm) located below the cultivation tray (4 nozzles for each cultivation tray). Water (nutrient solution: N-NO_3: 16.0 mM, N-NH_4: 2.0 mM, P: 2.0 mM, K: 10.0 mM, S: 2.5 mM, Ca: 4.5 mM, Mg: 1.0 mM, Fe: 40.0 µM, Cu: 1.0 µM, Zn: 5.0 µM, B: 30.0 µM, Mn: 5.0 µM, Mo: 1.0 µM) pH (5.9 $\pm$ 0.2) and EC (2.3 dS m^{-1} $\pm$ 0.2) were frequently monitored (96 times day^{-1}) and eventually corrected by a fertigator (NidoPro®, LogicSun, Cattolica, RN, Italy). Environmental conditions of the VF were regulated by a remote HVAC system (Monti&C srl, Borgo a Buggiano, PT, Italy) able to recover the water transpired and to renovate periodically 0.03 m^3 h^{-1} of the internal air. During the experiment, conditions were adjusted at day/night temperature of 24/21 ± 1°C and relative humidity of 70/75 ±10%, settled at 850 ppm of CO_2 concentration oscillating between 1000 and 1400 ppm along the cultivation levels, and at an air renovation of 0.03 m^3 h^{-1}.

Basil (*Ocimum basilicum* L. var. Italiano classico) was the plant selected for the study because of the high relevance in the Italian food market and the expertise gained upon indoor cultivation. 160 plugs of a biodegradable polymer (GROWFOAM®, Foamplant BV, Groningen, The Netherlands) contained in plastic net-pots were sowed with 2-3 seeds and positioned in a germination sector below RB_3 light (200 µmol m^{-2} s^{-1} e 16/8 h d^{-1} light/dark photoperiod) until occurrence of second true leaf (14 days). Aeroponic irrigation and light's intensity and photoperiod were set on the same conditions of the chosen cultivation sectors. Before the transfer to the growing sector extra plants were thinned out to provide one plant per pot. Seedlings were then distributed along the 3 levels of each light treatment, equally spaced (5 cm) over 55 central holes of the cultivation tray to receive homogeneous radiation, for a total plant

density of 104 plant m^{-2} (Pennisi et al., 2019). Plants were let developing for the following 40 days at the conditions of the farm.

7.2.2 Plant emission collection and monitored parameters

Streamlined representation of the sampling system is reported in Figure 7.1. The middle level of each RB_1 and RB_3 light treatment was sealed with a transparent LDPE cloth keeping the frontal long side open during the cultivation time that was closed only for the collection of plant emissions. The enclosing volume measured approximately 0.173 m^3 or 172.5 L (1.25 m length x 0.23 m height x 0.60 m width). Throughout the closing time inner environmental conditions were tracked continuously: T (°C) and RH (%) with wireless datalogger (model BL30, Trotec GmbH, China), CO_2 concentration (ppm) with a CARBOCAP® probe (Vaisala GMP343 ±0.5 % accuracy, Finland) and stomatal conductance (g_s, µmol m^{-2} s^{-1}) with a tweezer porometer (AP4, Delta-T Devices, Cambridge, UK) as indicator of leaves gaseous exchange. Additionally, CO_2 was supplied regularly through pure gas bottles under controlled management to sustain plant photosynthetic activity. Volatiles collection was achieved in static condition through dynamic sampling with coconut-shell charcoal sorbents (Anasorb: CSC, 6 x 70 mm – 100/50 mg; SKC) joined to dryer tubes (6 x 70 mm, 250 mg, 10/60 mesh; SKC) under fixed 0.25 L min^{-1} suction flow. Air measurements were taken at short intervals of 5 (1.25 L), 10 (2.5 L) and 15 (3.75 L) minutes to minimize the enclosing effect on targeted constitutive emissions, released at the normal farming conditions. Sampling was performed twice over the crop cycle collecting three replicates every time, respectively within 30-32 and 36-39 Day After Sowing (DAS) that corresponded to the developing (=young) and fully developed (=mature) stage. These terms were individuated after weekly tasks of stem sizing and leaves counting.

At the end of each sampling, 5 random plants from each LED treatment were harvested from the above or below level of the line and weighed first on their whole, then leaves and stem individually. Additionally, the projected leaves area was measured with a free mobile application Easy Leaf Area (University of California). Finally, fresh biomass was dried at 60 °C for three days in static oven to get corresponding dry weights.

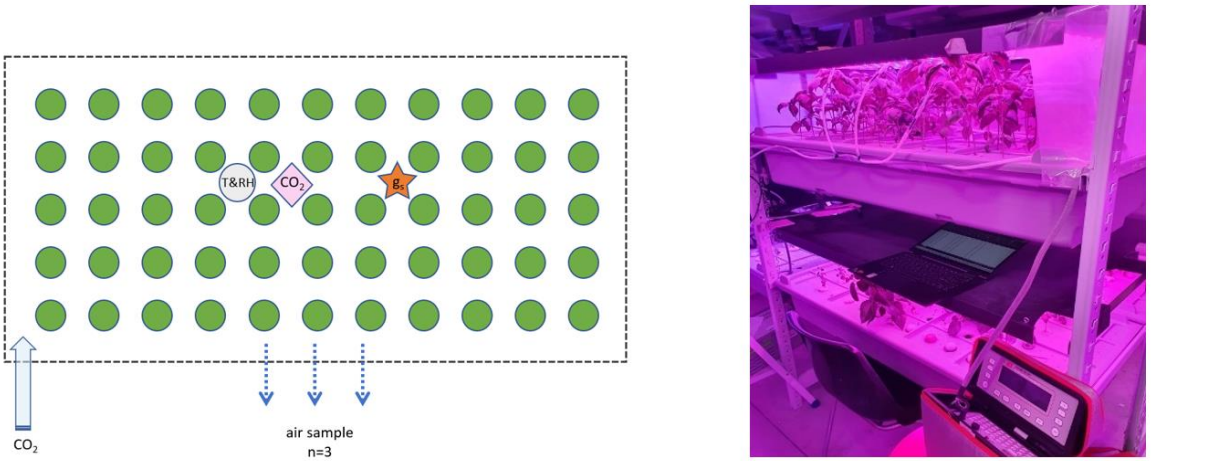

A.1 A.2

Figure 7. 1 A picture (A.2) of the volatile sampling set-up and its implementation and its simplified representation (A.1): sensors monitoring T&RH (green circle), CO_2 concentration (pink square) and g_s (orange star); reintegrated CO_2 (block arrow) and the total air samples taken (line arrows).

7.2.3 Post sampling analysis

5-, 10- and 15- minutes samples were all liquid extracted following NIOSH (1995) analytical protocol for terpene volatiles. Briefly, 1 mL of carbon disulfide (CS_2 for spectroscopy, ≥99.9%, Thermo Scientific) and the adsorbent material were collected in 1.5 mL vials and occasionally soaked 30 min prior to chromatographic analysis. From each extracted solution an aliquot of 2 µL was split-less injected (1 min, 240 °C) in the TG-WAXMS capillary column (TraceGOLDTM, 30 m x 0.32 mm x 1 µm, Thermo Scientific, USA) of the 7890A GC coupled to the 5975C inert MS (both Agilent Technologies, USA) and carried over at constant 3 mL min^{-1} flow by helium gas. GC ramp was set at an initial temperature of 35 °C for 2 min, followed by 10 °C min^{-1} gradient up to a final temperature of 215 °C for 4 min. MS transfer temperature was fixed at 250 °C and at 150 °C in the ion source; in the ion detector (70 eV) identification was carried out in scan mode at 50-550 amu (2.9 scan s^{-1}). 9 representative compounds out of the total BVOCs mixture were determined, based on standard solutions prepared with liquid CS_2 and external analytes (purity > 90%, TCI America), respectively: 1.8-cineole (OMT), a and β-pinene, β-myrcene and o-cymene (MTs), β-caryophyllene and trans-β-farnesene (STs), (E)-2-hexenal + (Z)-3-hexenal (LOX derivatives, "green VOC": stress signal), and methyl salicylate (PH). Qualitative determination was achieved by comparing the mass spectra of the peaks with the NIST library (NIST 17 Mass Spectral Library Software). Quantitation was carried out in SIM on single analyte RT and calibration curve (10^3–10^5 pg mL^{-1}) obtained by injecting increasing amounts of the smallest standards solution (10^3 pg mL^{-1}). This was determined on multiple replicates injected (n=5, RSD% ≤ 21%), and it was assumed as the instrument LOQ. All analytical steps were performed with the MassHunter Workstation 10.1 (Agilent).

7.2.4 Emission rates calculation

From the sampled concentrations (µg m^{-3}), the emission rate (ER) of each BVOC was determined for the two plant stages, respectively, expressed with the foliage (fresh/dry) biomass (g) and/or projected area (m^2) measured during the growing season. ER (µg g^{-1} h^{-1} or µg m^{-2} h^{-1}) calculation was based on a previous work (Stringari et al., 2023) adapted from the literature (Ortega and Helmig, 2008; Li et al., 2019). Equation (7.1) referred to the ER (µg g^{-1} h^{-1}) of a BVOC species (ER_{BVOC}) calculated from the product between the volatile concentration (C, µg m^{-3}) in the total sampled air and the volume (V, m^3) enclosing emitting plant, divided by the product of total enclosing time (Δt, h) and either the plant's (P) leaf area (m^2), LAI, or fresh/dry biomass (g). final ERs were reported in Table A7.1 of Annex III.

$$ER_{BVOC} = \frac{C \times V}{\Delta t \times P} \quad (7.1)$$

7.2.5 Statistical analysis

Emissions (µg m^{-3}) proceedings from the individual sampled volumes (1.25, 2.5, and 3.75 L) of each plant stage (young and mature) were contrasted first between themselves within the single light treatment, then between the treatments using ANOVA or Kruskal-Wallis, followed by either LSD (Least Significance Test) or Dunn (Bonferroni adjustment) post-hoc test. Similarly, environmental (temperature 'T', relative humidity 'RH', and CO_2 concentration) and physiological (stomatal conductance 'g_s') parameters related to each sampling interval were compared between the sampling intervals and between the light treatments. Data related to plant morphological development, which included biomass (g), height (cm), leaves number and area (m^2), was also used for the meaningful comparison. Furthermore, the relationships between plant emissions and the monitored parameters were measured through correlation tests (Spearman), using the mean value of the data collected. Significant differences were assumed at a $p \leq 0.05$, as well as for the individuated correlations between BVOC emissions and the recorded parameters, that were considered correlated at coefficient r_s comprised among ±0.8 and ±1. Statistical analysis was carried out with R software (version 4.2.2).

7.3 Results

7.3.1 Plants morphological development

Plants' morphological development between 30-32 and 36-39 DAS was marked by the increasing trend measured in the different parameters, individuating correctly the young and the mature stage. However, for none of them the increase appeared to be statistically significant (p> 0.05).

Similarly, there were no significant differences between light treatments within the individual stage. (Table 7.1).

Table 7. 1 Average ± SEM (n=5) of main morphological parameters measured over the young (Y) and the mature (M) stage of the cultivation cycle under RB1 and RB3 treatment. Different lowercase letters indicate significant difference at p≤ 0.05 between the light treatments within an individual stage, or between the growing stage within the same treatment.

Light treatment	Stem + leaves fresh weight (g plant^{-1})		Leaves fresh weight (g plant^{-1})		Stem + leaves dry weight (g plant^{-1})		Stem Height (cm plant^{-1})		Number of leaves per plant		Leaf Area (m^2 plant^{-1})	
YRB_1	4.31 ± 1.35	a	3.10 ± 0.93	a	0.44 ± 0.14	a	14.24 ± 2.89	a	13.40 ± 2.64	a	1.25 ± 0.36	a
YRB_3	3.63 ± 0.84	a	2.50 ± 0.46	a	0.39 ± 0.09	a	15.00 ± 2.96	a	11.40 ± 1.36	a	0.96 ± 0.16	a
MRB_1	6.43 ± 1.08	a	4.28 ± 0.73	a	1.00 ± 0.18	a	20.80 ± 1.86	a	20.40 ± 4.48	a	1.82 ± 0.34	a
MRB_3	7.67 ± 3.11	a	4.92 ± 1.95	a	0.88 ± 0.33	a	21.00 ± 2.20	a	21.20 ± 5.69	a	1.93 ± 0.81	a

7.3.2 Plants gaseous exchange and enclosing conditions

Results reported in this section are shown in Figure 7.2. Within the same growing stage environmental and physiological parameters during volatile collection were compared among each sampling interval between the two light treatments. Considering the first parameters, CO_2 levels were similar and not significantly different, in either the plant stages (Figure 7.2 A and B). Few significant differences for RH and T rates were detected. RH levels maintained generally higher under RB_3 light in both the growing stages. Significantly higher levels were individuated at 15-minutes interval ($p< 0.001$) in the young stage (Figure 7.2 C), and in all the intervals but progressively less significant in the mature one (Figure 7.2 D). Conversely, T levels were overall higher under RB_1 light in both the young and the mature stage, and significantly ($p< 0.01$) at 5- and 10-minutes interval (Figure 7.2 E and F). G_s, was mainly higher under RB_1 light in the young stage, but higher under RB_3 in the mature one (Figure 7.2 G and H). Overall, in the first sampling interval (5 minutes) g_s was higher under RB_1 light, and significantly only in the mature stage ($p< 0.05$). In the second interval (10 minutes), on the other hand, it was higher under RB_3 treatment and significantly in both the young ($p< 0.05$) and the mature ($p< 0.001$) stage. At 15 minutes g_s was slightly higher under RB_1 light in the young stage, but significantly lower ($p< 0.001$) in the mature stage.

Variation rates during the sampling (5 to 15 minutes) are shown in Table A7.2 of Annex III. With respect to CO_2, average levels remained overall similar to those measured in the VF (1490 ± 30

ppm). However, CO_2 showed a slight decreasing pattern under both light treatments in the young stage, which was significant ($p< 0.05$) only under RB_3 light, and a slight (not significant) increasing tendency in the mature stage (Table A7.2.1 and A7.2.2). Under both the treatments and in all the stages T and RH generally increased over the time of closure. T variations were minimal (circa ±1 °C), whereas RH ones were more pronounced (+2–13%). Significant variation differences of both T and RH between the light treatments were individuated (A7.2.3 and A7.2.4), consistent with those of the average levels (Figure 7.2 C, D, E and F), as well as between the sampling intervals of the same light treatment (A7.2.1 and A7.2.2). Strong variations ($p< 0.001$) of both T and RH were found under RB_1, of RH only under RB_3 light. RH variations in the mature stage were significant ($p< 0.01$) for both the treatments between 5-minutes interval and the following ones only. G_s showed a general decreasing pattern (-0.5–56 µmol $m^{-2}s^{-1}$) over the sampling length, in all the treatments, intervals, and plant stages. Strong significant differences ($p< 0.001$) were found in the mature stage between all the sampling intervals under RB_1 light, and between the first and the progressive intervals under RB_3.

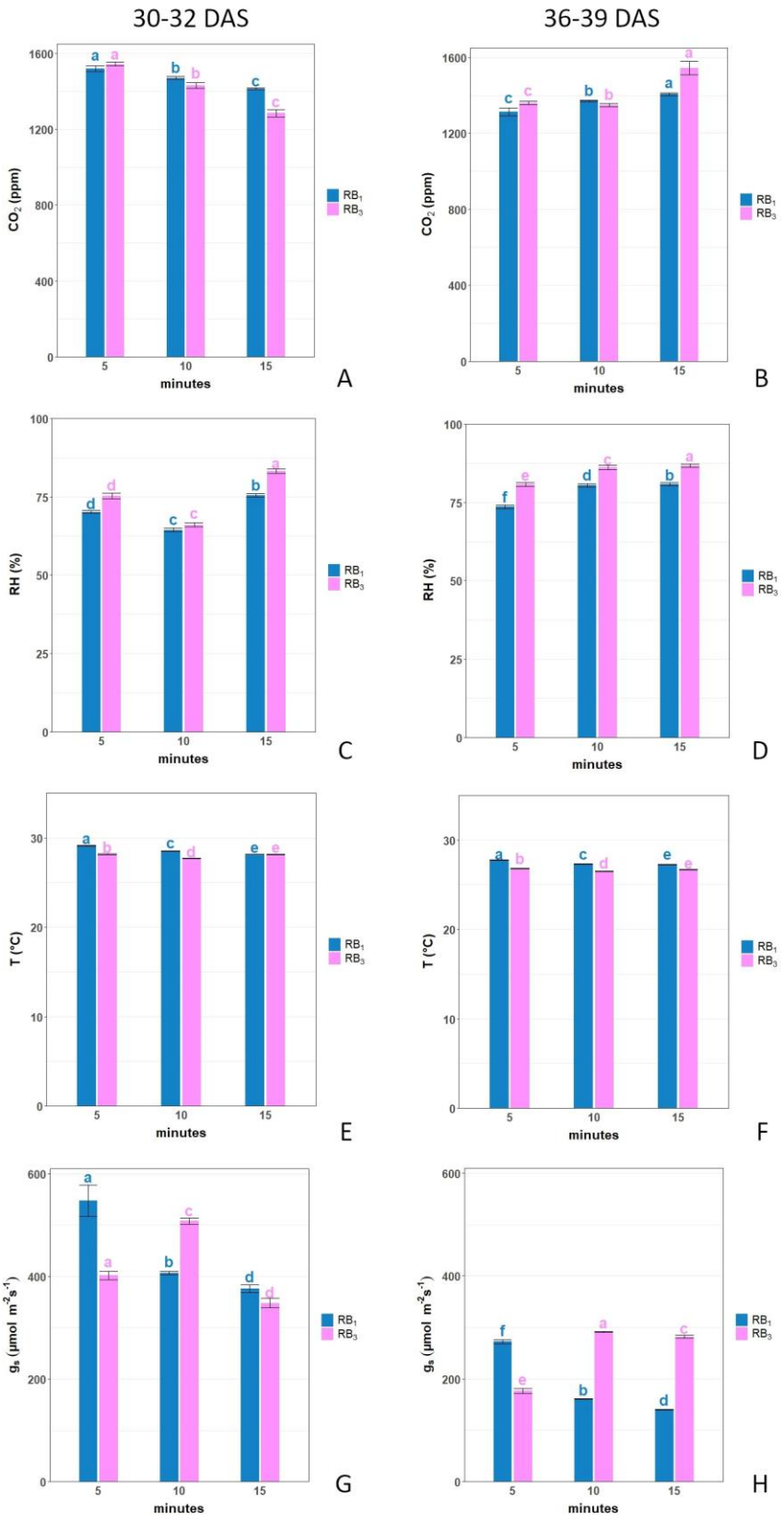

Figure 7. 2 CO_2 (A, B), RH (C, D), T (E, F), and g_s (G, H) ± SEM (n= 3) comparison between light treatments within the individual sampling interval, recorded during BVOCs collection in the young (left) and mature (right) plant stage. Different lowercase letters indicate significant differences between the treatments (p≤ 0.05).

7.3.3 BVOC emissions over the cultivation cycle

Detected BVOCs during the young and the mature plant stage are reported in Table 7.2 wrapped under the corresponding volatile class. In general, over the whole sampling, most of the BVOCs were found under RB_1 light in the young stage, under RB_3 in the mature one. Respectively, MTs, LOX derivatives and OMT were detected almost every time, at each sampling interval of each light treatment and growing stage. STs and PH compound occurrence instead was lower.

Table 7. 2 Summary of the detected (x) BVOCs belonging to MT, LOX derivative, PH, ST, and OMT class along the three consecutive sampling intervals (5, 10, and 15 minutes) under RB_1 and RB_3 at young (Y) and mature (M) plant stage. Superscripted number in parenthesis referred to the number of BVOCs out of the total detected in the considered stage, treatment, and sampling interval.

	MT			**LOX**			**PH**			**ST**			**OMT**		
	min			min			min			min			min		
	5	10	15	5	10	15	5	10	15	5	10	15	5	10	15
YRB_1	**x** (4)	**x** (4)	**x** (1)	**x**	**x**	**x**	**x**	**x**		**x** (1)	**x** (1)			**x**	**x**
YRB_3	**x** (1)	**x** (1)	**x** (1)	**x**	**x**	**x**							**x**	**x**	**x**
MRB_1	**x** (1)		**x** (1)	**x**	**x**					**x** (1)		**x** (1)	**x**	**x**	**x**
MRB_3	**x** (1)	**x** (1)	**x** (2)	**x**	**x**	**x**			**x**	**x** (2)	**x** (1)	**x** (1)	**x**	**x**	

The average (n=3) of the single BVOCs emission (μg m^{-3}) measured at each sampling interval under the two light treatments and growing stage are shown in Figure 7.3. As a general trend, BVOC emission levels were higher in the first 5 minutes of sampling, then progressively lower under both the light treatments and plant stages, although higher under RB_1 in the young stage, under RB_3 in the mature one. As a result of the statistical analysis, such decrease was found to be significant only for the LOX volatiles ($p< 0.001$) under RB_1 light in the young stage. In contrast, in the mature stage and under RB_3 light emissions did not always follow this pattern. Significant emission increase along the sampling length was found in fact for respectively OMT-1.8-cineole ($p< 0.05$) and MT-o-cymene ($p< 0.01$). However, the highest emission (116.17 μg m^{-3}) measured over the whole plant cycle was that of 1.8-cineole detected under RB_3 light in the mature stage within the first sampling interval Figure7.3 B). OMT emissions were also the most abundant collected in this stage under either RB_1 or RB_3 treatment.

Within the same stage and considering the young one (Figure 7.3 A, C, and E), MTs α-pinene, β-pinene, and β-myrcene were most abundant under RB_1 light following the decreasing tendency above mentioned. MT-o-cymene and characteristic OMT-1.8-cineole were barely detected,

under both the treatments and each interval, although OMT emission was higher under RB_3 than under RB_1 light. LOX derivatives showed a clear decreasing pattern under both the treatments, with significantly ($p< 0.05$) higher emissions under RB_1 light, at the 10-minutes interval. STs (β-caryophyllene) and the PH compound detected only under RB_1 light were found to decrease along the sampling. The highest emission in this stage was actually that of β-caryophyllene (58.53 μg m^{-3}), within the first sampling interval (Figure 7.3 A).

Considering the mature stage instead (Figure 7.3 B, D, and F), α-pinene, β-pinene, and β-myrcene were barely above the LOQ under both the light treatments. This was similar for MT-o-cymene whose emission was slightly higher under RB_3 light and significantly ($p< 0.01$) at the end of sampling (15 minutes). OMT-1.8-cineole emission was the highest in this stage and was detected in both the treatments at interval 5 and 10, showing a decreasing tendency, whereas at interval 15 it was detected only under RB_1. Although higher, emissions measured under RB_3 at minutes 5 and 10, were respectively not significant ($p> 0.13$) and significant ($p< 0.01$). LOX emissions did not show a clear tendency under any of the light treatments. Likewise, any remarks were observed for ST-β-caryophyllene and PH-methyl salicylate, which were barely detected. Conversely, ST-trans-β-farnesene emission (57.79 μg m^{-3}), was the third highest collected in this stage, under RB_3 light (Figure 7.3 B), and decreasing over the time.

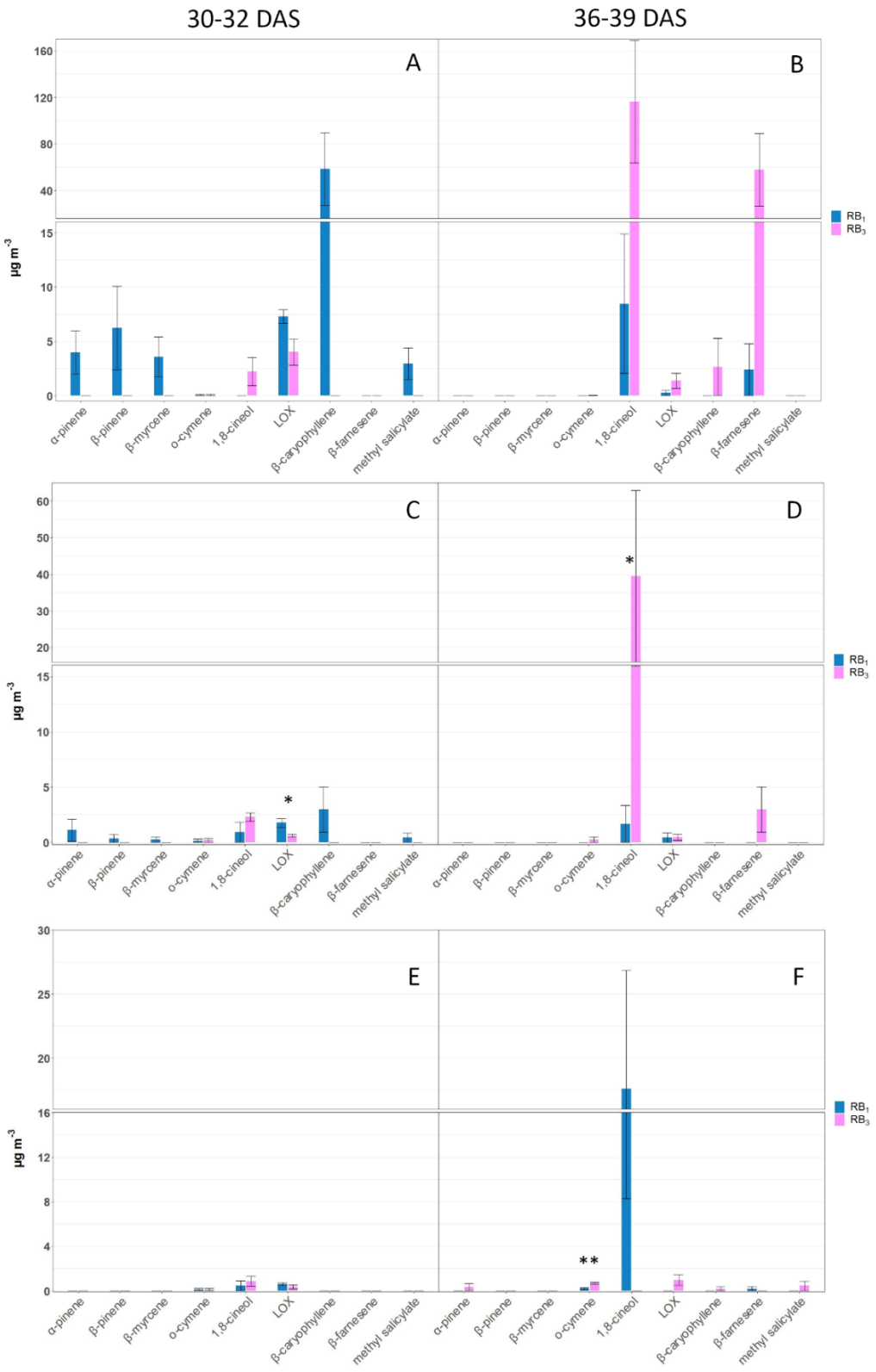

*Figure 7. 3 Average emissions (µg m^{-3}) ± SEM (n= 3) of the individual BVOC collected under RB_1 and RB_3 light at 5 (A, B), 10 (C, D), and 15 (E, F) minutes interval from young (30-32 DAS: A, C, E) and mature (36-39 DAS: B, D, F) plants; treatments comparison was performed on the individual volatile within the same interval and stage. Significant differences are indicated by '***', '**' or '*' (p ≤ 0.001, p ≤ 0.01 and p ≤ 0.05).*

Finally, comparing average and single emission levels within official EU-tables (Table 7.3), pretty all BVOCs were below the corresponding LCI values, except for LOX emissions collected under

RB_1. However, these levels refer to the single emission collected and not the averaged ones. Average levels instead were always below the LCI.

Table 7. 3 EU-LCI of the BVOCs listed in the European Framework against corresponding emission level measured in the VF under RB_1 and RB_3 treatment over the entire cultivation cycle, reported as the average (n=3) and the highest (not averaged) emission level, in parenthesis, detected.

	µg m^{-3}		
BVOC	**EU-LCI** (Report nº29)	**RB_1** *(VF)*	**RB_3** *(VF)*
α-pinene	2500	0.85 (6.37)	0.05 (0.96)
β-pinene	1400	1.10 (13.27)	Nd
o-cymene	1000	0.09 (0.47)	0.23 (0.79)
[a] 2-Hexenal	7	1.73 (**8.25**) *	1.29 (6.13)
other hydrocarbons	1400	[b] 0.27 (108.24)	[c] 26.32 (188.32)

[a] assumed for both investigated LOX derivatives. [b] referred to ST-β-caryophyllene, while [c] to OMT-1.8-cineole.

7.3.4 Measured effects of environmental and physiological conditions generated by the enclosing on plants emission

Perfect correlations (r_s ±1, p< 0.05) between the detected BVOCs and the monitored environmental and physiological parameters that were retrieved from the correlation test (Figure A7.3 of Annex III) are gathered in Table 7.4. In the text not perfect correlations (r_s ±0.8, p> 0.05) are referred as "slightly correlated" or to "slight correlation".

In the young stage, (Table 7.4 A and B), under RB_1 there were negative and slightly positive correlations between T increase and LOX derivatives and OMT-1,8-cineole respectively. Under RB_3 T increase was remarked by a positive correlation with the OMT and an unclear relation with the MT-o-cymene. Mainly negative (significant and slight) correlations between RH increase and MTs (β-pinene, β-myrcene and o-cymene), ST-β-caryophyllene, and PH-methyl salicylate were found under RB_1, except for the finally positive correlation with LOX derivatives. Under RB_3 RH showed instead a negative correlation with LOX derivatives, a finally positive correlation with the OMT, and a slightly positive correlation with o-cymene. Mainly negative correlations were individuated between CO_2 decrease and most of the BVOCs under RB_1, except for the final positive correlation with LOX derivatives. Under RB_3 CO_2 was negatively correlated with the OMT only, and unclearly correlated with o-cymene. G_s decrease was mainly positively correlated with most of the BVOCs under RB_1, except for the final negative correlation with o-cymene. Conversely, under RB_3 g_s was negatively correlated with LOX derivatives and only finally with the OMT, and (slightly) with o-cymene.

In the mature stage (Table 7.4 C and D), under both RB_1 and RB_3 still positive relationships were found with T increase, respectively, significantly with the OMT, slightly with LOX derivatives, ST-trans-β-farnesene, and (under RB_3) o-cymene. In contrast with the young stage, mainly positive correlations were individuated with the RH increase under both the treatments. There were slight correlations with LOX derivatives and trans-β-farnesene under RB_1, significant and slight with LOX derivatives and o-cymene respectively under RB_3, except for negative relation with the trans-β-farnesene. Under RB_1 CO_2 increase was associated only to slight correlations, positive with LOX derivatives and trans-β-farnesene, negative with the OMT. Under RB_3 still slight correlations were individuated, negative with MTs (o-cymene and α-pinene), LOX derivatives, and trans-β-farnesene. There was instead a positive correlation with the OMT. The correlation with G_s decrease under RB_1 was unclear, except for the slightly negative found with LOX derivatives. Under RB_3 mainly slightly negative correlations were found, respectively with o-cymene, the PH, ST-β-caryophyllene, and a significant one with LOX derivatives.

Relationships between the monitored parameters were also individuated. In the young stage (Figure A7.3.1), overall negative correlation was found between both increasing T and RH under RB_1 but not under RB_3. The correlation between decreasing g_s and increasing RH was tendentially negative under RB_3 but unclear under RB_1. The correlation between decreasing g_s and increasing T was unclear under both the treatments. Similarly, the correlation between increasing g_s and decreasing CO_2 was not resolved, except for the preliminary negative correlation found. Decreasing CO_2 was found to be overall negatively correlated with T and positively correlated with RH under RB_1. The same relationships remained unclear under RB_3.

In the mature stage (Figure A7.3.2), under the treatments the correlation between both increasing T and RH was initially unclear, although finally they resulted to be negatively correlated. Decreasing g_s was mainly negatively correlated with T under RB_1, and only initially (5 minutes) under RB_3. Its relationship with RH was not clear as it was initially negatively correlated, under both the treatments, then positive, under RB_1 only. Similarly, the correlation between decreasing g_s and increasing CO_2 was unclear as they were initially negatively correlated under RB_3 only, then finally positively correlated under both the treatments. CO_2 had a tendentially positive correlation with T under RB_3, negative under RB_1 tough in the last sampling term. Its correlation with RH was overall positive under RB_3, preliminary positive (5 minutes) under RB_1.

Table 7. 4 Correlations between detected BVOCs and environmental (T, RH, CO_2) and physiological (g_s) parameter along the three consecutive sampling intervals (5, 10, and 15 minutes) under RB_1 and RB_3 at young (Y) and mature (M) plants stage. Comparisons were performed within individual stages. Positive and negative correlations are indicated by '+' and '-' symbols, restrained or unrestrained in parenthesis referring either to perfect or not perfect correlation respectively, whereas blank spaces indicate missing correlations. Superscripted numbers in parentheses next to the correlation symbol indicate the number of BVOCs matching out of the total investigated. Up and down arrow next to sampling interval indicate parameter's increasing or decreasing trend.

	T			RH			CO_2			g_s		
	min			min			min			min		
YRB_1	5↓	10	15↑	5↑	10↑	15↑	5↓	10↑	15↓	5↓	10↓	15↓
MT					**(-)** [3]		**-** [1]	**(-)** [3]			**(+)** [3]	**(-)** [1]
LOX	**+**		**-**	**-**	**-**	**+**		**-**	**+**	**-**	**+**	
PH					**(-)**		**-**	**(-)**			**(+)**	
ST					**-** [1]			**-** [1]			**(+)** [1]	
OMT		**(+)**	**(+)**			**(-)**			**(-)**			

A

	T			RH			CO_2			g_s		
	min			min			min			min		
YRB_3	5↓	10↑	15↑	5↑	10↑	15↑	5↓	10↓	15↑	5↓	10↓	15↓
MT	**(+)** [1]	**(-)** [1]	**(+)** [1]		**(+)** [1]		**(-)** [1]		**(+)** [1]	**(+)** [1]	**(-)** [1]	
LOX					**-**						**-**	
PH												
ST												
OMT	**+**				**-**	**+**	**-**			**+**	**+**	**-**

B

	T			RH			CO_2			g_s		
	min			min			min			min		
MRB_1	5↓	10↑	15↑	5↑	10↑	15↑	5↓	10↑	15↓	5↓	10↓	15↑
MT												
LOX	**(+)**	**(+)**		**(+)**	**(+)**		**(+)**				**(-)**	
PH												
ST	**(+)** [1]			**(+)** [1]			**(+)** [1]					
OMT	**+**							**(-)**				

C

	T			RH			CO_2			g_s		
	min			min			min			min		
MRB_3	5	10↑	15↑	5↑	10↑	15↑	5↓	10↓	15↑	5↓	10↓	15↓
MT		**(+)** [1]			**(+)** [1]			**(+)** [1]	**(-)** [2]			**(-)** [2]
LOX	**(+)**			**(+)**	**+**		**(+)**		**-**			**-**
PH									**(-)**			**(-)**
ST	**-** [1]	**+** [1]		**-** [1]			**-** [1]	**+** [1]	**(-)** [1]	**(+)** [1]		**(-)** [1]
OMT		**+**						**+**				

D

7.4 Discussions

In this work we assessed the effect of the application of LED wavelengths on the BVOC emissions in an indoor vertical farming environment. Our objectives were the investigation of the qualitative and quantitative emission's response of basil plant grown under two different light treatments, RB_1 and RB_3 (to which the plant formerly responded differently in terms of growth and stomatal behaviour (Pennisi et al., 2019)), whose environmental levels were contrasted to current LCIs and databanks thresholds. For simplicity, emissions were collected in two distinctive terms of the cultivation cycle, further individuated at 30-32 and 36-39 DAS, which were respectively the plants' young and mature stage. Between the light treatments we obtained different outcomes in terms of emission chemical profile and amount, although some analogies in the related parameters were individuated. Likewise, within the same treatment both variations and resemblances were highlighted between the growing stages.

Along the whole plant cycle, most of the BVOC emissions were below or close to the instrumental LOQ. Occasional bursts collected from both RB_1 and RB_3 plants, mostly during the mature stage (Figure 7.3 B, D and F), misled the identification of a distinctive emission pattern under each of the light treatment. Nevertheless, both treatments and plant stages showed commonly higher emissions within the first 5 minutes of sampling (Figure 7.3 A and B) and a decreasing tendency along the time (from 10 to 15 minutes). However, during the young stage more BVOCs were detected under RB_1 light and at a slightly higher amount than under RB_3 (Figure 7.3 A, C and E). In the mature stage, emissions were conversely slightly higher and more variegated under RB_3 light (Figure 7.3 B, D and F). Usually, emission levels between the treatments were not significantly different, and whether significant differences were measured these were not maintained along the sampling. Hence, emission results were carefully analysed with respect to the environmental, physiological, and morphological parameters monitored during BVOCs collection and plants development.

In relation to the morphological aspect, all plant traits (stem height, leaf area, number, and biomass) were clearly increased along the cultivation term (Table 7.1) and increments were consistent with past works on basil cultivation under LED light (Pennisi et al., 2020; Wong et al., 2020b; Rahman et al., 2021)), although the growing stages were not remarked by significant differences. Indeed, significant biomass (leaves and stem) increase previously highlighted under RB_3 treatment (Pennisi et al., 2019; Lin et al., 2021; Chutimanukul et al., 2022; Montefiori et al., 2022), as well as significant stem growing (Larsen et al., 2020) and leaves compactness (Matysiak and Kowalski, 2019) under R:B ratios ≥1 was here not determined, in any of the measured traits. Therefore, plants development under the different wavelengths could be considered similar

throughout the cycle, assuming among them a similar emitting surface (similar leaf area and biomass).

G_s was the main physiological parameter considered with regards to the emissions, as regulating both the mechanism of production, connected with the secondary metabolism, and the release of BVOCs into the environment (Harley, 2013; Kanagendran et al., 2018; Li et al., 2023). Generally, g_s showed a decreasing tendency along the sampling under both treatments and plant stages (Figure 7.2 G and H; Table A7.2). Conversely, T and RH progressively increased (Figure 7.2 C, D, E and F), showing under both the treatments significant increases in the young stage and partially (only for RH within 5 minutes) in the mature one (Table A7.2.1 and Table A7.2.2), parallel to a decreasing g_s (Figure 7.2 G and H), mostly significant in mature plants (Table A7.2.2). G_s decrease could be associated to the negative correlations found with both T and RH (Figure A7.3). The simultaneous increase of these parameters was described to perform as negative feedback on the opening of stomata in condition of exceeding levels of vapour pressure deficit between the stoma and the external environment (Sussmilch et al., 2017; Yaaran et al., 2019). Such condition was usually observed, in the mature stage where increasing levels of RH (Figure 7.2 characterised by levels of g_s (Figure 7.2 H) much lower than the young stage. However, under RB_3, despite general low g_s, significantly higher g_s levels were registered over the closure time with respect to the first 5 minutes of sampling (Table A7.2.2) and than most of the levels registered under RB_1 treatment (Figure 7.2 H).

On the other hand, variable relationships were found between BVOC emissions and the CO_2 (Figure A7.3) which made unclear the understanding of its role on the volatiles' induction. Still, between the sampling intervals CO_2 levels, did not vary significantly (Table A7.2.1 and A7.2.2**,** with exception of mature RB_3 plants, between 5 and 15-minutes interval), overall confirming the correct CO_2 replenishment throughout plants closure and perhaps a minor impact on g_s performance. However, slight decreasing and increasing tendency of CO_2 in respectively young and mature plants were observed along the sampling and were common for both treatments. Although high concentrations of CO_2 could cause a reduction of the g_s (Hashimoto et al., 2006; Klein and Ramon, 2019), and interfere with the emission pathway of terpenes (Tiiva et al., 2017; Copolovici et al., 2021), this pattern was not remarked by the correlations found (Figure A7.3), especially in mature plants. For instance, higher CO_2 under RB_3 plants showed a positive correlation with g_s, while lower concentration under RB_1 showed a negative correlation (Figure A7.3.2).

The tight connection between g_s and the spectra of light has been assessed in multiple studies (Shimazaki et al., 2007; Clavijo-Herrera et al., 2018; Lanoue et al., 2018). Both blue and red wavelengths were found to interact with the phototropines present in the guard cells (Boccalandro et al., 2012; Doi et al., 2015), and activate multiple and different chemical pathways affecting g_s. Among these, K^+ exudation and CO_2 uptake were described as the main intracellular processes induced by respectively the blue and the red light, targeting stomata opening, increasing therefore g_s. However, blue light was found to perform higher and prolonged stomata stimulation with respect to red one (Shimazaki et al., 2007). Even though our results were in contrast with those reported by similar works on basil plant (Jensen et al., 2018; Pennisi et al., 2019; Lauria et al., 2023), g_s levels measured respectively under RB_1 in the young stage and under RB_3 in the mature one (Figure 7.2 H and G) and the respective BVOC emissions collected (Figure 7.3 A, C, E and B, D, F) were in line with the experimental findings derived from the study of the stomatal activity (Boccalandro et al., 2012; Doi et al., 2015; Hiyama et al., 2017).

The investigated BVOCs were then analysed under the related volatile class (MT, ST, LOX, PH, and OMT) attributing them to similar production and release patterns. MTs, STs, and the PH compound were mostly detected under RB_1 in the young stage, whereas at plants maturity they were overall less spread and mainly detected under RB_3 (Table 7.2). Evaluating the correlations individuated with the measured parameters (Table 7.4), in both treatments and stages MTs, STs and PH overall showed a positive correlation with the T (Räisänen et al., 2008; Tiiva et al., 2017), and a negative one with the RH (Tani et al., 2004; Xu and Zhang, 2011). These relationships were consistent with extensively reported trends regulating their releasing pathway (Niinemets and Reichstein, 2003; Harley, 2013). LOX derivatives, instead, were mainly ubiquitous along the sampling, the treatments, and the plant stages (Table 7.2). However, over the sampling time they showed often a significant negative correlation with the RH (higher than the positive correlation with T) (Table 7.4). This relationship was consistent with the releasing mechanism of 'green volatiles' occurring in a stress condition (Farag and Paré, 2002; A. C. Heiden et al., 2003; Jansen et al., 2010) that in our case was eventually reproduced by the closure (Ortega and Helmig, 2008; Pérez-Priego et al., 2015) producing the T and RH increase registered (Figure 7.2 C, D and E, F). In addition, individual LOX levels were generally high compared with the rest of the BVOCs (Table 7.3), supporting the stress hypothesis. Most countertrends were found in the emissions of the characteristic OMT-1.8-cineole. Among all BVOCs, it was the most abundant volatile and was found under both the light treatments, but its emission pattern was variable either between the sampling intervals, the growing stages, and the treatments (Figure 7.3). Low OMT emissions were detected in the young stage under both the treatments (Figure 7.3 A, C and E), whereas

much higher emissions were individuated at fully developed plants (Figure 7.3 B, D and F) that were significantly higher under RB_3 light than under RB_1. Increasing emissions along the development were previously detected (Carvalho et al., 2016), but under LED light with a similar percentage of red and blue. In contrast, similar emission levels were found under equivalent RB_1 and RB_3 light setup (Pennisi et al., 2019; Lauria et al., 2023). Considering the positive and negative correlation found between the OMT and respectively T and RH (Table 7.4), reported also in other assessments (Fischer et al., 2011; Walters et al., 2021) the releasing mechanism of 1,8-cineole was likely to follow the same pathway of the terpenoids detected (MT, ST, and PH compounds).

Although CO_2 variations measured along the sampling were minimal, significant correlations were individuated with some of the BVOC emissions (Table 7.4) in contrast with previous findings (Daussy and Staudt, 2020; Walters et al., 2021). However, both positive and negative correlations were found at either CO_2 increase or decrease under both the treatments, therefore the relationship with this variable remained unclear.

Concentrations of most of the investigated volatiles were below 10 µg m^{-3} among the treatments and plant stages, and below the related LCIs. Emission bursts were usually detected in the first sampling interval (Figure 7.3 A and B), mainly under mature RB_3 plants. LOX volatiles were the ones exceeding the referencing LCI (2-hexenal) (Table 7.3), although once and under RB_1 only. In contrast to the other BVOCs, average levels were below the LCI and substantially similar between the treatments and plant stages. In terms of health concern, assigned LCI referred to a read-across substance (2-pentenal), due to poor experimental data provided, indicating potential but not confirmed mutagenic effects (ECA, 2013; European Union, 2022). In the ECHA database, comprehensive dossier on (E)-2-hexenal (ECHA, 2023a) wrapped up the toxicological effects associated to its direct exposure. Skin irritation was reported in humans after 48 hours of uninterrupted contact, while acute toxicity was determined in rats after an oral administration of 780 mg kg^{-1} bw (body weight). No further adverse effects were mentioned, in parts due to the few studies conducted and the awaiting assessment. Among the highest concentrations detected, there were respectively OMT-1.8-cineole, and STs β-caryophyllene and trans-β-farnesene. All these volatiles were currently not associated to a determined LCI, but individual datasheets were compiled by ECHA. In the case of 1.8-cineole acute toxicity was found in animals (rats) at oral and dermal level, at relative high dosage of respectively 4.5 g kg^{-1} and 2 g kg^{-1} bw (ECHA, 2023) No adverse effects were reported with regards to the inhalation as further investigation on this administration was considered negligible. Among most frequent effects skin sensitization was reported. In the case of ST volatiles LCI could be roughly ascribed to hydrocarbon compounds. For β-caryophyllene ECHA indicated very low acute toxicity after oral

and dermal administration in respectively animals and humans, reporting for the sensitization effect (ECHA, 2023b). For trans-β-farnesene, exposure was tested in animals only, providing still small lethality for the oral and the dermal one, and toxicity after prolonged inhalation (4 hours) at relatively high concentrations (> 2.06 mg L^{-1}). (ECHA, 2023c).

Overall, for each of the investigated BVOCs emissions collected fell within the safety intervals determined by the clinical studies reported. In addition, all emissions were at least one order of magnitude (≤ ppb) below official levels calculated (ECA, 2013) and were highly variable over both the sampling and the cultivation term. Therefore, higher emission levels than current indoor limits (LCIs) registered at longer exposures than the considered intervals (5, 10, and 15 minutes) were unlikely to occur at the conditions of the VF studied.

7.5 Conclusions

Despite relevant differences found in the BVOC emissions of basil plant under RB_1 and RB_3 lighting, only few of them were statistically significant and were not maintained throughout the sampling. Therefore, in absence of remarked significances throughout the intervals we could not assess a clear emissions difference between the light treatments for any of the investigated BVOCs. In addition, emissions trend changed sensibly at plant full development, with much higher and variegated bursts with respect to the first cultivation term under RB_3 light characterised by volatiles that were typical of basil blend (1.8-cineole). We suggested, therefore, to focus the measurement on this stage when potentially higher emission levels are likely to occur, eventually discarding the significant differences found occasionally (e.g., at 10-minutes interval) between the treatments. BVOC emissions appeared to follow the physiological response of stomata under a specific wavelength, however, environmental conditions also seemed to play a significant role on the modulation of the emission release, especially RH and T parameters. Then, to fully understand plant emission response to a specific lightning monitoring these variables is recommended, as well as CO_2, which implication in our study remained unclear. In addition, depending on the sampling system adopted we suggest longer measurements simulating real emissions exposure (e.g., from 30 minutes to several hours). Since detected BVOC levels were considerably lower than the fixed indoor limits, we believed as the most likely repercussion on human sensitization to a determined BVOCs emitted by basil plant, in the case, the 1.8-cineole. Hence, we may consider basil cultivation indoor in VF system, under red and blue light, substantially safe. Complementary to our research other LED light combinations (wavelengths) could be object of further study within the framework of the indoor air quality.

PART III

Evaluation of field collection results and further relevant insights

Chapter 8

Research methodology assessment and additional relevant BVOC emission findings

Chapter 8: Research methodology assessment and additional relevant BVOC emission findings

Qualitative and quantitative outcomes of the different field collections achieved with Anasorb CSC tubes were finally compared on further measurements taken with TA tubes under analogous sampling setup and conditions to corroborate the obtained results. In contrast to LE Anasorb CSC tubes, TA tubes were designed for thermal desorption that was coupled to GC-FID. TA tubes were tested in advance of the field assessment.

8.1 Testing TA performance

First, sampling reproducibility of the TA tubes was tested measuring the BV. This consisted of replicate samplings taken with pair of tubes connected in series at common 250 mL min^{-1} air flow for 10-20 minutes length in a controlled environment. Both tubes were thermally desorbed using a Portable Thermal Desorber (Handy TD 265) and analysed in the GC-MS at the conditions reported in table 3.4 (section 3.2.8). BVOCs determination was done on 26 standards that encompassed a broad range of volatile classes, respectively, MTs, OMTs, and STs, LOX derivatives, and PHs. Following either EPA (1999) or HSE (1993) threshold (5%), breakthrough was observed for almost all the detected volatiles among those contained in the reference standard solution (9 out of 26), and similarly at both 2.5 and 5 L sampling volumes. These results were confirmed from further samplings conducted under cold conditions (0°C) (Figure 8.1). Overall, BV ranged between 7% and 140% for most of the MTs and LOX derivatives detected, and for the long chain volatiles detected (e.g., STs and PHs), respectively nonanal (LOX) and humulene (ST), it was among the highest. Safe Sample Volumes (SSV) were achieved for two BVOCs only, namely, octyl acetate (LOX) and linalool (OMT), given BV <5%. (Table 8.1). Based on these results comparative quantitative assessment with Anasorb CSC tubes was then carried out on these volatiles.

Table 8. 1 Breakthrough of the 26 BVOCs tested under different sampling conditions with respect to the temperature. Tolerable BV (<5%) is highlighted by green tones whereas progressively red tones match BV out of the tolerable range.

Class	BVOC	RT	BV% cold (0°C)	BV% room T (20°C)	BV% room T (20°C) x2*
MT	β-pinene	4.73	4.81		
MT	β-myrcene	5.06	40.10	0.00	0.00
MT	3-carene	5.06	0.00		
MT	α-phellandrene	5.18			
MT	α-terpinene	5.31			
MT	limonene	5.47	4.14	19.81	7.72
OMT	1.8-cineole	5.58			
LOX	trans-2-hexenal	5.67			
MT	g-terpinene	5.84		64.29	
MT	p-cymene	6.06	7.23	10.70	9.57
LOX	n-hexanol	6.50	73.92	29.20	39.19
LOX	cis-3-hexanol	6.72	94.02		
LOX	nonanal	6.94	71.78	55.72	70.26
LOX	**n-octyl acetate**	7.40		0.00	0.00
OMT	**linalool**	7.83		0.00	0.00
OMT	camphor	8.07			
ST	β-caryophyllene	8.52			
PH	methyl chavicol	8.91			
OMT	α-terpineol	8.96	82.27	0.00	68.78
ST	α-caryophyllene	9.01	142.60		
PH	methyl salicylate	9.69			
PH	methyl eugenol	10.77			
PH	methyl cinnamate	11.42			
PH	eugenol	11.87			

*From double sampled volume

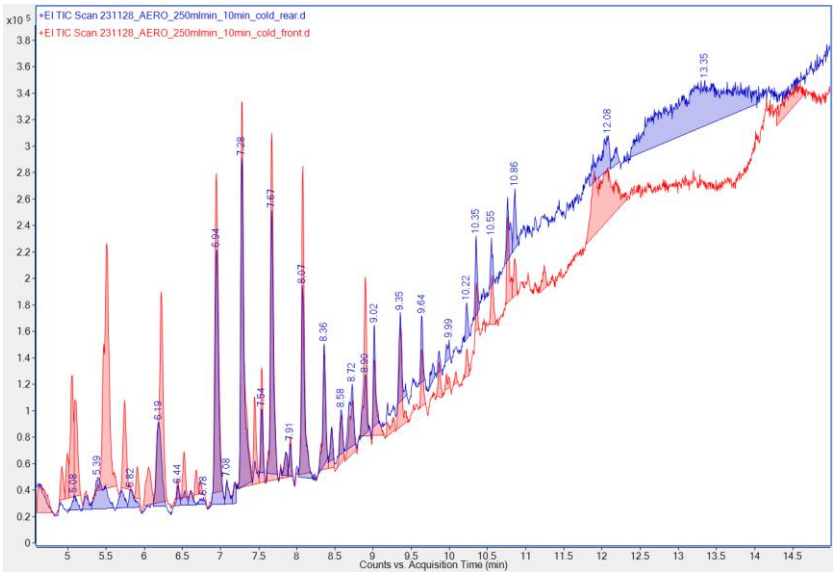

Figure 8. 1 Overlaid chromatograms of exemplary front (red) and rear (cold) TA tube samples collected at 0 ℃ (2.5 L) where most of the corresponding peaks (analogous RT) exhibited similar area among themselves.

8.2 Comparing field emissions collection of the two sorbents

In the iRTG-LAU2 a short-term basil crop was cultivated during the summer season of 2023 (June-July). Cultivation was led under drip irrigation recirculating the water leached from a crop of tomato plants (nutrient solution reported in table X.9 of Annex I section, pH= 5.54 ±0.1, CE=2.47 ±0.06 mS cm^{-1}) grown in neighbour iRTG-LAU1 over the same period. Weekly measurements of morphological traits, height, and leaves area provided information on plants' growth. At full development (32 DAT) 8 plants randomly chosen in the greenhouse were distributed in the 1 m^3 static enclosure described in table 3.3 (section 3.2.5.1) and connected to the soilless system (Figure 8.2). Environmental parameters during plants enclosing were continuously monitored by T, RH, and Rad sensors, as well as for CO_2, whose concentration was maintained constant (± 30 ppm) through supplementary purges. Triplicates of 2.5 L (250 mL 'in^{-1} x 10') air sample were simultaneously collected for each type of sorbent (Anasorb CSC and TA). Once solvent extraction of Anasorb CSC was realized (see section 3.2.7.1) samples were analysed in the GC-FID using thermal desorption technique at the conditions detailed in table 3.4, injecting an aliquot (7 µL) of LE samples, and extracting the entire sample of TA tubes. Volatiles determination and quantitation in the GC-FID was carried out on standard mixtures (paragraph 8.1) of different concentrations injected at a reproducible volume (7 µL) to provide robust CCs (10.5–210 ng) (see Table X.32 in Annex I). As shown in table 8.1 and Figure 8.3 different BVOCs were detected between the sorbents, excepting nonanal. Likewise, with respect to the meaningful volatiles for the comparison, linalool was detected in the TA and octyl acetate in the Anasorb CSC respectively, at quite low amount (0.72 µg m^3) the first and at much higher (139.79 µg m^3) the second. These differences may be due to the different volatile affinity between Anasorb CSC and TA sorbent material. To ensure consistent results, LE samples were investigated in the MS (7890A GC-5975C MS, Agilent) as well, in one case combining the injection with thermal desorption (LE-TD/GC-MS) at the instrument conditions described in the M&M (table 3.4). Quali- quantitative determination of BVOCs was carried out on target m/z chromatograms extracted from full scan-acquired TICs and on CCs within a much lower interval amount (0.002–0.1 ng) than FID machine (Table X.31). Pure CS_2 solutions (=no standards) were instead used as reference LOQ while the signal (peak area) of the lowest calibration point obtained in the FID machine (10.5 ng) acquired by the MS after its thermal injection was used for both the qualitative and quantitative determination of LE-TD samples (Table X.32), due to CC reproducibility issues at the working conditions. It should be noted that these final analyses were conducted after a cold storage over more than 4 months, due to conflicting laboratory schedules. Nevertheless, LE-TD samples provided consistent chromatographic results with the FID (Figure 8.3) and in addition, given the

high sensitivity supplied by the MS detector, further BVOCs were individuated (Figure 8.4), among which linalool (table 8.2). In contrast, LE-samples simply injected (without thermal desorption) provided an overall response factor below the LOD (Figure 8.5). Low response could be associated either to sample loss or manual error. However, the consistency between the quantitative outcomes (linalool) of LE-TD and TA samples, along with the complementary qualitative and quantitative information provided by Anasorb CSC tubes compared to TA samples, supported the results obtained from previous field collections and the research methodology employed. Moreover, coupling thermal desorption technique to LE samples was suggested to enhance the performance of both qualitative and quantitative analysis.

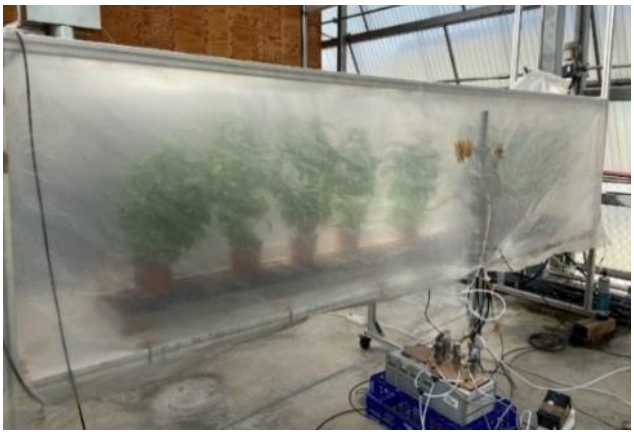

Figure 8. 2 BVOC emissions collection in the static enclosure from fully grown basil plants.

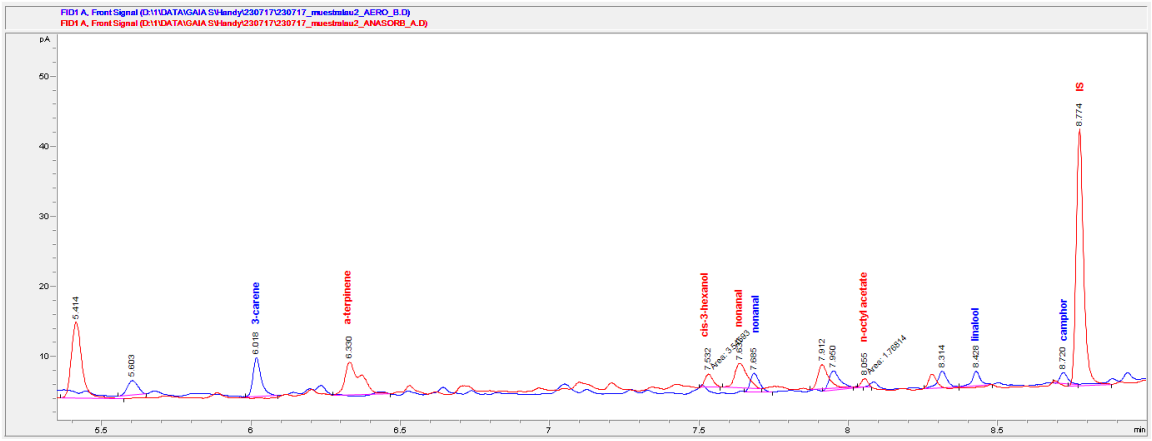

Figure 8. 3 Overlaid chromatograms of exemplary TA (blue) and Anasorb CSC (red) samples obtained after thermal desorption in the GC-FID.

Table 8. 2 Basil emissions (µg m^{-3}) detected in the GC-FID after thermal desorption (TD/GC-FID) of the two sorbents, TA and Anasorb CSC, and in the GC-MS re injecting LE samples (Anasorb CSC) after simple injection (LE/GC-MS) or thermal desorption (LE-TD/GC-MS). Empty cells indicate levels below the LOD. Symbol '' indicate emissions having only qualitative meaning due to significant sample loss (BV>5%) during air sampling.*

		TD/GC-FID		**LE/GC-MS**	**LE-TD/GC-MS**
Class	BVOC	***TA***	***Anasorb CSC***	***Anasorb CSC***	***Anasorb CSC***
MT	α-pinene				
	β-pinene	1.21*			
	3-carene	1.66*			0.84
	α-phellandrene				0.12
	α-terpinene		1091.50		0.51
	limonene				12.09
	γ-terpinene				
	p-cymene				3.95
OMT	β-myrcene				
	1.8-cineole				0.95
	linalool	**0.72**			**7.78**
	camphor	1.48*			9.28
	α-terpineol				
	eugenol				
ST	α-caryophyllene				
	β-caryophyllene				
LOX	n-hexanal	1.42*			
	trans-2-hexenal				
	n-hexanol				13.16
	cis-3-hexanol		276.32		
	nonanal	2.37*	628.32		130.83
	n-octyl acetate		**139.79**		**17.99**
PH	methyl chavicol				3.32
	methyl salicylate				
	methyl eugenol				2.52
	methyl cinnamate				4.48

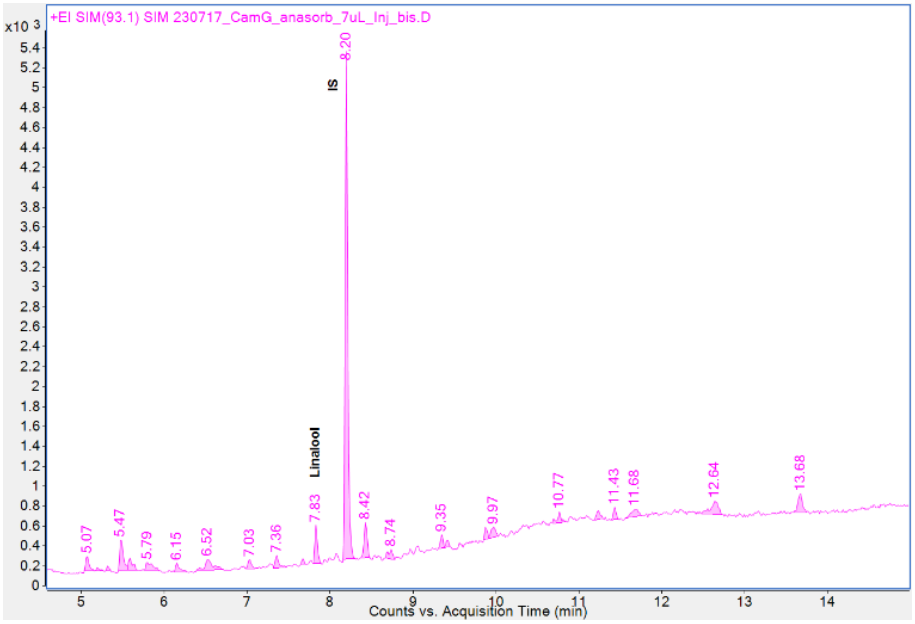

Figure 8. 4 Exemplary chromatogram (extracted SIM 93 m/z) of LE Anasorb CSC sample obtained after thermal desorption in the GC-MS.

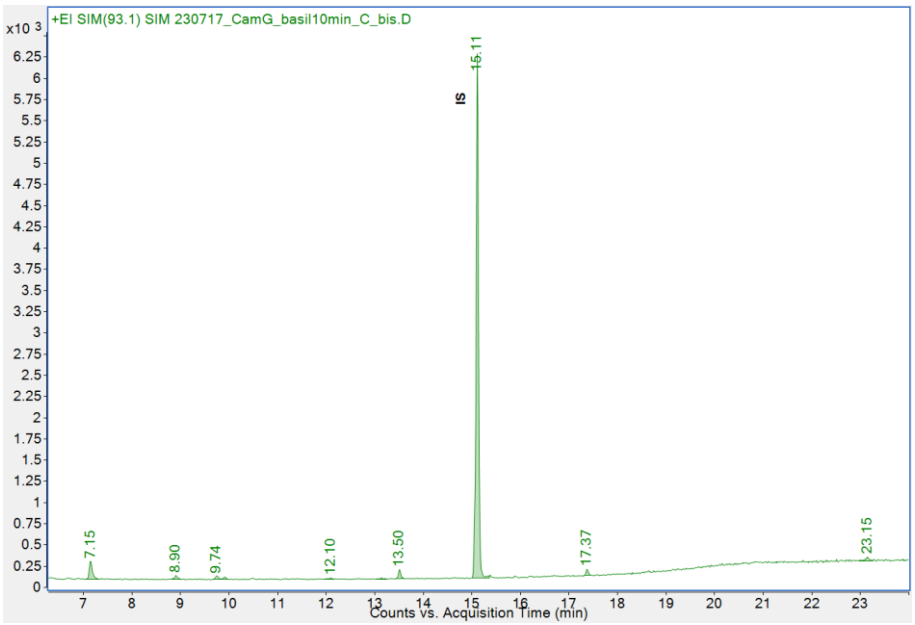

Figure 8. 5 Exemplary chromatogram (extracted SIM 93 m/z) of LE Anasorb CSC sample obtained after liquid injection (without thermal desorption) in the GC-MS.

8.3 Assessing BVOC emissions of the surrounding environment

Background emission levels of UA environments were also investigated. Among the two cases study this investigation was limited to the iRTG, being more exposed to air fluxes of surrounding building and the outdoors. The selected office described in section 3.1.1.1 was assigned as representative sample point for this purpose, because of its indoor configuration and apart location with respect to the cultivated floor (iRTG). Air samples (7.5 L) were taken straight in the environment without the use of static enclosure and in triplicates using TA sorbents since the tubes were featured for thermal desorption and the reconditioning, allowing faster and multiple samples analysis than consumable Anasorb CSC tubes. For the comparative purpose, side air samples were collected from the iRTGs during current tomato and basil campaigns and when plants were pulled out, and from the outdoors (Figure 8.6). Chromatographic analysis was carried out in the GC-FID at the conditions referenced above, including samples validation on blanks (=not sampled tube). BVOCs determination was done on the 26 standards previously mentioned. Due to the quantitative restriction related to TA performance, emission levels of the detected BVOCs were approximated to the peaks area exclusively, allowing only rough comparison between the emissions. As shown in Figure 8.7 most of the target BVOCs were detected in the background environment of the building (office) and at generally higher amount than in the rest of the sampled locations. Among the few exceptions, some monoterpenes (3-carene and p-cymene), oxygenated monoterpenes (camphor and α-terpineol), and phenylpropanoids (methyl chavicol and methyl eugenol) were higher in the iRTGs or outdoors or detected in these places only. However, between estimated emission levels there were overall slight differences.

Figure 8. 6 IRTGs LAU2 (left) and LAU1 (middle) during the cultivation season and outdoor rooftop (right) locations where side air samples were taken.

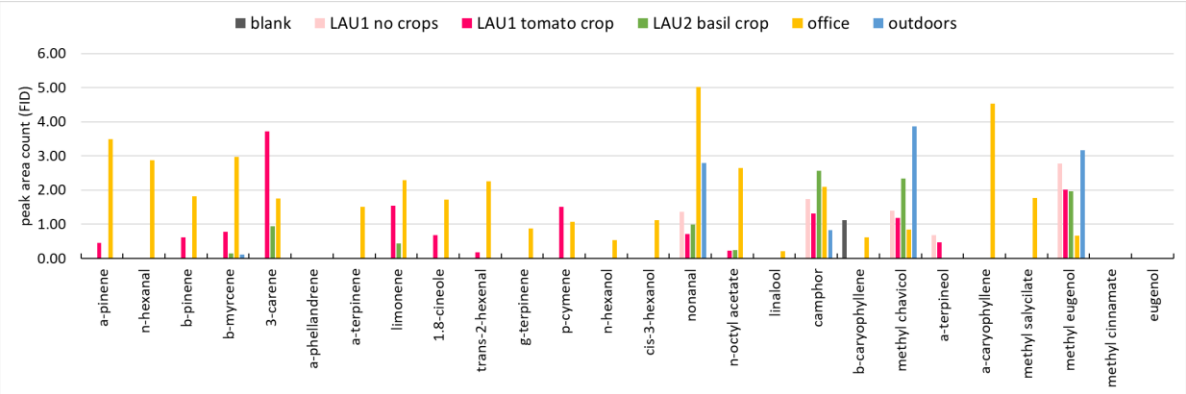

Figure 8. 7 Average (n=3) peaks area of the BVOCs collected with TA tubes detected in the different sampling locations: iRTGs during tomato (LAU1 tomato crop) and basil (LAU2 basil crop) cultivation, when plants were removed (LAU1 no crops), indoors and apart from the iRTGs (office), and outside from the building (outdoors).

Besides, accurate quantitation was performed for octyl acetate and linalool volatiles according to previously determined SSV. Calculated concentrations (Figure 8.8) were consistent with their preliminary estimations, individuating higher BVOC emissions (octyl acetate) in the office than in the iRTGs along crop season or individuating BVOC emissions (linalool) that were not detected (<LOQ) in the other spaces. Slight differences previously observed among peaks area were confirmed by the emission amounts calculated and in addition levels were much below reference LCIs (terpenes). Although partial, the results obtained by this preliminary assessment were encouraging because they suggested overall low BVOC emissions exposure in multiple originating locations. However, it demonstrated that levels indoors might increase and could be associated to sources different from biogenic ones (plants). In the case of the investigated office, furniture, plywood walls, and external objects introduced can all be responsible of volatiles release and can affect considerably indoor air quality (ECA, 1997a, 1997b).

Figure 8. 8 Average (n=3) emission amount (µg m^{-3}) and related SEM (=Standard Error of the Mean) of detected BVOCs octyl acetate (left) and linalool (right) in the air samples collected from different locations of the ICTA-UAB building.

PART IV

Discussion of the research outcomes

General conclusions

Further investigation

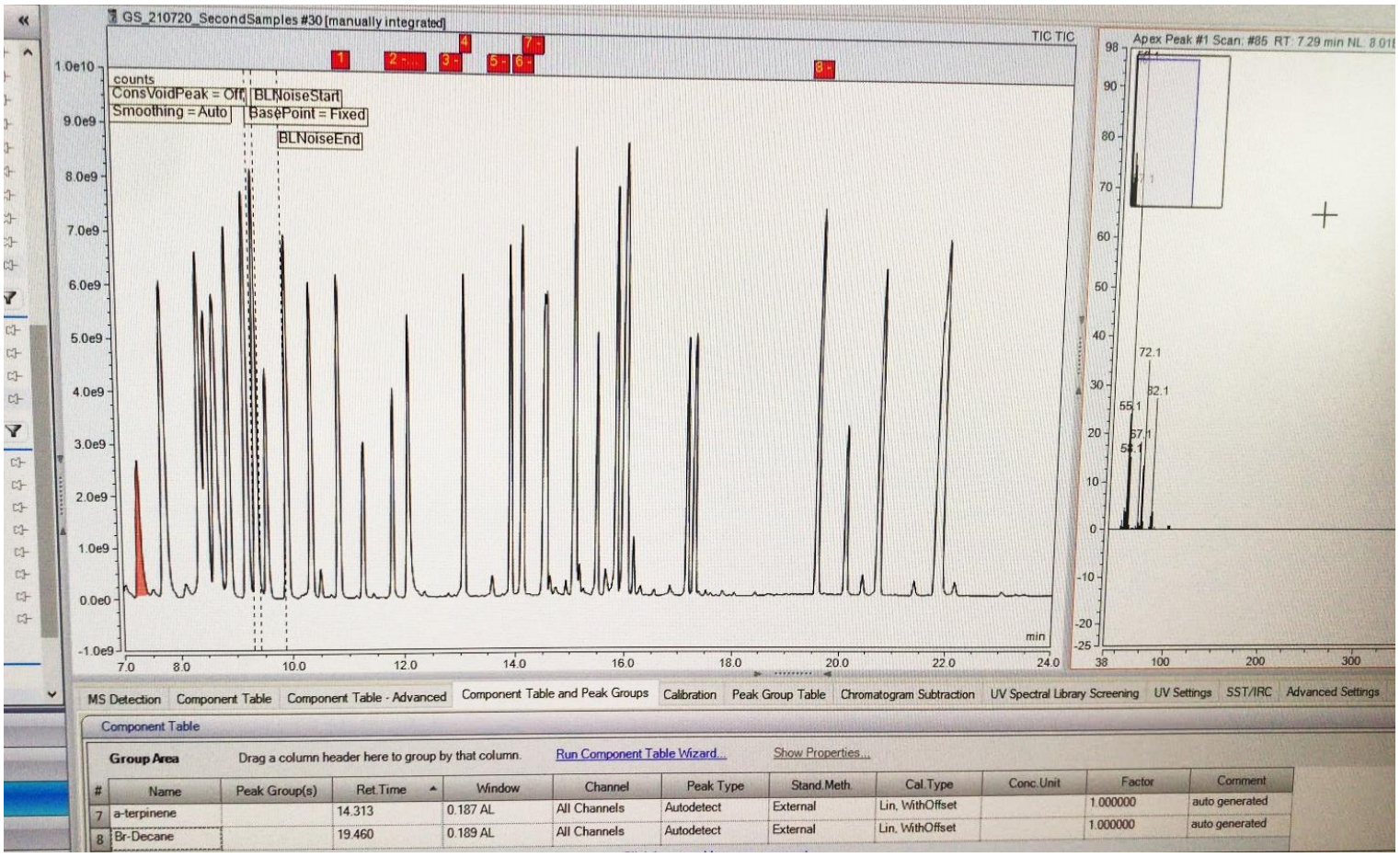

Chapter 9

Discussion of the research outcomes

Chapter 9: Discussion of the research outcomes

This dissertation presented a comprehensive assessment of BVOC emission levels resulting from crop cultivation in building-integrated and indoor UA environments, in relation to reported health-risk thresholds. The aim of the research was to evaluate the overall safety of UA implementation based on the assessed BVOC levels. Due to the growing interest in building-integrated rooftops and vertical farms and the availability of representative case studies, emission collection was restricted to these systems despite different plant species widespread in UA were involved in the investigation. Complementary to field collection, the study investigated the relationship between the implicated factors and the resulting emission response of the plants, particularly focusing on the environmental conditions defined by the cultivation system. Finally, the research methodology established prior to the official assessments was thoroughly validated through an additional technique developed during the latter stages of the investigation to corroborate the measured BVOC levels. This supplementary approach enhanced the applicability of the adopted methodology to the open environment, compared to a chamber-based approach, thereby enhancing the understanding of current emission levels. All these parts can be identified in summary Figure 9.1.

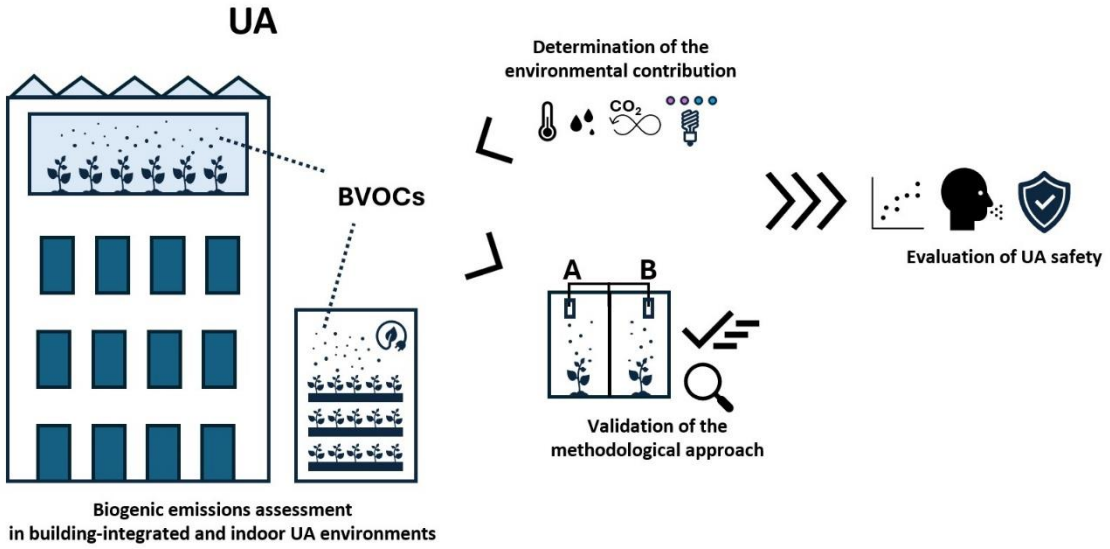

Figure 9. 1 Framework of the research highlighting the 4 main parts.

9.1 Methodological approach: sampling and post sampling

The feasibility and reproducibility of the sampling method were first investigated by implementing three different approaches in **chapter 4**. These approaches utilized both passive and active methods, namely open, semi-open, and closed sampling, in accordance with consolidated techniques described in the literature (Tholl et al., 2006; Li et al., 2019). These outcomes provided the technical information necessary for the selection and further

improvement of the sampling approach to be adopted for the next measurements, which involved dynamic sampling in a static enclosure. Two crucial aspects of the sampling performance were the qualitative and quantitative reproducibility of the sampled emissions. (Ortega and Helmig, 2008; Soria et al., 2015). To achieve them the enclosure was properly redesigned, as described in **Annexes A1.1** and **A1.3**, and the sampling length was fixed to shorter intervals, based on the measurements reported in **Annex A1.2**. Following these preliminary adjustments, comprehensive BVOC assessments were conducted on both short- and long-cycle crops grown in the iRTG (**chapters 5** and **6**) and indoor VF (**chapter 7**). Additionally, establishing a robust analytical method was crucial to ensure the reliability of the measured emission levels. For Anasorb CSC tubes, the post-sampling method, including sample extraction and analysis, was thoroughly defined in accordance with official protocols (HSE, 2002; NIOSH, 1996; EPA, 1999). Reliability was ensured through accurate and precise analytical conditions established with designated trials, as detailed in **Annex A3.1**. These trials were also applied in **chapter 8.1** to define the side methodology used with TA tubes. This was done in preparation for the comparative assessment with the official methodology conducted with Anasorb CSC tubes, as described in **chapter 8.2**. Due to breakthrough issues, the quantitation of most of the volatiles present in the emissions collected with TA tubes was considered unreliable. However, two of these volatiles were found to be usable for comparison purposes. Nonetheless, the emission data obtained remained valuable for qualitative purposes. The consistency observed in the quantitative outcomes between TA and Anasorb CSC samples, coupled with the broader sensitivity of Anasorb CSC sorbents, not only validated the emission levels measured in previous assessments but also provided reliability to the original methodology. Moreover, the higher qualitative and quantitative performance achieved with Anasorb CSC tubes highlighted the greater versatility of these sorbents compared to TA material. Nonetheless, the side methodology implemented brought significant technical benefits to both the sampling and post-sampling processes, as detailed in **Annex A3.2**. With regards to the first, it allowed for dynamic sampling application in the open field without the need of enclosing, along with longer sampling intervals (up to 30 minutes). Concerning the second, the coupling with thermal desorption technique enabled much faster analysis and reduced bias associated with sample handling and solvent interaction before analysis, which was suitable for Anasorb CSC tubes as well. These enhancements were therefore utilized for the measurements described in **chapter 8.3**.

9.2 Plant-system influence on the emissions

Monitoring BVOCs emission in distinctive UA environments throughout the cultivation of different plant species provided insights into the plant-system interaction. Despite the indoor

and building-integrated configurations in this research, the significant influence of plant metabolism on emission activity has been demonstrated, as supported by previous studies (Herrmann, 2010; Calfapietra et al., 2013b). For each short-cycle crops – leafy vegetables and herbs– whether in the iRTG or in the VF, higher emissions were measured during the plant's full development (mature stage, as detailed in chapters 5 and 7). During this phase of the growing cycle, emissions are primarily sustained by the plant's primary metabolism (Dudareva et al., 2013; Mozaffar et al., 2018). With reference to tomato (representing a long-cycle sprawling crop), predictability of higher emissions can be hypothesized or retrieved from literature, as sampling focused primarily on this stage. However, it was also noted that the emissions trend and chemical composition are significantly influenced by the surroundings. This included factors such as light spectra (**chapter 7**), CO_2 concentration (**chapter 6**), and temperature and relative humidity rates (**chapters 4**, **5**, **6**, and **7**). These findings confirmed the plant's responsiveness to external stimuli, which is primarily regulated by the secondary metabolism (Niinemets et al., 2013; Bouwmeester et al., 2019).

9.3 Environmental setting influence

Both qualitative and quantitative variations detected in BVOC emissions were attributed to the different environmental stimuli received by the plants, therefore correlations between them were deepened. T and RH were mostly found to increase during the sampling in the static enclosure which was usually correlated with an emission fall (**chapters 5**, **6**, and **7**). The consistency of this trend with a general issue remarked in reference assessments (Ortega and Helmig, 2008; Pérez-Priego et al., 2015), which attributed it to a poor sampling performance exacerbated by the length of the enclosure, was frequently highlighted in this dissertation. For this reason, short sampling intervals were preferred. The enclosing effect was estimated by monitoring or deriving, when not feasible, plant's physiological indicators such as the stomatal conductance (**chapter 6** and **7**) and the net photosynthesis (**chapter 6**). The decrease in stomatal conductance, coupled with the negative correlation between emissions and increasing T and RH shown in **chapter 7** hints at potential influence of the chamber, although this effect was limited to one specific condition (under RB_3 lighting). In previous analyses the combination of T and RH regulated by the Henry's Law constant has been demonstrated to decrease sensibly the total concentration of VOCs (Xu and Zhang, 2011; Zhou et al., 2017). Overall, this assumption could only be hypothesized. CO_2 fluctuations were also considered, although investigation was limited to the environmental levels of the case studies, where high concentrations (≥800 ppm) were faced in the VF system exceptionally. Although high CO_2 concentrations and T were found to reduce BVOC release (Dani et al., 2014; Daussy and Staudt, 2020), in the VF this was not

observed. Similarly, in the iRTG the progressive decrease in CO_2 concentration did not significantly affect either quantitative or qualitative emission pattern when compared with ambient CO_2 levels in **chapter 6**. In view of missing experimental arguments and based on main research findings CO_2 contribution to BVOC emissions remained unclear. Concerning light influence in the research little relevance was given to the solar radiation according to low levels registered inside the iRTG and in the chamber likewise (**chapter 5** and **6**) due to the double screening performed by the façade and the cloth. When examining the light spectra in **chapter 7** distinctive emission patterns were observed throughout the cycle under specific R:B light ratios but differences were not significant. Nevertheless, significantly different stomatal activity was recorded between the two treatments, supporting differences founded and literature findings (Carvalho et al., 2016; Pennisi et al., 2019; Lauria et al., 2023).

9.4 General BVOC emissions impact on UA safety

In the research each investigated plant species was found to emit detectable levels of BVOCs into the environment. Overall, the average concentrations measured in the assessments reported in **chapters 4**, **5**, **6**, **7**, and **8**, as well as the isolated bursts compiled in Table X.34 of **Annex 4** were below the reference LCIs indicated in Table X.33 (**Annex 4**). Although higher levels were registered nearby the vegetative stage of the plants, in both iRTG and VF systems plant emissions—whether concentrations or equivalent rates—were consistent with previous assessments conducted on analogous species such as tomato and basil plants. Additionally, under the exposed conditions of the iRTG, crop emissions were compared with outdoor levels (as discussed in **chapters 4** and **8**) and indoor amounts (office settings, as described in **chapter 8**). Regardless of the methodological approach adopted, basically no difference was observed between BVOC concentrations in the iRTG and outside. This data suggested the effectiveness of air renewal facilitated by the iRTG's framework (Muñoz-Liesa et al., 2022), aligning with certain strategic policies aimed at controlling volatile concentrations indoors (ECA 2006, 2020). On the contrary, higher concentrations observed in popular indoor environments unrelated to UA, such as the office described in **chapter 8**, corroborated remarks made by the ECA (1995, 1997) regarding the significance of both spatial configuration and layout, and the potential accumulation of BVOCs. Under the indoor conditions of the VF, emission levels were found to be within the range of iRTG levels, measured in parts per billion (ppb), despite differences in plant species and environmental setting. However, concerning occasional emission bursts, exceptionally higher levels of some LOX derivatives were detected (as shown in Table X.37, **Annex 4**), approaching the LCI of the reference aldehyde 2-hexenal. At such concentrations, however, clinical trials did not highlight significant harmful effects on human health, aside from superficial

sensitization (skin irritation) after prolonged exposure (ECHA, 2023). To the same extent, in the worst-case scenario of iRTG—characterized by poor or no air renovation—longer exposure to the high levels detected (as shown in Table X.34-35-36, Annex 4) would still result in contained adverse effects. Certain BVOCs, such as 1.8-cineole and β-caryophyllene in VF, as well as α-terpinene and nonanal in iRTG, exhibited relatively higher emissions compared to other volatile compounds present in the sampled blend. Nevertheless, without specific LCIs and toxicological knowledge, the risks associated with these species could only be anticipated based on the information available for similar compounds.

Chapter 10

General conclusions

Chapter 10: General conclusions

Based on reasoned discussions of the research outcomes, the four questions raised at the beginning of the investigation have now been systematically addressed.

Q.1 What are actual BVOC emission levels in the considered UA environments and which volatile compounds accumulate more?

Based on the quantitative assessments reported in **chapters 5**, **6**, **7**, **8**, and **Annex 4** the average BVOC levels were found to range within parts per billion in both building-integrated and indoor UA environments. Additionally, the highest levels measured along individual samplings were commonly within the ppb range. Throughout the crop cycle, the highest emissions (referring to calculated EFs or ERs) were observed during the initial stages, gradually decreasing as the plants matured. However, exceptions to this trend were primarily associated with distinct environmental conditions. For example, during basil cultivation in the VF, higher emissions were registered in the young stage of plants growing under RB_1 LED light, whereas they were higher under RB_3 light in the mature stage. With respect to the quantitative distribution the iRTG and the VF did not show comparable patterns. In the iRTG, monoterpenes dominated BVOCs blend (77%) but showed a decreasing tendency along the growing cycle (19%) and were replaced by Lipoxygenase derivatives (from 15% to 65%), and oxygenated monoterpenes (from 2% to 16%), whereas sesquiterpenes and phenylpropanoids accounted for only 0.2% and 0.3% over the time. Although emission trends over the cultivation were tracked in **chapter 5** only (beans), similar percentages were observed in **chapter 6** (tomato plants) as well. In the VF, emission trends were distinctive of each light treatment, although OMTs were found to be the most abundant (from 36% to 74%), followed by LOX derivatives (from 1% to 60%), STs (from 0% to 29%), MTs (from 0% to 11%), and PHs (from 0 to 1%). It is noteworthy that while OMTs (1.8-cineole) were the most abundant in the VF, consistent with the originating plant species (basil), they did not predominate in the iRTG when the same species was cultivated (**chapter 8**). Once more, such discrepancies could be attributed to the external factors previously mentioned.

Q.2 Are the measured BVOC emission levels within the safety range fixed by official frameworks and/or most updated databanks?

BVOCs referenced LCIs reported in ECA lists (European Union, 2022) are still limited to few compounds, despite the broad spectrum of plant emissions. When a defined LCI was unavailable for the target volatile, it was attributed to the LCI provided for the most similar compound in terms of chemical composition. Based on the assessments conducted, it was observed that the

average emission levels of investigated BVOCs in both building-integrated and indoor UA environments were notably lower than the reference LCIs (Annex X.33 Table, **Annex 4**), by at least one order of magnitude. Individual samplings, though, revealed slightly higher emissions of lipoxygenase derivatives compared to the fixed health-risk threshold (7 μg m^{-3}) for the reference aldehyde 2-hexenal, across all considered plant species (bean, tomato, and basil) in both UA settings. However, these levels were deemed irrelevant for health concerns because their release was limited to specific plant states for relatively short durations, as determined by correlation matches found in **chapters 5**, **6**, and **7**. To guarantee/ensure safe levels, high emissions found for the unlisted BVOCs were compared against REACH registered factsheets of ECHA Dossier (2023b), among which STs-β-caryophyllene and trans-β-farnesene and OMT-1.8-cineole. Overall, the measured concentrations suggested that experiencing the health complications outlined in the factsheets was unlikely. It was hypothesized that volatile exposure would most likely result in localized sensitization, such as skin irritation or allergic reactions, depending on the individual.

Q.3 Which are the factors implicated in final BVOC emissions in the considered UA environments?

Throughout the research it was proved that carrying out UA indoors multiple factors can affect the internal conditions. Moreover, in an iRTG, the influence of the external environment must be considered despite its integration with the building. Variations of simple environmental parameters, like T, RH, and CO_2 concentration, shared among these two systems, but also the lighting setting, in the case of the VF, were found to significantly ($p \leq$ 0.001-0.05) affect plant's emission response, more than species influence. T and RH, and to some extent CO_2, were additionally affected by the BVOC sampling arrangement, leading to an increased impact on total emissions as discussed in **chapter 5**, **6**, and **7**. However, the actual implication of CO_2 at the current ambient and controlled concentrations in each building-integrated and indoor environment was not demonstrated in any of the assessments conducted. On the other hand, radiation was suggested to have a minor impact on plant emissions in building-integrated systems, particularly in the considered iRTG, where light screening is intensified by the polycarbonate facade material, even during peak season (summer) and highest exposure (LAU-1), as described in **chapter 6** and **Annex A1.2**. Conversely, artificial light in an indoor system, the VF, was believed to modulate the emission blend and quantity based on literature findings and observations reported **in chapter 7**. However, our assessment failed to confirm this hypothesis due to the poor significance of correlations (r_s< 0.8; p> 0.05) measured with two different R:B ratios. Finally, another relevant factor in both UA environments was the biological development

of the plants, as discussed in **chapters 5** (iRTG) and **7** (VF). Across subsequent stages, both qualitative and quantitative variations in BVOC emissions were observed. However, due to the lack of significant morphological differences between the stages and the absence of further evaluative elements, such impact could not be conclusively determined.

Q.4 Based on the overall investigation, do UA environments bring about unsafe conditions to human health? And if so, how could the BVOCs accumulation be contained and/or prevented?

The average BVOC emissions, including any incidental outbreaks, measured in the considered building-integrated and indoor UA systems were demonstrated to be significantly lower than established levels of concern, and resembled outdoor levels. Despite crop's emission release throughout the cultivation, the assumption of frequent air renewal associated with the iRTG's structure was then confirmed. Moreover, the research highlighted air turnovers even in the VF, as indicated by the different CO_2 concentrations measured across cultivation levels (±1600 ppm vs 800 ppm), although there was no proof of significant implication in the BVOCs trend. It was concluded that the internal conditions of these spaces largely maintained indoor BVOC concentrations at tolerable levels, thereby preventing the occurrence of dangerous scenarios. These observations strongly supported the implementation of UA integrated into households or public buildings, as well as in indoor spaces specifically designed for plant cultivation, such as VFs. Our findings were further confirmed by the additional assessment conducted at different locations related to the iRTG, as reported in **chapter 8**. Current BVOCs pattern measured across individual spaces reaffirmed emissions dilution under building-integrated conditions but also revealed BVOCs presence in common indoor environments disconnected from UA, such as the working offices. While this observation should be confirmed through more accurate estimations, it stressed out the potential impact of traditional indoor spaces despite green certifications provided, such as LEED of ICTA-UAB. Considering people's daily exposure to their emissions, it should be relevant the compliance with official qualitative air standards outlined by local institutions and frameworks, with particular emphasis on European ones in our case (ECA, 2006, 2020; European Parliament, 2021). This may be achieved by implementing the indicated assessments regularly.

Chapter 11

Further investigation

Chapter 11: Further investigation

In this final chapter, the suggested improvements derived from the research findings are briefly compiled as follows.

- Based on this preliminary study on Controlled-Environment Agriculture, further investigation could explore additional plant species and/or varieties, not only under standard cultivation regimes but also under different fertigation treatments. For example, the use of recovered fertilizers, such as struvite or compost, which have been recently introduced in UA, could significantly influence BVOC emissions, potentially varying according to the plant species and/or variety involved. Similarly, exploring alternative environmental conditions resulting from different combinations of light, CO_2, temperature, and relative humidity factors could significantly affect BVOC emission levels and profiles.
- Refining the quantitation analysis of TA tubes can be achieved by adjusting the sampling method, such as optimizing pump flow rates, sampling duration, and the environmental conditions throughout it. Additionally, exploring alternative sorbents with different polarity, such as Carbopack, could improve the sampling methodology. This approach would enhance the applicability of active sampling due to the simplified analytical procedure of reusable stainless-steel tubes, involving thermal desorption and further conditioning, while also enabling reliable sampling without static enclosure. By implementing these refinements, the scope of BVOCs investigation can be expanded to encompass multiple UA settings integrated with different cultivation systems (e.g., green walls). Furthermore, this methodology can be applied to assess air quality in diverse indoor environments.
- Exploring the feasibility of similar sampling techniques, such as Solid Phase Microextraction (SPME), within the methodology used, leveraging the insights gained from the research. SPME offers potential integration into dynamic sampling within static enclosures and presents additional technical advantages. Similar to TA and Carbopack tubes, SPME sorbent fibers can be thermally extracted and reconditioned afterward, rendering them cost-effective. This would therefore enhance the versatility of this sampling method and potentially provide valuable insights into BVOCs.
- Expanding the qualitative and quantitative investigation of BVOCs to include their derivatives resulting from the chemical reactions with airborne molecules, among others, ozone. Many of these volatile compounds are reactive species, such as NO, NO_x, and OH^-, which are associated with indoor air pollution. By broadening the scope of the

investigation to encompass these reactive species, a more comprehensive understanding of indoor air quality can be achieved.

〉 Applying the technical findings of this research across various investigation levels of BVOCs, shifting the focus towards the positive effects highlighted in the literature regarding, for instance, their role as biostimulants. The outcomes derived from this approach have the potential to benefit both plant cultivation and production, as well as human well-being attributed to the pleasant effects exerted on the nervous system. It is believed that these improvements will sustain the diffusion of UA in the city area.

References

Aguilar-Rodríguez, C.E., Flores -Velázquez, J., Rojano-Aguilar, F., Ojeda-Bustamante, W., Iñiguez-Covarrubias, M., 2020. Tomato (Solanum lycopersicum L.) crop cycle estimation in greenhouse, based on degree day heat (GDC) simulated in CFD. Tecnologia y Ciencias del Agua 11, 27–57. https://doi.org/10.24850/j-tyca-2020-04-02

Appolloni, E., Orsini, F., Specht, K., Thomaier, S., Sanyé-Mengual, E., Pennisi, G., Gianquinto, G., 2021. The global rise of urban rooftop agriculture: A review of worldwide cases. J Clean Prod 296, 126556. https://doi.org/https://doi.org/10.1016/j.jclepro.2021.126556

Arena, C., Tsonev, T., Doneva, D., de Micco, V., Michelozzi, M., Brunetti, C., Centritto, M., Fineschi, S., Velikova, V., Loreto, F., 2016. The effect of light quality on growth, photosynthesis, leaf anatomy and volatile isoprenoids of a monoterpene-emitting herbaceous species (Solanum lycopersicum L.) and an isoprene-emitting tree (Platanus orientalis L.). Environ Exp Bot 130, 122–132. https://doi.org/10.1016/j.envexpbot.2016.05.014

Armanda, D.T., Guinée, J.B., Tukker, A., 2019. The second green revolution: Innovative urban agriculture's contribution to food security and sustainability – A review. Glob Food Sec. https://doi.org/10.1016/j.gfs.2019.08.002

Avgoustaki, D.D., Xydis, G., 2021. Energy cost reduction by shifting electricity demand in indoor vertical farms with artificial lighting. Biosyst Eng 211, 219–229. https://doi.org/https://doi.org/10.1016/j.biosystemseng.2021.09.006

Baek, S.-O., Kim, Y.-S., Perry, R., 1997. Indoor air quality in homes, offices and restaurants in Korean urban areas—indoor/outdoor relationships. Atmos Environ 31, 529–544. https://doi.org/https://doi.org/10.1016/S1352-2310(96)00215-4

Bajomo, E.M., Aing, M.S., Ford, L.S., Niemeyer, E.D., 2022. Chemotyping of commercially available basil (Ocimum basilicum L.) varieties: Cultivar and morphotype influence phenolic acid composition and antioxidant properties. NFS Journal 26, 1–9. https://doi.org/https://doi.org/10.1016/j.nfs.2022.01.001

Ball, J.T., Woodrow, I.E., Berry, J.A., 1987. A Model Predicting Stomatal Conductance and its Contribution to the Control of Photosynthesis under Different Environmental Conditions, in: Biggins, J. (Ed.), Progress in Photosynthesis Research: Volume 4 Proceedings of the VIIth International Congress on Photosynthesis Providence, Rhode Island, USA, August 10–15, 1986. Springer Netherlands, Dordrecht, pp. 221–224. https://doi.org/10.1007/978-94-017-0519-6_48

Ballhorn, D.J., Kautz, S., Lion, U., Heil, M., 2008. Trade-offs between direct and indirect defences of lima bean (Phaseolus lunatus). Journal of Ecology 96, 971–980. https://doi.org/10.1111/j.1365-2745.2008.01404.x

Banerjee, A., Paul, K., Varshney, A., Nandru, R., Badhwar, R., Sapre, A., Dasgupta, S., 2022. Chapter 8 - Soilless indoor smart agriculture as an emerging enabler technology for food and nutrition security amidst climate change, in: Kumar, V., Srivastava, A.K., Suprasanna, P.

(Eds.), Plant Nutrition and Food Security in the Era of Climate Change. Academic Press, pp. 179–225. https://doi.org/https://doi.org/10.1016/B978-0-12-822916-3.00004-4

Barrett, G.E., Alexander, P.D., Robinson, J.S., Bragg, N.C., 2016. Achieving environmentally sustainable growing media for soilless plant cultivation systems – A review. Sci Hortic 212, 220–234. https://doi.org/https://doi.org/10.1016/j.scienta.2016.09.030

Bartual, J., Doctor, S., Químicas, C., 1986. NTP 151: Toma de muestras con captadores pasivos. Barcelona.

Benke, K., Tomkins, B., 2017. Future food-production systems: Vertical farming and controlled-environment agriculture. Sustainability: Science, Practice, and Policy 13, 13–26. https://doi.org/10.1080/15487733.2017.1394054

Boccalandro, H.E., Giordano, C. V., Ploschuk, E.L., Piccoli, P.N., Bottini, R., Casal, J.J., 2012. Phototropins but not cryptochromes mediate the blue light-specific promotion of stomatal conductance, while both enhance photosynthesis and transpiration under full sunlight. Plant Physiol 158, 1475–1484. https://doi.org/10.1104/pp.111.187237

Bouwmeester, H., Schuurink, R.C., Bleeker, P.M., Schiestl, F., 2019. The role of volatiles in plant communication. The Plant Journal 100, 892–907. https://doi.org/https://doi.org/10.1111/tpj.14496

Brilli, F., Fares, S., Ghirardo, A., de Visser, P., Calatayud, V., Muñoz, A., Annesi-Maesano, I., Sebastiani, F., Alivernini, A., Varriale, V., Menghini, F., 2018. Plants for Sustainable Improvement of Indoor Air Quality. Trends Plant Sci. https://doi.org/10.1016/j.tplants.2018.03.004

Buehler, D., Junge, R., 2016. Global Trends and Current Status of Commercial Urban Rooftop Farming. Sustainability 8. https://doi.org/10.3390/su8111108

Burge, H.A., Solomon, W.R., Muilenberg, M.L., 1982. Evaluation of indoor plantings as allergen exposure sources. Journal of Allergy and Clinical Immunology 70, 101–108. https://doi.org/https://doi.org/10.1016/0091-6749(82)90236-6

Buscaroli, E., Braschi, I., Cirillo, C., Fargue-Lelièvre, A., Modarelli, G.C., Pennisi, G., Righini, I., Specht, K., Orsini, F., 2021. Reviewing chemical and biological risks in urban agriculture: A comprehensive framework for a food safety assessment of city region food systems. Food Control 126, 108085. https://doi.org/https://doi.org/10.1016/j.foodcont.2021.108085

Bušić, A., Vojvodić, A., Komes, D., Akkermans, C., Belščak-Cvitanović, A., Stolk, M., Hofland, G., 2014. Comparative evaluation of CO2 drying as an alternative drying technique of basil (Ocimum basilicum L.) — The effect on bioactive and sensory properties. Food Research International 64, 34–42. https://doi.org/https://doi.org/10.1016/j.foodres.2014.06.013

Caballero-Casero, N., Rubio, S., 2022. Identification of bisphenols and derivatives in greenhouse dust as a potential source for human occupational exposure. Anal Bioanal Chem 414, 5397–5409. https://doi.org/10.1007/s00216-021-03863-x

Cai, M., An, C., Guy, C., 2021. A scientometric analysis and review of biogenic volatile organic compound emissions: Research hotspots, new frontiers, and environmental implications. Renewable and Sustainable Energy Reviews 149, 111317. https://doi.org/https://doi.org/10.1016/j.rser.2021.111317

Calfapietra, C., Pallozzi, E., Lusini, I., Velikova, V., 2013a. Modification of BVOC Emissions by Changes in Atmospheric [CO2] and Air Pollution 253–284. https://doi.org/10.1007/978-94-007-6606-8_10

Calfapietra, C., Pallozzi, E., Lusini, I., Velikova, V., Monson, R.K., Niinemets, Ü., 2013b. Biology, controls and models of tree volatile organic compound emissions, Biology, Controls and Models of Tree Volatile Organic Compound Emissions. https://doi.org/10.1007/978-94-007-6606-8

Carotti, L., Pistillo, A., Zauli, I., Meneghello, D., Martin, M., Pennisi, G., Gianquinto, G., Orsini, F., 2023. Improving water use efficiency in vertical farming: Effects of growing systems, far-red radiation and planting density on lettuce cultivation. Agric Water Manag 285, 108365. https://doi.org/10.1016/j.agwat.2023.108365

Carvalho, S.D., Schwieterman, M.L., Abrahan, C.E., Colquhoun, T.A., Folta, K.M., 2016. Light quality dependent changes in morphology, antioxidant capacity, and volatile production in sweet basil (Ocimum basilicum). Front Plant Sci 7. https://doi.org/10.3389/fpls.2016.01328

Catola, S., Centritto, M., Cascone, P., Ranieri, A., Loreto, F., Calamai, L., Balestrini, R., Guerrieri, E., 2018. Effects of single or combined water deficit and aphid attack on tomato volatile organic compound (VOC) emission and plant-plant communication. Environ Exp Bot 153, 54–62. https://doi.org/10.1016/j.envexpbot.2018.05.001

Chang, X., Alderson, P.G., Wright, C.J., 2008. Solar irradiance level alters the growth of basil (Ocimum basilicum L.) and its content of volatile oils. Environ Exp Bot 63, 216–223. https://doi.org/10.1016/j.envexpbot.2007.10.017

Chen, J., Tang, J., Yu, X., 2020. Environmental and physiological controls on diurnal and seasonal patterns of biogenic volatile organic compound emissions from five dominant woody species under field conditions. Environmental Pollution 259, 113955. https://doi.org/10.1016/j.envpol.2020.113955

Chuang, M.-T., Zhang, Y., Kang, D., 2011. Application of WRF/Chem-MADRID for real-time air quality forecasting over the Southeastern United States. Atmos Environ 45, 6241–6250. https://doi.org/https://doi.org/10.1016/j.atmosenv.2011.06.071

Churkina, G., Kuik, F., Bonn, B., Lauer, A., Grote, R., Tomiak, K., Butler, T., 2017. Effect of VOC Emissions from Vegetation on Air Quality in Berlin during a Heatwave. Environ Sci Technol 51, 6120–6130. https://doi.org/10.1021/acs.est.6b06514

Chutimanukul, P., Wanichananan, P., Janta, S., Toojinda, T., Darwell, C.T., Mosaleeyanon, K., 2022. The influence of different light spectra on physiological responses, antioxidant capacity and chemical compositions in two holy basil cultivars. Sci Rep 12. https://doi.org/10.1038/s41598-021-04577-x

Cirone, F., Masotti, M., Prosperi, P., Bosi, S., Dinelli, G., Vittuari, M., 2023. Business strategy pathways for short food supply chains: Sharing value between consumers and producers. Sustain Prod Consum 40, 458–470. https://doi.org/https://doi.org/10.1016/j.spc.2023.07.017

Clavijo-Herrera, J., Van Santen, E., Gómez, C., 2018. Growth, Water-Use Efficiency, Stomatal Conductance, and Nitrogen Uptake of Two Lettuce Cultivars Grown under Different Percentages of Blue and Red Light. Horticulturae 4. https://doi.org/10.3390/horticulturae4030016

Coggon, M.M., Gkatzelis, G.I., McDonald, B.C., Gilman, J.B., Schwantes, R.H., Abuhassan, N., Aikin, K.C., Arendd, M.F., Berkoff, T.A., Brown, S.S., Campos, T.L., Dickerson, R.R., Gronoff, G., Hurley, J.F., Isaacman-Vanwertz, G., Koss, A.R., Li, M., McKeen, S.A., Moshary, F., Peischl, J., Pospisilova, V., Ren, X., Wilson, A., Wu, Y., Trainer, M., Warneke, C., 2021. Volatile chemical product emissions enhance ozone and modulate urban chemistry. Proc Natl Acad Sci U S A 118. https://doi.org/10.1073/pnas.2026653118

Colston, N.M., Vadjunec, J.M., Wakeford, T., 2015. Exploring the entry points for citizen science in urban sustainability initiatives. Curr Opin Environ Sustain 17, 66–71. https://doi.org/https://doi.org/10.1016/j.cosust.2015.11.006

Copolovici, L., Kännaste, A., Pazouki, L., Niinemets, Ü., 2012. Emissions of green leaf volatiles and terpenoids from Solanum lycopersicum are quantitatively related to the severity of cold and heat shock treatments. J Plant Physiol 169, 664–672. https://doi.org/10.1016/j.jplph.2011.12.019

Copolovici, L., Kännaste, A., Remmel, T., Niinemets, Ü., 2014. Volatile organic compound emissions from Alnus glutinosa under interacting drought and herbivory stresses. Environ Exp Bot 100, 55–63. https://doi.org/10.1016/j.envexpbot.2013.12.011

Copolovici, L., Popitanu, A.C., Copolovici, D.M., 2021. Volatile organic compound emission and residual substances from plants in light of the globally increasing CO2 level. Curr Opin Environ Sci Health. https://doi.org/10.1016/j.coesh.2020.10.004

Cozzolino, R., Pace, B., Cefola, M., Martignetti, A., Stocchero, M., Fratianni, F., Nazzaro, F., De Giulio, B., 2016. Assessment of volatile profile as potential marker of chilling injury of basil leaves during postharvest storage. Food Chem 213, 361–368. https://doi.org/10.1016/j.foodchem.2016.06.109

Croft, K.P.C., Jüttner, F., Slusarenko, A.J., 1993. Volatile products of the lipoxygenase pathway evolved from Phaseolus vulgaris (L.) leaves inoculated with Pseudomonas syringae pv phaseolicola. Plant Physiol 101, 13–24. https://doi.org/10.1104/pp.101.1.13

Cruz, S., van Santen, E., Gómez, C., 2022. Evaluation of Compact Tomato Cultivars for Container Gardening Indoors and under Sunlight. Horticulturae 8. https://doi.org/10.3390/horticulturae8040294

Cummings, B.E., Waring, M.S., 2020. Potted plants do not improve indoor air quality: a review and analysis of reported VOC removal efficiencies. J Expo Sci Environ Epidemiol 30, 253–261. https://doi.org/10.1038/s41370-019-0175-9

Dani, K.G.S., Jamie, I.M., Prentice, I.C., Atwell, B.J., 2014. Evolution of isoprene emission capacity in plants. Trends Plant Sci. https://doi.org/10.1016/j.tplants.2014.01.009

Daussy, J., Staudt, M., 2020. Do future climate conditions change volatile organic compound emissions from Artemisia annua? Elevated CO2 and temperature modulate actual VOC emission rate but not its emission capacity. Atmos Environ X 7, 100082. https://doi.org/https://doi.org/10.1016/j.aeaoa.2020.100082

Degenhardt, D.C., Refi-Hind, S., Stratmann, J.W., Lincoln, D.E., 2010. Systemin and jasmonic acid regulate constitutive and herbivore-induced systemic volatile emissions in tomato, Solanum lycopersicum. Phytochemistry 71, 2024–2037. https://doi.org/10.1016/j.phytochem.2010.09.010

Delorme, M., Santini, A., 2022. Energy-efficient automated vertical farms. Omega (Westport) 109, 102611. https://doi.org/https://doi.org/10.1016/j.omega.2022.102611

Dodman, D.M., Hayward, B., Pelling, M., Broto, V., Chow, W., Chu, E., Dawson, R., Khirfan, L., McPherson, T., Prakash, A., Zheng, Y., Ziervogel, G., Archer, D., Bertolin, C., Brail, S., Cartwright, A., Chester, M., Colenbrander, S., Dhar, T., Westman, L., 2022. Cities, Settlements and Key Infrastructure. In: Climate Change 2022: Impacts, Adaptation and Vulnerability. Contribution of Working Group II to the Sixth Assessment Report of the Intergovernmental Panel on Climate Change. https://doi.org/10.1017/9781009325844.008

Doi, M., Kitagawa, Y., Shimazaki, K.I., 2015. Stomatal blue light response is present in early vascular plants. Plant Physiol 169, 1205–1213. https://doi.org/10.1104/pp.15.00134

Domingo, J.L., Nadal, M., 2009. Domestic waste composting facilities: A review of human health risks. Environ Int 35, 382–389. https://doi.org/10.1016/j.envint.2008.07.004

D'Ostuni, M., Zaffi, L., Appolloni, E., Orsini, F., 2022. Understanding the complexities of Building-Integrated Agriculture. Can food shape the future built environment? Futures 144, 103061. https://doi.org/https://doi.org/10.1016/j.futures.2022.103061

Dou, H., Niu, G., Gu, M., Masabni, J.G., 2018. Responses of sweet basil to different daily light integrals in photosynthesis, morphology, yield, and nutritional quality. HortScience 53, 496–503. https://doi.org/10.21273/HORTSCI12785-17

Drewer, J., Howard, D., McNamara, N., 2018. Greenhouse Gas (GHG) and Biogenic Volatile Organic Compound (bVOC) Fluxes Associated With Land-Use Change to Bioenergy Crops, Greenhouse Gas Balances of Bioenergy Systems. Elsevier Inc. https://doi.org/10.1016/B978-0-08-101036-5.00006-9

Duan, C., Liao, H., Wang, K., Ren, Y., 2023. The research hotspots and trends of volatile organic compound emissions from anthropogenic and natural sources: A systematic quantitative review. Environ Res 216, 114386. https://doi.org/https://doi.org/10.1016/j.envres.2022.114386

Dudareva, N., Klempien, A., Muhlemann, J.K., Kaplan, I., 2013. Biosynthesis, function and metabolic engineering of plant volatile organic compounds. New Phytologist 198, 16–32. https://doi.org/10.1111/nph.12145

Duhl, T.R., Helmig, D., Guenther, A., 2008. Sesquiterpene emissions from vegetation: A review. Biogeosciences 5, 761–777. https://doi.org/10.5194/bg-5-761-2008

Engler, N., Krarti, M., 2021. Review of energy efficiency in controlled environment agriculture. Renewable and Sustainable Energy Reviews 141, 110786. https://doi.org/https://doi.org/10.1016/j.rser.2021.110786

Ercilla-Montserrat, M., Izquierdo, R., Belmonte, J., Montero, J.I., Muñoz, P., De Linares, C., Rieradevall, J., 2017. Building-integrated agriculture: A first assessment of aerobiological air quality in rooftop greenhouses (i-RTGs). Science of the Total Environment 598, 109–120. https://doi.org/10.1016/j.scitotenv.2017.04.099

European Chemicals Agency (ECHA), 2023a. REACH Dossier (Last updated 01 December 2023) [WWW Document]. URL https://www.echa.europa.eu/information-on-chemicals (accessed 12.4.23).

European Chemicals Agency (ECHA), 2023b. REACH registered substance factsheets: trans-hex-2-enal, EC number 229-778-1 [WWW Document]. InfoCard. URL https://echa.europa.eu/es/registration-dossier/-/registered-dossier/25168 (accessed 12.4.23).

European Chemicals Agency (ECHA), 2023c. REACH registered substance factsheets: Cineole, EC number 207-431-5 [WWW Document]. InfoCard. URL https://echa.europa.eu/es/registration-dossier/-/registered-dossier/13231/7/3/1 (accessed 12.4.23).

European Chemicals Agency (ECHA), 2023d. REACH registered substance factsheets: Caryophyllene, EC number 201-746-1 [WWW Document]. InfoCard. URL https://www.echa.europa.eu/web/guest/registration-dossier/-/registered-dossier/13231 (accessed 12.4.23).

European Chemicals Agency (ECHA), 2023e. REACH registered substance factsheets: (E)-7,11-dimethyl-3-methylenedodeca-1,6,10-triene, EC number 242-582-0 [WWW Document]. InfoCard. URL https://echa.europa.eu/es/registration-dossier/-/registered-dossier/10936/7/3/3 (accessed 12.4.23).

European Collaborative Action (ECA), 2020. Urban Air, Indoor Environment and Human Exposure, Report No.30, Framework for health-based ventilation guidelines in Europe. Luxembourg. https://doi.org/10.2788/17476

European Collaborative Action (ECA), 2006. Urban Air, Indoor Environment and Human Exposure, Report no.25, Strategies to determine and control the contributions of indoor air pollution to total inhalation exposure: STRATEX. Publications Office, Luxembourg.

European Collaborative Action (ECA), 2000. Urban Air, Indoor Environment and Human Exposure, Report no. 22, Risk assessment in relation to indoor air quality. Office for Official Publications of the European Communities, Luxembourg.

European Collaborative Action (ECA), 1997a. Indoor Air and its Impact on man, Report No.18, Evaluation of VOC emissions from building products. Solid flooring materials. , Luxembourg.

European Collaborative Action (ECA), 1997b. Indoor Air Quality and its Impact on man, Report no.19, Total Volatile Organic Compounds (TVOC) in indoor air quality investigations. Office for Official Publications of the European Communities, Luxembourg.

European Collaborative Action (ECA), 1995. Indoor Air and its Impact on man, Report No.16, Determination of VOCs emitted from indoor materials and products : Second interlaboratory comparison of small chamber measurements. Commission of the European Communities, Directorate General for Science, Research and Development Joint Research Centre - Institute for the Environment , Luxembourg.

European Collaborative Action (ECA), 1991a. Indoor Air Quality and its Impact on man, Report no. 10, Effects of Indoor Air pollution on Human Health. Luxembourg .

European Collaborative Action (ECA), 1991b. Indoor Air Quality and its Impact on man, Report no. 9, Project Inventory. 2nd Updated Edition. Luxembourg.

European Collaborative Action (ECA), 1989. Indoor Air and its Impact on man, Report No.6, Strategy for sampling. chemicals Substances in Indoor Air. Luxembourg.

European Collaborative Agency (ECA), 2007. Urban Air, Indoor Environment and Human Exposure, Report No. 26, Impact of ozone-initiated terpene chemistry on indoor air quality and human health. Publications Office, Luxembourg.

European Commission, 2019. COMMUNICATION FROM THE COMMISSION TO THE EUROPEAN PARLIAMENT, THE EUROPEAN COUNCIL, THE COUNCIL, THE EUROPEAN ECONOMIC AND SOCIAL COMMITTEE AND THE COMMITTEE OF THE REGIONS - The European Green Deal, EUR-Lex. Brussels.

European Food Safety Authority (EFSA), 2014. EFSA Guidance Document on clustering and ranking of emissions of active substances of plant protection products and transformation products of these active substances from protected crops (greenhouses and crops grown under cover) to relevant environmental compartments. EFSA Journal 12, 3615. https://doi.org/https://doi.org/10.2903/j.efsa.2014.3615

European Parliament, 2021. Implementation of the Ambient Air Quality Directives - European Parliament resolution of 25 March 2021 on the implementation of the Ambient Air Quality Directives: Directive 2004/107/EC and Directive 2008/50/EC (2020/2091(INI)), Official Journal of the European Union.

European Union, 2022. Agreed EU-LCI values (December 2022). Luxemburg.

European Union, 2013. Urban Air, Indoor Environment and Human Exposure: Harmonisation framework for health based evaluation of indoor emissions from construction products in the European Union using the EU-LCI concept. Office for Official Publications of the European Communities, Luxembourg.

European Union, 2008. Impact of ozone-initiated terpene chemistry on indoor air quality and human health. European collaborative action: Urban air, indoor environment and human exposure. Environment and Quality of Life Report no.26. Luxembourg.

Fabbri, B., Valt, M., Parretta, C., Gherardi, S., Gaiardo, A., Malagù, C., Mantovani, F., Strati, V., Guidi, V., 2020. Correlation of gaseous emissions to water stress in tomato and maize crops: From field to laboratory and back. Sens Actuators B Chem 303. https://doi.org/10.1016/j.snb.2019.127227

Falara, V., Akhtar, T.A., Nguyen, T.T.H., Spyropoulou, E.A., Bleeker, P.M., Schauvinhold, I., Matsuba, Y., Bonini, M.E., Schilmiller, A.L., Last, R.L., Schuurink, R.C., Pichersky, E., 2011. The tomato terpene synthase gene family. Plant Physiol 157, 770–789. https://doi.org/10.1104/pp.111.179648

Farag, M.A., Paré, P.W., 2002. C6-green leaf volatiles trigger local and systemic VOC emissions in tomato. Phytochemistry 61, 545–554. https://doi.org/10.1016/S0031-9422(02)00240-6

Fisch, G., 2004. Biogenic VOC emissions from forested Amazonian landscapes 651–662. https://doi.org/10.1111/j.1529-8817.2003.00758.x

Fischer, R., Nitzan, N., Chaimovitsh, D., Rubin, B., Dudai, N., 2011. Variation in essential oil composition within individual leaves of sweet basil (Ocimum basilicum L.) is more affected by leaf position than by leaf age. J Agric Food Chem 59, 4913–4922. https://doi.org/10.1021/jf200017h

Fox-Kämper, R., Kirby, C.K., Specht, K., Cohen, N., Ilieva, R., Caputo, S., Schoen, V., Hawes, J.K., Ponizy, L., Béchet, B., 2023. The role of urban agriculture in food-energy-water nexus policies: Insights from Europe and the U.S. Landsc Urban Plan 239, 104848. https://doi.org/https://doi.org/10.1016/j.landurbplan.2023.104848

Fu, P., Kawamura, K., Kanaya, Y., Wang, Z., 2010. Contributions of biogenic volatile organic compounds to the formation of secondary organic aerosols over Mt. Tai, Central East China. Atmos Environ 44, 4817–4826. https://doi.org/10.1016/j.atmosenv.2010.08.040

Geron, C.D., Pierce, T.E., Guenther, A.B., 1995. Reassessment of biogenic volatile organic compound emissions in the Atlanta area. Atmos Environ 29, 1569–1578. https://doi.org/10.1016/1352-2310(94)00274-O

Glotfelty, T., Zhang, Y., Karamchandani, P., Streets, D.G., 2016. Changes in future air quality, deposition, and aerosol-cloud interactions under future climate and emission scenarios. Atmos Environ 139, 176–191. https://doi.org/10.1016/j.atmosenv.2016.05.008

Gould, D., Caplow, T., 2012. 8 - Building-integrated agriculture: a new approach to food production, in: Zeman, F. (Ed.), Metropolitan Sustainability, Woodhead Publishing Series

in Energy. Woodhead Publishing, pp. 147–170. https://doi.org/https://doi.org/10.1533/9780857096463.2.147

Graamans, L., Baeza, E., van den Dobbelsteen, A., Tsafaras, I., Stanghellini, C., 2018. Plant factories versus greenhouses: Comparison of resource use efficiency. Agric Syst 160, 31–43. https://doi.org/10.1016/j.agsy.2017.11.003

Guenther, A., Karl, T., Harley, P., Wiedinmyer, C., Palmer, P.I., Geron, C., 2006. Estimates of global terrestrial isoprene emissions using MEGAN (Model of Emissions of Gases and Aerosols from Nature). Atmos Chem Phys 6, 3181–3210. https://doi.org/10.5194/acp-6-3181-2006

Gumisiriza, M.S., Ndakidemi, P., Nalunga, A., Mbega, E.R., 2022. Building sustainable societies through vertical soilless farming: A cost-effectiveness analysis on a small-scale non-greenhouse hydroponic system. Sustain Cities Soc 83, 103923. https://doi.org/https://doi.org/10.1016/j.scs.2022.103923

Gunawardena, K., Steemers, K., 2019. Living walls in indoor environments. Build Environ. https://doi.org/10.1016/j.buildenv.2018.11.014

Hammock, H.A., Kopsell, D.A., Sams, C.E., 2021. Narrowband Blue and Red LED Supplements Impact Key Flavor Volatiles in Hydroponically Grown Basil Across Growing Seasons. Front Plant Sci 12. https://doi.org/10.3389/fpls.2021.623314

Hantson, S., Knorr, W., Schurgers, G., Pugh, T.A.M., Arneth, A., 2017. Global isoprene and monoterpene emissions under changing climate, vegetation, CO2 and land use. Atmos Environ 155, 35–45. https://doi.org/10.1016/j.atmosenv.2017.02.010

Harley, P.C., 2013. The Roles of Stomatal Conductance and Compound Volatility in Controlling the Emission of Volatile Organic Compounds from Leaves, in: Niinemets Ülo and Monson, R.K. (Ed.), Biology, Controls and Models of Tree Volatile Organic Compound Emissions. Springer Netherlands, Dordrecht, pp. 181–208. https://doi.org/10.1007/978-94-007-6606-8_7

Hashimoto, M., Negi, J., Young, J., Israelsson, M., Schroeder, J.I., Iba, K., 2006. Arabidopsis HT1 kinase controls stomatal movements in response to CO2. Nat Cell Biol 8, 391–397. https://doi.org/10.1038/ncb1387

Health and Safety Executive (HSE), 2002. MDHS no 96 Volatile organic compounds in air - Laboratory method using pumed solid sorbent tubes, solvent desorption and gas chromatography, in: Methods for the Determination of Hazardous Substances (MDHS) . Crown, Norwich , pp. 1–24.

Health and Safety Executive (HSE), 1993. MDHS no 72 Volatile organic compounds in air - Laboratory method using pumped solid sorbent tubes and gas chromatography, in: Methods for the Determination of Hazardous Substances (MDHS) . Crown , Norwich.

Heiden, A. C., Kobel, K., Langebartels, C., Schuh-Thomas, G., Wildt, J., 2003. Emissions of oxygenated volatile organic compounds from plants part I: Emissions from lipoxygenase activity. J Atmos Chem 45, 143–172. https://doi.org/10.1023/A:1024069605420

Heiden, A C, Kobel, K., Langebartels, C., Schuh-Thomas, G., Wildt, J., 2003. Emissions of Oxygenated Volatile Organic Compounds from Plants Part I: Emissions from Lipoxygenase Activity, Journal of Atmospheric Chemistry.

Herrmann, A., 2010. The Chemistry and Biology of Volatiles, The Chemistry and Biology of Volatiles. https://doi.org/10.1002/9780470669532

Hiyama, A., Takemiya, A., Munemasa, S., Okuma, E., Sugiyama, N., Tada, Y., Murata, Y., Shimazaki, K.I., 2017. Blue light and CO2 signals converge to regulate light-induced stomatal opening. Nat Commun 8. https://doi.org/10.1038/s41467-017-01237-5

Holzke, C., Dindorf, T., Kesselmeier, J., Kuhn, U., Koppmann, R., 2006. Terpene emissions from European beech (Fagus sylvatica L.): Pattern and emission behaviour over two vegetation periods. J Atmos Chem 55, 81–102. https://doi.org/10.1007/s10874-006-9027-9

HUI, L.C., JIM, C.Y., TIAN, Y., 2022. Public views on green roofs and green walls in two major Asian cities and implications for promotion policy. Urban For Urban Green 70, 127546. https://doi.org/https://doi.org/10.1016/j.ufug.2022.127546

Iaquinta, D.L., Drescher, A.W., 2015. Urban Agriculture: A Comparative Review of Allotment and Community Gardens, in: Urban Ecosystem Ecology. John Wiley & Sons, Ltd, pp. 199–226. https://doi.org/10.2134/agronmonogr55.c10

INSHT, 1983. NTP 151: Toma de muestras con captadores pasivos, in: Bartual Sánchez, J. (Ed.), . INSHT, Barcelona, p. 5.

International Agency for Research on Cancer, 2016. Outdoor Air Pollution. IARC Monograph 109.

International Organization for Standardization (ISO), 2003. ISO 16017-2. Indoor, ambient and workplace air — Sampling and analysis of volatile organic compounds by sorbent tube/thermal desorption/capillary gas chromatography — Part 2: Diffusive sampling. Geneva.

International Organization for Standardization (ISO), 2000. ISO 16017-1. Indoor, ambient and workplace air — Sampling and analysis of volatile organic compounds by sorbent tube/thermal desorption/capillary gas chromatography — Part 1: Pumped sampling. Geneva.

IPCC, 2023. SYNTHESIS REPORT OF THE IPCC SIXTH ASSESSMENT REPORT (AR6), Diriba Korecha Dadi. Panmao Zhai, INTERLAKEN, Switzerland.

IPCC, 2022. Climate Change 2022: Impacts, Adaptation, and Vulnerability. Contribution of Working Group II to the Sixth Assessment Report of the Intergovernmental Panel on Climate Change. Cambridge, UK and New York, NY, USA. https://doi.org/10.1017/9781009325844

IPCC, 2021. Technical Summary. Contribution of Working Group I to the Sixth Assessment Report of the Intergovernmental Panel on Climate Change. Climate Change 2021: The Physical Science Basis. 3949.

Jamloki, A., Bhattacharyya, M., Nautiyal, M.C., Patni, B., 2021. Elucidating the relevance of high temperature and elevated CO2 in plant secondary metabolites (PSMs) production. Heliyon 7, 1–13. https://doi.org/10.1016/j.heliyon.2021.e07709

Jansen, R.M.C., Hofstee, J.W., Wildt, J., Vanthoor, B.H.E., Verstappen, F.W.A., Takayama, K., Bouwmeester, H.J., van Henten, E.J., 2010. Health monitoring of plants by their emitted volatiles: A model to predict the effect of Botrytis cinerea on the concentration of volatiles in a large-scale greenhouse. Biosyst Eng 106, 37–47. https://doi.org/10.1016/j.biosystemseng.2010.01.009

Jansen, R.M.C., Hofstee, J.W., Wildt, J., Verstappen, F.W.A., Bouwmeester, H.J., Posthumus, M.A., van Henten, E.J., 2009. Health monitoring of plants by their emitted volatiles: Trichome damage and cell membrane damage are detectable at greenhouse scale. Annals of Applied Biology 154, 441–452. https://doi.org/10.1111/j.1744-7348.2008.00311.x

Jansen, R.M.C., Wildt, J., Kappers, I.F., Bouwmeester, H.J., Hofstee, J.W., van Henten, E.J., 2011. Detection of Diseased Plants by Analysis of Volatile Organic Compound Emission. Annu Rev Phytopathol 49, 157–174. https://doi.org/10.1146/annurev-phyto-072910-095227

Jensen, N.B., Clausen, M.R., Kjaer, K.H., 2018. Spectral quality of supplemental LED grow light permanently alters stomatal functioning and chilling tolerance in basil (Ocimum basilicum L.). Sci Hortic 227, 38–47. https://doi.org/10.1016/j.scienta.2017.09.011

Juuti, S., Arey, J., Atkinson, R., 1990. Monoterpene emission rate measurements from a Monterey pine. J Geophys Res 95, 7515. https://doi.org/10.1029/jd095id06p07515

Kanagendran, A., Pazouki, L., Bichele, R., Külheim, C., Niinemets, Ü., 2018. Temporal regulation of terpene synthase gene expression in Eucalyptus globulus leaves upon ozone and wounding stresses: relationships with stomatal ozone uptake and emission responses. Environ Exp Bot 155, 552–565. https://doi.org/10.1016/j.envexpbot.2018.08.002

Kari, E., Miettinen, P., Yli-Pirilä, P., Virtanen, A., Faiola, C.L., 2018. PTR-ToF-MS product ion distributions and humidity-dependence of biogenic volatile organic compounds. Int J Mass Spectrom 430, 87–97. https://doi.org/10.1016/j.ijms.2018.05.003

Karl, T., Guenther, A., Turnipseed, A., Patton, E.G., Jardine, K., 2008. Chemical sensing of plant stress at the ecosystem scale. Biogeosciences 5, 1287–1294. https://doi.org/10.5194/bg-5-1287-2008

Kasal-Slavik, T., Eschweiler, J., Kleist, E., Mumm, R., Goldbach, H.E., Schouten, A., Wildt, J., 2017. Early biotic stress detection in tomato (Solanum lycopersicum) by BVOC emissions. Phytochemistry 144, 180–188. https://doi.org/10.1016/j.phytochem.2017.09.006

Kim, H.H., Lee, J.Y., Yang, J.Y., Kim, K.J., Lee, Y.J., Shin, D.C., Lim, Y.W., 2011. Evaluation of indoor air quality and health related parameters in office buildings with or without indoor plants. Journal of the Japanese Society for Horticultural Science 80, 96–102. https://doi.org/10.2503/jjshs1.80.96

Kim, J.-C., Kim, K.-J., Kim, D.-S., Han, J.-S., 2005. Seasonal variations of monoterpene emissions from coniferous trees of different ages in Korea. Chemosphere 59, 1685–1696. https://doi.org/10.1016/j.chemosphere.2004.10.048

Klein, T., Ramon, U., 2019. Stomatal sensitivity to CO2 diverges between angiosperm and gymnosperm tree species. Funct Ecol 33, 1411–1424. https://doi.org/10.1111/1365-2435.13379

Klimánková, E., Holadová, K., Hajšlová, J., Čajka, T., Poustka, J., Koudela, M., 2008. Aroma profiles of five basil (Ocimum basilicum L.) cultivars grown under conventional and organic conditions. Food Chem 107, 464–472. https://doi.org/10.1016/j.foodchem.2007.07.062

Kobayashi, Y., Kotilainen, T., Carmona-García, G., Leip, A., Tuomisto, H.L., 2022. Vertical farming: A trade-off between land area need for crops and for renewable energy production. J Clean Prod 379, 134507. https://doi.org/https://doi.org/10.1016/j.jclepro.2022.134507

Komenda, M., Parusel, E., Wedel, A., Koppmann, R., 2001. Measurements of biogenic VOC emissions: Sampling, analysis and calibration. Atmos Environ 35, 2069–2080. https://doi.org/10.1016/S1352-2310(00)00502-1

Kozai, T., Niu, G., 2016. Chapter 4 - Plant Factory as a Resource-Efficient Closed Plant Production System, in: Kozai, T., Niu, G., Takagaki, M. (Eds.), Plant Factory. Academic Press, San Diego, pp. 69–90. https://doi.org/https://doi.org/10.1016/B978-0-12-801775-3.00004-4

Kulmala, M., Nieminen, T., Chellapermal, R., Makkonen, R., Bäck, J., Kerminen, V.-M., 2013. Climate Feedbacks Linking the Increasing Atmospheric CO2 Concentration, BVOC Emissions, Aerosols and Clouds in Forest Ecosystems, in: Niinemets, Ü., Monson, R.K. (Eds.), Biology, Controls and Models of Tree Volatile Organic Compound Emissions. Springer Netherlands, Dordrecht, pp. 489–508. https://doi.org/10.1007/978-94-007-6606-8_17

Kutralam-Muniasamy, G., Shruti, V.C., Pérez-Guevara, F., 2023. Citizen involvement in reducing end-of-life product waste in Mexico City. Sustain Prod Consum 41, 167–178. https://doi.org/https://doi.org/10.1016/j.spc.2023.08.010

Lampinen, J., García-Antúnez, O., Olafsson, A.S., Kavanagh, K.C., Gulsrud, N.M., Raymond, C.M., 2022. Envisioning carbon-smart and just urban green infrastructure. Urban For Urban Green 75, 127682. https://doi.org/https://doi.org/10.1016/j.ufug.2022.127682

Langemeyer, J., Madrid-Lopez, C., Mendoza Beltran, A., Villalba Mendez, G., 2021. Urban agriculture — A necessary pathway towards urban resilience and global sustainability? Landsc Urban Plan 210, 104055. https://doi.org/10.1016/J.LANDURBPLAN.2021.104055

Lanoue, J., Leonardos, E.D., Grodzinski, B., 2018. Effects of light quality and intensity on diurnal patterns and rates of photo-assimilate translocation and transpiration in tomato leaves. Front Plant Sci 9. https://doi.org/10.3389/fpls.2018.00756

Laothawornkitkul, J., Taylor, J.E., Paul, N.D., Hewitt, C.N., 2009. Biogenic volatile organic compounds in the Earth system: Tansley review. New Phytologist 183, 27–51. https://doi.org/10.1111/j.1469-8137.2009.02859.x

Larsen, D.H., Woltering, E.J., Nicole, C.C.S., Marcelis, L.F.M., 2020. Response of Basil Growth and Morphology to Light Intensity and Spectrum in a Vertical Farm. Front Plant Sci 11. https://doi.org/10.3389/fpls.2020.597906

Lauria, G., Lo Piccolo, E., Davini, A., Ruffini Castiglione, M., Pieracci, Y., Flamini, G., Martens, S., Angeli, A., Ceccanti, C., Guidi, L., Pellegrini, E., Incrocci, L., Landi, M., 2023. Modulation of VOC fingerprint and alteration of physiological responses after supplemental LED light in green- and red-leafed sweet basil (Ocimum basilicum L.). Sci Hortic 315. https://doi.org/10.1016/j.scienta.2023.111970

Li, H., Zhao, Y., Sützl, B., Kubilay, A., Carmeliet, J., 2022. Impact of green walls on ventilation and heat removal from street canyons: Coupling of thermal and aerodynamic resistance. Build Environ 214, 108945. https://doi.org/https://doi.org/10.1016/j.buildenv.2022.108945

Li, L., Guenther, A.B., Xie, S., Gu, D., Seco, R., Nagalingam, S., Yan, D., 2019. Evaluation of semi-static enclosure technique for rapid surveys of biogenic volatile organic compounds (BVOCs) emission measurements. Atmos Environ 212, 1–5. https://doi.org/10.1016/j.atmosenv.2019.05.029

Li, S., Harley, P.C., Niinemets, Ü., 2017. Ozone-induced foliar damage and release of stress volatiles is highly dependent on stomatal openness and priming by low-level ozone exposure in Phaseolus vulgaris. Plant Cell Environ 40, 1984–2003. https://doi.org/10.1111/pce.13003

Li, Shuangjiang, Agathokleous, E., Li, Shenglan, Yuan, X., Du, Y., Feng, Z., 2023. Sensitivity of isoprene emission rate to ozone in greening trees is concurrently determined by isoprene synthesis capacity and stomatal conductance. Science of The Total Environment 164325. https://doi.org/10.1016/j.scitotenv.2023.164325

Lin, K.H., Huang, M.Y., Hsu, M.H., 2021. Morphological and physiological response in green and purple basil plants (Ocimum basilicum) under different proportions of red, green, and blue LED lightings. Sci Hortic 275. https://doi.org/10.1016/j.scienta.2020.109677

LLorach Massana, P., 2017. Mitigating the environmental impacts of Urban Agriculture: innovative materials, GHG emissions analysis and new by-products. UAB.

Llusi, J., Pe, J., Gimeno, B.S., 2002. Seasonal and species-specific response of VOC emissions by Mediterranean woody plant to elevated ozone concentrations, Atmospheric Environment.

Loreto, F., Barta, C., Brilli, F., Nogues, I., 2006. On the induction of volatile organic compound emissions by plants as consequence of wounding or fluctuations of light and temperature. Plant Cell Environ 29, 1820–1828. https://doi.org/10.1111/j.1365-3040.2006.01561.x

Loreto, F., Schnitzler, J.P., 2010. Abiotic stresses and induced BVOCs. Trends Plant Sci. https://doi.org/10.1016/j.tplants.2009.12.006

Lun, X., Lin, Y., Chai, F., Fan, C., Li, H., Liu, J., 2020. Reviews of emission of biogenic volatile organic compounds (BVOCs) in Asia. Journal of Environmental Sciences 95, 266–277. https://doi.org/https://doi.org/10.1016/j.jes.2020.04.043

Lundgren, B., Crump, D.R., Knoppel, H., Laurent, A.M., Lebret, E., Rothweiler, H., Seifert, B., Wolkoff, P., Cavallo, D., 1994. Report No. 14, Sampling Strategies for Volatile Organic Compounds (VOCs) in Indoor Air, Indoor Air Quality & Its I Pact on Man. European Commission, Joint Research Centre - Environment Institute, Luxembourg.

Madsen, A.M., Tendal, K., Thilsing, T., Frederiksen, M.W., Baelum, J., Hansen, J. V, 2013. Fungi, β-Glucan, and Bacteria in Nasal Lavage of Greenhouse Workers and Their Relation to Occupational Exposure. Ann Occup Hyg 57, 1030–1040. https://doi.org/10.1093/annhyg/met019

Maffei, M.E., 2010. Sites of synthesis, biochemistry and functional role of plant volatiles. South African Journal of Botany 76, 612–631. https://doi.org/10.1016/j.sajb.2010.03.003

Maffei, M.E., Gertsch, J., Appendino, G., 2011. Plant volatiles: Production, function and pharmacology. Nat Prod Rep 28, 1359–1380. https://doi.org/10.1039/c1np00021g

Magwaza, S.T., Magwaza, L.S., Odindo, A.O., Mditshwa, A., 2020. Hydroponic technology as decentralised system for domestic wastewater treatment and vegetable production in urban agriculture: A review. Science of the Total Environment 698, 134154. https://doi.org/10.1016/j.scitotenv.2019.134154

Mahilang, M., Deb, M.K., Pervez, S., 2021. Biogenic secondary organic aerosols: A review on formation mechanism, analytical challenges and environmental impacts. Chemosphere 262, 127771. https://doi.org/https://doi.org/10.1016/j.chemosphere.2020.127771

Malik, T.G., Gajbhiye, T., Pandey, S.K., 2018. Plant specific emission pattern of biogenic volatile organic compounds (BVOCs) from common plant species of Central India. Environ Monit Assess 190. https://doi.org/10.1007/s10661-018-7015-6

Manco, A., Brilli, F., Famulari, D., Gasbarra, D., Gioli, B., Vitale, L., Tommasi, P. di, Loubet, B., Arena, C., Magliulo, V., 2021. Cross-correlations of Biogenic Volatile Organic Compounds (BVOC) emissions typify different phenological stages and stressful events in a Mediterranean Sorghum plantation. Agric For Meteorol 303. https://doi.org/10.1016/j.agrformet.2021.108380

Martin, M., Weidner, T., Gullström, C., 2022. Estimating the Potential of Building Integration and Regional Synergies to Improve the Environmental Performance of Urban Vertical Farming. Front Sustain Food Syst 6. https://doi.org/10.3389/fsufs.2022.849304

Martins, S.J., Faria, A.F., Pedroso, M.P., Cunha, M.G., Rocha, M.R., Medeiros, F.H.V., 2019. Microbial volatiles organic compounds control anthracnose (Colletotrichum lindemuthianum) in common bean (Phaseolus vulgaris L.). Biological Control 131, 36–42. https://doi.org/10.1016/j.biocontrol.2019.01.003

Materić, D., Bruhn, D., Turner, C., Morgan, G., Mason, N., Gauci, V., 2015. Methods in Plant Foliar Volatile Organic Compounds Research. Appl Plant Sci 3, 1500044. https://doi.org/10.3732/apps.1500044

Matysiak, B., Kowalski, A., 2019. White, blue and red LED lighting on growth, morphology and accumulation of flavonoid compounds in leafy greens. Zemdirbyste 106, 281–286. https://doi.org/10.13080/z-a.2019.106.036

Maye, D., 2019. 'Smart food city': Conceptual relations between smart city planning, urban food systems and innovation theory. City, Culture and Society 16, 18–24. https://doi.org/https://doi.org/10.1016/j.ccs.2017.12.001

Mehdizadeh Khorrami, B., Soleimani, A., Pinnarelli, A., Brusco, G., Vizza, P., 2023. Forecasting heating and cooling loads in residential buildings using machine learning: a comparative study of techniques and influential indicators. Asian Journal of Civil Engineering. https://doi.org/10.1007/s42107-023-00834-8

Milford, A.B., Kårstad, S., Verheul, M., 2019. Exploring the opportunities for building a rooftop greenhouse Case study from Bergen, Norway, NIBIO Rapport. ed.

Miner, G.L., Bauerle, W.L., Baldocchi, D.D., 2017. Estimating the sensitivity of stomatal conductance to photosynthesis: a review. Plant Cell Environ 40 7, 1214–1238.

Mohd Hanif, N., Limi Hawari, N.S.S., Othman, M., Abd Hamid, H.H., Ahamad, F., Uning, R., Ooi, M.C.G., Wahab, M.I.A., Sahani, M., Latif, M.T., 2021. Ambient volatile organic compounds in tropical environments: Potential sources, composition and impacts – A review. Chemosphere 285, 131355. https://doi.org/https://doi.org/10.1016/j.chemosphere.2021.131355

Montefiori, F., Pennisi, G., Pistillo, A., Orsini, F., Nicola, S., Fèrnandez, J.A., Crepaldi, A., Gianquinto, G., 2022. Optimal red:blue LED lighting ratio for a sustainable indoor cultivation of rocket salad and chicory, in: Acta Horticulturae. International Society for Horticultural Science, pp. 25–30. https://doi.org/10.17660/ActaHortic.2022.1337.4

Montero, J.I., Baeza, E., Heuvelink, E., Rieradevall, J., Muñoz, P., Ercilla, M., Stanghellini, C., 2017. Productivity of a building-integrated roof top greenhouse in a Mediterranean climate. Agric Syst 158, 14–22. https://doi.org/10.1016/J.AGSY.2017.08.002

Mozaffar, A., Schoon, N., Bachy, A., Digrado, A., Heinesch, B., Aubinet, M., Fauconnier, M.L., Delaplace, P., du Jardin, P., Amelynck, C., 2018. Biogenic volatile organic compound emissions from senescent maize leaves and a comparison with other leaf developmental stages. Atmos Environ 176, 71–81. https://doi.org/10.1016/j.atmosenv.2017.12.020

Müller, K., Pelzing, M., Gnauk, T., Kappe, A., Teichmann, U., Spindler, G., Haferkorn, S., Jahn, Y., Herrmann, H., 2002. Monoterpene emissions and carbonyl compound air concentrations during the blooming period of rape (Brassica napus). Chemosphere 49, 1247–1256. https://doi.org/10.1016/S0045-6535(02)00610-0

Muñoz-Liesa, J., Royapoor, M., Cuerva, E., Gassó-Domingo, S., Gabarrell, X., Josa, A., 2022. Building-integrated greenhouses raise energy co-benefits through active ventilation

systems. Build Environ 208, 108585. https://doi.org/https://doi.org/10.1016/j.buildenv.2021.108585

Muñoz-Liesa, J., Royapoor, M., López-Capel, E., Cuerva, E., Rufí-Salís, M., Gassó-Domingo, S., Josa, A., 2020. Quantifying energy symbiosis of building-integrated agriculture in a mediterranean rooftop greenhouse. Renew Energy 156, 696–709. https://doi.org/https://doi.org/10.1016/j.renene.2020.04.098

Muñoz-Liesa, J., Toboso-Chavero, S., Mendoza Beltran, A., Cuerva, E., Gallo, E., Gassó-Domingo, S., Josa, A., 2021. Building-integrated agriculture: Are we shifting environmental impacts? An environmental assessment and structural improvement of urban greenhouses. Resour Conserv Recycl 169, 105526. https://doi.org/10.1016/J.RESCONREC.2021.105526

Nadal, A., Llorach-Massana, P., Cuerva, E., López-Capel, E., Montero, J.I., Josa, A., Rieradevall, J., Royapoor, M., 2017. Building-integrated rooftop greenhouses: An energy and environmental assessment in the mediterranean context. Appl Energy 187, 338–351. https://doi.org/10.1016/j.apenergy.2016.11.051

Naranjani, B., Najafianashrafi, Z., Pascual, C., Agulto, I., Chuang, P.-Y.A., 2022. Computational analysis of the environment in an indoor vertical farming system. Int J Heat Mass Transf 186, 122460. https://doi.org/https://doi.org/10.1016/j.ijheatmasstransfer.2021.122460

Nicole, C.C.S., Krijn, M.P.C.M., van Slooten, U., 2019. Chapter 1.4 - Postharvest Quality of Leafy Greens Growing in a Plant Factory, in: Anpo, M., Fukuda, H., Wada, T. (Eds.), Plant Factory Using Artificial Light. Elsevier, pp. 33–43. https://doi.org/https://doi.org/10.1016/B978-0-12-813973-8.00005-1

Niinemets, Ü., Kännaste, A., Copolovici, L., 2013. Quantitative patterns between plant volatile emissions induced by biotic stresses and the degree of damage. Front Plant Sci 4, 1–15. https://doi.org/10.3389/fpls.2013.00262

Niinemets, Ü., Kuhn, U., Harley, P.C., Staudt, M., Arneth, A., Cescatti, A., Ciccioli, P., Copolovici, L., Geron, C., Guenther, A., Kesselmeier, J., Lerdau, M.T., Monson, R.K., Peñuelas, J., 2011. Estimations of isoprenoid emission capacity from enclosure studies: Measurements, data processing, quality and standardized measurement protocols. Biogeosciences. https://doi.org/10.5194/bg-8-2209-2011

Niinemets, Ü., Loreto, F., Reichstein, M., 2004. Physiological and physicochemical controls on foliar volatile organic compound emissions. Trends Plant Sci 9, 180–186. https://doi.org/10.1016/j.tplants.2004.02.006

Niinemets, Ü., Peñuelas, J., 2008. Gardening and urban landscaping: significant players in global change. Trends Plant Sci 13, 60–65. https://doi.org/10.1016/j.tplants.2007.11.009

Niinemets, Ü., Reichstein, M., 2003. Controls on the emission of plant volatiles through stomata: Differential sensitivity of emission rates to stomatal closure explained. Journal of Geophysical Research D: Atmospheres 108, 1–17. https://doi.org/10.1029/2002jd002620

NIOSH, 1996. Terpenes: METHOD 1552. Fourth Edition Measurement 13–16.

NIOSH, 1995. Volatile Organic Compounds (Screening) METHOD 2549. Fourth Edition Measurement 1–8.

Nowak, D.J., 2019. Air Pollution and Greenhouse Gases, Understanding Urban Ecology: An Interdisciplinary ….

Opitz, I., Berges, R., Piorr, A., Krikser, T., 2016. Contributing to food security in urban areas: differences between urban agriculture and peri-urban agriculture in the Global North. Agric Human Values 33, 341–358. https://doi.org/10.1007/s10460-015-9610-2

Oquendo-Di Cosola, V., Olivieri, F., Ruiz-García, L., 2022. A systematic review of the impact of green walls on urban comfort: temperature reduction and noise attenuation. Renewable and Sustainable Energy Reviews 162, 112463. https://doi.org/https://doi.org/10.1016/j.rser.2022.112463

Orsini, F., Gasperi, D., Marchetti, L., Piovene, C., Draghetti, S., Ramazzotti, S., Bazzocchi, G., Gianquinto, G., 2014. Exploring the production capacity of rooftop gardens (RTGs) in urban agriculture: the potential impact on food and nutrition security, biodiversity and other ecosystem services in the city of Bologna. Food Secur 6, 781–792. https://doi.org/10.1007/s12571-014-0389-6

Orsini, Francesco, Pennisi, G., Michelon, N., Minelli, A., Bazzocchi, G., Sanyé-Mengual, E., Gianquinto, G., 2020a. Features and Functions of Multifunctional Urban Agriculture in the Global North: A Review. Front Sustain Food Syst 4, 1–27. https://doi.org/10.3389/fsufs.2020.562513

Orsini, F., Pennisi, G., Zulfiqar, F., Gianquinto, G., 2020. Sustainable use of resources in plant factories with artificial lighting (PFALs). Eur J Hortic Sci. https://doi.org/10.17660/eJHS.2020/85.5.1

Orsini, Francesco, Pennisi, G., Zulfiqar, F., Gianquinto, G., 2020b. Sustainable use of resources in plant factories with artificial lighting (PFALs). Eur J Hortic Sci 85, 297–309. https://doi.org/10.17660/eJHS.2020/85.5.1

Ortega, J., Helmig, D., 2008. Approaches for quantifying reactive and low-volatility biogenic organic compound emissions by vegetation enclosure techniques - Part A. Chemosphere 72, 343–364. https://doi.org/10.1016/j.chemosphere.2007.11.020

Ortega, J., Helmig, D., Daly, R.W., Tanner, D.M., Guenther, A.B., Herrick, J.D., 2008. Approaches for quantifying reactive and low-volatility biogenic organic compound emissions by vegetation enclosure techniques - Part B: Applications. Chemosphere 72, 365–380. https://doi.org/10.1016/j.chemosphere.2008.02.054

OSRAM, 2017a. OSLON SSL 89 Datasheet Version 2.0. GB CS8PM1.24. [WWW Document]. URL https://www.mouser.com/datasheet/2/311/GH%20CS8PM1.24%20-%20OSLON%20SSL%2080%20(EnglishDeutsch)-1073965.pdf (accessed 12.4.23).

OSRAM, 2017b. OSLON SSL 80 Datasheet Version 1.0. GB CS8PM1.13 [WWW Document]. URL https://www.mouser.com/datasheet/2/311/GB%20CS8PM1.13%20-%20OSLON%20SSL%2080%20(EnglishDeutsch)-1073992.pdf (accessed 12.4.23).

Owen, S.M., Harley, P., Guenther, A., Hewitt, C.N., 2002. Light dependency of VOC emissions from selected Mediterranean plant species, Atmospheric Environment.

Pandey, V., Patel, A., Patra, D.D., 2016. Integrated nutrient regimes ameliorate crop productivity, nutritive value, antioxidant activity and volatiles in basil (Ocimum basilicum L.). Ind Crops Prod 87, 124–131. https://doi.org/https://doi.org/10.1016/j.indcrop.2016.04.035

Parada, F., Gabarrell, X., Rufí-Salís, M., Arcas-Pilz, V., Muñoz, P., Villalba, G., 2021. Optimizing irrigation in urban agriculture for tomato crops in rooftop greenhouses. Science of The Total Environment 794, 148689. https://doi.org/10.1016/J.SCITOTENV.2021.148689

Parmesan, C., Morecroft, M.D., Trisurat, R., Adrian, Y., Anshari, G.Z., Arneth, A., Gao, Q., Gonzalez, P., Harris, R., Price, J., Stevens, N., Talukdar, G.H., 2022. Terrestrial and Freshwater Ecosystems and their Services. In: Climate Change 2022: Impacts, Adaptation, and Vulnerability. Contribution of Working Group II to the Sixth Assessment Report of the Intergovernmental Panel on Climate Change. Cambridge, UK and New York, NY, USA. https://doi.org/10.1017/9781009325844.004

Pazouki, L., Kanagendran, A., Li, S., Kännaste, A., Rajabi Memari, H., Bichele, R., Niinemets, Ü., 2016. Mono- and sesquiterpene release from tomato (Solanum lycopersicum) leaves upon mild and severe heat stress and through recovery: From gene expression to emission responses. Environ Exp Bot 132, 1–15. https://doi.org/10.1016/j.envexpbot.2016.08.003

Peña, A., Rovira-Val, M.R., Mendoza, J.M.F., 2022. Life cycle cost analysis of tomato production in innovative urban agriculture systems. J Clean Prod 367. https://doi.org/10.1016/j.jclepro.2022.133037

Pennisi, G., Blasioli, S., Cellini, A., Maia, L., Crepaldi, A., Braschi, I., Spinelli, F., Nicola, S., Fernandez, J.A., Stanghellini, C., Marcelis, L.F.M., Orsini, F., Gianquinto, G., 2019. Unraveling the role of red:Blue LED lights on resource use efficiency and nutritional properties of indoor grown sweet basil. Front Plant Sci 10. https://doi.org/10.3389/fpls.2019.00305

Pennisi, G., Pistillo, A., Orsini, F., Cellini, A., Spinelli, F., Nicola, S., Fernandez, J.A., Crepaldi, A., Gianquinto, G., Marcelis, L.F.M., 2020. Optimal light intensity for sustainable water and energy use in indoor cultivation of lettuce and basil under red and blue LEDs. Sci Hortic 272. https://doi.org/10.1016/j.scienta.2020.109508

Peñuelas, J., Llusià, J., 1997. Effects of carbon dioxide, water supply, and seasonality on terpene content and emission by Rosmarinus officinalis. J Chem Ecol 23, 979–993. https://doi.org/10.1023/B:JOEC.0000006383.29650.d7

Peñuelas, J., Llusiaá, J., Gimeno, B.S., 1999. Effects of ozone concentrations on biogenic volatile organic compounds emission in the Mediterranean region.

Peñuelas, J., Staudt, M., 2010. BVOCs and global change. Trends Plant Sci 15, 133–144. https://doi.org/10.1016/j.tplants.2009.12.005

Pérez-Priego, O., López-Ballesteros, A., Sánchez-Cañete, E.P., Serrano-Ortiz, P., Kutzbach, L., Domingo, F., Eugster, W., Kowalski, A.S., 2015. Analysing uncertainties in the calculation of fluxes using whole-plant chambers: random and systematic errors. Plant Soil 393, 229–244. https://doi.org/10.1007/s11104-015-2481-x

Persiani, S., 2021. Benefits of Using Plants in Indoor Environments: Exploring Common Research Gaps. Architecture 1, 83–98. https://doi.org/10.3390/architecture1020008

Picazo-Aragonés, J., Terrab, A., Balao, F., 2020. Plant volatile organic compounds evolution: Transcriptional regulation, epigenetics and polyploidy. Int J Mol Sci. https://doi.org/10.3390/ijms21238956

Pinstrup-Andersen, P., 2018. Is it time to take vertical indoor farming seriously? Glob Food Sec 17, 233–235. https://doi.org/https://doi.org/10.1016/j.gfs.2017.09.002

Pistillo, A., Pennisi, G., Crepaldi, A., Giorgioni, M.E., Minelli, A., Orsini, F., Gianquinto, G., 2022. Influence of red:blue ratio in LED lighting for indoor cultivation of edible marigold flowers, in: Acta Horticulturae. International Society for Horticultural Science, pp. 249–254. https://doi.org/10.17660/ActaHortic.2022.1337.33

Pons, O., Nadal, A., Sanyé-Mengual, E., Llorach-Massana, P., Cuerva, E., Sanjuan-Delmàs, D., Muñoz, P., Oliver-Solà, J., Planas, C., Rovira, M.R., 2015. Roofs of the Future: Rooftop Greenhouses to Improve Buildings Metabolism. Procedia Eng 123, 441–448. https://doi.org/10.1016/j.proeng.2015.10.084

Popkova, E.G., 2022. Vertical Farms Based on Hydroponics, Deep Learning, and AI as Smart Innovation in Agriculture, in: Popkova, E.G., Sergi, B.S. (Eds.), Smart Innovation in Agriculture. Springer Nature Singapore, Singapore, pp. 257–262. https://doi.org/10.1007/978-981-16-7633-8_28

Prabhakaran, J., Jayabal, S., Ramesh Kumar, A., Vinoth, V., 2022. Air quality assessment in indoor and outdoor environments: A review. Mater Today Proc 66, 1260–1266. https://doi.org/https://doi.org/10.1016/j.matpr.2022.05.124

Pradhan, P., Callaghan, M., Hu, Y., Dahal, K., Hunecke, C., Reusswig, F., Lotze-Campen, H., Kropp, J.P., 2023. A systematic review highlights that there are multiple benefits of urban agriculture besides food. Glob Food Sec 38, 100700. https://doi.org/https://doi.org/10.1016/j.gfs.2023.100700

Puppim de Oliveira, J.A., Bellezoni, R.A., Shih, W., Bayulken, B., 2022. Innovations in Urban Green and Blue Infrastructure: Tackling local and global challenges in cities. J Clean Prod 362, 132355. https://doi.org/https://doi.org/10.1016/j.jclepro.2022.132355

Quintana-Rodriguez, E., Morales-Vargas, A.T., Molina-Torres, J., Ádame-Alvarez, R.M., Acosta-Gallegos, J.A., Heil, M., 2015. Plant volatiles cause direct, induced and associational resistance in common bean to the fungal pathogen Colletotrichum lindemuthianum. Journal of Ecology 103, 250–260. https://doi.org/10.1111/1365-2745.12340

Rahman, M.M., Vasiliev, M., Alameh, K., 2021. Led illumination spectrum manipulation for increasing the yield of sweet basil (Ocimum basilicum l.). Plants 10, 1–13. https://doi.org/10.3390/plants10020344

Räisänen, T., Ryyppö, A., Kellomäki, S., 2008. Effects of elevated CO2 and temperature on monoterpene emission of Scots pine (Pinus sylvestris L.). Atmos Environ 42, 4160–4171. https://doi.org/10.1016/j.atmosenv.2008.01.023

Ramasubramanian, P., Starry, O., Rosenstiel, T., Gall, E.T., 2019. Pilot study on the impact of green roofs on ozone levels near building ventilation air supply. Build Environ 151, 43–53. https://doi.org/10.1016/j.buildenv.2019.01.023

Rao, N., Patil, S., Singh, C., Roy, P., Pryor, C., Poonacha, P., Genes, M., 2022. Cultivating sustainable and healthy cities: A systematic literature review of the outcomes of urban and peri-urban agriculture. Sustain Cities Soc 85, 104063. https://doi.org/https://doi.org/10.1016/j.scs.2022.104063

Richardson, M.L., Arlotta, C.G., 2022. Producing Cherry Tomatoes in Urban Agriculture. Horticulturae 8. https://doi.org/10.3390/horticulturae8040274

Rufí-Salís, M., Petit-Boix, A., Villalba, G., Sanjuan-Delmás, D., Parada, F., Ercilla-Montserrat, M., Arcas-Pilz, V., Muñoz-Liesa, J., Rieradevall, J., Gabarrell, X., 2020. Recirculating water and nutrients in urban agriculture: An opportunity towards environmental sustainability and water use efficiency? J Clean Prod 261, 121213. https://doi.org/https://doi.org/10.1016/j.jclepro.2020.121213

Sabeh, N., 2020. Rooftop plant production systems in urban areas. Plant Factory: An Indoor Vertical Farming System for Efficient Quality Food Production: Second Edition 129–135. https://doi.org/10.1016/B978-0-12-816691-8.00007-8

Saeed Meo, M., Karim, M.Z.A., 2022. The role of green finance in reducing CO2 emissions: An empirical analysis. Borsa Istanbul Review 22, 169–178. https://doi.org/10.1016/J.BIR.2021.03.002

Saha, S., Monroe, A., Day, M.R., 2016. Growth, yield, plant quality and nutrition of basil (Ocimum basilicum L.) under soilless agricultural systems. Annals of Agricultural Sciences 61, 181–186. https://doi.org/10.1016/j.aoas.2016.10.001

Sanjuan-Delmás, D., Llorach-Massana, P., Nadal, A., Ercilla-Montserrat, M., Muñoz, P., Montero, J.I., Josa, A., Gabarrell, X., Rieradevall, J., 2018. Environmental assessment of an integrated rooftop greenhouse for food production in cities. J Clean Prod 177, 326–337. https://doi.org/10.1016/j.jclepro.2017.12.147

Sanyé-Mengual, E., Llorach Massana, P., Sanjuan Demás, D., Oliver-Solà, J., Josa Garcia-Tornel, A., Montero, J.I., Rieradevall Pons, J., 2014. The ICTA-ICP Rooftop Greenhouse Lab (RTG-Lab): closing metabolic flows (energy, water, CO2) through integrated Rooftop Greenhouses. Finding Places for Productive Cities. Proceedings of 6th International AESOP Sustainable Food Planning Conference 693–701. https://doi.org/10.13140/RG.2.1.5016.7206

Sanyé-Mengual, E., Martinez-Blanco, J., Finkbeiner, M., Cerdà, M., Camargo, M., Ometto, A.R., Velásquez, L.S., Villada, G., Niza, S., Pina, A., Ferreira, G., Oliver-Solà, J., Montero, J.I., Rieradevall, J., 2018. Urban horticulture in retail parks: Environmental assessment of the potential implementation of rooftop greenhouses in European and South American cities. J Clean Prod 172, 3081–3091. https://doi.org/https://doi.org/10.1016/j.jclepro.2017.11.103

Schilmiller, A.L., Schauvinhold, I., Larson, M., Xu, R., Charbonneau, A.L., Schmidt, A., Wilkerson, C., Last, R.L., Pichersky, E., 2009. Monoterpenes in the glandular trichomes of tomato are synthesized from a neryl diphosphate precursor rather than geranyl diphosphate.

Seco, R., Karl, T., Guenther, A., Hosman, K.P., Pallardy, S.G., Gu, L., Geron, C., Harley, P., Kim, S., 2015. Ecosystem-scale volatile organic compound fluxes during an extreme drought in a broadleaf temperate forest of the Missouri Ozarks (central USA). Glob Chang Biol 21, 3657–3674. https://doi.org/10.1111/gcb.12980

Seco, R., Peñuelas, J., Filella, I., 2007. Short-chain oxygenated VOCs: Emission and uptake by plants and atmospheric sources, sinks, and concentrations. Atmos Environ 41, 2477–2499. https://doi.org/10.1016/j.atmosenv.2006.11.029

Shao, Y., Li, J., Zhou, Z., Hu, Z., Zhang, F., Cui, Y., Chen, H., 2021a. The effects of vertical farming on indoor carbon dioxide concentration and fresh air energy consumption in office buildings. Build Environ 195, 107766. https://doi.org/https://doi.org/10.1016/j.buildenv.2021.107766

Shao, Y., Li, J., Zhou, Z., Hu, Z., Zhang, F., Cui, Y., Chen, H., 2021b. The effects of vertical farming on indoor carbon dioxide concentration and fresh air energy consumption in office buildings. Build Environ 195. https://doi.org/10.1016/j.buildenv.2021.107766

Shao, Y., Zhou, Zhiwei, Chen, H., Zhang, F., Cui, Y., Zhou, Zhenghuan, 2022. The potential of urban family vertical farming: A pilot study of Shanghai. Sustain Prod Consum 34, 586–599. https://doi.org/https://doi.org/10.1016/j.spc.2022.10.011

Sharkey, T.D., Monson, R.K., 2014. The future of isoprene emission from leaves, canopies and landscapes. Plant Cell Environ 37, 1727–1740. https://doi.org/10.1111/pce.12289

Sharma, S., Bakht, A., Jahanzaib, M., Lee, H., Park, D., 2022. Evaluation of the Effectiveness of Common Indoor Plants in Improving the Indoor Air Quality of Studio Apartments. Atmosphere (Basel) 13. https://doi.org/10.3390/atmos13111863

Shimazaki, K.I., Doi, M., Assmann, S.M., Kinoshita, T., 2007. Light regulation of stomatal movement. Annu Rev Plant Biol. https://doi.org/10.1146/annurev.arplant.57.032905.105434

Simon, S., 2023. The role of Design Thinking to promote a sustainability transition within participatory urban governance: Insights from urban agriculture initiatives in Lisbon. Urban Governance. https://doi.org/https://doi.org/10.1016/j.ugj.2023.05.003

Song, X., Li, H., Li, C., Xu, J., Hu, D., 2016. Effects of VOCs from leaves of Acer truncatum Bunge and Cedrus deodara on human physiology and psychology. Urban For Urban Green 19, 29–34. https://doi.org/10.1016/j.ufug.2016.06.021

Soria, A.C., García-Sarrió, M.J., Sanz, M.L., 2015. Volatile sampling by headspace techniques. TrAC - Trends in Analytical Chemistry 71, 85–99. https://doi.org/10.1016/j.trac.2015.04.015

Souza, S.R., Blande, J.D., Holopainen, J.K., 2013. Pre-exposure to nitric oxide modulates the effect of ozone on oxidative defenses and volatile emissions in lima bean. Environmental Pollution 179, 111–119. https://doi.org/10.1016/j.envpol.2013.03.065

Srbinovska, A., Gasparotto, L., Conchione, C., Menegoz Ursol, L., Lambertini, F., Suman, M., Moret, S., 2023. Mineral oil contamination in basil pesto from the Italian market: Ingredient contribution and market survey. Journal of Food Composition and Analysis 115, 104914. https://doi.org/https://doi.org/10.1016/j.jfca.2022.104914

Staudt, M., Morin, X., Chuine, I., 2017. Contrasting direct and indirect effects of warming and drought on isoprenoid emissions from Mediterranean oaks. Reg Environ Change 17, 2121–2133. https://doi.org/10.1007/s10113-016-1056-6

Stringari, G., Moraleda, N., Rosell, A., Rieradevall, J., Orsini, F., Gabarrell, X., 2022. Potential volatile organic compounds emission in indoor urban farming: a case study. Acta Hortic 1356, 117–126. https://doi.org/https://doi.org/10.17660/ActaHortic.2022.1356.17

Stringari, G., Villanueva, J., Rosell-Melé, A., Moraleda-Cibrián, N., Orsini, F., Villalba, G., Gabarrell, X., 2023. Assessment of greenhouse emissions of the green bean through the static enclosure technique. Science of The Total Environment 874, 162319. https://doi.org/10.1016/j.scitotenv.2023.162319

Sussmilch, F.C., Brodribb, T.J., McAdam, S.A.M., 2017. Up-regulation of NCED3 and ABA biosynthesis occur within minutes of a decrease in leaf turgor but AHK1 is not required. J Exp Bot 68, 2913–2918. https://doi.org/10.1093/jxb/erx124

Syed, A.M., Hachem, C., 2019. Review of Construction; Geometry; Heating, Ventilation, and Air-Conditioning; and Indoor Climate Requirements of Agricultural Greenhouses. Journal of Biosystems Engineering 44, 18–27. https://doi.org/10.1007/s42853-019-00005-1

Tablada, A., Kosorić, V., 2022. 11 - Vertical farming on facades: transforming building skins for urban food security, in: Gasparri, E., Brambilla, A., Lobaccaro, G., Goia, F., Andaloro, A., Sangiorgio, A. (Eds.), Rethinking Building Skins. Woodhead Publishing, pp. 285–311. https://doi.org/https://doi.org/10.1016/B978-0-12-822477-9.00015-2

Takayama, K., Jansen, R.M.C., van Henten, E.J., Verstappen, F.W.A., Bouwmeester, H.J., Nishina, H., 2012. Emission index for evaluation of volatile organic compounds emitted from tomato plants in greenhouses. Biosyst Eng 113, 220–228. https://doi.org/10.1016/j.biosystemseng.2012.08.004

Tangpao, T., Charoimek, N., Teerakitchotikan, P., Leksawasdi, N., Jantanasakulwong, K., Rachtanapun, P., Seesuriyachan, P., Phimolsiripol, Y., Chaiyaso, T., Ruksiriwanich, W.,

Jantrawut, P., Van Doan, H., Cheewangkoon, R., Sommano, S.R., 2022. Volatile Organic Compounds from Basil Essential Oils: Plant Taxonomy, Biological Activities, and Their Applications in Tropical Fruit Productions. Horticulturae. https://doi.org/10.3390/horticulturae8020144

Tani, A., Hayward, S., Hansel, A., Hewitt, C.N., 2004. Effect of water vapour pressure on monoterpene measurements using proton transfer reaction-mass spectrometry (PTR-MS). Int J Mass Spectrom 239, 161–169. https://doi.org/10.1016/j.ijms.2004.07.020

Tholl, D., Boland, W., Hansel, A., Loreto, F., Röse, U.S.R., Schnitzler, J.P., 2006. Practical approaches to plant volatile analysis. Plant Journal 45, 540–560. https://doi.org/10.1111/j.1365-313X.2005.02612.x

Tholl, D., Hossain, O., Weinhold, A., Röse, U.S.R., Wei, Q., 2021. Trends and applications in plant volatile sampling and analysis. Plant Journal 106, 314–325. https://doi.org/10.1111/tpj.15176

Tiiva, P., Tang, J., Michelsen, A., Rinnan, R., 2017. Monoterpene emissions in response to long-term night-time warming, elevated CO2 and extended summer drought in a temperate heath ecosystem. Science of the Total Environment 580, 1056–1067. https://doi.org/10.1016/j.scitotenv.2016.12.060

Tiwari, A., Kumar, P., Baldauf, R., Zhang, K.M., Pilla, F., Di Sabatino, S., Brattich, E., Pulvirenti, B., 2019. Considerations for evaluating green infrastructure impacts in microscale and macroscale air pollution dispersion models. Science of the Total Environment 672, 410–426. https://doi.org/10.1016/j.scitotenv.2019.03.350

Tiwary, A., Namdeo, A., Fuentes, J., Dore, A., Hu, X.M., Bell, M., 2013. Systems scale assessment of the sustainability implications of emerging green initiatives. Environmental Pollution 183, 213–223. https://doi.org/10.1016/j.envpol.2013.03.049

Toboso-Chavero, S., Montealegre, A.L., García-Pérez, S., Sierra-Pérez, J., Muñoz-Liesa, J., Gabarrell Durany, X., Villalba, G., Madrid-López, C., 2023. The potential of local food, energy, and water production systems on urban rooftops considering consumption patterns and urban morphology. Sustain Cities Soc 95, 104599. https://doi.org/https://doi.org/10.1016/j.scs.2023.104599

Tomson, M., Kumar, P., Barwise, Y., Perez, P., Forehead, H., French, K., Morawska, L., Watts, J.F., 2021. Green infrastructure for air quality improvement in street canyons. Environ Int 146, 106288. https://doi.org/https://doi.org/10.1016/j.envint.2020.106288

Tong, Z., Whitlow, T.H., Landers, A., Flanner, B., 2016. A case study of air quality above an urban roof top vegetable farm. Environmental Pollution 208, 256–260. https://doi.org/https://doi.org/10.1016/j.envpol.2015.07.006

Torpy, F., Zavattaro, M., 2018. Bench-study of green-wall plants for indoor air pollution reduction.

Trettel, J.R., Gazim, Z.C., Gonçalves, J.E., Stracieri, J., Magalhães, H.M., 2017. Volatile essential oil chemical composition of basil (Ocimum basilicum L. 'Green') cultivated in a

greenhouse and micropropagated on a culture medium containing copper sulfate. In Vitro Cellular and Developmental Biology - Plant 53, 631–640. https://doi.org/10.1007/s11627-017-9868-8

United Nations Department of Economic and Social Affairs, P.D., 2022. World Population Prospects 2022: Summary of Results., 3rd ed, World Population Prospects. UN DESA/POP/TR, New York. https://doi.org/10.18356/cd7acf62-en

United States Environmental Action (EPA), 1988. NATIONAL AMBIENT VOLATILE ORGANIC COMPOUNDS (VOCs) DATA BASE UPDATE. Portland, OR.

United States Environmental Protection Agency (EPA), 1999. Compendium of Methods for the Determination of Toxic Organic Compounds in Ambient Air Second Edition Compendium Method TO-17 Determination of Volatile Organic Compounds in Ambient Air Using Active Sampling Onto Sorbent Tubes. Cincinnati.

Velikova, V., Tsonev, T., Barta, C., Centritto, M., Koleva, D., Stefanova, M., Busheva, M., Loreto, F., 2009. BVOC emissions, photosynthetic characteristics and changes in chloroplast ultrastructure of Platanus orientalis L. exposed to elevated CO 2 and high temperature. Environmental Pollution 157, 2629–2637. https://doi.org/10.1016/j.envpol.2009.05.007

Veremeichik, G.N., Grigorchuk, V.P., Makhazen, D.S., Subbotin, E.P., Kholin, A.S., Subbotina, N.I., Bulgakov, D. V., Kulchin, Y.N., Bulgakov, V.P., 2023. High production of flavonols and anthocyanins in Eruca sativa (Mill) Thell plants at high artificial LED light intensities. Food Chem 408. https://doi.org/10.1016/j.foodchem.2022.135216

Vuorinen, T., Reddy, G.V.P., Nerg, A.M., Holopainen, J.K., 2004. Monoterpene and herbivore-induced emissions from cabbage plants grown at elevated atmospheric CO2 concentration. Atmos Environ 38, 675–682. https://doi.org/10.1016/j.atmosenv.2003.10.029

Wada, T., Fukuda, H., Ogura, T., 2019. Chapter 6.1 - Fundamental Components and Points to Consider in the Design of a Plant Factory: An Example of OPU New-Generation Plant Factory, in: Anpo, M., Fukuda, H., Wada, T. (Eds.), Plant Factory Using Artificial Light. Elsevier, pp. 231–241. https://doi.org/https://doi.org/10.1016/B978-0-12-813973-8.00006-3

Walters, K.J., Lopez, R.G., Behe, B.K., 2021. Leveraging Controlled-Environment Agriculture to Increase Key Basil Terpenoid and Phenylpropanoid Concentrations: The Effects of Radiation Intensity and CO2 Concentration on Consumer Preference. Front Plant Sci 11. https://doi.org/10.3389/fpls.2020.598519

Wang, C.T., Wiedinmyer, C., Ashworth, K., Harley, P.C., Ortega, J., Vizuete, W., 2019. Leaf enclosure measurements for determining volatile organic compound emission capacity from Cannabis spp. Atmos Environ 199, 80–87. https://doi.org/10.1016/j.atmosenv.2018.10.049

Wang, J., Tuduri, L., Mercury, M., Millet, M., Briand, O., Montury, M., 2009. Sampling atmospheric pesticides with SPME: Laboratory developments and field study.

Environmental Pollution 157, 365–370. https://doi.org/https://doi.org/10.1016/j.envpol.2008.10.006

Wang, L., Iddio, E., 2022. Energy performance evaluation and modeling for an indoor farming facility. Sustainable Energy Technologies and Assessments 52, 102240. https://doi.org/https://doi.org/10.1016/j.seta.2022.102240

Wang, Y., Bakker, F., de Groot, R., Wörtche, H., 2014. Effect of ecosystem services provided by urban green infrastructure on indoor environment: A literature review. Build Environ 77, 88–100. https://doi.org/https://doi.org/10.1016/j.buildenv.2014.03.021

Wang, Y., Yang, T., He, Z., Sun, L., Yu, X., Zhao, J., Hu, Y., Zhang, S., Xiong, J., 2020. A general regression method for accurately determining the key parameters of VOC emissions from building materials/furniture in a ventilated chamber. Atmos Environ 231, 117527. https://doi.org/10.1016/j.atmosenv.2020.117527

Weidner, T., Yang, A., Hamm, M.W., 2021. Energy optimisation of plant factories and greenhouses for different climatic conditions. Energy Convers Manag 243, 114336. https://doi.org/https://doi.org/10.1016/j.enconman.2021.114336

Wilkinson, M.J., Monson, R.K., Trahan, N., Lee, S., Brown, E., Jackson, R.B., Polley, H.W., Fay, P.A., Fall, R., 2009. Leaf isoprene emission rate as a function of atmospheric CO2 concentration. Glob Chang Biol 15, 1189–1200. https://doi.org/10.1111/j.1365-2486.2008.01803.x

Wiśniewska-Paluszak, J., Paluszak, G., Fiore, M., Coticchio, A., Galati, A., Lira, J., 2023. Urban agriculture business models and value propositions: Mixed methods approach based on evidence from Polish and Italian case studies. Land use policy 127, 106562. https://doi.org/https://doi.org/10.1016/j.landusepol.2023.106562

Wong, C.E., Teo, Z.W.N., Shen, L., Yu, H., 2020a. Seeing the lights for leafy greens in indoor vertical farming. Trends Food Sci Technol 106, 48–63. https://doi.org/https://doi.org/10.1016/j.tifs.2020.09.031

Wong, C.E., Teo, Z.W.N., Shen, L., Yu, H., 2020b. Seeing the lights for leafy greens in indoor vertical farming. Trends Food Sci Technol. https://doi.org/10.1016/j.tifs.2020.09.031

World Health Organization, 2021. WHO global air quality guidelines: particulate matter (PM2.5 and PM10), ozone, nitrogen dioxide, sulfur dioxide and carbon monoxide. World Health Organization 1–1302.

World Health Organization (WHO), 2020. Methods for sampling and analysis of chemical pollutants in indoor air: supplementary publication to the screening tool for assessment of health risks from combined exposure to multiple chemicals in indoor air in public settings for children. World Health Organization. Regional Office for Europe.

Xu, J., Szyszkowicz, M., Jovic, B., Cakmak, S., Austin, C.C., Zhu, J., 2016. Estimation of indoor and outdoor ratios of selected volatile organic compounds in Canada. Atmos Environ 141, 523–531. https://doi.org/https://doi.org/10.1016/j.atmosenv.2016.07.031

Xu, J., Zhang, J.S., 2011. An experimental study of relative humidity effect on VOCs' effective diffusion coefficient and partition coefficient in a porous medium. Build Environ 46, 1785–1796. https://doi.org/10.1016/j.buildenv.2011.02.007

Yaaran, A., Negin, B., Moshelion, M., 2019. Role of guard-cell ABA in determining steady-state stomatal aperture and prompt vapor-pressure-deficit response. Plant Science 281, 31–40. https://doi.org/10.1016/j.plantsci.2018.12.027

Yamada, Y., Ohtani, K., Imajo, A., Izu, H., Nakamura, H., Shiraishi, K., 2015. Comparison of the neurotoxicities between volatile organic compounds and fragrant organic compounds on human neuroblastoma SK-N-SH cells and primary cultured rat neurons. Toxicol Rep 2, 729–736. https://doi.org/10.1016/j.toxrep.2015.05.002

Yang, D.S., Son, K.C., Kays, S.J., 2009a. Volatile organic compounds emanating from indoor ornamental plants. HortScience 44, 396–400. https://doi.org/10.21273/hortsci.44.2.396

Yang, D.S., Son, K.C., Kays, S.J., 2009b. Volatile organic compounds emanating from indoor ornamental plants. HortScience 44, 396–400. https://doi.org/10.21273/hortsci.44.2.396

Yang, Q., Du, X., Wang, Z., Meng, Z., Ma, Z., Zhang, Q., 2023. A review of core agricultural robot technologies for crop productions. Comput Electron Agric 206, 107701. https://doi.org/10.1016/J.COMPAG.2023.107701

Yang, Y., Zhang, Z., Zhang, L., Song, F., Ren, Y., Zhang, X., Zhang, J., Liew, R.K., Foong, S.Y., Chong, W.W.F., Lam, S.S., Verma, M., Ng, H.S., Sonne, C., Ge, S., 2023. Recent advances in the control of volatile organic compounds emissions from indoor wood-based panels: A comprehensive review. Science of The Total Environment 884, 163741. https://doi.org/https://doi.org/10.1016/j.scitotenv.2023.163741

Yin, J., Liu, X., Miao, Y., Gao, Y., Qiu, R., Zhang, M., Li, H., Li, M., 2019. Measurement and prediction of tomato canopy apparent photosynthetic rate. International Journal of Agricultural and Biological Engineering 12, 156–161. https://doi.org/10.25165/j.ijabe.20191205.4982

Ysebaert, T., Koch, K., Samson, R., Denys, S., 2021. Green walls for mitigating urban particulate matter pollution—A review. Urban For Urban Green 59, 127014. https://doi.org/https://doi.org/10.1016/j.ufug.2021.127014

Yuan, C., Shan, R., Adelia, A.S., Tablada, A., Lau, S.K., Lau, S.S.-Y., 2019. Effects of vertical farming on natural ventilation of residential buildings. Energy Build 185, 316–325. https://doi.org/https://doi.org/10.1016/j.enbuild.2018.12.028

Yudelson, J., 2012. Green building trends: Europe. Island Press.

Zambrano, P., Muñoz Liesa, J., Josa, A., Rieradevall, J., Alamús, R., Gassó, S., Gabarrell Durany, X., 2021. Assessment of the food-water-energy nexus suitability of rooftops. Methodological remote sensing approach in a urban Mediterranean area. Sustain Cities Soc 75, 103287. https://doi.org/10.1016/j.scs.2021.103287

Zauli, I., Appolloni, E., Carotti, L., Paucek, I., Quaini, S., Pennisi, G., Orsini, F., Gianquinto, G., 2022. Effects of different LEDs wavelengths on secondary metabolites accumulation in medicinal plants cultivated in vitro: A review of recent literature, in: Acta Horticulturae. International Society for Horticultural Science, pp. 233–239. https://doi.org/10.17660/ActaHortic.2022.1337.31

Zhang, H., Zhang, Y., Huang, Z., Acton, W.J.F., Wang, Z., Nemitz, E., Langford, B., Mullinger, N., Davison, B., Shi, Z., Liu, D., Song, W., Yang, W., Zeng, J., Wu, Z., Fu, P., Zhang, Q., Wang, X., 2020. Vertical profiles of biogenic volatile organic compounds as observed online at a tower in Beijing. Journal of Environmental Sciences 95, 33–42. https://doi.org/https://doi.org/10.1016/j.jes.2020.03.032

Zhou, C., Zhan, Y., Chen, S., Xia, M., Ronda, C., Sun, M., Chen, H., Shen, X., 2017. Combined effects of temperature and humidity on indoor VOCs pollution: Intercity comparison. Build Environ 121, 26–34. https://doi.org/10.1016/j.buildenv.2017.04.013

Zorić, M., Simić, M., Orlović, S., Mladenović, E., Babić, Z., 2019. Indoor Ecosystem Services: Impacts of Plants on Air Quality. Contemporary Agriculture 68, 12–16. https://doi.org/10.2478/contagri-2019-0003

https://webbook.nist.gov/chemistry/

PART V

Annexes

List of Tables and Figures Annex I

List of Tables and Figures Annex II

List of Tables and Figures Annex III

Annex I

Elements of the experimental methodology for practical BVOC emissions measurement and analysis

Annex I: Elements of the experimental methodology for practical BVOC emissions measurement and analysis

A1 Testing the sampling system

A1.1 Chamber design

The very first measurements using the active sampling method in static enclosure (elected method) are reported in **Ch. 4**. In figure X.1 are shown the prototypes used to test the frame and the dimension of the static enclosure. The open chamber of 9 m^3 hosting 32 plants in bag modules of 4-plants initially built provided scarce reproducible samples and overall BVOC emissions >LOQ. Therefore, a small-scale chamber of 0.33 m^3 hosting one bag module (=4 plants) was assembled and sealed to evaluate the emission levels of the enclosed plants. According to the positive results (>LOQ), all future chambers were then designed to be totally closed during air collection (=static enclosure) to compensate emission dispersion and reduce estimation error. This can be seen in the further chamber of 1 m^3 (figure X.2) that reproduced the same internal dispersion provided by the small prototype (0.083 m^3 $plant^{-1}$).

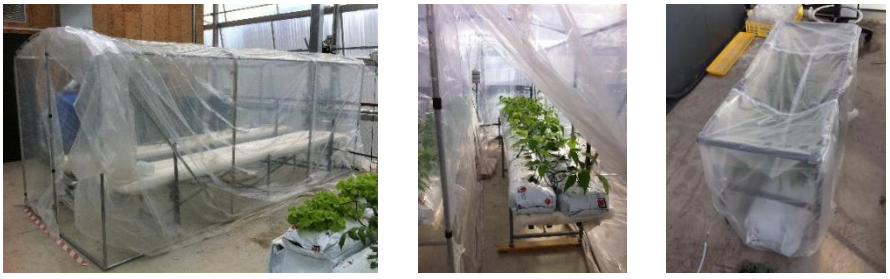

Annex X. 1 First prototype chambers: Open (left) with its internal arrangement (middle) and closed (right).

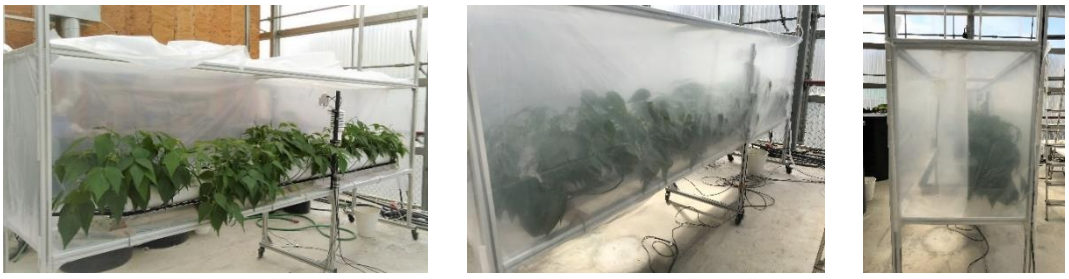

Annex X. 2 New closed chamber: arrangement at normal conditions (left) and during air sampling, longitudinal (middle) and frontal (right) view.

A1.2 Sampling length

Alongside chamber construction sampling length was also evaluated. This step involved activated charcoal tubes (Anasorb CSC) and the static enclosure described in **Ch. 5**, though it was performed in advance to the reported assessment. In static condition short sampling was

generally recommended to minimize sample bias associated to breakthrough and artifacts (Tholl et al., 2006; Ortega and Helmig, 2008; Li et al., 2019). Sampling artifacts are particularly connected to plants transpiration that over static closing tends to increase enhancing relative humidity levels up to the saturation point (Xu and Zhang, 2011; Pérez-Priego et al., 2015). In the test intervals of 15 and 30 minutes were then considered, measuring BVOC emissions of bean plants in the empty (=control) and the filled (=12 plants) side of the static enclosure simultaneously, monitoring temperature (T) and relative humidity (RH) variation throughout. Triplicates of parallel 15- and 30-minutes samples (=long- and short-interval sample) were collected plus 15 minutes sample interposed between the two intervals. Short-interval samples were then compared among each other to observe emission trend along static closing. Similarly, their sum providing theorical long-interval samples were compared with the original ones to evaluate overall sampling performance according to the total emission amount. All sample tubes were analysed at the instrumental conditions detailed in **Ch. 5**, focusing on few volatiles representing 4 typical BVOC classes of plants emission profile, namely, MTs, OMTs, STs, LOX derivates, and PH.

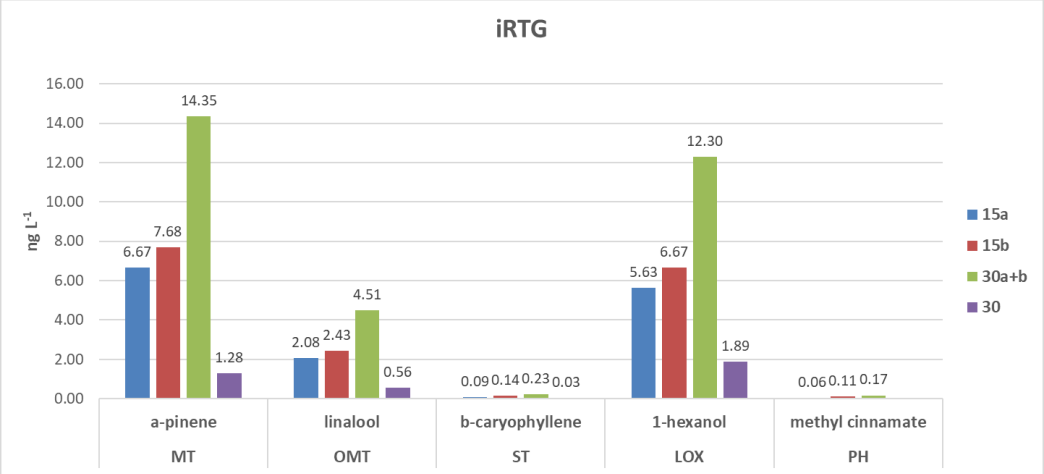

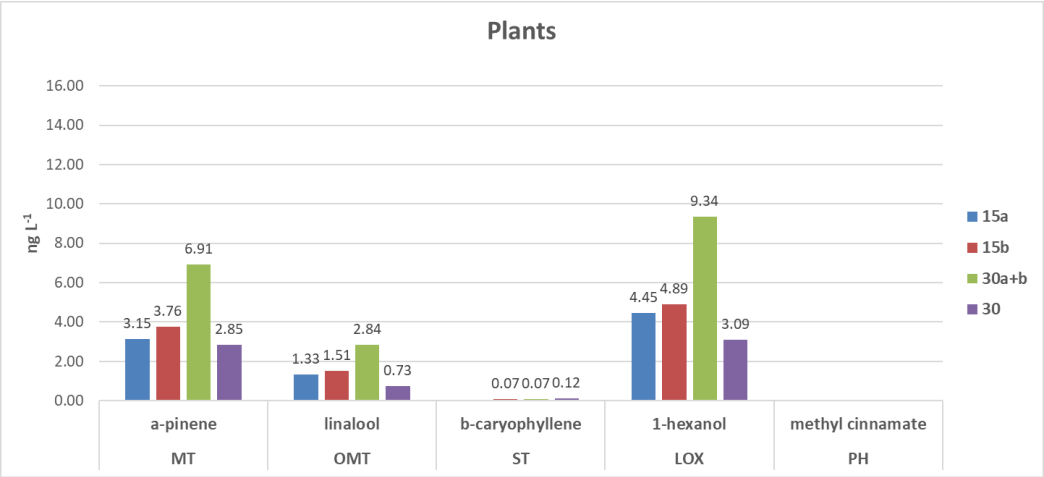

Annex X. 3 Average emissions of 4 representative BVOCs found in the empty (=iRTG) and filled (=plants) side of the static enclosure after 15 (a and b) and 30 (original and theorical summing a and b 15-minutes samples) minutes of sampling.

As shown in figure X.3 overall low emission levels were detected and among the two sides emission patterns were mostly identical. Between 15-minutes samples (15a and 15b) slight differences were observed, where MT, OMT, and ST emissions were slightly lower in initial (15a) than consecutive (15b) samples. On the other hand, differences between 30-minutes samples (original and theorical) were considerable. Indeed, BVOC levels of theorical samples (30a+b) were more than double of original (30) long-interval samples. Considering ST and PH emissions instead, differences were irrelevant as concentrations were mostly below the instrument LOQ.

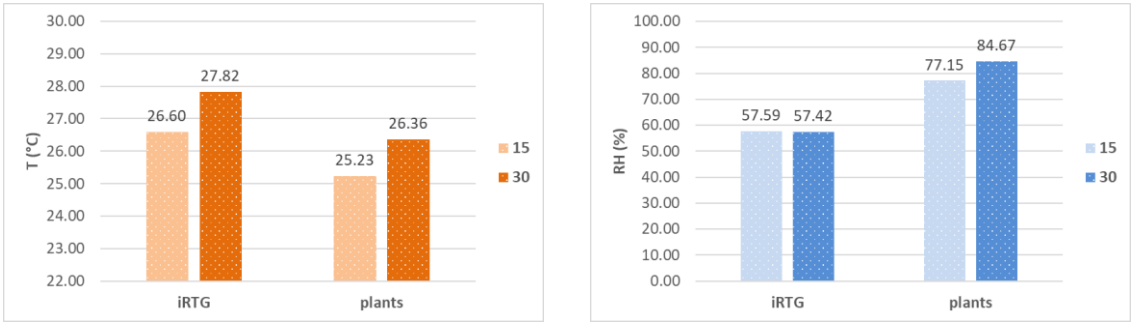

Annex X. 4 Mean temperature (left) and relative humidity (right) measured in the empty (=iRTG) and filled (=plants) side over 15- and 30-minutes sampling.

Regarding the environmental variables monitored (figure X.4), temperature and relative humidity, both usually showed an increasing tendency along the sampling time, except for RH measured in the empty side. T increase was slightly higher in the empty side, whereas the raise of RH in the plants side was mostly close to the saturation point for either the short or the long interval. Therefore, trends suggested that in the side filled with plants transpiration occurred and was positively correlated to the length of the static closing. Because of the increase of air humidity levels slight T decrease was then predictable (cooling effect). According to these results, we confirmed literature findings on long-interval sampling which was more susceptible to

technical error and sample overestimation. With the perspective of sampling on plants in the static enclosure, short intervals provided higher emissions and more reproducible samples even between consecutive intervals. However, fractionating sampling in short intervals was discouraged because of the environmental instability in the chamber. Hence, to minimize static closing effect on physiological plants' emissions further assessments were generally carried out within 15-minutes intervals.

A similar test was also performed meanwhile the assessment described in **Ch. 6**. Three consecutive sampling intervals of 5', 10' (short), and 45' (long) were carried out in three different locations, respectively, the static enclosure, the iRTG, and outdoor the greenhouse (rooftop), in the morning and afternoon terms of daytime. BVOC emissions collected were compared between the sampling intervals within an individual site and between the three locations within the single interval. Results aimed at providing a quick overview of the performance of the static enclosure and of the sampling length in terms of total emission sampled. These results can be found in the Annex II (Annex X. 36).

A1.2 Inertia of tubular static enclosure

Based on the last configuration mentioned in section A1.1, static enclosure was then adapted for the collection of BVOC emissions from bulky species, in this case tomato plant (**Ch. 6**). Following a previous work (Takayama et al., 2012) a tubular-shaped chamber designed to accommodate a single plant for air measurement was constructed and hung from the ceiling. The chamber's wall effect on the enclosed plant was then measured monitoring internal conditions throughout at different closure settings, respectively, open-top/bottom and sealed. Environmental variables recorded were temperature (°C), relative humidity (%), CO_2 concentration (ppm), and solar radiation (W m^{-2}). Measurements were taken in the middle of the greenhouse initially in the empty chamber, and subsequently with the accommodated plant, both at open top/bottom setting. The radiation curve was only measured in the empty chamber and compared with records provided by sensors located at different levels (height) of the iRTG. As can be seen in figure X.5, chamber's cloth performed a relevant shadowing effect on the solar radiation as did the roof polycarbonate windows on the total radiation measured inside the iRTG.

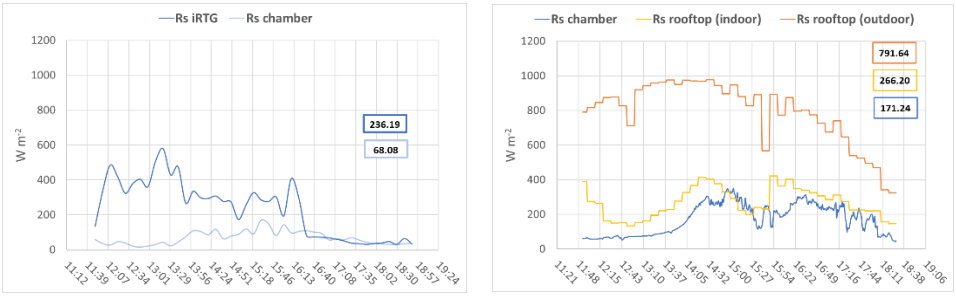

Annex X. 5 Radiation (Rs) recorded in the empty chamber and in the iRTG at different height levels, where average Rs records are reported in square boxes.

Additionally, air velocity (m s^{-1}) was monitored to determine its impact on the variation of CO_2. Air velocity in the empty chamber was mostly close to 0 m s^{-1} in either open-top/bottom or sealed configuration, even when the iRTG was fully open (results not showed). Therefore, measurements were taken directly in the iRTG, monitoring environmental fluxes both near and far from tomato plants. As shown in figure X.6, under similar trends of air velocity (11:45-15:00), slight differences between CO_2 levels (±20 ppm) were identified, whereas no differences were observed under much different air trends (15:00-18:40). Based on these outcomes, an overall negligible contribution of air stream to CO_2 evolution was considered.

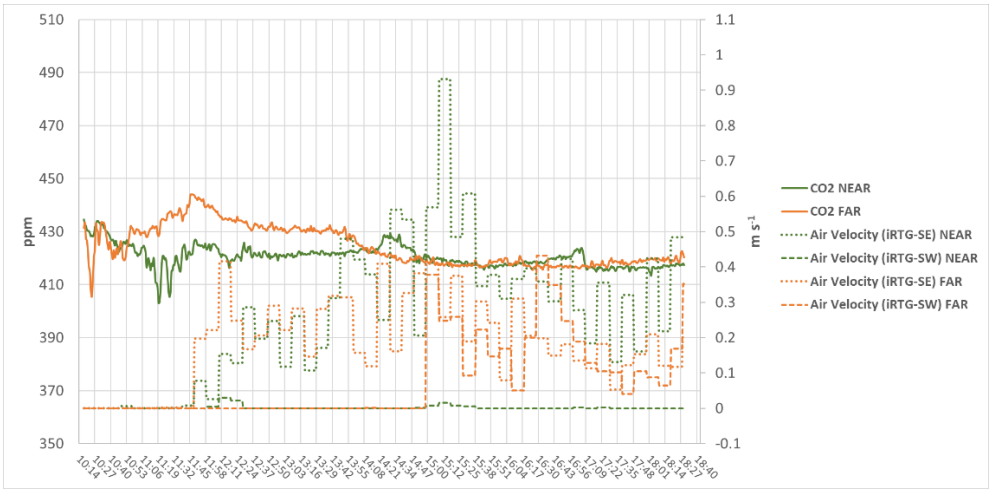

Annex X. 6 CO_2 measured in the iRTG near and far from plants and air velocity recorded during the respective scenario.

Figure X.7 illustrates the curves of the rest of the variables measured in the chamber with and without plant. As can be seen, no relevant variations were observed for the temperature (X.7.1), whereas plant presence inside the chamber produced an increase (+20%) in relative humidity (X.7.2), and a decrease (-40 ppm) in CO_2 concentration (X.7.3), both within the first 10 minutes. However, in the case of relative humidity a parallel increase was also measured in the iRTG.

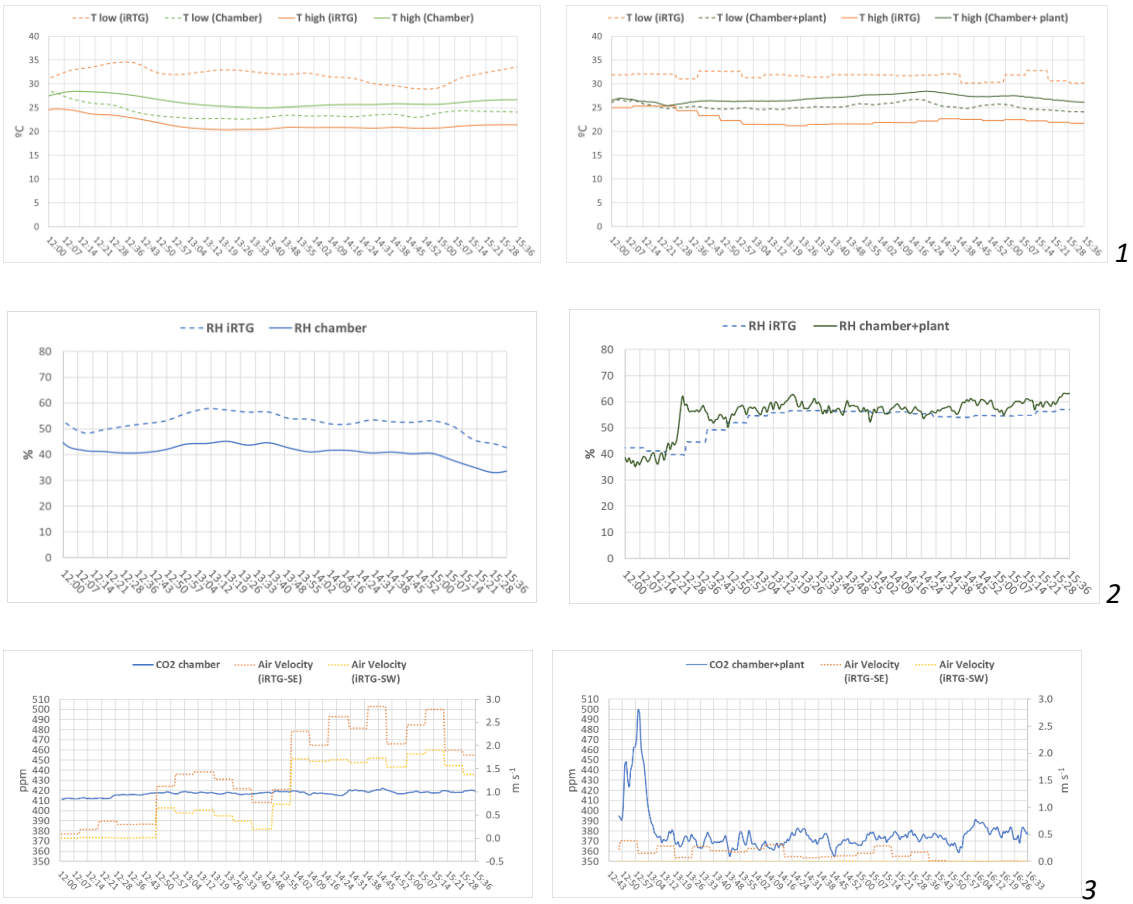

Annex X. 7 Variation curve of the T (7.1), RH (7.2), and CO2 and air velocity (7.3) measured in the open-top/bottom chamber while empty (left side) and during plant enclosing (right side).

According to these results, further measurements were carried out with the enclosed plant comparing relative trends under open open/bottom and sealed chamber setting, respectively (figure X.8). During the closure CO_2 decrease and final concentration were substantially similar between the settings (figure X.8.1). However, slightly different curves of temperature and relative humidity were observed, showing under open top/bottom condition a higher increase in humidity levels (+12%) along with lower temperature rates compared to the sealed setting (figure X.8.2). Because measurements were conducted on different days, the environmental conditions of the iRTG were not identical as well as the affected internal conditions of the chamber. Hence, according to the inverse proportionality between temperature and relative humidity trends observed were consistent. Based on these final outcomes chamber configurations were considered similar with respect to the measured parameters. Regardless of the chamber setting, for the BVOCs assessment conducted afterwards (**Ch. 6**) special attention was given to the length of sampling concerning CO_2 and relative humidity variables.

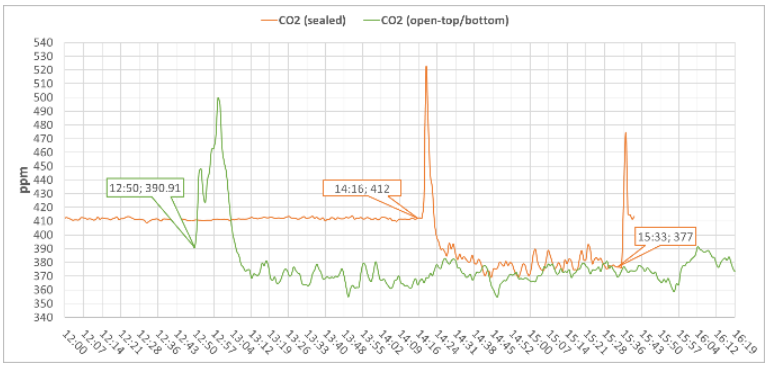

1

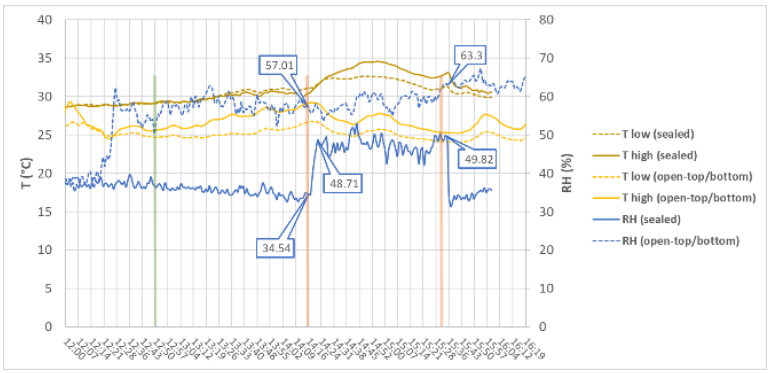

2

Annex X. 8 Comparing chamber performance during plant enclosing at open-top/bottom or sealed setting condition with respect to the variation curve of CO2 concentration (left), T, and RH (right). For each setting condition the time of closure is highlighted by data-called outs (8.1) or by corresponding-coloured perpendicular bars (8.2).

A2 Plant cultivation system

A2.1 Nutrient recipes

Annex X. 9 Nutrients concentration delivered to the plants along the cultivation (months). In the case of tomato plant mid-term recipe is reported. Data in red indicates water solution of a parallel crop (tomato) whose leachates were used for the fertigation of considered species (basil).

				Nutrient concentration (mg L^{-1})							
				#1 tank			*#2 tank*				
Ch.	*UA case study*	*species*	*months*	**KPO_4H_2**	**KNO_3**	**K_2SO_4**	**$Ca(NO_3)_2$**	**$CaCl_2$**	**$Mg(NO_3)_2$**	**Hortilon**	**Sequestren**
4, 5	iRTG-LAU2	bean	3	136	101	217	164	111	148.3	0.1	0.1
6	iRTG-LAU1	tomato	6	140	50	350	490	140	150	10	10
8	iRTG-LAU2	basil	2	170	0	501	451	194	185	–[a]	10

a

NH_4NO_3	**$Na_2B_4O_7$**	**$MnSO_4$**	**$ZnSO_4$**	**$CuSO_4$**	**$NaMoO_4$**
40	2.1	1.7	1.7	0.3	0.2

				*Nutrient concentration (*mM or ** µM)*												
Ch	*UA system*	*species*	*months*	*NO_3	*NH_4	*P	*K	*S	*Ca	*Mg	**Fe	**Cu	**Zn	**B	**Mn	**Mo
7	VF	basil	2	16.0	2.0	2.0	10.0	2.5	4.5	1.0	40.0	1.0	5.9	30.0	5.0	1.0

A3 Testing the post sampling method: sample handling and processing

A3.1 Performance of activated carbon material

Sampling method with activated carbon sorbents was further assessed on the measure of breakthrough volumes, desorption efficiency, and recovery of the sampled material, following MDHS 96 (HSE, 2002) and NIOSH 1552 (1996) protocols.

A3.1.1 Sample breakthrough

At the beginning of the test described in paragraph A1.2 breakthrough was evaluated. First samples obtained after 15- and 30-minutes sampling from both chamber sides (*control* and *plants*) were analysed extracting the two parts of the adsorption bed separately, respectively the front and the back part, according to procedure 3.2.7.1 of the M&M. Samples were analysed in the GC-MS at the conditions above mentioned (A1.2), focusing on MT-limonene given its higher volatility compared to bigger BVOC species and its ubiquity in plant emission profile. In figure *X.10* is shown an exemplary of the chromatograms obtained from the analysis of the front and the back part individually of one sorbent tube. As reported in table X.11, all samples provided

acceptable BVs (<5%), even double-interval ones (30 minutes). These results provided evidence of a correct performance of sorbent tubes under the set sampling conditions.

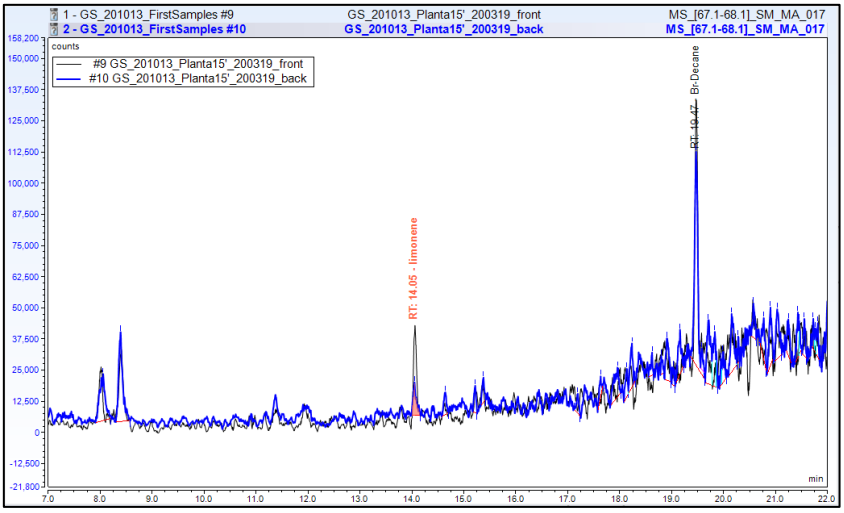

Annex X. 10 Overlaid chromatograms (MS channel 67.1-68.1) obtained from analysed sorbent's front and back part where limonene peak is highlighted. In this case are shown the short-air samples (15 minutes) collected from chambers' plants side (=12 bean plants).

Annex X. 11 Table illustrating limonene signal (peak area) detected in respectively the front and the back adsorbent part of air samples collected along short and long sampling from the two chamber sides, and the corresponding breakthrough volumes (BV) calculated.

sample	sampling length	tube-front (area*counts)	tube-back (area*counts)	front - back (area*counts)	BV%
control	15'	5345.72	159.50	5186.22	3.0
control	30'	4012.03	185.40	3826.63	4.6
plants	15'	2887.60	94.18	2793.42	3.3
plants	30'	37840.75	1044.06	36796.69	2.8

A3.1.2 Sample desorption efficiency

This parameter consisted in the measurement of the amount of analyte recovered from an entire sorbent bed after its liquid extraction with a selected solvent. Standard solutions containing four representative BVOC analytes, respectively, α-pinene, β-pinene, 3-carene, and limonene, diluted in pure CS_2 were prepared: 50, 10, 200, and 400 ng μL^{-1}. 10 µL of each standard solution was then purged into individual Anasorb CSC tubes following sampling direction. Sorbent material was subsequently extracted with 1 mL of the same CS_2 solvent, obtaining 4 different extracts containing the mixed standards at the respective theorical amounts: 0.5, 1, 2, and 4 ng. One extra tube was purged with only CS_2 and extracted as well as the previous ones. All extracts contained in addition a fixed concentration (105 ng μL^{-1}) of IS, 1-bromodecane. 1 µL of each

extract was then injected and analysed in the GC-MS at the conditions mentioned in paragraph A1.2. As can be seen in in figure X.12 for most of the analytes the recovered amount in the extracted tubes was equivalent to the measured one in the injected standard solutions. No analytes were detected in blank (CS_2) extracts. Following the definition of MDHS 96 (HSE, 2002), DE for activated carbon tube should not be lower than 0.75 (or 75%). Figure X.13 indeed, confirmed found equivalences, except for the slightly lower DE of the highest amount of β-pinene analyte (0.71). However, considering that mixtures of standards were prepared, chemical interactions were likely to occur, though quite irrelevant in this case due to overall compatibility among the selected analytes.

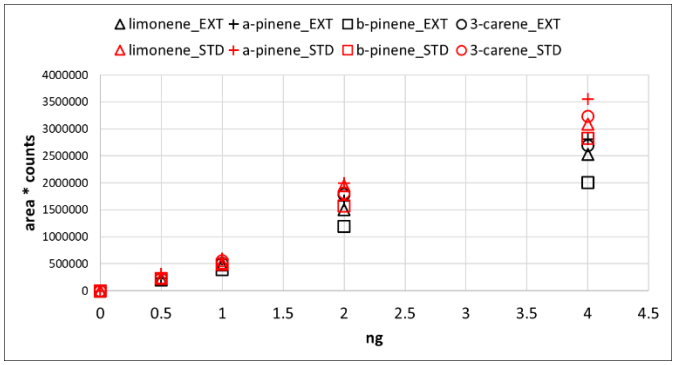

Annex X. 12 Analytes amount (ng) in the original standard solutions (STD) and in corresponding purged tube extracts (EXT) plotted against relative signal area counts.

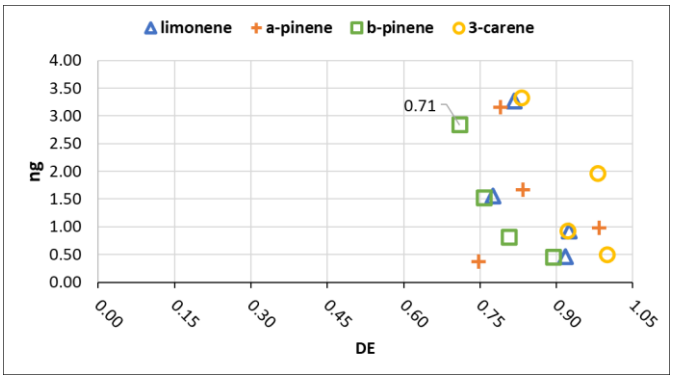

Annex X. 13 Analytes amount (ng) in tube extracts plotted against relative desorption efficiency (DE) measured. Data callout highlights DE level lower than the minimum one (75%).

A3.1.3 Sample recovery

This parameter was assessed to define the storing boundary under optimal conditions of the samples collected with Anasorb CSC tubes. Samples conservation after the period of storage was measured as a function of the total recovery of the analytes amount with respect to the starting one before the storage. Storage was kept at stable 4°C temperature following NIOSH 1552

protocol for 4 months because this was the longest interval occurred between sample collection and analysis according to laboratory schedules. Two of the least concentrated standard solutions were considered for the test, 0.001 and 0.005 ng μL^{-1}, that were respectively the first (=LOQ) and the second level of the reference calibration curve. Triplicates of each solution were prepared with 27 standards and injected individually into virgin Anasorb CSC tubes following the sampling direction. Three additional tubes were purged with pure CS_2 providing blanks. At complete solvent evaporation, tubes were capped and stored in glass jars filled with additional silica gel to prevent humidity for the following 4 months. At the end of the storing period, all tubes were let acquaint at room temperature, then extracted, and analysed as reported above (A3.1.1). Sample recovery was fixed at a percentage of at least the 50% of the initial amount. As reported in table X.14 most than a half of the standards of each class and reference concentration was not fully recovered (<50%). Among the recovered standards though, many exceeded the total amount of injected solutions (>100%). Indeed, there were few analytes detected in the blanks, suggesting contamination either from the environment or between the capped samples. Based on these outcomes, storage longer than 4 months was discouraged. If shorter terms were unavoidable, sample loss was then considered in the final results.

Annex X. 14 Analytes amount (ng μL^{-1}) in the starting standard solutions (STD) and in the stored samples (TEST and blank) and the corresponding total recovery (%) after 4 months of cool storage. Samples conservation is achieved with recovery >50% (green). Recovery >100% (underlined) indicates sample contamination occurred.

		STD	*TEST*	*STD*	*TEST*	*blank*	*Recovery (%)*	
Class	**VOC**	**0.005**		**0.001**		**-**	**0.005**	**0.001**
MT	α-pinene	0.005	0.002	0.002	0.002	0.001	33.3	109.9
	β-pinene	0.006	0.002	0.001	0.002	0.002	32.8	151.9
	β-myrcene	0.006	0.002	0.001	0.002	0.002	40.6	164.4
	3-carene	0.005	0.002	0.001	0.001	0.001	32.7	68.2
	α-phellandrene	0.005	0.001	0.001	0.001	0.001	18.5	89.6
	α-terpinene	0.005	0.000	0.001	0.000	0.000	0.0	0.0
	limonene	0.005	0.051	0.002	0.049	0.001	993.5	2209.0
	g-terpinene	0.005	0.000	0.001	0.000	0.000	0.0	0.0
	p-cymene	0.005	0.008	0.001	0.001	0.000	154.3	105.3
	o-cymene	0.005	0.007	0.001	0.000	0.000	146.7	0.0
	β-phellandrene	0.005	0.001	0.001	0.000	0.000	28.4	0.0
OMT	1.8-cineole	0.005	0.008	0.001	0.001	0.000	170.1	74.1
	linalool	0.005	0.001	0.001	0.000	0.000	13.3	22.7
	camphor	0.005	0.013	0.002	0.004	0.000	256.4	258.1
	α-terpineol	0.005	0.002	0.001	0.003	0.000	41.7	514.3
ST	β-caryophyllene	0.005	0.000	0.001	0.000	0.001	0.0	0.0
	trans-β-farnesene	0.006	0.000	0.001	0.000	0.001	5.6	0.0

	α-caryophyllene	0.005	0.000	0.002	0.000	0.000	0.0	22.2
HT	TMTT	0.005	0.000	0.001	0.000	0.000	0.0	0.0
LOX	n-octyl acetate	0.004	0.007	0.004	0.000	0.001	170.7	0.0
	n-hexanol	0.005	0.008	0.002	0.009	0.000	166.7	446.3
	cis-3-hexenal	0.006	0.024	0.006	0.021	0.018	394.4	364.7
	cis-3-hexenol	0.005	0.005	0.002	0.005	0.000	95.2	277.2
PH	methyl chavicol	0.005	0.000	0.001	0.001	0.000	6.7	51.9
	2-tert-butylphenol	0.005	0.000	0.001	0.000	0.000	0.0	0.0
	methyl cinnamate	0.005	0.002	0.002	0.001	0.000	40.0	82.5
	methyl eugenol	0.005	0.000	0.001	0.000	0.000	6.8	0.0

A3.2 Side sampling method

A3.2.1 Handy TD setup on TA tube

A processing method for TA tubes analysis was developed in the GC-FID (8860, Agilent) instrument and thermal desorption machine (Handy TD265, GL-Sciences) transversely. Analytical conditions of the GC-FID were based on examples provided by Handy TD265 manufacturer, adjusted on current column and carrier gas. Critical parameters were the desorber machine (Handy TD265) setting and the GC injection, straight connected with tube's packing material and the targeted volatiles. In particular, pressure, heating temperature and time along the desorption process were tested under several combinations. In figure X.15 are showed the configurated desorbing conditions.

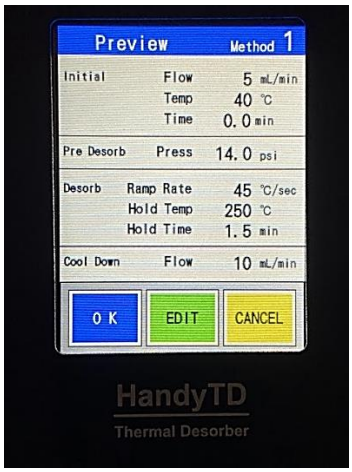

Annex X. 15 Thermal desorption method established for the Handy TD256 after multiple combination tests of the shown parameters.

Concurrently, injection setting was adjusted accordingly, testing different split ratios. It was individuated a clear inverse correlation between the signal outputs (peaks area) and the split ratio for both the compounds with the highest and the lowest volatility that were present in the standard mixture injected (Figure X.16).

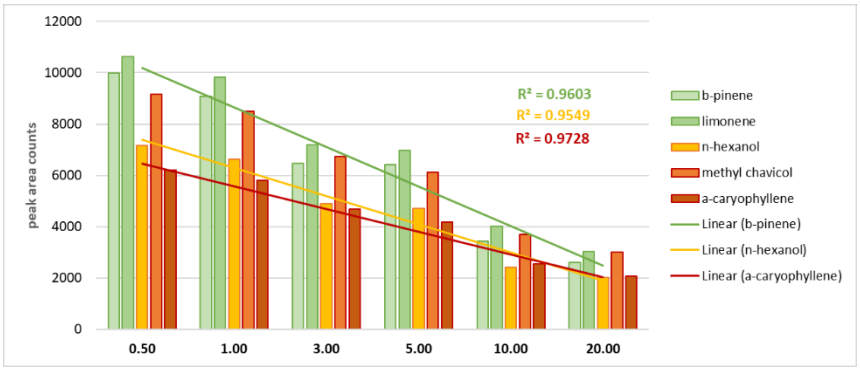

Annex X. 16 Increasing split ratios (0.5, 1.00, 3.00, 5.00, 10.00, 20.00) tested under fixed amount of injected standard mixture plotted against the peaks area of five BVOCs with different volatility, representing the most and the least volatile species (from green to red-coloured bars), and corresponding linear relations.

Among these tests the load of known concentrations of standard mixtures to be injected was also determined comparing the chromatographic resolution obtained loading (purging) different aliquots (µL) of mixtures onto a liner. As shown in figure X.17, increasing the sample load (7 and 9 µL) chromatographic resolution improved. However, higher loads also increased the time lapse of solvent evaporation from the liner, which was necessary to prevent machine's issues, considerably affecting the reliability of sample.

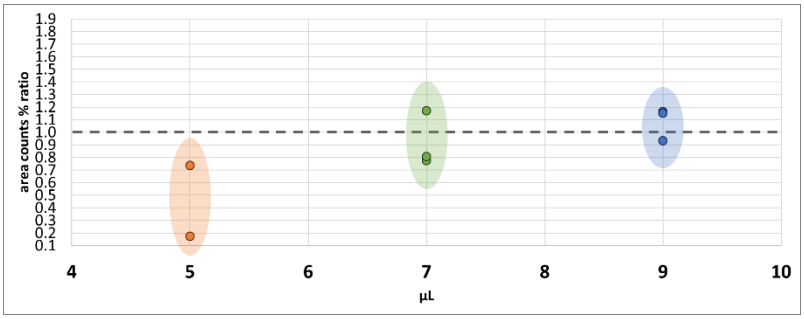

Annex X. 17 Peaks area (area counts) ratio (%) between the least (β-pinene) and the most (α-caryophyllene) volatile compound present in the standard mixture injected at different sample loads (5, 7, and 9 µL).

Overall parameters were related, but they affected each other with a different impact (table X.18).

Annex X. 18 Relations degree among the individual parameters of instruments and sample.

		Sample parameter		
Instrument	**Instrument parameter**	Tube's packing material	Target volatiles	Chromatographic analysis
Liner/Sorbent	Sample load	++	+++	+++
Handy TD265	Pressure	+ + +		
	Heating temperature	++	+++	++
	Heating time	++	+++	++
	Gas flow	+		
GC-FID	Split ratio		+++	+++
	GC setting (T gradients, time, gas flow)			+++
	FID setting (T, gas flow)			+++

A3.2.2 Chromatographic performance

Chromatographic accuracy was determined by multiple injections (triplicates) of known concentrations of standard mixtures at the processing methods established, where reproducibility and repeatability of the results were evaluated according to peak's retention time within 0.05 interval and related features (X.19).

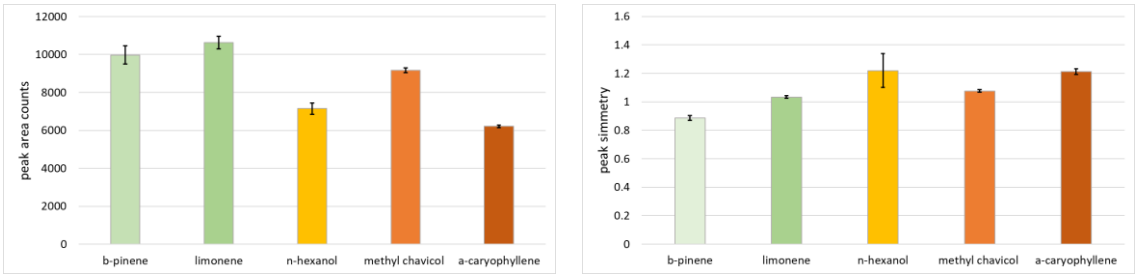

Annex X. 19 Average (=n3) peak's area (left) and symmetry (right) with relative SEM of each analyte of the standard mixture injected at established machine and instrument conditions.

Similarly, this step was realized for real samples, but considering high variability of both amount and composition of BVOC emissions additional information about environmental background were necessary. Moreover, sampling interval was tested. Field sampling was carried out in iRTG-LAU1 during tomato plants cultivation (March-July 2023). BVOC emissions were collected over 120 minutes in the greenhouse uninterruptedly along increasing intervals of 30, 60, 90 and 120 minutes (=cumulative samples). In parallel, four consecutive samples of 30 minutes each were collected, the sums of which were compared to the equivalent sample volumes provided by corresponding 60, 90 and 120-minutes cumulative samples. Meaningful T, RH, solar radiation, and CO_2 data were recorded throughout the sampling period. Overall, there was low

resemblance between cross-samples, where BVOCs amount in cumulative samples was generally lower (figure X.20*J*).

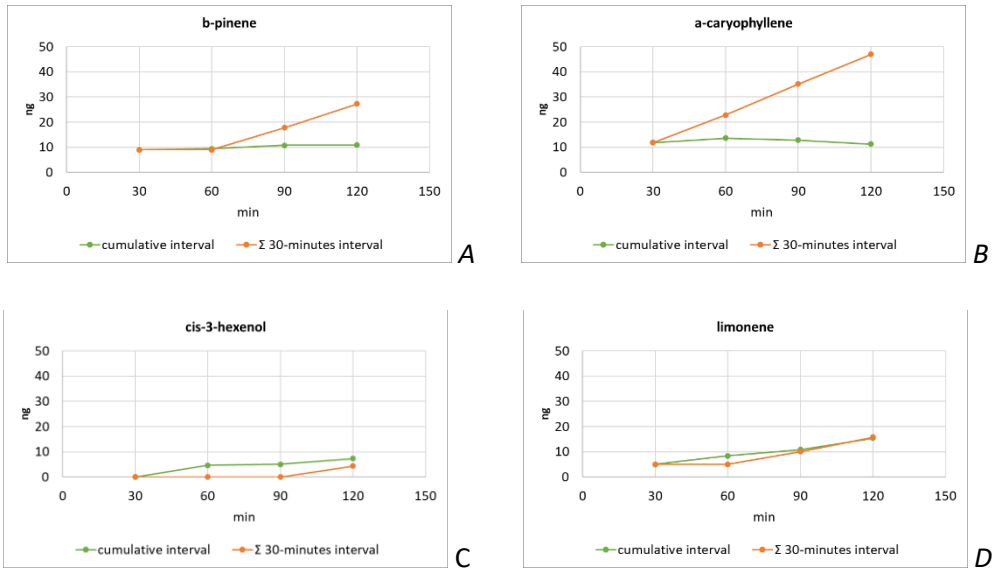

Annex X. 20 Individual BVOC emission (ng) curves obtained plotting the amount detected in cumulative samples (green) and in corresponding 30-minutes summed samples (orange). Curves of the most (A) and the least (B) volatile terpenes, of a LOX compound (C), and of a monoterpene with the highest samples resemblance are reported as example.

Resemblance degree (percentage) among cumulative and summed BVOC emissions is shown in figure X.21, where some distribution patterns were individuated. Indeed, only few monoterpenes (α-pinene, 3-carene, and limonene) had the highest match (>80%), the rest of them and other terpenoids had similar low matches (20-40%), as well as one LOX volatile (cis-3-hexenol), which amount was instead higher in the cumulative samples (X.20.C).

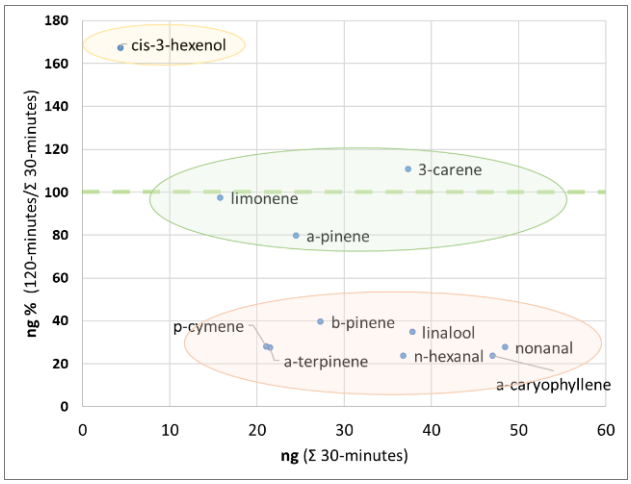

Annex X. 21 BVOC emissions match (%) between cumulative 120-minutes sample and corresponding summed one. Similar percentage matches are wrapped in coloured circles.

These findings were therefore compared with the environmental trends measured meanwhile (X.22). Over the whole sampling period a progressive temperature increase along with the solar

radiation increment and a slight relative humidity decrease were registered. CO_2 concentration, instead, fluctuated within ±12 ppm every approximately 30 minutes. Hence, it was considered relevant the impact of background conditions on sampled emissions, especially after longer exposure intervals (>30 minutes). Conversely, overall proportionality between BVOCs emission amount and sampling interval obtained summing individual 30-minutes samples, this length was therefore suggested as elective sampling interval to provide most accurate chromatographic outputs.

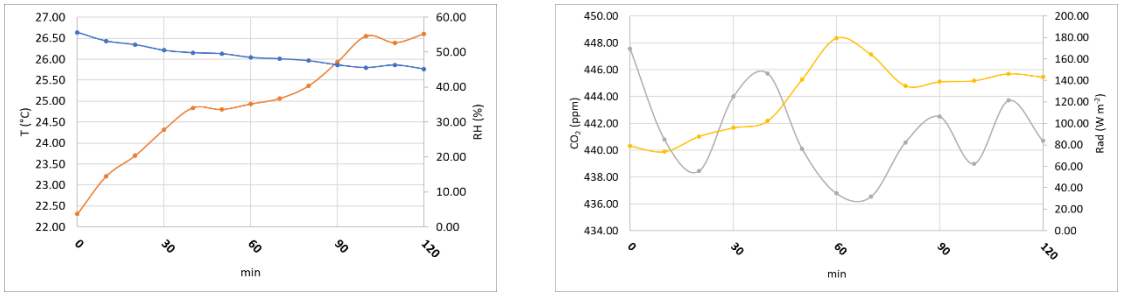

Annex X. 22 T (°C), RH (%), solar radiation (W m^{-2}), and CO_2 concentration (ppm) curves registered along the whole sampling period (120 minutes) in the iRTG-LAU1. Measurements were conducted between 10:00 and 12:00 hour.

A3.3 Analytical processing methods

Annex X. 23 SIM acquisition table list of the target BVOCs, related retention time (RT), and mass ion charge m/z applied for the quantitation analysis carried out with the ISQ7000 MS (Thermo Scientific) in Ch. 5.

compound	**RT (min)**	**target m/z**
α-pinene	6.35	93.1
n-hexanal	7.37	57.1
β-pinene	7.82	93.1
3-carene	8.46	93.1
β-myrcene	8.55	69.1
α-phellandrene	8.73	93.1
α-terpinene	8.99	121.1
limonene	9.28	68.1
1.8-cineole	9.44	139.1
β-phellandrene	9.45	136.1
cis-3-hexenal	9.63	69.1
trans-2-hexenal	9.63	98.1
γ-terpinene	9.99	93.1
p-cymene	10.42	119.1
o-cymene	10.91	119.1
n-hexanol	11.32	56.1
cis-3-hexenol	11.85	67.1
nonanal	12.14	82.1
n-octyl acetate	13.18	61.1
linalool	13.98	93.1
camphor	14.22	95.1
1-bromodecane*	14.61	135.1
β-caryophyllene	15.19	133.1
trans-β-farnesene	15.69	93.1
methyl chavicol	15.95	148.1
α-caryophyllene (Humulene)	16.12	80.1
α-terpineol	16.16	59.1
(3E,7E)-4,8,12-trimethyltrideca-1,3,7,11-tetraene (TMTT)	17.26	69.1
methyl salicylate	17.41	92.1
methyl eugenol	19.69	178.1
methyl cinnamate	20.87	131.1
2-tert-butylphenol	21.99	135.1
eugenol	22.05	164.1

*IS

Annex X. 24 Complete information of the calibration curves retrieved with the ISQ7000 MS (Thermo Scientific) in SIM scan mode for the quantitation analysis carried out in Ch. 5. Red-highlighted data indicate unreliable calibration curves (> 99% Correlation Coeff.). Fixed IS amount was used for all calibration levels (8).

Compound	*Calibration type*	*points n.*	*RSE (%)*	*Correlation Coeff. (%)*	*Variation Coeff. (%)*	*SD (%)*	*RSD (%)*	*Determination Coeff.*	***Intercept (ng)***	***Slope (ng area counts^{-1} min^{-1})***	***Curve***
α-pinene	Quad, WithOffset, 1/A²	8	9.78	99.71	5.50	95.40	10.08	0.99	233.17	493371.43	-26427.69
n-hexanal	Lin, WithOffset	8	424.24	97.11	18.53	1406.78	33.95	0.94	468.00	75778.46	0.00
β-pinene	Lin, WithOffset	8	64.21	99.91	3.50	1253.59	6.93	1.00	-614.04	385567.96	0.00
3-carene	Quad, WithOffset, 1/A²	8	8.33	99.73	5.61	74.33	10.84	0.99	116.65	393304.61	-3234.62
β-myrcene	Quad, WithOffset	8	85.69	99.76	4.07	849.65	8.68	1.00	-513.29	237551.51	-183126.53
α-phellandrene	Quad, WithOffset	8	38.73	99.81	1.36	790.56	3.05	1.00	-438.88	453649.93	658677.25
α-terpinene	Quad, WithOffset, 1/A²	8	1.58	98.77	4.61	34.80	11.56	1.00	-12.59	214531.92	534952.42
limonene	Lin, WithOffset, 1/A²	8	9.58	99.57	6.37	68.01	10.09	0.99	221.30	313055.04	0.00
1.8-cineole	Quad, WithOffset	8	43.62	99.87	1.02	78.35	2.24	1.00	41.57	61759.22	70404.64
β-phellandrene	Quad, WithOffset	8	34.33	99.75	1.07	68.26	2.38	1.00	27.40	47298.01	82637.75
trans-2-hexenal	Lin, WithOffset	7	n.a.	99.80	4.68	116.14	8.11	1.00	179.86	22712.47	0.00
cis-3-hexenal	Lin, WithOffset	8	69.16	99.90	3.27	249.03	5.58	1.00	861.66	74283.84	0.00
γ-terpinene	Quad, WithOffset	8	11.83	99.82	0.35	128.28	0.76	1.00	19.85	289103.24	413613.39
p-cymene	Lin, WithOffset, 1/A	8	15.71	99.96	2.70	690.70	10.24	1.00	212.77	1539598.08	0.00
o-cymene	Quad, WithOffset	8	19.76	99.95	0.44	394.61	0.94	1.00	214.04	783901.59	539728.92
n-hexanol	Quad, WithOffset, 1/A²	8	1.74	99.81	4.26	26.54	7.51	1.00	106.89	170326.84	4320.56
cis-3-hexenol	Lin, WithOffset, 1/A²	8	6.68	99.83	4.47	14.36	8.15	1.00	21.55	106839.71	0.00
nonanal	Quad, WithOffset, 1/A²	8	37.14	96.77	15.53	25.94	25.07	0.94	44.41	40892.83	-19569.43
n-octyl acetate	Lin, WithOffset, 1/A	8	32.36	99.64	8.14	80.44	33.27	0.99	-11.68	59721.03	0.00
linalool	Quad, WithOffset, 1/A²	8	2.13	99.94	2.38	6.39	5.12	1.00	3.76	83567.28	23629.01
camphor	Quad, WithOffset, 1/A	8	9.23	99.85	1.92	55.41	8.61	1.00	15.24	142028.51	123659.63
1-bromodecane*	**Lin, WithOffset**	**8**	**n.a.**	**99.95**	**n.a.**	**n.a.**	**n.a.**	**n.a.**	**0.00**	**0.00**	**0.00**
β-caryophyllene	Lin, WithOffset, 1/A²	8	5.52	99.87	3.97	8.77	7.45	1.00	9.50	74806.41	0.00
trans-β-farnesene	Quad, WithOffset	8	14.89	99.83	1.07	24.49	2.36	1.00	-1.75	18053.37	24495.16
methyl chavicol	Lin, WithOffset, 1/A	8	9.76	99.82	5.72	255.53	24.21	1.00	-95.84	271273.45	0.00
α-caryophyllene (Humulene)	Quad, WithOffset, 1/A	8	9.95	99.88	2.13	43.39	9.46	1.00	11.06	101908.21	73319.82
α-terpineol	Lin, WithOffset, 1/A	8	15.26	99.94	3.09	69.75	9.32	1.00	189.68	131709.29	0.00
TMTT	Lin, WithOffset, 1/A²	8	5.66	99.74	6.25	18.78	14.51	0.99	-32.41	111894.66	0.00
methyl salicylate	Lin, WithOffset	8	117.52	96.32	19.99	56.89	34.53	0.93	33.86	2698.50	0.00
methyl eugenol	Lin, WithOffset, 1/A	8	10.49	99.81	5.89	138.22	24.08	1.00	-28.83	142018.96	0.00
methyl cinnamate	Quad, WithOffset, 1/A²	8	13.84	99.42	7.47	51.02	13.28	0.99	107.72	191195.41	-46942.82
2-tert-butylphenol	Lin, WithOffset, 1/A²	8	4.25	99.85	4.41	30.02	8.78	1.00	-3.22	238581.19	0.00
eugenol	Quad, WithOffset, 1/A²	8	62.84	91.27	33.85	62.50	87.46	0.85	-0.93	49560.61	114623.92

***IS**

Annex X. 25 BVOCs theorical LOD and LOQ (ng μL^{-1}) retrieved from calibration curve slope and multiple injections (n=6) of the lowest calibration level (STDs L1; 0.001 ng μL^{-1}) which peaks area RSD (≤25%) was used to assess the LOQ for the quantitation analysis carried out with the ISQ7000 MS (Thermo Scientific) in ch.5. Red-highlighted compounds failed the LOQ due to RSD>25% or unreliable calibration curves (bold text).

Compound	*Curve slope*	*STDs L1 (n=6)*	*SD*	***RSD***	*theorical LOD*	*theorical LOQ*	*STDs L1 (n=6)*	***LOQ****
	ng area counts $^{-1}$ min $^{-1}$	*area*counts*	*%*		*ng μL^{-1}*			
α-pinene	493371.43	995.06	164.89	16.57	0.003	0.005	0.002	0.002
n-hexanal	**75778.46**	**2452.89**	**885.46**	**36.10**	**0.071**	**0.149**	**0.031**	-
β-pinene	385567.96	453.12	80.15	17.69	0.002	0.003	0.001	0.001
3-carene	393304.61	694.02	111.30	16.04	0.003	0.005	0.001	0.001
β-myrcene	237551.51	229.53	51.53	22.45	0.002	0.003	0.001	0.001
α-phellandrene	453649.93	439.80	53.51	12.17	0.001	0.002	0.001	0.001
α-terpinene	214531.92	249.74	32.49	13.01	0.002	0.003	0.001	0.001
limonene	313055.04	924.88	261.59	28.28	0.006	0.011	0.002	-
1.8-cineole	61759.22	60.37	8.13	13.46	0.001	0.002	0.001	0.001
β-phellandrene	47298.01	60.75	10.38	17.08	0.002	0.003	0.001	0.001
trans-2-hexenal	**22712.47**	**312.58**	**35.37**	**11.32**	**0.019**	**0.029**	**0.003**	**0.003**
cis-3-hexenal	74283.84	1369.83	188.70	13.78	0.027	0.044	0.006	0.006
γ-terpinene	289103.24	339.19	58.54	17.26	0.002	0.003	0.001	0.001
p-cymene	1539598.08	1714.18	153.92	8.98	0.001	0.002	0.001	0.001
o-cymene	783901.59	771.10	68.67	8.91	0.001	0.002	0.001	0.001
n-hexanol	170326.84	451.28	99.31	22.01	0.005	0.008	0.002	0.002
cis-3-hexenol	106839.71	199.93	38.92	19.47	0.003	0.006	0.002	0.002
nonanal	**40892.83**	**163.89**	**48.88**	**29.82**	**0.008**	**0.016**	**0.003**	-
n-octyl acetate	59721.03	229.56	78.37	34.14	0.008	0.017	0.004	-
linalool	83567.28	125.83	25.72	20.44	0.003	0.005	0.001	0.001
camphor	142028.51	232.10	52.74	22.72	0.003	0.005	0.002	0.002
β-caryophyllene	18053.37	100.00	15.98	15.98	0.008	0.014	0.001	0.001
trans-β-farnesene	271273.45	26.05	9.00	34.54	0.000	0.000	0.001	-
methyl chavicol	101908.21	284.88	49.48	17.37	0.004	0.008	0.001	0.001
α-caryophyllene (Humulene)	131709.29	160.66	41.27	25.69	0.002	0.004	0.002	-
α-terpineol	111894.66	234.17	133.81	57.14	0.006	0.014	0.001	-
TMTT	2698.50	99.90	11.55	11.57	0.051	0.080	0.001	0.001
methyl salicylate	**142018.96**	**46.24**	**11.60**	**25.09**	**0.001**	**0.001**	**0.002**	-
methyl eugenol	191195.41	187.46	43.74	23.33	0.002	0.003	0.001	0.001
methyl cinnamate	238581.19	418.79	98.46	23.51	0.003	0.006	0.002	0.002
2-tert-butylphenol	49560.61	286.36	30.43	10.63	0.008	0.012	0.001	0.001
eugenol	**49560.61**	**59.18**	**27.05**	**45.71**	**0.003**	**0.007**	**0.001**	-

***RSD≤25%**

Annex X. 26 SIM acquisition table list of the target BVOCs, related retention time (RT), and mass ion charge m/z applied for the quantitation analysis carried out with the 5975C MS (Agilent) in chapters 6 and 7.

compound	**RT (min)**	**target m/z**
α-pinene	6.75	93.1
n-hexanal	7.85	56.1
β-pinene	8.29	93.1
3-carene	8.96	93.1
β-myrcene	9.10	69.1
α-phellandrene	9.24	93.1
α-terpinene	9.48	121.1
limonene	9.79	68.1
1.8-cineole	9.96	139.1
trans-2-hexenal + cis-3-hexenal	10.18	69.1
γ-terpinene	10.54	93.1
p-cymene	10.97	119.1
o-cymene	11.46	119.1
n-hexanol	11.95	56.1
cis-3-hexenol	12.46	67.1
nonanal	12.73	98.1
n-octyl acetate	13.73	56.1
linalool	14.59	93.1
camphor	14.76	95.1
1-bromodecane*	15.17	135.1
β-caryophyllene	15.69	93.1
trans-β-farnesene	16.16	69.1
methyl chavicol	16.52	148.1
α-caryophyllene (Humulene)	16.62	93.1
α-terpineol	16.69	136.1
TMTT	17.83	69.1
methyl salicylate	17.97	121.1
methyl eugenol	20.21	178.1
methyl cinnamate	21.27	131.1
2-tert-butylphenol	22.28	135.1
eugenol	22.36	164.1

*IS

Annex X. 27 Complete information of the calibration curves retrieved with the 5975C MS (Agilent) in SIM scan mode for the quantitation analysis carried out in chapters 6 and 7. Fixed IS amount was used for all calibration levels (7).

Compound	*Calibration type*	*points n.*	*Origin*	*Weight*	*Accuracy Max. Dev. (%)*	*Correlation Coeff. (%)*	*RSD (%)*	*Curve formula*
α-pinene	Linear	7	Ignore	1/x	20	99.62	28.51	y = 0.111512 * x + 111.767365
n-hexanal	Linear	7	Ignore	1/x	20	98.58	19.09	y = 0.026275 * x + 535.364084
β-pinene	Linear	7	Ignore	1/x	20	99.73	7.15	y = 0.106716 * x + 14.604326
3-carene	Linear	7	Ignore	1/x	20	99.70	11.66	y = 0.102681 * x + 48.230189
β-myrcene	Linear	7	Ignore	1/x	20	99.79	12.26	y = 0.059366 * x - 14.234149
α-phellandrene	Linear	7	Ignore	1/x	20	99.73	8.94	y = 0.178313 * x - 34.248942
α-terpinene	Linear	7	Ignore	1/x	20	99.54	6.02	y = 0.067687 * x - 1.136729
limonene	Linear	7	Ignore	1/x	20	99.75	39.02	y = 0.077891 * x + 110.095548
1.8-cineole	Linear	7	Ignore	1/x	20	99.84	4.15	y = 0.017180 * x + 0.835548
trans-2-hexenal + cis-3-hexenal[a]	Linear	7	Ignore	1/x	20	99.67	153.80	y = 0.019052 * x + 367.662543
γ-terpinene	Linear	7	Ignore	1/x	20	99.71	6.81	y = 0.112506 * x - 3.310487
p-cymene	Linear	7	Ignore	1/x	20	99.79	14.72	y = 0.245912 * x + 126.303861
o-cymene	Linear	7	Ignore	1/x	20	99.72	7.51	y = 0.229082 * x + 54.190060
n-hexanol	Linear	7	Ignore	1/x	20	99.53	9.48	y = 0.060162 * x + 21.914595
cis-3-hexenol	Linear	7	Ignore	1/x	20	99.52	8.87	y = 0.041215 * x + 12.301419
nonanal	Linear	7	Ignore	1/x	20	99.43	40.29	y = 0.011143 * x + 53.971423
n-octyl acetate	Linear	7	Ignore	1/x	20	99.77	10.02	y = 0.024062 * x - 64.643716
linalool	Linear	7	Ignore	1/x	20	99.64	10.35	y = 0.033398 * x - 1.316166
camphor	Linear	7	Ignore	1/x	20	99.62	11.50	y = 0.053770 * x + 16.766705
1-bromodecane[b]	**Linear**	7	**Ignore**	**1/x**	**20**	**-516.99**	**11.82**	**y = 0.062500 * x + 0.000000E+000**
β-caryophyllene	Linear	7	Ignore	1/x	20	99.60	6.72	y = 0.034933 * x + 6.071118
trans-β-farnesene	Linear	7	Ignore	1/x	20	99.20	13.95	y = 0.011866 * x - 116.207905
methyl chavicol	Linear	7	Ignore	1/x	20	99.46	8.32	y = 0.074111 * x + 4.660630
α-caryophyllene (Humulene)	Linear	7	Ignore	1/x	20	99.70	6.76	y = 0.087542 * x + 13.124266
α-terpineol	Linear	7	Ignore	1/x	20	99.41	9.92	y = 0.031852 * x + 4.309500
TMTT	Linear	7	Ignore	1/x	20	99.66	7.03	y = 0.049987 * x + 34.869431
methyl salicylate	Linear	7	Ignore	1/x	20	96.89	46.73	y = 0.004016 * x + 66.195451
methyl eugenol	Linear	7	Ignore	1/x	20	99.61	14.61	y = 0.069069 * x - 9.033223
methyl cinnamate	Linear	7	Ignore	1/x	20	99.50	6.41	y = 0.075382 * x + 27.881882
2-tert-butylphenol	Linear	7	Ignore	1/x	20	99.69	45.55	y = 0.107207 * x + 207.613725
eugenol	Linear	7	Ignore	1/x	20	98.23	18.31	y = 0.028618 * x + 45.169763

[a]co-eluting compounds; [b]IS

Annex X. 28 BVOCs LOQ (pg mL^{-1}) used for the quantitation analysis carried out with the 5975C MS (Agilent) in chapters 6 and 7. LOQ was retrieved from multiple injections (n=5) of the lowest calibration levels (L1, L2, L3, or L4) where the RSD of peaks area was ≤25%. Red-highlighted compounds failed the LOQ whether at the LOD or the RSD (>25%).

STDs Level	*Compound*	*area counts (n=5)*	*SD*	*RSD (%)*	***LOQ****	
					(pg mL^{-1})	*(ng µL^{-1})*
L1	α-pinene	175.29	35.52	20.26	569.62	0.001
-	n-hexanal	-	-	-	-	-
L1	β-pinene	108.24	14.23	13.15	877.39	0.001
L1	3-carene	143.92	9.56	6.64	931.89	0.001
L1	β-myrcene	53.92	9.01	16.71	1148.03	0.001
L1	α-phellandrene	164.87	12.58	7.63	1116.69	0.001
L1	α-terpinene	79.31	8.54	10.76	1188.47	0.001
L1	limonene	140.25	26.23	18.70	387.09	0.000
L2	1.8-cineole	57.53	10.68	18.57	3300.08	0.003
L1	trans-2-hexenal + cis-3-hexenal[a]	349.55	26.85	7.68	193.94	0.000
L1	γ-terpinene	113.15	7.51	6.64	1035.14	0.001
L1	p-cymene	422.75	49.56	11.72	1205.51	0.001
L1	o-cymene	270.95	18.17	6.70	946.23	0.001
L1	n-hexanol	56.07	16.41	29.26	-	-
L2	cis-3-hexenol	98.71	26.60	26.95	-	-
L2	nonanal	46.77	21.20	45.34	-	-
L4	n-octyl acetate	189.68	8.53	17.42	10569.78	0.011
L1	linalool	34.46	7.11	20.65	1071.11	0.001
L1	camphor	49.15	11.60	23.61	602.22	0.001
L2	β-caryophyllene	81.35	12.17	14.96	2155.04	0.002
-	trans-β-farnesene	-	-	-	-	-
L1	methyl chavicol	87.17	18.20	20.88	1113.38	0.001
L1	α-caryophyllene (Humulene)	83.92	7.58	9.03	808.72	0.001
L1	α-terpineol	40.80	11.54	28.27	-	-
L3	TMTT	198.57	36.41	18.34	3274.77	0.003
L4	methyl salicylate	113.93	11.68	21.64	11884.96	0.012
L1	methyl eugenol	57.28	9.45	16.49	960.03	0.001
L1	methyl cinnamate	288.12	103.97	36.09	-	-
L1	2-tert-butylphenol	211.82	53.46	25.24	-	-
L2	eugenol	66.25	66.25	100.00	-	-

***RSD≤25%** **[a]co-eluting compounds**

Annex X. 29 Complete information of the target BVOCs and their calibration curves retrieved with the GC-FID 8860 (Agilent) for the quantitation analysis carried out in Ch. 8. Co-eluting compounds were prepared in different solutions (1 and 2). Fixed IS amount was used for all calibration levels (5), present in each BVOC solution.

RT	solution	Compound	Calibration type	Points n.	Correlation Coeff. (%)	Accuracy Max. Dev. (%)	Residual ($ng_{measured}$ - $ng_{teorical}$)	Curve formula	Slope (ng area counts min^{-1}) (a)	Determination Coeff. (b)	Origin (c)
5.27	2	α-pinene	Linear	5	99.96	20	1.21	y = ax + b	0.809	0.809	0
5.65	1	n-hexanal	Quadratic	5	99.71	20	3.23	$y = ax^2 + bx + c$	0.002	0.455	0
5.89	1	β-pinene	Quadratic	5	99.63	20	7.86	$y = ax^2 + bx + c$	0.003	0.796	0
6.07	2	β-myrcene	Linear	5	99.62	20	9.94	y = mx		0.964	0
6.12	1	3-carene	Quadratic	5	99.72	20	7.91	$y = ax^2 + bx + c$	0.003	0.803	0
6.21	2	α-phellandrene	Linear	5	99.79	20	14.44	y = mx		1.053	0
6.31	1	α-terpinene	Quadratic	5	99.73	20	7.81	$y = ax^2 + bx + c$	0.003	0.841	0
6.44	2	limonene	Linear	5	99.74	20	8.16	y = mx		1.006	0
6.54	2	1.8-cineole	Linear	5	99.96	20	2.13	y = ax + b	1.264	1.264	0
6.60	1	trans-2-hexenal	Quadratic	5	99.76	20	5.34	$y = ax^2 + bx + c$	0.002	0.583	0
6.73	1	γ-terpinene	Linear	5	99.66	20	14.43	y = ax + b	1.513	1.513	0
6.92	2	p-cymene	Linear	5	99.76	20	7.66	y = mx		0.991	0
7.21	1	n-hexanol	Quadratic	5	99.93	20	4.36	$y = ax^2 + bx + c$	0.001	0.839	0
7.46	1	cis-3-hexanol	Quadratic	5	99.90	20	5.05	$y = ax^2 + bx + c$	0.001	0.773	0
7.64	2	nonanal	Linear	5	99.96	20	2.12	y = ax + b	0.922	0.922	0
8.04	2	n-octyl acetate	Linear	5	99.89	20	6.28	y = ax + b	1.042	1.042	0
8.41	2	linalool	Linear	5	99.80	20	8.13	y = ax + b	1.192	1.192	0
8.72	2	camphor	Linear	5	99.89	20	1.83	y = ax + b	0.463	0.463	0
8.78	**1,2**	**1-bromodecane***	**Linear**	**6**	**99.85**	**20**	**5.08**	**y = ax + b**	**0.780**	**0.000**	**0**
9.12	2	β-caryophyllene	Linear	5	99.76	20	12.49	y = ax + b	1.475	1.475	0
9.43	2	methyl chavicol	Linear	5	99.92	20	8.04	y = ax + b	1.733	1.733	0
9.49	1	α-terpineol	Linear	5	99.85	20	11.16	y = ax + b	1.460	1.460	0
9.56	1	α-caryophyllene (Humulene)	Linear	5	99.83	20	9.24	y = ax + b	1.073	1.073	0
10.19	1	methyl salicylate	Linear	5	99.78	20	6.26	y = ax + b	0.755	0.755	0
11.24	2	methyl eugenol	Linear	5	99.80	20	6.07	y = ax + b	1.054	1.054	0
11.94	2	methyl cinnamate	Linear	5	99.80	20	4.84	y = ax + b	0.676	0.676	0
12.48	1	eugenol	Linear	5	99.88	20	8.11	y = ax + b	1.134	1.134	0

***IS**

Annex X. 30 BVOCs LOD (ng), and/or LOQ (ng) for those analytes having BV <5% (bold text) used for the qualitative and/or quantitative analysis carried out with the GC-FID 8860 (Agilent) in Ch.8. LOD and/or LOQ was retrieved from multiple injections (n=5) of the lowest calibration level (1.5 ng μL^{-1}; 7µL injected) of each of the standard solutions (1 and 2) where the RSD of peaks area was ≤25%.

Solution	*Compound*	*peak area counts (n=5)*	*SD*	*RSD (%)*	*LOD - **LOQ** * (ng)*
2	α-pinene	9.96	1.04	10.43	12.03
1	n-hexanal	8.45	2.05	24.32	17.21
1	β-pinene	12.65	2.84	22.45	17.39
2	β-myrcene	10.17	2.33	22.87	10.57
1	3-carene	12.49	2.24	17.94	15.09
2	α-phellandrene	10.93	1.98	18.08	10.39
1	α-terpinene	13.24	2.52	19.02	15.04
2	limonene	10.66	2.36	22.15	10.58
2	1.8-cineole	11.43	1.44	12.58	9.15
1	trans-2-hexenal	8.68	2.02	23.27	14.01
1	γ-terpinene	12.81	2.10	16.43	9.95
2	p-cymene	10.52	2.43	23.05	10.56
1	n-hexanol	10.78	2.20	20.42	12.50
1	cis-3-hexanol	10.00	2.10	20.99	12.73
2	nonanal	9.24	1.94	21.01	8.75
2	**n-octyl acetate**	**8.86**	**1.68**	**18.95**	**8.52**
2	**linalool**	**8.97**	**1.58**	**17.56**	**7.49**
2	camphor	8.65	1.63	18.79	7.86
2	β-caryophyllene	11.04	2.29	20.78	7.60
2	methyl chavicol	13.42	1.57	11.69	8.73
1	α-terpineol	13.06	2.39	18.26	8.98
1	α-caryophyllene	10.24	2.41	23.56	9.58
1	methyl salicylate	9.95	1.17	11.79	13.15
2	methyl eugenol	12.64	2.59	20.53	14.96
2	methyl cinnamate	9.97	1.48	14.87	14.71
1	eugenol	12.45	2.09	16.82	11.70

***RSD≤25%**

Annex X. 31 Complete information of the target BVOCs retrieved with the 5975C MS (Agilent) for the quantitation analysis of LE samples carried out in Ch. 8 (LE/GC-MS). Co-eluting compounds were prepared in different solutions (1 and 2). Information include the SIM scan acquired m/z, RT, calibration curves, and LOQ determined from multiple injections (n=5) of the lowest calibration levels (L1, L2, or L3) where the RSD of peaks area (not shown) was ≤25%. Fixed IS amount was used for all calibration levels (5), present in each BVOC solution.

RT	Solution	Compound	SIM	Calibration type	points n.	Origin	Weight	Accuracy Max. Dev. (%)	Correlation Coeff. (%)	RSD (%)	Curve formula	LOQ (pg mL^{-1}) L1	L2	L3
6.70	2	α-pinene	93.1	Linear	5	Ignore	None	20	99.61	43.45	y = 56.028786 * x + 3.665738E-004	1.03	5.72	10.75
7.81	1	n-hexanal[a]	56.1	Linear	5	Ignore	None	20	99.43	20.59	y = 21.276759 * x + 4.514481E-004	0.00	3.33	5.49
8.23	1	β-pinene	93.1	Linear	5	Ignore	None	20	99.76	13.20	y = 49.502907 * x + 2.336610E-004	0.09	5.48	10.58
8.90	1	3-carene	93.1	Linear	5	Ignore	None	20	99.64	21.58	y = 52.685854 * x + 2.167689E-004	0.69	5.80	10.93
9.06	2	β-myrcene	69.1	Linear	5	Ignore	None	20	99.62	12.18	y = 35.293257 * x - 5.397920E-005	1.14	5.04	11.28
9.19	2	α-phellandrene	93.1	Linear	5	Ignore	None	20	99.21	27.49	y = 38.448256 * x - 1.668867E-004	1.44	5.83	10.55
9.43	1	α-terpinene	121.1	Linear	5	Ignore	None	20	99.96	13.02	y = 17.500590 * x + 1.691078E-004	0.00	4.72	10.56
9.74	2	limonene	68.1	Linear	5	Ignore	None	20	99.68	31.86	y = 44.271387 * x + 2.277088E-004	0.86	5.46	11.05
9.91	2	1.8-cineole	81.1	Linear	5	Ignore	None	20	99.61	10.38	y = 24.646366 * x + 7.681400E-005	0.20	4.89	11.37
10.14	1	trans-2-hexenal	55.1	Quadratic	5	Ignore	None	20	100.00	37.77	y = 48002.537536 * x ^ 2 + 3.597477 * x + 0.001733	17.79	24.78	10.00
10.49	1	γ-terpinene	93.1	Linear	5	Ignore	None	20	99.63	13.11	y = 56.446192 * x + 1.497816E-004	0.63	5.88	10.91
10.92	2	p-cymene	119.1	Linear	5	Ignore	None	20	99.65	12.90	y = 145.481416 * x + 9.872030E-004	0.00	4.74	11.40
11.90	1	n-hexanol	56.1	Linear	5	Ignore	None	20	99.69	28.13	y = 33.136770 * x + 1.152697E-004	1.05	5.53	10.77
12.42	1	cis-3-hexanol	67.1	Linear	5	Ignore	None	20	99.73	9.85	y = 23.710554 * x + 1.878472E-005	1.01	5.54	10.70
12.67	2	nonanal	57.1	Linear	5	Ignore	None	20	99.72	85.47	y = 56.103500 * x + 0.001195	0.94	4.25	9.55
13.67	2	n-octyl acetate	56.1	Linear	5	Ignore	None	20	99.62	6.71	y = 21.347654 * x - 6.636915E-005		5.45	10.88
14.54	2	linalool	93.1	Linear	5	Ignore	None	20	99.96	26.09	y = 20.524057 * x + 8.924152E-005	0.82	5.52	10.07
14.71	2	camphor	95.1	Linear	5	Ignore	None	20	99.70	10.44	y = 17.134258 * x + 2.829427E-005		5.61	10.55
15.11	**1,2**	**1-bromodecane[b]**	**135.1**		**5**			**20**	**0.00**	**4.78**				
15.63	2	β-caryophyllene	93.1	Linear	5	Ignore	None	20	99.94	14.71	y = 17.513912 * x + 6.184014E-005	0.64	5.05	10.78
16.46	2	methyl chavicol	148.1	Linear	5	Ignore	None	20	99.74	14.12	y = 70.070632 * x + 1.983612E-004	0.73	5.24	11.20
16.56	1	α-caryophyllene (Humulene)	80.1	Linear	5	Ignore	None	20	99.81	28.45	y = 10.873575 * x + 3.741127E-005	1.07	5.00	10.96
16.64	1	α-terpineol	59.1	Linear	5	Ignore	None	20	99.93	32.39	y = 30.761370 * x + 1.296863E-004	1.05	5.40	10.15
17.92	1	methyl salicylate	92.1	Linear	5	Ignore	None	20	99.84	17.65	y = 19.488194 * x + 7.918743E-005	0.00	5.51	10.93
20.17	2	methyl eugeneol	178.1	Linear	5	Ignore	None	20	99.94	25.81	y = 33.134763 * x + 1.615874E-004	0.71	5.49	10.35
21.20	2	methyl cinnamate	131.1	Linear	5	Ignore	None	20	99.98	21.65	y = 28.801015 * x + 4.253429E-004		5.21	10.04
22.27	1	eugenol	164.1	Linear	5	Ignore	None	20	99.74	16.12	y = 22.908077 * x + 1.895731E-004	0.00	5.67	11.19
		[a]sample loss; [b]IS												

Annex X. 32 Information of the BVOCs targeted in the samples collected with TA and Anasorb CSC tubes in Ch. 8 that were analysed under thermal desorption, in the 8860 FID (Agilent), both the tubes (TD/GC-FID), and in the 5975C MS (Agilent), Anasorb CSC tubes only (only (LE-TD/GC-MS). LOQ in the GC-FID was calculated with the general formula based on blank signal (n=5) and standards calibration curve. In the GC-MS, no calibration was carried out, thus blank signal (n=5) was assigned as the LOQ and subtracted to the sample. The final sample amount was retrieved from signal provided by the lowest calibration level of the FID machine, that were injected and analysed in the MS at sample conditions. Red-highlighted data refer to compound's RT out of MS acquisition time.

		8860 (GC-) FID					(7890A GC-) 5975C MS			
Solution	*Compound*	*RT*	*Curve slope [a] (ng area counts $^{-1}$ min $^{-1}$)*	*SD blank [b] (n=5) (area counts)*	*LOD [c] (area counts)*	*LOQ [d] (area counts)*	*RT*	*SIM (m/z)*	*blank [be] (n=5) (area counts)*	*L1 [e] (n=5) (area counts)*
2	α-pinene	5.27	0.809	0.00	0.00	0.00	4.21	-	-	-
1	n-hexanal	5.65	0.455	0.00	0.00	0.00	4.55	-	-	-
1	β-pinene	5.89	0.796	0.00	0.00	0.00	4.74	93.1	77.30	146930.24
1	β-myrcene	6.07	0.803	0.00	0.00	0.00	5.06	93.1	0.00	189510.90
2	3-carene	6.12	0.964	0.00	0.00	0.00	5.06	69.1	65.73	239486.12
2	α-phellandrene	6.21	1.053	0.00	0.00	0.00	5.18	93.1	0.00	393914.89
1	α-terpinene	6.31	0.841	0.00	0.00	0.00	5.31	121.1	75.15	224114.58
2	limonene	6.44	1.006	0.00	0.00	0.00	5.47	68.1	72.58	214597.76
2	1.8-cineole	6.54	1.264	0.00	0.00	0.00	5.58	81.1	48.67	118769.35
1	trans-2-hexenal	6.60	0.583	0.00	0.00	0.00	5.67	55.1	0.00	75620.52
1	γ-terpinene	6.73	1.513	0.00	0.00	0.00	5.84	93.1	73.14	303787.74
2	p-cymene	6.92	0.991	0.00	0.00	0.00	6.06	119.1	0.00	539492.97
1	n-hexanol	7.21	0.839	0.00	0.00	0.00	6.46	56.1	36.83	197830.28
1	cis-3-hexanol	7.46	0.773	0.00	0.00	0.00	6.75	67.1	36.33	149025.66
2	nonanal	7.64	0.922	0.00	0.00	0.00	6.92	57.1	0.00	115312.75
2	n-octyl acetate	8.04	1.042	0.00	0.00	0.00	7.40	56.1	0.00	97400.40
2	linalool	8.41	1.192	0.00	0.00	0.00	7.83	93.1	66.71	52711.82
2	camphor	8.72	0.463	0.00	0.00	0.00	8.07	95.1	81.62	91880.46
1, 2	**1-bromodecane***	**8.78**					**8.20**	**135.1**	**0.00**	**108320.89**
2	β-caryophyllene	9.12	1.475	3.35	6.81	22.71	8.52	93.1	0.00	65459.85
2	methyl chavicol	9.43	1.733	0.00	0.00	0.00	8.91	148.1	0.00	368726.99
1	α-terpineol	9.49	1.460	0.00	0.00	0.00	8.96	59.1	0.00	101155.47
1	α-caryophyllene (Humulene)	9.56	1.073	0.00	0.00	0.00	9.01	80.1	38.92	53090.79
1	methyl salicylate	10.19	0.755	0.00	0.00	0.00	9.69	92.1	0.00	161362.81
2	methyl eugenol	11.24	1.054	0.00	0.00	0.00	10.77	178.1	0.00	194112.79
2	methyl cinnamate	11.94	0.676	0.00	0.00	0.00	11.42	131.1	0.00	195307.22
1	eugenol	12.48	1.134	0.00	0.00	0.00	11.87	164.1	11.68	179025.94

***IS**

[a] retrieved from calibration points (5) betwen 10.5-210 ng

[b] blank= pure CS2

[c] based on general formula, applied to blank: LOD= 3*(SD blank/Curve slope)

[d] based on general formula applied to blank: LOD= 10*(SD blank/Curve slope)

[e] lowest calibration level (10.5 ng) used to retrieve sample amount after substraction of blank signal, assigned as LOQ

Annex II

Summary of complete BVOC emissions and Emission Factors

Annex II: Summary of complete BVOC emissions and Emission Factors

Annex 4 BVOC emissions of main field collections

Annex X. 33 EU-LCIs table list for the investigated BVOCs adapted from most updated Master list (European Union, 2022).

No.	CAS no.	Compound	EU-LCI (µg m^{-3})	Status of EU-LCI value	Year of adoption
1		***Aromatic hydrocarbons***			
1-8*	527-84-4 535-77-3 99-87-6 25155-15-1	Cymene (o-, m- ,p-,) (1-isopropyl-2(3,4)-methylbenzene) and mix of o-, m-, and p-cymene	2200	Derived EU-LCI	2022
3		***Terpenes***			
3-1*	498-15-7	3-Carene	2500	Derived EU-LCI	2022
3-2	80-56-8	α-Pinene	2500	Derived EU-LCI	2013
3-3	127-91-3	β-Pinene	1400	Ascribed EU-LCI	2013
3-4	138-86-3 5989-27-5 5989-54-8	Limonene	5000	Derived EU-LCI	2014
3-5		Other terpene hydrocarbons	1400	Ascribed EU-LCI	2013
4		***Aliphatic alcohols***			
4-5	111-27-3	1-Hexanol	2100	Ascribed EU-LCI	2013
7		***Aldehydes***			
7-6	66-25-1	Hexanal	900	Derived EU-LCI (read-across)	2013
7-10	124-19-6	Nonanal	900	Derived EU-LCI (read-across)	2013
7-14	6728-26-3 505-57-7 16635-54-4 1335-39-3 73543-95-0	2-Hexenal	7	Derived EU-LCI (read-across)	2015

*new or altered

Annex X. 34 Table of the highest BVOC emissions (µg m^{-3}) measured along the considered growing stages of investigated plant species, bean (Ch.5), tomato (Ch.6), and basil (Ch.7), within the shortest sampling interval of each (15'-beans, 5'-tomato, and 5'-basil) carried out in the static enclosure (n= number of enclosed plants). Gradient colors highlighted emissions distribution (amount) over the cycle. BVOCs in bold were reported in the Master EU-LCIs list.

		µg m^{-3}									
		bean (n=12)				**tomato-~~CO_2~~** (n=1)	**tomato-CO_2** (n=1)	**basil RB_1** (n=55)		**basil RB_3** (n=55)	
Class	**BVOC**	*blossoming*	*mature*	*productive*	*senescence*	*mature*	*mature*	*young*	*mature*	*young*	*mature*
MT	**α-pinene**	16.53	29.87	9.07	0	21.60	0	6.37	0	0	0.96
	β-pinene		1.09	0	0	0	0	13.27	0	0	0
	3-carene	23.09	62.53	8.88	1.04	6.56	0	0	0	0	0
	α-phellandrene	0	0	0	0	0	0	0	0	0	0
	α-terpinene	0	1.92	0	0	5.28	0	1.56	0	0	0
	limonene	35.31	167.39	10.99	0	50.88	11.93	4.83	0.67	0.26	0.64
	γ-terpinene	0.37	1.73	0	0	1.04	0	2.27	0	0	0
	p-cymene	26.75	37.60	10.56	1.28	36.24	0	1.69	0	0	0
	β-phellandrene	0	0.35	0	0	1.44	-	-	-	-	-
	o-cymene	0	0.43	0	0	0	0	0.84	0.93	0.95	0.35
OMT	β-myrcene	0	0.42	0	0	0	0	5.99	0	0	0
	1.8-cineole	0.56	0.72	0.32	0	1.92	0	189.07	5.40	5.22	36.14
	linalool	2.35	16.69	2.11	0.77	0	0	0	0	0	0
	camphor	3.44	9.84	4.19	1.44	1.84	0	0	0	0	0
	α-terpineol	-	-	-	-	-	0	0	0	0	0
	eugenol	-	-	-	-	-	-	-	-	-	-
ST	β-caryophyllene	0	0.61	0	0	0	0	108.24	0	0	7.90
	α-caryophyllene (Humuler	-	-	-	-	-	0	0	0	0	0
	trans-β-farnesene	-	-	-	-	-	0	1.86	0	0	0.41
HT	TMTT	0	0	0	0	0	0	0	0	0	0
LOX	**n-hexanal**	-	-	-	-	-	0	0	0	0	0
	trans-2-hexenal*	-	-	-	-	-	6.63	2.69	3.82	6.68	1.34
	n-hexanol	5.65	16.59	9.68	4.59	4.56	-	-	-	-	-
	cis-3-hexanol	4.64	20.64	10.21	4.24	2.00	0	0	0	0	0
	nonanal	-	-	-	-	-	-	-	-	-	-
	n-octyl acetate	-	-	-	-	-	0	0	0	0	0
	cis-3-hexenal*	2.03	4.67	1.89	0	0	-	-	-	-	-
PH	methyl chavicol	0	0	0	0	0	0	0	0	0	0
	methyl salicylate	-	-	-	-	-	0	4.58	0	0	1.32
	methyl eugenol	0	0	0	0	0	0	0	0	0	0
	methyl cinnamate	0	0	0	0	1.36	0.00	0	0	0	0
	2-tert-butylphenol	0	0	0	0	0	0	0	0	0	0

* reference LCI for 2-hexenal

0 : not detected

- : not determined

Annex X. 35 Comparative table between the highest BVOC emissions (µg m^{-3}) measured along bean plants cultivation in the empty (=iRTG) and planted (=Plants) section of the static enclosure within short (15') and long (30') sampling intervals in the assessment reported in Ch.5 and A1.2. The number of enclosed plants (n) is indicated. Gradient colors highlighted emissions distribution (amount) over the cycle between short and long sampling intervals. BVOCs in bold were reported in the Master EU-LCIs list.

		Plants (n=12)								*iRTG* (n=0)							
		15'				**30'**				**15'**				**30'**			
Class	**BVOC**	*blossoming*	*mature*	*productive*	*senescence*	*blossoming*	*mature*	*productive*	*senescence*	*blossoming*	*mature*	*productive*	*senescence*	*blossoming*	*mature*	*productive*	*senescence*
MT	**α-pinene**	16.53	29.87	9.07	0	3.87	6.93	18.13	2.67	0	27.20	25.33	3.73	5.07	13.73	3.6	0
	β-pinene		1.09	0	0	0	0	0	0	0	0.83	0.48	0	0.00	0.2	0	0
	3-carene	23.09	62.53	8.88	1.04	9.41	17.11	9.55	7.07	2.21	56.08	42.75	4.83	10.72	24.87	6.57	0.28
	α-phellandrene	0	0	0	0	0	0	0	0	0	0	0	0	0	0	0	0
	α-terpinene	0	1.92	0	0	0	0.25	0.23	0	0	2.11	0.8	0	0.23	0.85	0	0
	limonene	35.31	167.39	10.99	0	20.05	38.40	30.91	11.84	2.45	160.64	89.15	2.08	32.91	121.31	16.45	0
	γ-terpinene	0.37	1.73	0	0	0.00	0.28	0.25	0	0	1.84	0.85	0	0.25	0.72	0	0
	p-cymene	26.75	37.60	10.56	1.28	9.84	9.16	10.37	6.36	2.88	40.21	45.60	3.87	12.15	13.77	6.16	0.23
	β-phellandrene	0	0.35	0	0	0	0	0.2	0	0	0.37	0	0	0	0	0	0
	o-cymene	0	0.43	0	0	0	0.13	0.88	0	0	0.45	0.32	0	0	0.19	0	0
OMT	β-myrcene	0	0.42	0	0	0	0	4.72	0.17	0	0	0	0	0	0	0	0
	1.8-cineole	0.56	0.72	0.32	0	0.25	0.27	1.76	0.61	0	0.69	0.88	0	0.28	0.37	0.17	0
	linalool	2.35	16.69	2.11	0.77	1.01	3.28	1.96	0.81	1.20	15.41	6.03	0.72	1.19	3.49	1.20	0.21
	camphor	3.44	9.84	4.19	1.44	1.76	2.21	7.05	1.43	1.25	9.79	8.53	1.01	1.96	2.89	1.88	0.40
	α-terpineol	-	-	-	-	-	-	-	-	-	-	-	-	-	-	-	-
	eugenol	-	-	-	-	-	-	-	-	-	-	-	-	-	-	-	-
ST	β-caryophyllene	0	0.61	0	0	0.17	0	0.88	0.16	0	0.61	0.59	0	0.17	0.16	0.16	0
	α-caryophyllene	-	-	-	-	-	-	-	-	-	-	-	-	-	-	-	-
	trans-β-farnesene	-	-	-	-	-	-	-	-	-	-	-	-	-	-	-	-
HT	TMTT	0	0	0	0	0	0	0	0	0	0	0	0	0	0	0	0
LOX	**n-hexanal**	-	-	-	-	-	-	-	-	-	-	-	-	-	-	-	-
	trans-2-hexenal*	-	-	-	-	-	-	-	-	-	-	-	-	-	-	-	-
	n-hexanol	5.65	16.59	9.68	4.59	2.91	2.87	13.73	3.48	3.68	16.00	13.73	3.57	2.88	3.56	3.83	1.87
	cis-3-hexanol	4.64	20.64	10.21	4.24	2.39	4.63	8.25	2.77	3.81	20.56	13.60	3.60	1.92	4.85	3.83	1.77
	nonanal	-	-	-	-	-	-	-	-	-	-	-	-	-	-	-	-
	n-octyl acetate	-	-	-	-	-	-	-	-	-	-	-	-	-	-	-	-
	cis-3-hexenal*	2.03	4.67	1.89	0	1.39	0	8.87	0	0	4.43	2.93	0	0.80	0.95	0.95	0
PH	methyl chavicol	0	0	0	0	0	0	0	0	0	0	0	0	0	0	0	0
	methyl salicylate	-	-	-	-	-	-	-	-	-	-	-	-	-	-	-	-
	methyl eugenol	0	0	0	0	0	0	0	0	0	0	0	0	0	0	0	0
	methyl cinnamate	0	0	0	0	0	0	0	0	0	0	0.59	0	0	0	0	0
	2-tert-butylphenol	0	0	0	0	0	0	0	0	0	0	0	0	0	0	0	0

* reference LCI for 2-hexenal

0 : not detected

- : not determined

Annex X. 36 Comparative tables between the highest BVOC emissions (µg m^{-3}) measured in the chamber (n= 1 plant), and directly (no chamber) in the iRTG (n=177 plants) and in the outdoor along three consecutive sampling intervals (short, 5' and 10', and long, 45') and two different daytimes during tomato crop cultivation (reference assessment Ch.6, 2021). Note that during plant enclosing no CO2 replenishment was applied, meaning that extremely untrustworthy emissions from long sampling must be supposed. Gradient colors highlighted emissions distribution (amount) between the sampling intervals within the individual sampling point (1), and between the sampling points within a single sampling interval (2). BVOCs in bold were reported in the Master EU-LCIs list.

		Morning									Afternoon								
		chamber (n=1)			*iRTG (n=177)*			*outdoor (rooftop)*			*chamber (n=1)*			*iRTG (n=177)*			*outdoor (rooftop)*		
Class	**BVOC**	**5'**	**10'**	**45'**	**5'**	**10'**	**45'**	**5'**	**10'**	**45'**	**5'**	**10'**	**45'**	**5'**	**10'**	**45'**	**5'**	**10'**	**45'**
MT	**α-pinene**	21.60	9.20	1.42	2.40	1.20	0.80	1.60	2.00	1.33	9.60	5.60	0.80	2.40	1.60	0.18	0	0	0.18
	β-pinene	0	0	0	0	0	0	0	0	0	0	0	0.44	0	0	0	0	0	0
	3-carene	6.56	2.96	0.60	1.92	1.00	0.25	1.84	1.08	0.35	4.24	2.56	12.51	2.48	1.52	0.47	1.20	0.60	0.28
	α-phellandrene	0	0	0	0	0	0	0	0	0	0	0	0.72	0	0	0	0	0	0
	α-terpinene	5.28	2.48	0.41	0	0	0	0	0.64	0.16	2.56	1.72	7.38	0	0	0	0	0	0
	limonene	50.88	20.76	2.77	2.80	1.92	0.29	1.12	1.92	0	16.64	8.48	58.52	2.32	0	0	0	0	0
	γ-terpinene	1.04	0	0	0	0	0	0	0	0	0	0	2	0	0	0	0	0	0
	p-cymene	36.24	15.32	3.29	2.48	1.48	1.49	2.88	4.24	0.92	29.04	14.88	41.67	2.00	4.60	0.64	0.88	0.48	0.21
	β-phellandrene	1.44	0.56	0.12	0	0	0	0	0	0	0	0	1.97	0	0	0	0	0	0
	o-cymene	0	0	0	0	0	0	0	0	4.92	0	0	0	0	0	0	0	0	0
OMT	β-myrcene	0	0	0	0	0	0	0	0	0	7.56	3.28	0.22	0	0.62	0.18	0	0	0
	1.8-cineole	1.92	1.04	0.27	1.84	1.48	0.27	1.92	1.04	0.37	3.20	1.40	0.52	2.72	1.12	0.33	0.96	1.00	0.20
	linalool	0	0	0	0	0	0	0	0	0	0	0	0	0	0	0	0	0	0
	camphor	1.84	0.92	0.25	2.32	1.48	0.24	2.40	1.04	0.28	3.20	1.36	0.20	2.24	1.00	0.30	1.44	0.88	0.28
	α-terpineol	-	-	-	-	-	-	-	-	-	-	-	-	-	-	-	-	-	-
	eugenol	-	-	-	-	-	-	-	-	-	-	-	-	-	-	-	-	-	-
ST	β-caryophyllene	0	0	0	0	0	0.11	0	0.48	0	0	0.48	0	0	0	0	0	0	0
	α-caryophyllene	-	-	-	-	-	-	-	-	-	-	-	-	-	-	-	-	-	-
	trans-β-farnesene	-	-	-	-	-	-	-	-	-	-	-	-	-	-	-	-	-	-
HT	TMTT	0	0	0	0	0	0	0	0	0	0	0	0	0	0	0	0	0	0
LOX	**n-hexanal**	-	-	-	-	-	-	-	-	-	-	-	-	-	-	-	-	-	-
	trans-2-hexenal*	-	-	-	-	-	-	-	-	-	-	-	-	-	-	-	-	-	-
	n-hexanol	4.56	3.32	0.73	7.68	4.60	0.72	6.96	2.96	0.73	10.32	4.32	0.82	7.84	2.96	0.76	2.72	2.40	0.58
	cis-3-hexanol	2.00	1.68	0.36	2.24	1.64	0.25	3.12	1.32	0.49	3.44	1.20	0.24	4.56	1.04	0.40	1.68	1.36	0.31
	nonanal	-	-	-	-	-	-	-	-	-	-	-	-	-	-	-	-	-	-
	n-octyl acetate	-	-	-	-	-	-	-	-	-	-	-	-	-	-	-	-	-	-
	cis-3-hexenal*	0	0	0.63	0	5.32	0.66	0	0	0	12.80	6.16	1.42	4.32	2.80	0.92	0	0	0
PH	methyl chavicol	0	0	0	0	0	0	0	0	0	0	0	0	0	0	0	0	0	0
	methyl salicylate	-	-	-	-	-	-	-	-	-	-	-	-	-	-	-	-	-	-
	methyl eugenol	0	0	0	0	0	0	0	0	0	0	0	0	0	0	0	0	0	0
	methyl cinnamate	1.36	0.68	0	1.36	0	0	0	0	0	1.60	0	0	0	0	0.20	0	0	0
	2-tert-butylphenol	0	0	0	0	0	0	0	0	0	0	0	0	0	0	0	0	0	0

* reference LCI for 2-hexenal

0 : not detected

- : not determined

1

		Morning									Afternoon								
		5′			*10′*			*45′*			*5′*			*10′*			*45′*		
Class	**BVOC**	**chamber**	**iRTG**	**outdoor**	**chamber**	**iRTG**	**outdoor**	**chamber**	**iRTG**	**outdoor**	**chamber**	**iRTG**	**outdoor**	**chamber**	**iRTG**	**outdoor**	**chamber**	**iRTG**	**outdoor**
MT	**α-pinene**	21.60	2.40	1.60	9.20	1.20	2.00	1.42	0.80	1.33	9.60	2.40	0	5.60	1.60	0	0.80	0.18	0.18
	β-pinene	0	0	0	0	0	0	0	0	0	0	0	0	0	0	0	0.44	0	0
	3-carene	6.56	1.92	1.84	2.96	1.00	1.08	0.60	0.25	0.35	4.24	2.48	1.20	2.56	1.52	0.60	12.51	0.47	0.28
	α-phellandrene	0	0	0	0	0	0	0	0	0	0	0	0	0	0	0	0.72	0	0
	α-terpinene	5.28	0	0	2.48	0	0.64	0.41	0	0.16	2.56	0	0	1.72	0	0	7.38	0	0
	limonene	50.88	2.80	1.12	20.76	1.92	1.92	2.77	0.29	0	16.64	2.32	0	8.48	0	0	58.52	0	0
	γ-terpinene	1.04	0	0	0	0	0	0	0	0	0	0	0	0	0	0	2	0	0
	p-cymene	36.24	2.48	2.88	15.32	1.48	4.24	3.29	1.49	0.92	29.04	2.00	0.88	14.88	4.60	0.48	41.67	0.64	0.21
	β-phellandrene	1.44	0	0	0.56	0	0	0.12	0	0	0	0	0	0	0	0	1.97	0	0
	o-cymene	0	0	0	0	0	0	0	0	4.92	0	0	0	0	0	0	0	0	0
OMT	β-myrcene	0	0	0	0	0	0	0	0	0	7.56	0	0	3.28	0.62	0	0.22	0.18	0
	1.8-cineole	1.92	1.84	1.92	1.04	1.48	1.04	0.27	0.27	0.37	3.20	2.72	0.96	1.40	1.12	1.00	0.52	0.33	0.20
	linalool	0	0	0	0	0	0	0	0	0	0	0	0	0	0	0	0	0	0
	camphor	1.84	2.32	2.40	0.92	1.48	1.04	0.25	0.24	0.28	3.20	2.24	1.44	1.36	1.00	0.88	0.20	0.30	0.28
	α-terpineol	-	-	-	-	-	-	-	-	-	-	-	-	-	-	-	-	-	-
	eugenol	-	-	-	-	-	-	-	-	-	-	-	-	-	-	-	-	-	-
ST	β-caryophyllene	0	0	0	0	0	0.48	0	0.11	0	0	0	0	0.48	0	0	0	0	0
	α-caryophyllene	-	-	-	-	-	-	-	-	-	-	-	-	-	-	-	-	-	-
	trans-β-farnesene	-	-	-	-	-	-	-	-	-	-	-	-	-	-	-	-	-	-
HT	TMTT	0	0	0	0	0	0	0	0	0	0	0	0	0	0	0	0	0	0
LOX	**n-hexanal**	-	-	-	-	-	-	-	-	-	-	-	-	-	-	-	-	-	-
	trans-2-hexenal*	-	-	-	-	-	-	-	-	-	-	-	-	-	-	-	-	-	-
	n-hexanol	4.56	7.68	6.96	3.32	4.60	2.96	0.73	0.72	0.73	10.32	7.84	2.72	4.32	2.96	2.40	0.82	0.76	0.58
	cis-3-hexanol	2.00	2.24	3.12	1.68	1.64	1.32	0.36	0.25	0.49	3.44	4.56	1.68	1.20	1.04	1.36	0.24	0.40	0.31
	nonanal	-	-	-	-	-	-	-	-	-	-	-	-	-	-	-	-	-	-
	n-octyl acetate	-	-	-	-	-	-	-	-	-	-	-	-	-	-	-	-	-	-
	cis-3-hexenal*	0	0	0	0	5.32	0	0.63	0.66	0	12.80	4.32	0	6.16	2.80	0	1.42	0.92	0
PH	methyl chavicol	0	0	0	0	0	0	0	0	0	0	0	0	0	0	0	0	0	0
	methyl salicylate	-	-	-	-	-	-	-	-	-	-	-	-	-	-	-	-	-	-
	methyl eugenol	0	0	0	0	0	0	0	0	0	0	0	0	0	0	0	0	0	0
	methyl cinnamate	1.36	1.36	0	0.68	0	0	0	0	0	1.60	0	0	0	0	0	0	0.20	0
	2-tert-butylphenol	0	0	0	0	0	0	0	0	0	0	0	0	0	0	0	0	0	0

* reference LCI for 2-hexenal

0 : not detected

- : not determined

Annex X. 37 Comparative table between the highest BVOC emissions (µg m^{-3}) of young and mature basil plants under the two R:B light ratios measured during the static enclosing along three consecutive sampling intervals (5', 10', and 15') in the assessment reported in Ch.7. Gradient colors highlighted emissions distribution (amount) between the sampling intervals within each stage. BVOCs in bold were reported in the Master EU-LCIs list.

		YOUNG						*MATURE*					
		RB_1			**RB_3**			RB_1			**RB_3**		
Class	BVOC	5'	10'	15'	5'	10'	15'	5'	10'	15'	5'	10'	15'
MT	**α-pinene**	6.37	3.07	0	0	0	0	0	0	0	0	0	0.96
	β-pinene	13.27	1.07	0	0	0	0	0	0	0	0	0	0
	3-carene	0	0	0	0	0	0	0	0	0	0	0	0
	α-phellandrene	0	0	0	0	0	0	0	0	0	0	0	0
	α-terpinene	1.56	0	0	0	0	0	0	0	0	0	0	0
	limonene	4.83	1.43	0	0	0.26	0.11	0.67	0	0	0	0	0.64
	γ-terpinene	2.27	0	0	0	0	0	0	0	0	0	0	0
	p-cymene	1.69	0.60	0	0	0	0	0	0	0	0	0	0
	β-phellandrene	-	-	-	-	-	-	-	-	-	-	-	-
	o-cymene	0.84	0.79	0.77	0.95	0.60	0.32	0.93	0	0	0	0	0.35
OMT	β-myrcene	5.99	0.73	0	0	0	0	0	0	0	0	0	0
	1.8-cineole	189.07	86.31	0	5.22	3.08	1.44	5.40	2.07	0	21.76	4.99	36.14
	linalool	0	0	0	0	0	0	0	0	0	0	0	0
	camphor	0	0	0	0	0	0	0	0	0	0	0	0
	α-terpineol	0	0	0	0	0	0	0	0	0	0	0	0
	eugenol	-	-	-	-	-	-	-	-	-	-	-	-
ST	β-caryophyllene	108.24	6.92	0	0	0	0	0	0	0	7.90	0	0.54
	α-caryophyllene (Humulene)	0	0	0	0	0	0	0	0	0	0	0	0
	trans-β-farnesene	0.64	1.86	0	0	0	0	0	0	0	0	0	0.41
HT	TMTT	0	0	0	0	0	0	0	0	0	0	0	0
LOX	**n-hexanal**	0	0	0	0	0	0	0	0	0	0	0	0
	trans-2-hexenal + cis-3-hexenal*	2.69	0.62	0.93	6.68	0.51	0.02	3.82	0.33	0	1.34	0.94	0
	n-hexanol	-	-	-	-	-	-	-	-	-	-	-	-
	cis-3-hexanol	0	0	0	0	0	0	0	0	0	0	0	0
	nonanal	-	-	-	-	-	-	-	-	-	-	-	-
	n-octyl acetate	0	0	0	0	0	0	0	0	0	0	0	0
PH	methyl chavicol	0	0	0	0	0	0	0	0	0	0	0	0
	methyl salicylate	4.58	1.28	0	0	0	0	0	0	0	0	0	1.32
	methyl eugenol	0	0	0	0	0	0	0	0	0	0	0	0
	methyl cinnamate	0	0	0	0	0	0	0	0	0	0	0	0
	2-tert-butylphenol	0	0	0	0	0	0	0	0	0	0	0	0

* reference LCI for 2-hexenal

0 : not detected

- : not determined

Annex 5 Derived BVOC Emission Factors of main field assessments

Annex X. 38 Tables reporting the calculated BVOC EFs with respect to the fresh leaf biomass (1) and leaf area (2) along the considered growing stages of investigated plant species: bean (Ch.5), tomato (Ch.6), and basil (Ch.7). EFs were retrieved from average concentration values. Gradient colors highlighted EFs distribution (amount) over the cycle. BVOCs in bold were reported in the Master EU-LCIs list.

		EF (ng h^{-1} g^{-1})								
		bean				tomato	basil (RB_1)		basil (RB_3)	
Class	BVOC	*blossoming*	*mature*	*productive*	*senescence*	*mature*	*young*	*mature*	*young*	*mature*
MT	**α-pinene**	41.82	31.87	14.24	0	101.89	48.39	0	0	0
	β-pinene	0	1.17	0	0	0	75.73	0	0	0
	3-carene	65.70	70.86	16.39	3.14	41.42	0	0	0	0
	α-phellandrene	0	0	0	0	0	0	0	0	0
	α-terpinene	0	2.05	0	0	18.54	12.58	0	0	0
	limonene	94.71	180.80	17.26	0	243.89	32.39	1.97	0	0
	γ-terpinene	0.94	1.85	0	0	2.17	16.02	0	0	0
	p-cymene	77.71	45.71	20.51	3.56	195.25	6.82	0	0	0
	β-phellandrene	0	0.37	0	0	4.68	-	-	-	-
	o-cymene	0	0.46	0	0	0	3.40	2.72	4.77	0
OMT	β-myrcene	0	0.45	0	0	0	43.43	0	0	0
	1.8-cineole	1.42	0.77	0.35	0	15.70	1419.47	15.84	40.73	68.57
	linalool	10.05	21.57	5.05	2.03	0	0	0	0	0
	camphor	13.83	13.86	8.80	3.69	3.84	0	0	0	0
	α-terpineol	-	-	-	-	0	0	0	0	0
	eugenol	-	-	-	-	-	-	-	-	-
ST	β-caryophyllene	0	0.65	0	0	0	710.59	0	0	20.13
	α-caryophyllene (Humulene)	-	-	-	-	0	0	0	0	0
	trans-β-farnesene	-	-	-	-	0	2.60	0	0	0
HT	TMTT	0	0	0	0	0	0	0	0	0
LOX	**n-hexanal**	-	-	-	-	0	0	0	0	0
	trans-2-hexenal*	0	0	0	0	110.70	21.08	20.72	68.81	3.42
	n-hexanol	29.75	25.33	20.57	11.64	76.13	-	-	-	-
	cis-3-hexanol	26.64	33.18	20.60	11.04	4.18	0	0	0	0
	nonanal	-	-	-	-	-	-	-	-	-
	n-octyl acetate	-	-	-	-	0	0	0	0	0
	cis-3-hexenal*	5.13	4.98	2.06	0	0	-	-	-	-
PH	methyl chavicol	0	0	0	0	0	0	0	0	0
	methyl salicylate	-	-	-	-	0	35.67	0	0	0
	methyl eugenol	0	0	0	0	0	0	0	0	0
	methyl cinnamate	0	0	0	0	2.84	0	0	0	0
	2-tert-butylphenol	0	0	0	0	0	0	0	0	0

* reference LCI for 2-hexenal

0 : not detected

- : not determined

1

		EF (µg h^{-1} m^{-2})								
		bean				tomato	basil (RB_1)		basil (RB_3)	
Class	BVOC	*blossoming*	*mature*	*productive*	*senescence*	*mature*	*young*	*mature*	*young*	*mature*
MT	**α-pinene**	49.11	89.17	37.26	0	65.69	0.12	0	0	0
	β-pinene	0	3.26	0	0	0	0.19	0	0	0
	3-carene	77.15	198.25	42.89	0.51	26.71	0	0	0	0
	α-phellandrene	0	0	0	0	0	0	0	0	0
	α-terpinene	0	5.73	0	0	11.95	0.03	0	0	0
	limonene	111.21	505.80	45.17	0	157.24	0.08	0.00	0	0
	γ-terpinene	1.11	5.18	0	0	1.40	0.04	0	0	0
	p-cymene	91.25	127.86	53.69	0.57	125.88	0.02	0	0	0
	β-phellandrene	0	1.04	0	0	3.02	-	-	-	-
	o-cymene	0	1.27	0	0	0	0.01	0.01	0.01	0
OMT	β-myrcene	0	1.25	0	0	0	0.11	0	0	0
	1.8-cineole	1.66	2.15	0.90	0	10.12	3.52	0.04	0.11	0.17
	linalool	11.80	60.35	13.21	0.33	0	0	0	0	0
	camphor	16.24	38.77	23.04	0.59	2.48	0	0	0	0
	α-terpineol	-	-	-	-	0	0	0	0	0
	eugenol	-	-	-	-	-	-	-	-	-
ST	β-caryophyllene	0	1.83	0	0	0	1.76	0	0	0.05
	α-caryophyllene (Humulene)	-	-	-	-	0	0	0	0	0
	trans-β-farnesene	-	-	-	-	0	0.01	0	0	0
HT	TMTT	0	0	0	0	0	0	0	0	0
LOX	**n-hexanal**	-	-	-	-	0	0	0	0	0
	trans-2-hexenal*	0	0	0	0	71.37	0.05	0.05	0.18	0.01
	n-hexanol	34.93	70.86	53.84	1.87	49.08	-	-	-	-
	cis-3-hexanol	31.29	92.83	53.92	1.78	2.69	0	0	0	0
	nonanal	-	-	-	-	-	-	-	-	-
	n-octyl acetate	-	-	-	-	0	0	0	0	0
	cis-3-hexenal*	6.02	13.93	5.40	0	0	-	-	-	-
PH	methyl chavicol	0	0	0	0	0	0	0	0	0
	methyl salicylate	-	-	-	-	0	0.09	0	0	0
	methyl eugenol	0	0	0	0	0	0	0	0	0
	methyl cinnamate	0	0	0	0	1.83	0	0	0	0
	2-tert-butylphenol	0	0	0	0	0	0	0	0	0

* reference LCI for 2-hexenal

0 : not detected

- : not determined

2

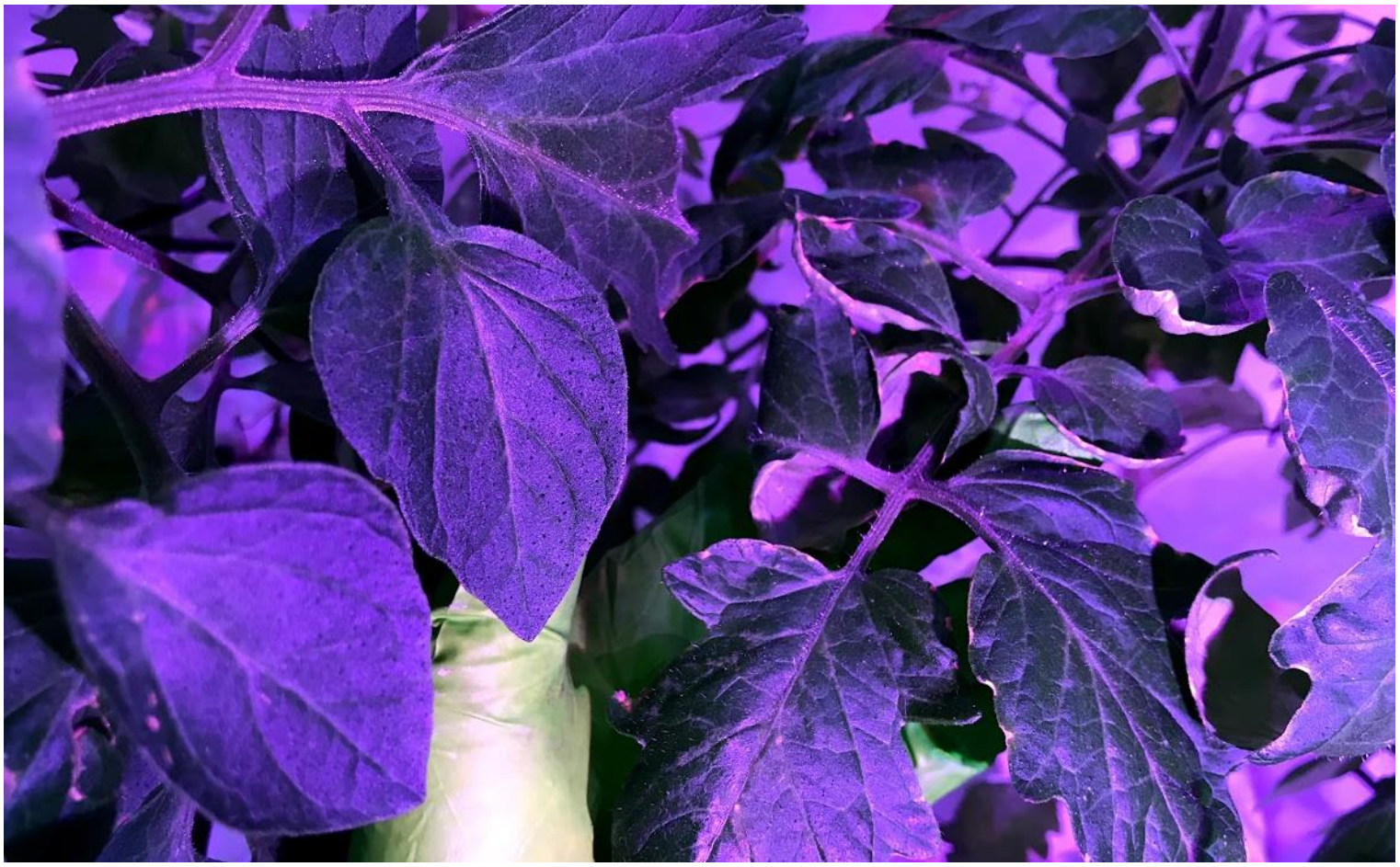

Annex III

Supplementary Information

Annex III: Supplementary Information

Annex A5. 1 Instrumental conditions of the analytical processing method (MS SIM) for the determination of mono- and sesqui- terpenes (MT, ST), oxygenated monoterpene (OMT) and lipoxygenase derivate (LOX) compounds: the retention time (RT), the selected ion mass (m/z), the lowest limit of quantitation (LOQ) and the relative standard deviation (RSD) of calculated LLOQs.

Order	RT (min)	SIM (m/z)	BVOC Class	Compound name	LOQ (ng µL^{-1})	RSD (%)
1	6.35	93.1	MT	α-pinene	0.0018	16.57
2	13.98	56.1	OMT	linalool	0.0015	15.98
3	15.19	98.1	ST	β-caryophyllene	0.0012	19.47
4	11.85	178.1	LOX	cis-3-hexenol	0.0017	20.44

untitled0.py*

```
import numpy as np
import matplotlib.pyplot as plt
from skimage import io
from skimage.color import rgb2gray
from skimage.filters import threshold_otsu
img = io.imread('C:/Users/gaiaR/Desktop/pathcarpeta/file.png o .jpg')
img_bw = rgb2gray(img)
threshold = threshold_otsu(img_bw)
img_binary = img_bw < threshold
area_tot_scan = 660
area = np.sum(img_binary) / np.prod(img_bw.shape) * area_tot_scan
# Plot the binarized image
plt.imshow(img_binary)
plt.show()
print('The area is', area)
```

Annex A5. 2 Python 3.8 script (Spyder 4.1.5) for leaf area calculation from leaves pictures.

Annex A5. 3 Emission Factor (average of nearby air measurements) of the reviewed BVOCs over the crop cycle in the i-RTG according to measured leaf area (1) and calculated LAI index (2).

	BVOC EF ($\mu g\ m^{-2}\ h^{-1}$)			
Plant phenological stage	**α-Pinene**	**Linalool**	**cis-3-hexenol**	**β-caryophyllene**
Full vegetative	89.07	60.28	92.73	1.83
Reproductive	49.56	11.91	31.57	0.00
Productive	37.41	13.26	54.13	0.00
Senescent	0.00	0.33	1.78	0.00

1

	BVOC EF ($\mu g\ h^{-1}$)			
Plant phenological stage	**α-Pinene**	**Linalool**	**cis-3-hexenol**	**β-caryophyllene**
Full vegetative	8.91	6.03	9.27	0.18
Reproductive	4.96	1.19	3.16	0.00
Productive	3.74	1.33	5.41	0.00
Senescent	0.00	0.03	0.18	0.00

2

Annex A6. 1 Common constitutive and induced volatiles emitted by tomato plants (Solanum lycopersicum L.), retrieved from the literature (Farag and Paré, 2002; Jansen et al., 2009, 2010; Degenhardt et al., 2010; Copolovici et al., 2012;

Takayama et al., 2012; Pazouki et al., 2016; Kasal-Slavik et al., 2017; Catola et al., 2018). In bold are those considered for the emissions assessment.

BVOC classes			
Terpenoids		LOX (Lypoxygenase) derivatives	Shikimic acid derivatives (Phenolics)
Monoterpenes	α-Pinene β-pinene β-myrcene **limonene** 2-carene α-phellandrene β-phellandrene α-terpinene γ-terpinene linalool β-elemelene	n-Hexanal n-Hexanol **(Z)-3-Hexenal** (E)-2-Hexenal (Z)-3-Hexenol	methyl salicylate (3E,7E)-4,8,12-trimethyl-1, 3,7,11-tridecatetraene tert-butylphenol p-cymene o-cymene
Sesquiterpenes	α-copaene β-caryophyllene* α-humulene δ-elemene		
Others	nonanal decanal		

Annex A6. 2 MS SIM conditions of each instrument processing method (compound retention time, RT, compound selected ion mass, m/z), the calibration curve results (Correlation Coefficient 'CF', RSD, n=5), the lower limit of quantitation calculated (LOQ) and its RSD (n=6) applied for the determination of MT-limonene and LOX-cis-3-hexenal.

BVOC class	BVOC name	RT (min)	SIM (m/z)	Curve CF (r_s)	Curve RSD (%)	LOQ (ng µL^{-1})	LOQ RSD (%)
MT	Limonene	9.27[1]; 9.79[2]	68.1	0.99[1]; 0.99[2]	10.09[1]; 39.02[2]	0.0022[1]; 0.0004[2]	8.71[1]; 20.91[2]
LOX	Cis-3-hexenal	9.63[1]; 10.18[2]	69.1	1.0[1]; 0.99[2]	5.58[1]; 153.79[2]	0.0056[1]; 0.00002[2]	13.78[1]; 8.59[2]

[1] ISQ7000 MS; [2] 5975C inert MSD

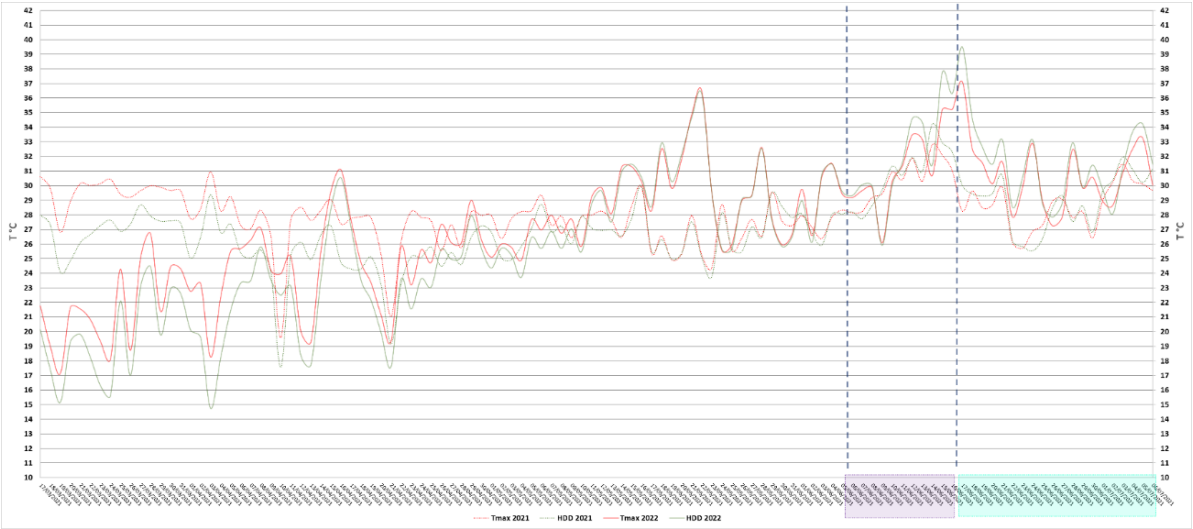

Annex A6. 3 Graph reporting daily heat degree day (HDD) and maximum temperature (T max) registered in the i-RTG throughout the experimental seasons from plant transplant until the last day of volatile collection. Sampling intervals in 2021 (blue area) and 2022 (violet area) are highlighted.

Annex A6. 4 Mean ± SD (n=9, 2021; n=5, 2022) of average fresh weights of individual and total organ biomass, leaf area, leaf area index (LAI) and height of tomato plants measured in 2021 and 2022.

	m	***gfw****				***m²***	
year	*height*	*total biomass*	*leaves*	*green biomass (leaves + stem)*	*fruits*	*leaves area*	*LAI*
2021	*3.0 ± 0.3*	*4228.3 ± 674.6*	*1044.7 ± 159.6*	*1621.5 ± 184.6*	*2597.3 ± 614.3*	*1.6 ± 0.4*	*19.7 ± 4.4*
2022	*2.5 ± 0.4*	*3079.7 ± 639.5*	*889.4 ± 199.2*	*1700.1 ± 286.4*	*1379.6 ± 560.2*	*1.4 ± 0.6*	*11.5 ± 5.2*

*grams of fresh weight

Annex A6. 5 Calculated emission rates (ERs) according to leaf and total (stem + leaves + fruits) fresh biomass and projected leaf area of average ± SEM (n=9, 2021; n=5, 2022) emission (µg m^{-3}) of MT-limonene (1) and LOX-cis-3-hexenal (2) collected at 5- and 10- minute sampling under unadministered CO_2 (2021) and administered CO_2 (2022). In bold and between parenthesis next to the average ER are reported the highest ERs measured on the whole season calculated from an individual emission collected.

Limonene (MT)		ng gfw^{-1} h^{-1}	ng gfw^{-1} h^{-1}	µg m^{-2} h^{-1}
Condition	interval	leaves (ER)	total biomass (ER)	leaves area (ER)
Unadministered CO_2	5'	280.53 (**1752.19**) ± 189.14	59.09 (**352.09**) ± 37.97	181.74 (**1080.84**) ± 116.88
Administered CO_2		291.66 ± 74.07	90.04 ± 22.89	251.20 ± 56.88
Unadministered CO_2	10'	82.46 ± 39.42	18.13 ± 8.22	54.78 ± 25.05
Administered CO_2		79.30 ± 10.15	25.34 ± 5.17	67.17 ± 13.54

1

Cis-3-hexenal (LOX)		ng gfw^{-1} h^{-1}	ng gfw^{-1} h^{-1}	µg m^{-2} h^{-1}
Condition	interval	leaves (ER)	total biomass (ER)	leaves area (ER)
Unadministered CO_2	5'	ND	ND	ND
Administered CO_2		128.56 (**181.84**) ± 20.44	41.22 (**81.41**) ± 10.75	113.87 (**227.18**) ± 31.24
Unadministered CO_2	10'	ND	ND	ND
Administered CO_2		29.86 ± 7.71	9.26 ± 2.77	23.77 ± 5.58

2

Annex A6. 6 Mean ± SD (n=9, 2021; n=5, 2022) of average CO_2 concentration, temperature (T), relative humidity (RH), and radiation (Rs) measured in the i-RTG environment and in the chamber during 5 and 10 minutes of sampling under administered and unadministered CO_2 conditions. Different superscript lowercase letter indicates significantly different levels between the assays (p> 0.05).

Year	location	CO_2 (ppm ± SD)	T (°C ± SD)	RH (% ± SD)	Rs (W m^{-2} ± SD)
2021 (Unadministered CO_2)	i-RTG	441.85 ± 37.04	25.96 ± 2.67	62.82 ± 13.65	234.70* ± 133.62
	Chamber (5')	427.00 ± 31.79	26.59 ± 2.91	71.85[a] ± 14.56	64.57 ± 67.17
	Chamber (10')	411.43 ± 24.35	26.80 ± 2.98	74.51[a] ± 12.94	67.40 ± 68.08
2022 (Administered CO_2)	i-RTG	415.81 ± 23.15	28.01 ± 2.92	52.43 ± 13.63	178.99* ± 15.83
	Chamber (5')	423.60 ± 24.51	28.21 ± 2.73	55.47[b] ± 11.60	84.66 ± 14.89
	Chamber (10')	426.14 ± 30.46	28.29 ± 2.70	56.22[b] ± 11.15	85.70 ± 12.39

Annex A6. 7 Mean ± SD (n=9, 2021; n=5, 2022) of average photosynthetic rate (Pn) and stomatal conductance (g_s) predicted during 5 and 10 minutes of sampling under administered and unadministered CO_2 conditions. Different superscript lowercase letter indicates significantly different levels between the assays (p> 0.05).

Year	interval	Pn (μmol CO_2 m^{-2} s^{-1} ± SD)	g_s (mmol m^{-2} s^{-1} ± SD)
2021 (Unadministered CO_2)	5'	10.12 ± 6.62	278.90 ± 193.91
	10'	6.14 ± 3.64	181.89[a] ± 112.17
2022 (Administered CO_2)	5'	4.01 ± 3.77	86.72 ± 72.43
	10'	2.63 ± 1.97	57.80[b] ± 41.92

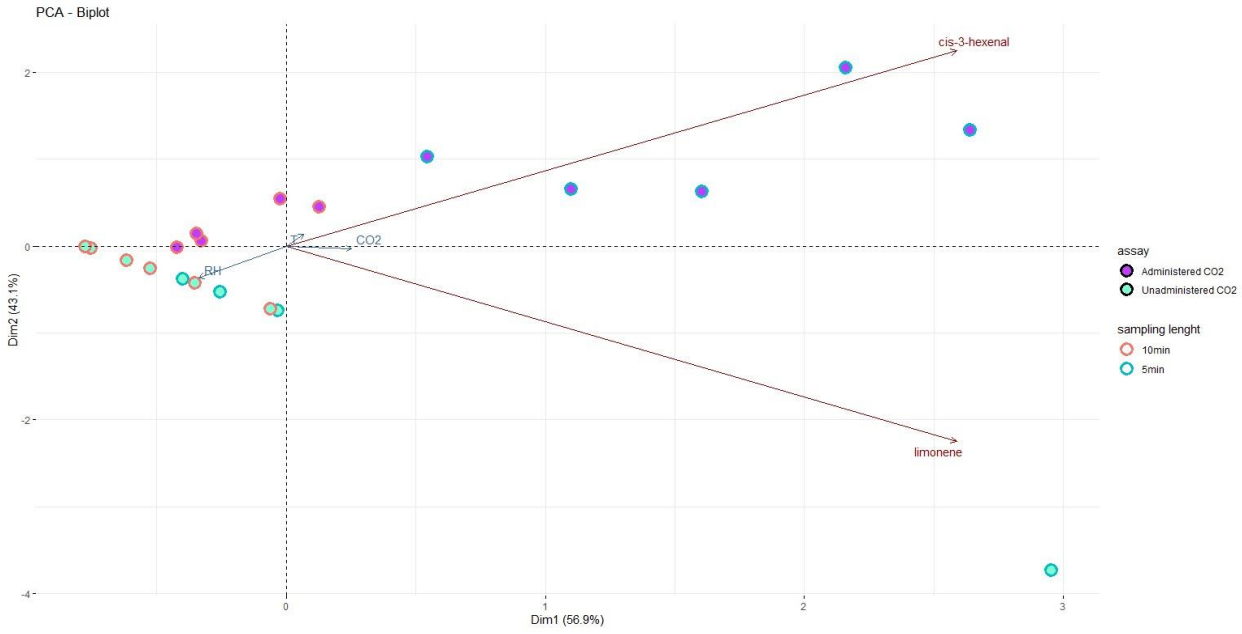

Annex A6. 8 Principal component analysis (PCA) performed with the mean emission rates of MT (limonene) and LOX (cis-3-hexenal) volatiles, temperature (T), relative humidity (RH), CO_2 concentration, photosynthetic rate (Pn), and stomatal conductance (g_s) measured or predicted (g_s and Pn) at 5- and 10-minute sampling under administered and unadministered CO_2 assays.

Annex A6. 9 Summary of the main results from the principal component analysis (PCA).

Eigenvalues	Dim.1	Dim.2
Variance	1.138	0.862
Proportion of variance (%)	56.896	43.104
Cumulative proportion (%)	56.896	100

Individuals	sampling interval	replicate	Dist	Dim.1	ctr	cos2	Dim.2	ctr	cos2
Unadministered CO_2	5-minutes	1	4.757	2.952	27.357	0.385	-3.729	57.619	0.615
		2	0.744	-0.034	0.004	0.002	-0.743	2.287	0.998
		3	0.778	-0.778	1.899	1.000	0.001	0.000	0.000
		4	0.778	-0.778	1.899	1.000	0.001	0.000	0.000
		5	0.581	-0.255	0.204	0.192	-0.522	1.130	0.808
		6	0.778	-0.778	1.899	1.000	0.001	0.000	0.000
		7	0.778	-0.778	1.899	1.000	0.001	0.000	0.000
		8	0.550	-0.400	0.503	0.530	-0.377	0.588	0.470
		9	0.778	-0.778	1.899	1.000	0.001	0.000	0.000
	10-minutes	1	0.718	-0.062	0.012	0.007	-0.715	2.120	0.993
		2	0.583	-0.526	0.867	0.814	-0.251	0.262	0.186
		3	0.778	-0.778	1.899	1.000	0.001	0.000	0.000
		4	0.777	-0.777	1.894	1.000	0.000	0.000	0.000
		5	0.638	-0.617	1.196	0.937	-0.160	0.106	0.063
		6	0.754	-0.754	1.784	0.999	-0.023	0.002	0.001
		7	0.778	-0.778	1.899	1.000	0.001	0.000	0.000
		8	0.552	-0.352	0.389	0.407	-0.425	0.748	0.593
		9	0.778	-0.778	1.899	1.000	0.001	0.000	0.000
Administered CO_2	5-minutes	1	2.962	2.640	21.872	0.794	1.343	7.475	0.206
		2	1.164	0.543	0.924	0.217	1.030	4.397	0.783
		3	1.725	1.604	8.079	0.865	0.634	1.664	0.135
		4	2.983	2.158	14.617	0.523	2.059	17.569	0.477
		5	1.281	1.098	3.781	0.734	0.661	1.810	0.266
	10-minutes	1	0.552	-0.025	0.002	0.002	0.552	1.261	0.998
		2	0.335	-0.329	0.339	0.963	0.065	0.017	0.037
		3	0.470	0.125	0.049	0.071	0.453	0.850	0.929
		4	0.378	-0.346	0.376	0.842	0.150	0.094	0.158
		5	0.421	-0.421	0.556	1.000	-0.009	0.000	0.000

Variables	Dim.1	ctr	cos2	Dim.2	ctr	cos2
limonene	0.754	50	0.569	-0.657	50	0.431
cis-3-hexenal	0.754	50	0.569	0.657	50	0.431

Supplementary continuous variables	Dim.1	cos2	Dim.2	cos2
T	0.069	0.005	0.14	0.019
RH	-0.337	0.113	-0.362	0.131
CO_2	0.253	0.064	-0.029	0.001
Pn	-0.145	0.021	-0.393	0.154
g_s	-0.200	0.040	-0.365	0.133

Supplementary categories	Dist	Dim.1	cos2	v.test	Dim.2	cos2	v.test
Administered CO_2	0.989	0.705	0.508	2.559	0.694	0.492	2.894
Unadministered CO_2	0.549	-0.392	0.508	-2.559	-0.385	0.492	-2.894
10-minutes	0.459	-0.458	0.997	-2.233	-0.026	0.003	-0.144
5-minutes	0.459	0.458	0.997	2.233	0.026	0.003	0.144

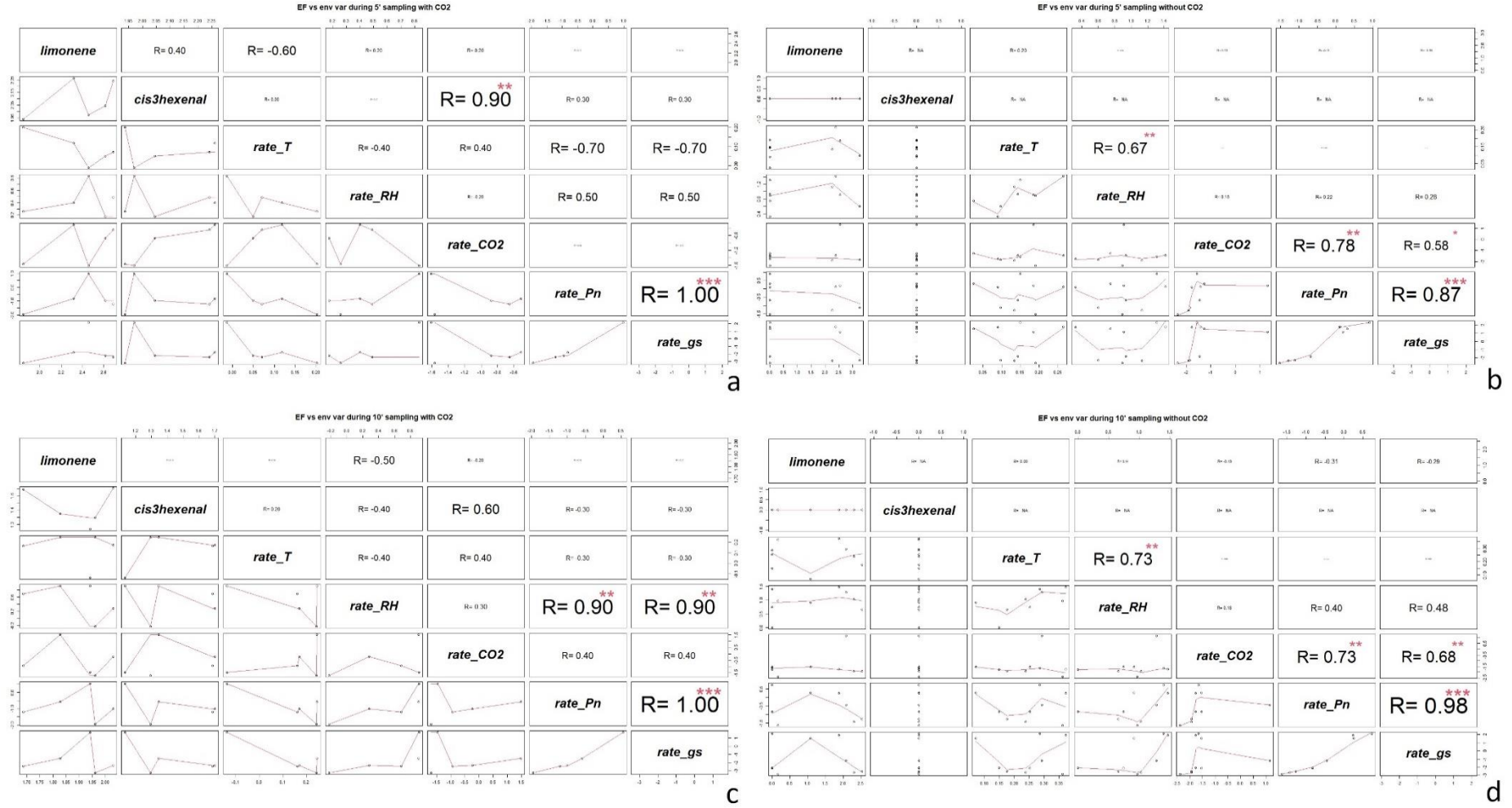

*Annex A6. 10 Matrices showing positive and negative Spearman rs correlations between the mean ER of sampled BVOCs (MT-limonene and LOX-cis-3-hexenal) and the mean variation rates of the variables registered and predicted (mean rate of CO_2 concentration, RH, air T, Pn, and g_s: rate_CO2, rate_RH, rate_T, rate_Pn, and rate_gs) along dynamic sampling in the static enclosure under administered CO_2 at 5 (a) and 10 (c) minutes and unadministered CO_2 at 5 (b) and 10 (d) minutes. Significant $p \leq 0.001$, $p \leq 0.01$ and $p \leq 0.05$ are indicated by the symbols '***', '**' and '*'; rs between ± 0.50 and ± 1 accounts for a correlation.*

Annex A7. 1 ERs of the BVOCs determined at the three sampling intervals (5, 10, and 15 minutes) under RB_1 and RB_3 treatments, for the young (YRB_1, YRB_3) and the mature (MRB_1, MRB_3) stage. ERs are referred to the fresh rather than dry foliage biomass (g) (1), since volatile emissions were collected from living plants, and the projected leaf area (m^2) (2), measured during each term.

		µg g^{-1} h^{-1}								
	(min)	α-pinene	β-pinene	β-myrcene	o-cymene	1.8-cineole	LOX	β-caryophyllene	trans-β-farnesene	methyl salicylate
YRB_1	5	50.34	78.79	45.18	0.72	0.00	91.90	739.24	0.00	37.11
	10	6.70	2.11	1.45	0.92	5.35	10.54	17.71	0.00	2.53
	15	0.00	0.00	0.00	0.41	1.82	2.42	0.00	0.00	0.00
YRB_3	5	0.00	0.00	0.00	1.08	34.68	63.10	0.00	0.00	0.00
	10	0.00	0.00	0.00	1.47	16.92	4.43	0.00	0.00	0.00
	15	0.00	0.00	0.00	0.53	4.24	1.76	0.00	0.00	0.00
MRB_1	5	0.00	0.00	0.00	0.00	77.64	2.41	0.00	21.86	0.00
	10	0.00	0.00	0.00	0.00	7.18	1.91	0.00	0.00	0.00
	15	0.00	0.00	0.00	0.58	50.56	0.00	0.00	0.52	0.00
MRB_3	5	0.00	0.00	0.00	0.26	926.10	10.92	20.98	460.65	0.00
	10	0.00	0.00	0.00	0.98	147.76	1.72	0.00	11.18	0.00
	15	0.80	0.00	0.00	1.71	0.00	2.40	0.45	0.00	1.10

1

		µg m^{-2} h^{-1}								
	(min)	α-pinene	β-pinene	β-myrcene	o-cymene	1.8-cineole	LOX	β-caryophyllene	trans-β-farnesene	methyl salicylate
YRB_1	5	124.70	195.16	111.91	1.79	0.00	227.64	1831.09	0.00	91.91
	10	16.59	5.23	3.58	2.28	13.26	26.11	43.87	0.00	6.26
	15	0.00	0.00	0.00	1.01	4.51	5.99	0.00	0.00	0.00
YRB_3	5	0.00	0.00	0.00	2.81	90.11	163.95	0.00	0.00	0.00
	10	0.00	0.00	0.00	3.81	43.97	11.52	0.00	0.00	0.00
	15	0.00	0.00	0.00	1.37	11.01	4.56	0.00	0.00	0.00
MRB_1	5	0.00	0.00	0.00	0.00	182.70	5.68	0.00	51.44	0.00
	10	0.00	0.00	0.00	0.00	16.90	4.48	0.00	0.00	0.00
	15	0.00	0.00	0.00	1.37	118.98	0.00	0.00	1.22	0.00
MRB_3	5	0.00	0.00	0.00	0.65	2361.11	27.83	53.49	1174.42	0.00
	10	0.00	0.00	0.00	2.51	376.71	4.39	0.00	28.50	0.00
	15	2.04	0.00	0.00	4.36	0.00	6.11	1.15	0.00	2.81

2

*Annex A7. 2 Variation rates (positive and negative) of environmental (T, RH, CO_2) and physiological (G_s) parameters along the sampling under RB_1 and RB_3 light in the young and mature plant stage. In 1 and 2 are highlighted the significant differences of the variation rates of the individual parameter between the sampling intervals within the same treatment, indicated by different lowercase letters. In 3 and 4 are reported the significant differences of the variation rates of the individual parameter between the treatments within the same sampling interval. Symbols '***', '**', and '*', refer to a significance of a p value ≤0.001, 0.01, and 0.05 respectively.*

30-32 DAS

parameter	interval	RB1		p	RB3		p
CO2	5	-6.13	a		-55.13	a	*
CO2	10	19.90	a		-102.67	ab	
CO2	15	-4.50	a		42.23	b	*
T	5	-0.13	a	***	-0.07	a	
T	10	0.00	b	***	0.17	b	*
T	15	0.23	c	***	0.17	a	
RH	5	6.20	a	***	6.03	a	***
RH	10	4.47	b	***	3.17	b	***
RH	15	1.97	c	***	4.90	c	***
Gs	5	-39.33	a		-13.83	a	
Gs	10	-8.50	a		-11.83	b	*
Gs	15	-24.77	a		-56.07	a	

1

36-39 DAS

parameter	interval	RB1		p	RB3		p
CO2	5	-36.93	a		-89.90	a	
CO2	10	7.13	a		-131.90	a	
CO2	15	-4.50	a		293.27	a	
T	5	-0.07	a	*	0.00	a	
T	10	0.27	b		0.10	a	
T	15	0.23	b		0.27	a	
RH	5	2.17	a	**	6.93	a	**
RH	10	3.30	b		12.57	b	
RH	15	1.97	b		11.47	b	
Gs	5	-1.20	a	***	-6.03	a	***
Gs	10	-3.97	b	***	-0.43	b	
Gs	15	3.23	c	***	-12.93	b	

2

30-32 DAS

parameter	interval	RB1	RB3	p
CO2	5	-6.13	-55.13	
CO2	10	19.90	-102.67	
CO2	15	-4.50	42.23	
T	5	-0.13	-0.07	**
T	10	0.00	0.17	***
T	15	0.23	0.17	
RH	5	6.20	6.03	
RH	10	4.47	3.17	
RH	15	1.97	4.90	***
Gs	5	-39.33	-13.83	
Gs	10	-8.50	-11.83	*
Gs	15	-24.77	-56.07	

3

36-39 DAS

parameter	interval	RB1	RB3	p
CO2	5	-36.93	-89.90	
CO2	10	7.13	-131.90	
CO2	15	-4.50	293.27	
T	5	-0.07	0.00	***
T	10	0.27	0.10	**
T	15	0.23	0.27	
RH	5	2.17	6.93	***
RH	10	3.30	12.57	**
RH	15	1.97	11.47	*
Gs	5	-1.20	-6.03	**
Gs	10	-3.97	-0.43	***
Gs	15	3.23	-12.93	***

4

30-32 DAS

RB1

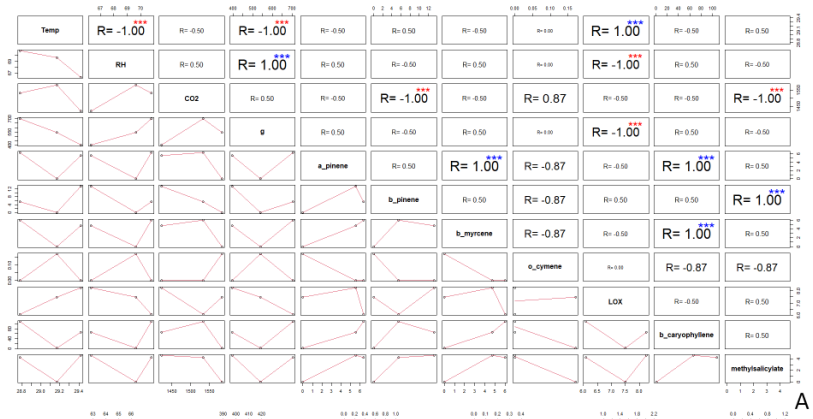

A

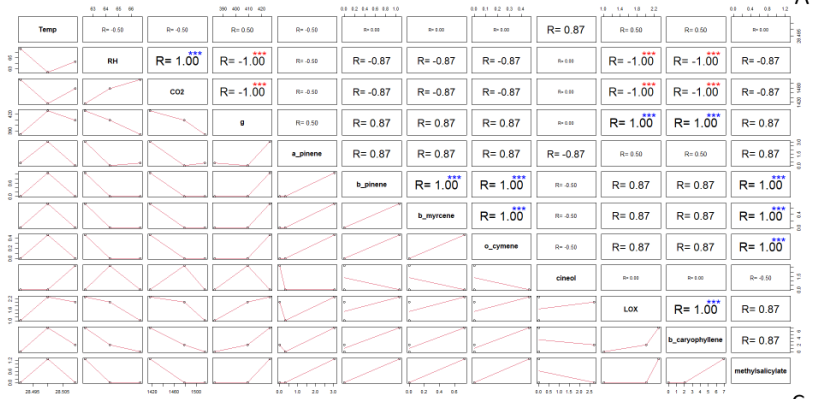

C

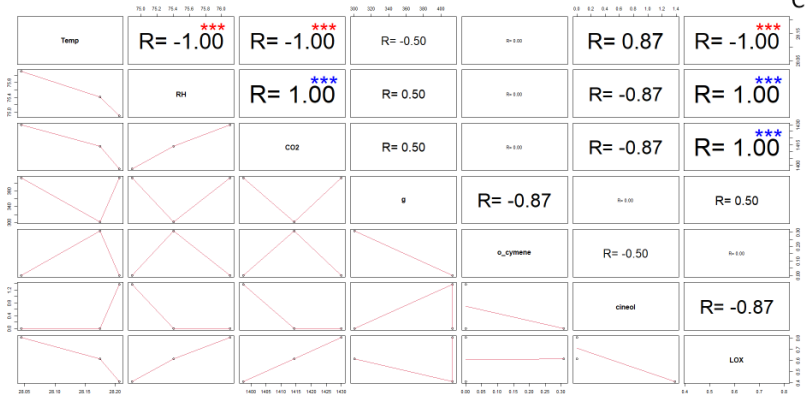

E

RB3

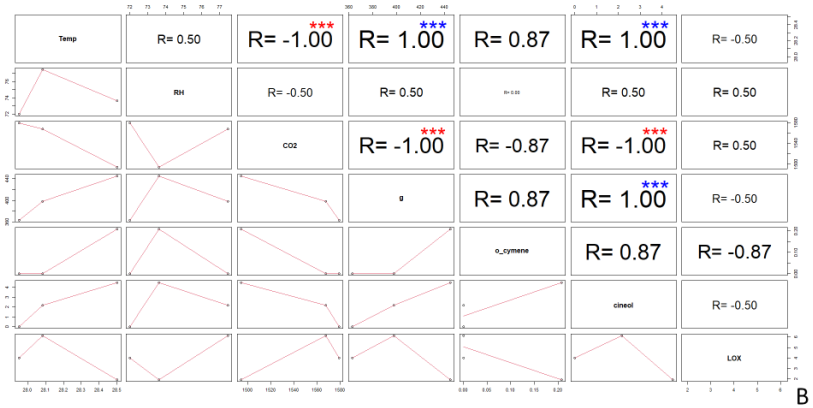

B

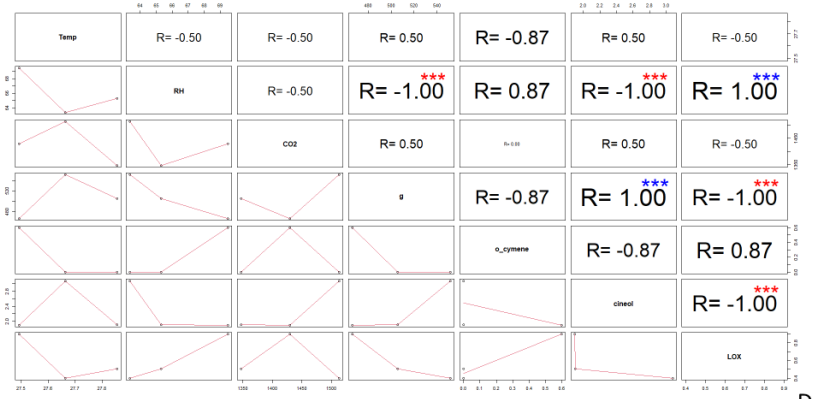

D

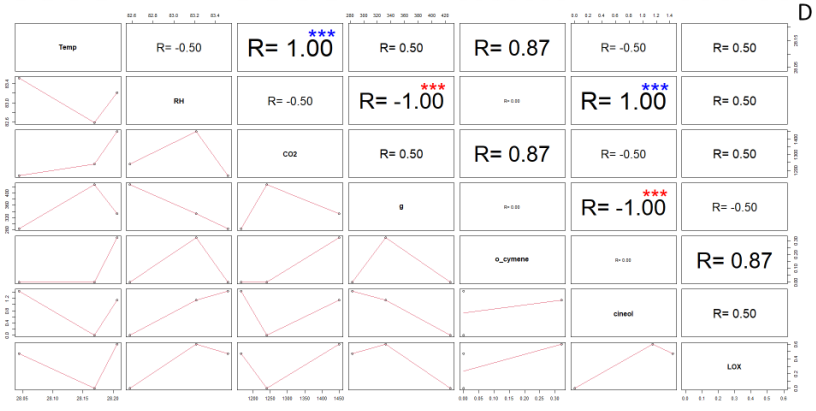

F

1

2

*Annex A7. 3 Correlation matrices showing positive and negative Spearman ('R'= r_s) correlations between the detected BVOC emissions and the levels of the environmental (T, RH, CO_2) and physiological ('g'= g_s) parameters monitored during volatile collection in the young (1) and mature (2) plant stage under RB1 and RB3 light along respectively 5- (A, B), 10- (C, D) and 15- (E, F) minutes interval. Symbols '***' above Spearman r_s indicate perfect correlations (rs ±1, $p \leq 0.05$), although not significant ($p > 0.05$) not perfect correlations having r_s ±0.8 were considered meaningful.*